Advances in Meteorology

Advances in Urban Biometeorology

Guest Editors: Panagiotis Nastos, Andreas Matzarakis, Marialena Nikolopoulou, and Tzu-Ping Lin

Advances in Urban Biometeorology

Advances in Meteorology

Advances in Urban Biometeorology

Guest Editors: Panagiotis Nastos, Andreas Matzarakis, Marialena Nikolopoulou, and Tzu-Ping Lin

Editorial Board

Contents

Hindawi Publishing Corporation
Advances in Meteorology
Volume 2013, Article ID 427413, 3 pages
http://dx.doi.org/10.1155/2013/427413

Editorial

Advances in Urban Biometeorology

Panagiotis Nastos,[1] Andreas Matzarakis,[2] Marialena Nikolopoulou,[3] and Tzu-Ping Lin[4]

[1] *Laboratory of Climatology and Atmospheric Environment, University Campus, University of Athens, 15784 Athens, Greece*
[2] *Meteorology and Climatology, Albert-Ludwigs-University of Freiburg, Werthmannstraße 10, 79085 Freiburg, Germany*
[3] *Kent School of Architecture, University of Kent, Canterbury, Kent CT2 7NR, UK*
[4] *Department of Architecture, National Cheng Kung University, 1 University Road, Tainan 701, Taiwan*

Correspondence should be addressed to Panagiotis Nastos; nastos@geol.uoa.gr

Received 27 November 2013; Accepted 27 November 2013

With the increase of urbanization, a significant factor playing an important role in global warming, the scientific community has been required to provide solutions addressing the negative impact of climate and the general atmospheric environment on cities, along with the improvement of these conditions for humans. The urban heat island affects not only quality of life, but in many cases also affects morbidity and mortality. Urban planning plays a very important role in this, and various studies have shown the importance of taking into account human thermal sensation in order to mitigate the negative consequences of urbanization and strengthen the resilience of the society [1–8]. This special issue focuses on the assessment/modeling of human thermal sensation and exposure to ambient air pollution within urban agglomerations. The various papers focus on different scales and climatic contexts, all with the common theme of identifying the effect of urban configurations, such as buildings, parks, and streets, on humans' health and well-being.

More specifically, the paper of H. Lee et al. "*Modification of human-biometeorologically significant radiant flux densities by shading as local method to mitigate heat stress in summer within urban street canyons*" analyzes the physical processes, which are characteristic of shading in terms of urban human biometeorology, through experimental investigations into the thermal effects of shading by a building and tree canopies, conducted in Freiburg, southwest Germany, during typical Central European summer weather. Urban human biometeorology, that is, the human-biometeorological concept to assess the thermal environment, refers to the variables of air temperature Ta, mean radiant temperature Tmrt, and physiologically equivalent temperature PET—based on the energy balance model of the human body. With respect to both shading devices, the Ta reduction did not exceed 2°C, while PET as a measure for human heat stress was lowered by two thermal sensation steps. The results show the crucial significance of the horizontal radiant flux densities for Tmrt and consequently PET.

The effect of urban structures on thermal comfort indices in the extreme climate region of the Russian Far East, as well as the seasonal dynamics in different urban zones at the capital of the Jewish Autonomous Region, Birobidzhan, was studied by J. L. Bauche et al. in "*Human-biometeorological assessment of urban structures in extreme climate conditions: the example of birobidzhan, Russian Far East.*" The difference of thermal values for three zones with different vegetation and build-up density shows the influence of urban planning on the local microclimate. The moderating effect of dense built-up and inner city vegetation on extreme thermal conditions becomes clear when comparing all zones. Through the analysis of daily and monthly timelines it was possible to determine preferable times of the day for inner city outdoor activities. The results indicate that, with a total of 170 days per year with PET values below 0°C, Birobidzhan can be considered as a region of extreme cold stress. This suggests that adaptation based solely on behaviour and clothing is not sufficient, but adaptation of the urban surroundings and therefore the identification and choice of preferable urban structures are necessary.

In a similar work, P. T. Nastos and A. Matzarakis "*Human bioclimatic conditions, trends, and variability in the Athens University Campus, Greece*" attempt to identify human thermal bioclimatic conditions in the Athens University Campus (AUC). The quantification of human thermal sensation in such a place was considered of a great significance due to the great gathering of student body and members of University. The analysis of the bioclimate is carried out, using PET. Results reveal that approximately 45%–65% of the days within the year, from 08:00 to 19:00, experience PET values greater than 18°C (thermal comfort), while 13%–23% of the days (mainly during summer period) are characterized by strong/extreme thermal stress from 09:00 to 16:00. Regarding the strong/extreme cold stress, it appeared for almost 50% of days from midnight to early morning hours (06:00). Regarding the extreme conditions, the intense heat waves that occurred during summer 2007 along with extreme cold during December 2003–February 2004 were also analyzed. These were compared to the respective average bioclimatic conditions of the study period, indicating that the occurrence of extreme human-biometeorological conditions is of high concern for the future climate, especially for very crowed areas, such as AUC.

Long-term estimations in a tropical coastal city of Dar es Salaam, Tanzania are carried out by E. L. Ndetto and A. Matzarakis in "*Effects of urban configuration on human thermal conditions in a typical tropical African coastal city,*" in order to determine the effects of buildings' heights and street orientations on human thermal conditions at pedestrian level. A typical urban street and a park were chosen as representative urban environments. Results, as interpreted in terms of the thermal comfort parameters of mean radiant (Tmrt) and PET, indicate that urban configurations influence significantly the two parameters. In particular, optimal reduction of Tmrt and PET values are observed on the north-south reoriented streets and with increased building heights. Simulation results on a small urban garden provide a novelty in design implications and management of open spaces in cities.

In the study of C. H. Lin et al. "*Thermal comfort for urban parks in subtropics: understanding visitor's perceptions, behavior and attendance,*" an effort towards thermal comfort assessment for urban parks under the climatic conditions of Taiwan is conducted, through field interviews, observations, and micrometeorological measurements. The WBGT is used as the thermophysiological index to investigate the effects of thermal conditions on visitors' thermal perception and adaptive behaviors in outdoor urban spaces. Observation results show that the overall attendance is influenced by sun and thermal conditions. There is a robust relationship between thermal sensation votes, as well as thermal acceptability, and thermal environment, in terms of WBGT. The upper and lower limits of 80% acceptability are 26°C WBGT and 20°C WBGT, respectively.

L. A. Égerházi et al. in "*Application of microclimate modelling and onsite survey in planning practice related to an urban micro-environment*" perform numerical simulations of thermal comfort conditions by means of the urban microclimate model ENVI-met in a popular children's playground located in Szeged, Hungary. Bioclimatic conditions are quantified using PET and thermal stress maps are created in two different periods of typical summer and autumn days. The study aims to reveal the seasonal and diurnal spatial patterns of the simulated thermal conditions and thus the degree of heat stress in different parts of the playground. Furthermore, the momentary spatial distributions of the visitors triggered by the microclimatic conditions of the area are analyzed. Remarkable differences in the thermal conditions are found depending on the sun elevation and the resulting shaded conditions as well as the radiation of the heated surfaces. The spatial distribution of the visitors seems to be highly influenced by the patterns of the thermal conditions, but the location and the preference of the playground equipment also affect this. To evaluate the possible causes of the people's behavior, an on-site questionnaire survey was conducted with possible modification requirements related to the design of the playground.

In the modeling aspect of outdoor biometeorological conditions, K. P. Moustris et al. "*One-day prediction of biometeorological conditions in a mediterranean urban environment using artificial neural networks modeling*" deal with the 24-hour prognosis of the outdoor human-biometeorological conditions in an urban monitoring site within the greater Athens area, Greece. For this purpose, artificial neural networks (ANNs) are applied in order to predict the maximum and the minimum value of the PET, one day ahead, as well as the persistence of the hours with extreme human-biometeorological conditions. The results show that extreme heat stress appears in 10% of the examined hours within the warm period of the year, against extreme cold stress for 22.8% of the hours during the cold period of the year. Finally, human thermal comfort sensation accounts for 81.8% of the hours during the year. Concerning the PET forecast, ANNs have a remarkable forecasting ability to predict the extreme daily PET values one day ahead, as well as the persistence of extreme conditions during the day, at a significant statistical level of $P < 0.01$.

Findings of the study by A. Lopes et al. in "*Lisbon urban heat island updated: new highlights about the relationships between thermal patterns and wind regimes*" update the results of the research published in 2007 and bring more precise information about the relationship between the UHI (urban heat island) and the regional and local wind systems in Lisbon. The highest frequencies of temperature differences higher than 0°C are found in the city centre. In the green park of Monsanto, the highest frequency occurred between −2 and 0°C. During the summer, the effect of the breezes is observed in Belém, lowering the air temperature. The "strong" UHI (intensity > 4°C) occurred more often during the summer, with median values of 2°C by night and 1.8°C by day. The highest frequencies of UHI occur for winds between 2 and 6 m/s, and are not associated with atmospheric calm events, as pointed out in the literature. Winds above 8 m/s inhibit the occurrence of strong UHI in Lisbon.

The assessment and comparison of variations in air temperature and vapour pressure (vis-à-vis relative humidity) against a crowd of runners—the herd effect—are studied by P. Wong et al. in "*Microclimate variations between semienclosed*

and open sections of a marathon route." The work evaluates conditions in two different environmental settings along the marathon course, a semienclosed (tunnel) versus an open space (suspension bridge). A series of small iButtons was deployed at strategic locations along the course to undertake minute-by-minute measurements of air temperature and relative humidity. It is found that herd effects of varying degrees are present in both the semienclosed and open settings. Various environmental differences also play a role in ameliorating or amplifying the climatological effects of the herd of runners. Microclimatic variations in different environmental settings and crowd conditions could have an impact on runners. This knowledge can inform the design of marathon routes and establishes the feasibility of employing the iButton logging sensors for widespread deployment and monitoring of meteorological situations.

The last paper in this volume is by J. H. Amorim et al. "*Pedestrian exposure to air pollution in cities: modeling the effect of roadside trees,*" who evaluate the exposure of students to traffic-emitted carbon monoxide (CO) in their daily walk to school, with a particular emphasis on the effect of trees and route choice. The study is focused on the city centre of Aveiro, in central Portugal. Time evolution of the georeferenced location of an individual was tracked with a GPS for different alternative walking routes to a school. Spatial distribution of CO concentration was simulated with a computational fluid dynamics (CFD) model. An exposure model was developed that associates the georeferenced location of the student with the computed air quality levels (at an average breathing height) for that specific grid cell. For each individual the model calculates the instantaneous exposure at each time frame and the mean value for a given period. Results show a general benefit induced by the trees over the mean exposure of the student in each route. However, in the case of instantaneous exposure values this is not consistent along the entire period. Also, the variability of the estimated exposure values indicates the potential error that can be committed when using a single value of air quality as a surrogate of air pollution exposure.

We expect that this special issue will help journal readers to understand better the impacts of various aspects of urban biometeorology. We trust that this volume will be a valuable reference to researchers, academics, planning authorities, practitioners, and policy makers.

Acknowledgments

As Guest Editors of this special issue, we would like to thank all the authors for their contributions to this volume and their adherence to the strict reviewing rules. We also wish to express our sincere appreciation to the international panel of reviewers for making their expertise available in the effort to achieve the highest scientific value of this volume.

Panagiotis Nastos
Andreas Matzarakis
Marialena Nikolopoulou
Tzu-Ping Lin

References

[1] M. Nikolopoulou, "Outdoor thermal comfort," *Frontiers in Bioscience*, vol. 3, pp. 1552–1568, 2011.

[2] M. Nikolopoulou and S. Lykoudis, "Thermal comfort in outdoor urban spaces: analysis across different European countries," *Building and Environment*, vol. 41, no. 11, pp. 1455–1470, 2006.

[3] P. T. Nastos and A. Matzarakis, "Variability of tropical days over Greece within the second half of the twentieth century," *Theoretical and Applied Climatology*, vol. 93, no. 1-2, pp. 75–89, 2008.

[4] T.-P. Lin, "Thermal perception, adaptation and attendance in a public square in hot and humid regions," *Building and Environment*, vol. 44, no. 10, pp. 2017–2026, 2009.

[5] A. Matzarakis and P. T. Nastos, "Human-biometeorological assessment of heat waves in Athens," *Theoretical and Applied Climatology*, vol. 105, no. 1, pp. 99–106, 2011.

[6] T.-P. Lin, R. de Dear, and R.-L. Hwang, "Effect of thermal adaptation on seasonal outdoor thermal comfort," *International Journal of Climatology*, vol. 31, no. 2, pp. 302–312, 2011.

[7] P. T. Nastos and A. Matzarakis, "The effect of air temperature and human thermal indices on mortality in Athens, Greece," *Theoretical and Applied Climatology*, vol. 108, no. 3-4, pp. 591–599, 2012.

[8] A. Matzarakis, "Stadtklima vor dem Hintergrund des Klimawandels," *Gefahrstoffe*, vol. 73, pp. 115–118, 2013.

Hindawi Publishing Corporation
Advances in Meteorology
Volume 2013, Article ID 487695, 11 pages
http://dx.doi.org/10.1155/2013/487695

Research Article

Lisbon Urban Heat Island Updated: New Highlights about the Relationships between Thermal Patterns and Wind Regimes

António Lopes,[1] Elis Alves,[1,2] Maria João Alcoforado,[1] and Raquel Machete[1]

[1] *Institute of Geography and Spatial Planning (IGOT-UL), Center of Geographical Studies (Climate Change and Environmental Systems Research Group), University of Lisbon, Av. Prof. Gama Pinto, 1649-003 Lisboa, Portugal*
[2] *São Carlos School of Engineering, University of São Paulo, Brazil*

Correspondence should be addressed to António Lopes; antonio.lopes@campus.ul.pt

Received 26 July 2013; Accepted 2 October 2013

Academic Editor: Marialena Nikolopoulou

Urban growth implies significant modifications in the urban climate. To understand the influence of the city of Lisbon on the urban boundary layer, a mesoscale meteorological network was installed in 2004. The main goals of the present study are to update the results of the research published in 2007 and to bring more precise information about the relationship between the Urban Heat Island (UHI) and the regional and local wind systems. The highest frequencies of the UHI were found in the city centre (Restauradores). In the green park of Monsanto, the highest frequency occurred between −2 and 0°C. During the summer, the effect of the breezes was observed in Belém, lowering the temperature. The "strong" UHI (intensity >4°C) occurred more often during the summer, with median values of 2°C by night and 1.8°C by day. The highest frequencies of UHI occurred for winds between 2 and 6 m/s and were not associated with atmospheric calm, as pointed out in the literature. Winds above 8 m/s inhibit the occurrence of strong UHI in Lisbon. Summer nighttime strong UHI should be further investigated, due to the heat stress consequences on the population and probable increase of energy consumption.

1. Introduction

Urban growth and land use changes imply considerable modifications on the atmospheric dynamics and induce local climatic changes. The consequent changes in aerodynamic roughness also induce alterations in the wind flows, which act as one of the major factors in urban climate and microclimates [1]. The authors of this study [1] found a reduction of about 30% in the mean wind speed in the Lisbon urban boundary layer, due to both topography and built-up areas, when compared with the wind speed simulations where only regional winds and the local topography were taken into account. These values may reach 40%, if the roughness length increases to 1.5 m windward of the city. This will contribute to increase the heat stress and urban atmospheric pollution, with major negative consequences on human health and quality of life for the urban population.

In recent years the problems caused by urban climate modifications led to an increasing number of studies about thermal bioclimates [2–4], also bringing about new ideas and solutions to solve them [5–8].

Amongst the climatic effects of urbanization, the urban heat island (UHI) pattern is the best documented example of involuntary human climatic modification [2, 9–11].

The urban heat island is defined by the difference of temperature between the city centre and the surrounding areas [12]. This clear and simple definition has led to the development of different methodologies to effectively calculate the UHI in different cities (the definition used in this study is presented in Section 2).

Lisbon is located on the western coast of Portugal, at the latitude of 38°43′ N and the longitude of 9°9′ W. The city is located about 30 km to the east of the Atlantic Ocean, on the right bank of the Tagus River (Figure 1). It occupies an area of 84 km^2 and has 547733 inhabitants, while the Metropolitan Area population has more than 2 M people (2011 census). The topography of the city is well differentiated: the maximum altitude is about 226 m (in the Monsanto Park, a small hill in

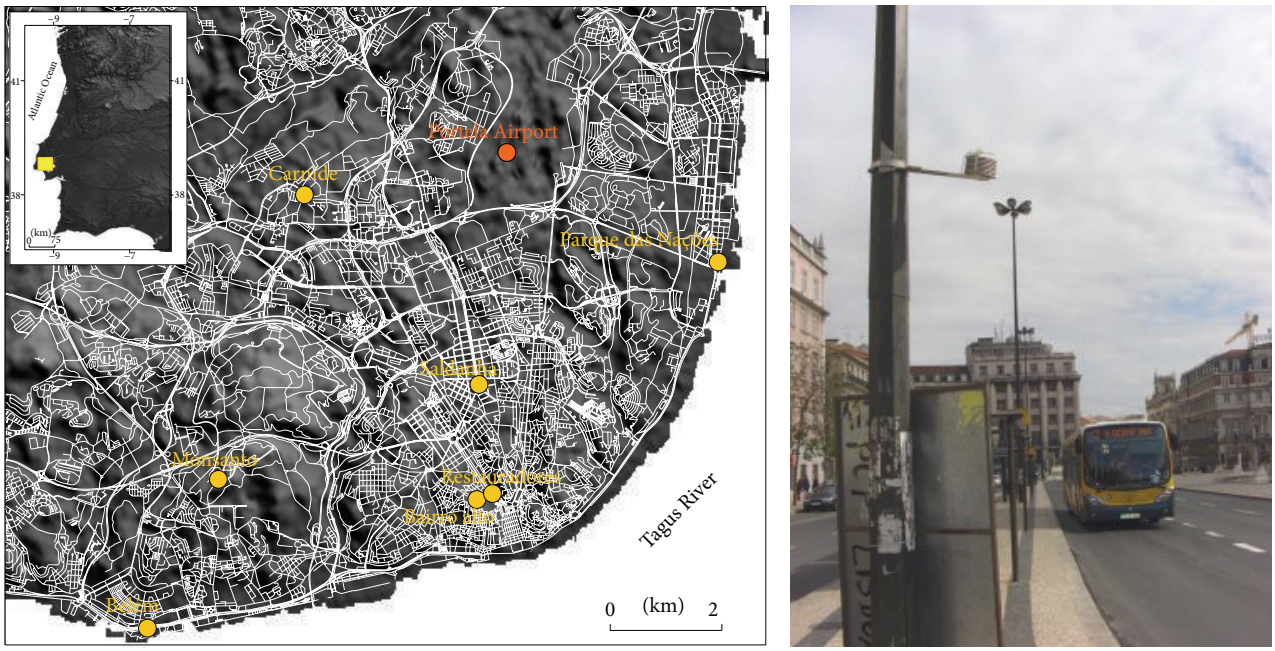

Figure 1: Location of the measurement sites of the Lisbon mesoscale network. On the right, the radiation shield, containing the thermohygrometer, in "Restauradores," is shown.

Table 1: Characterization of the measurement sites of the Lisbon mesoscale network (RES: Restauradores, BAI: Bairro Alto, SAL: Saldanha, CAR: Carnide, MON: Monsanto, BEL: Belém, and PAR: Parque das Nações).

	Measurements sites						
	RES	BAI	SAL	CAR	MON	BEL	PAR
Mean altitude* (m)	32.4	55.8	85.1	106.7	160.8	5.8	4.2
Minimum distance to the Tagus River (m)	1225	1168	3765	7810	2635	181	75
Buildings* (%)	65.7	73.6	70.8	24.7	0.6	19.8	21.6
Mean building height* (m)	11.6	11.4	16.2	15	7.5	9.9	16.5
NDVI (normalized difference vegetation index)	0.1	0.1	−0.1	−0.14	0.12	0	0.29

*Measured within a square of 500 m, centred over the observation site (based on Alves and Biudes [13]).
Source: adapted from Alcoforado et al. [14]

the western part of the city) and 160 m in the urbanized area [5].

According to Andrade [15] the urban heat island effect occurs normally in the south, with undefined boundaries. This thermal pattern is also influenced in Lisbon by a set of nonurban features, such as the relief and the proximity to the Tagus estuary and to the ocean.

In Lisbon, the wind blows predominantly from the north and northwest throughout the year. Western and southwestern as well as eastern and northeastern winds are also frequent in the cold season [16]. However, for 45% of the spring and summer days, a relatively strong north wind (the *Nortada*) dominates [17]. This natural north ventilation is very important because it promotes pollutant dispersion and reduces natural and anthropogenic heat loads. However, in the last 20/30 years Lisbon has been growing towards the north; the buildings create an enormous barrier to the north wind and environmental problems for the south of the city can occur [1].

After numerous studies based on field measurements in the 1980s and 1990s [2], a mesoscale meteorological network was set up in 2004 by the CEG/CliMA (Climate and Environmental Changes research group) of the University of Lisbon (Figure 1), in order to understand the influence of the city of Lisbon on the urban heat island effect. Based on the first temporal data series [2, 14] the researchers concluded that the heat island effect occurs more frequently during the night, especially in situations of weak and moderate wind (5 m/s). This was justified by the urban effect together with shelter from the northern winds, usually cool or cold, in summer and in winter [2, 14]. During winter and summer days, situations of heat island interchange with "cool islands"; these are due to cool air advection from the Tagus estuary, "shadow effect" from the buildings and other modifications of the energy balance (such as heat stored inside the buildings during the day) [18]. The mean intensity of the nocturnal UHI (representing the difference between the average temperature in the city centre and "rural" areas), varies from 0.5°C to 4°C,

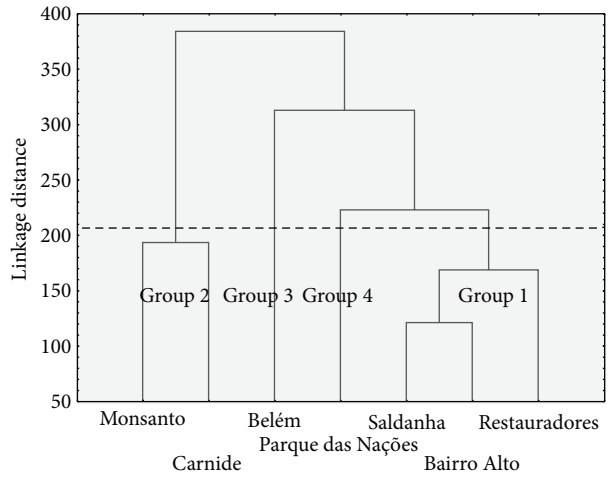

Figure 2: Similarity groups of the thermal deviations of each station of the urban mesoscale network and the Portela Airport. Data: CliMA-CEG and IPMA.

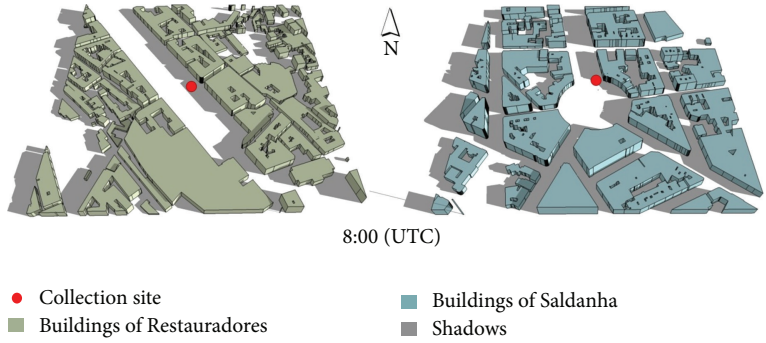

Figure 3: Building's shadow effect during the equinox in Restauradores and Saldanha sites.

as found by Alcoforado and Andrade [2]. In 2007, Alcoforado et al. [14], based on new data collected during a period 678 days from the Lisbon mesometeorological network, concluded that the urban heat island effect had a mean intensity of 3°C.

The main goal of the present study is to update the results with new observational data and to bring new light on the relationships between the UHI patterns and the wind conditions in Lisbon.

2. Material and Methods

The results presented here are based on data measured by a mesoscale network currently consisting of seven thermo-hygrographs. The network was first installed in the early 2000s, as a temporary network, and the first results were divulged in 2003 [15]. From 2004 onwards, a permanent mesoscale network was installed and results were presented in a paper in 2007 [14]. In the present paper 31000 hourly data were analysed, for the period 2004–2012 (with some gaps due to technical problems). The CliMA research group, of the Centre of Geographical Studies of the University of Lisbon, maintains this network. To assess data quality, the thermohygrometers are regularly (every 2 to 3 years) submitted to tests to verify for the need for calibration. No meaningful differences were reported between the devices since the beginning of the observations, and therefore we consider that data quality is insured.

In the present study several temporal scales of analysis were used as follows:

(a) hourly data, frequency of temperature deviations; urban heat island intensity;

(b) Daytime and nighttime, urban heat island intensity (see explanation bellow);

(c) Seasonal, mean hourly temperature deviations; urban heat island intensities; hourly mean wind speed and directions.

The measurement sites are open (SVF ≥ 0.69), so that the microclimatic influence of buildings or nearby trees are banned. Following the advice given by T. R. Oke, a consultant for one of our projects on urban climatology (CLIMLIS) and based on [20], this network aims to study the mesoscale features of the Lisbon thermal fields. The instruments are Gemini data loggers (model TinyTag Plus) and are located on public lighting poles, about 3.5 m above the ground [21], inside a radiation protection shield (Figure 1).

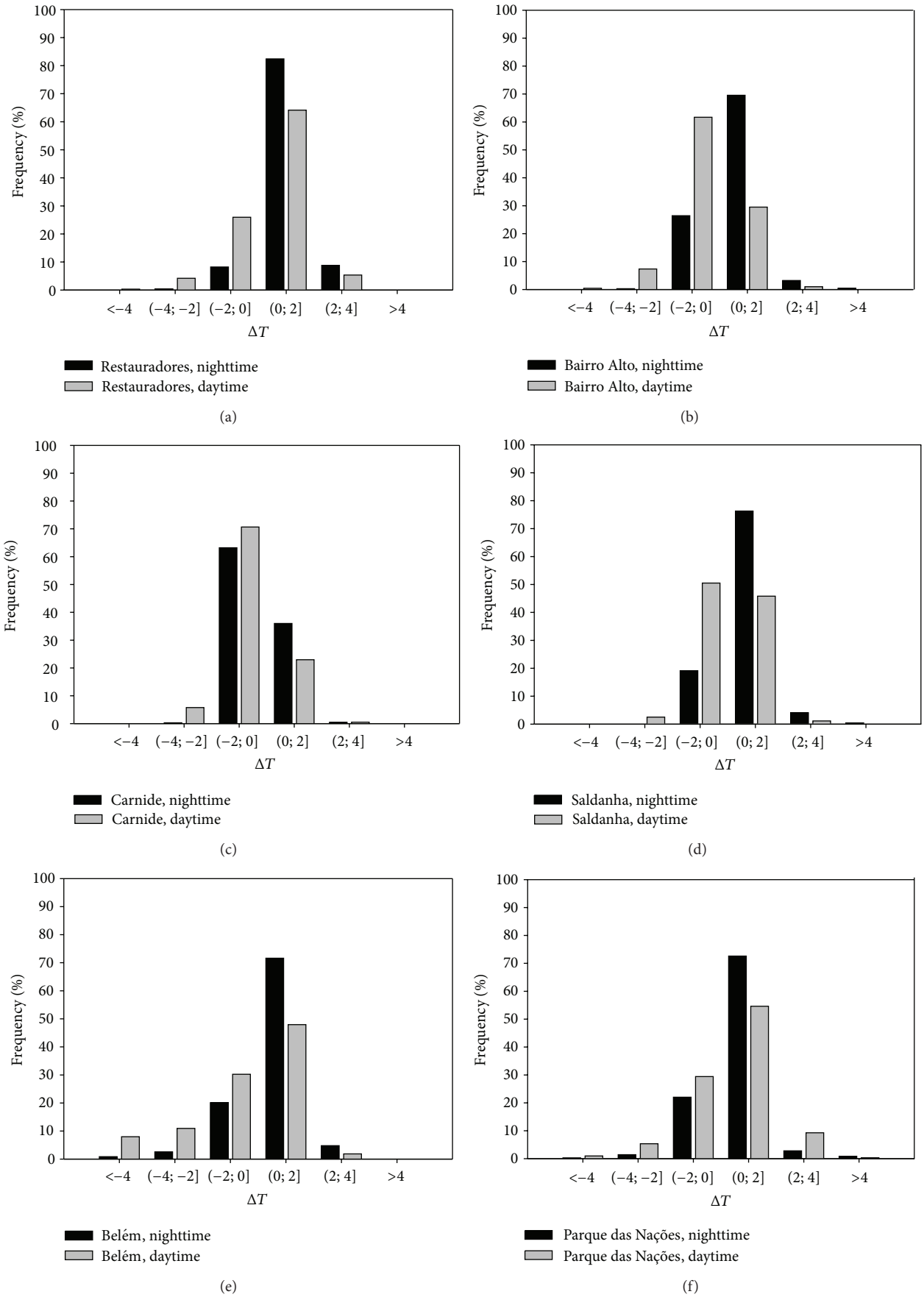

Figure 4: Continued.

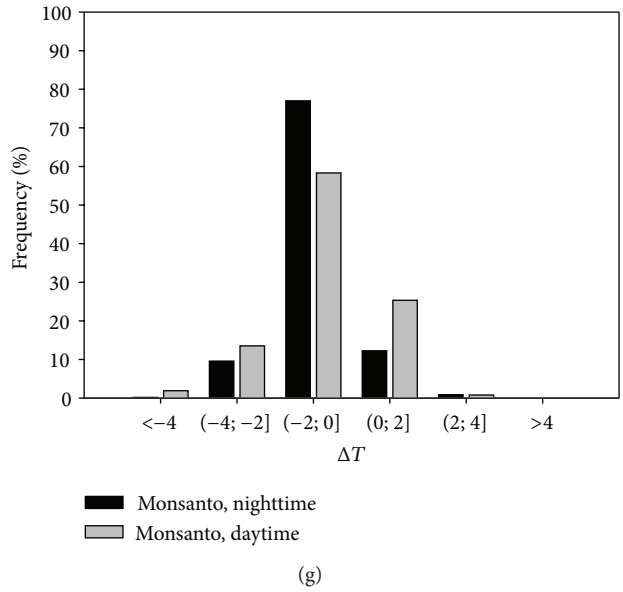

(g)

Figure 4: Frequencies of air temperature deviations between the observation points and the Portela Airport meteorological station. *Low intensity*: urban-rural differences up to 2°C; medium intensity: from 2 to 4°C; *strong intensity*: >4°C (Classification based on García [19]).

The measurements are undertaken every 15 minutes, but the present analysis is based on hourly averages. The location and features of each measurement site are indicated in Figure 1 and Table 1.

The (ΔT) frequencies were obtained from the differences between all measuring sites and the Portela Airport meteorological station. Alcoforado and Andrade [2] (such as other authors, in several different cities [10, 22]), applied this concept in Lisbon, as described in

$$\Delta T = T_U - T_A, \quad (1)$$

where T_U corresponds to the air temperature of each measuring or collecting site in the city and T_A is the air temperature representative of a nonurban area. To follow the same methodology [2], the analysis of the thermal deviations between urban stations and a reference one was carried out. In order to do so, the meteorological data from the Portela Airport was used (orange point in Figure 1) as reference (T_A). In order to assess the thermal similarities between the city measurement sites, a tree clustering analysis with all data was carried out (Figure 2). As a result, the measurement sites were divided into 4 groups. Group 1 comprises the central city sites (Restauradores, Bairro Alto, and Saldanha), group 2 the peripheral sites (Monsanto and Carnide), and 3 and 4 are only represented by the riverside sites—Belém and Parque das Nações, respectively. These sites are representative of the oceanic influence and sea breezes (Belém) and the Tagus estuarine breezes (Parque das Nações).

It is difficult to find an universal criteria to calculate the UHI intensity (UHII) [20]. According to Andrade [15], the UHI in Lisbon was considered to occur each time the temperature in the central sites (group 1) was superior to the temperature registered in the peripheral places (group 2). The intensity of the UHI was calculated as the difference, at a specific moment, between the central and the peripheral sites following

$$\text{UHII} = T_C - T_P, \quad (2)$$

where T_C corresponds to the highest air temperature among the central sites and T_P to the lowest air temperature among the peripheral sites.

The riverside areas (Belém and Parque das Nações) were not considered in this analysis, because their thermal behaviour is specific only to them, due to the frequent Tagus and Ocean breezes [5, 14].

The UHI intensities were classified according to García [19]: *low*: urban-rural differences up to 2°C; *medium* with differences ranging from 2 to 4°C; *strong* from 4 to 6°C; and *very strong* with UHI intensities superior to 6°C.

However, particularly during the day, "negative" UHI or cool islands occur in Lisbon, as referred above.

Due to the large range of daytime UHI intensities in Lisbon [2, 15], for the analysis of the temperature variation (ΔT) and frequency of UHI intensities, the data was divided into nighttime (20:00 to 6:00 h) and daytime observations (10:00 to 18:00 h). By selecting these periods, the radiation conditions that can cause thermal anomalies due to the facets shadowing near sunrise and sunset is partially avoided. In fact, depending on the hour, the day, the season and the position of the buildings, some microclimatic differences may arise, unrelated to the mesoclimatic factors (Figure 3).

3. Results and Discussion

3.1. Temperature Differences (ΔT). The frequencies of the various ΔT classes can be observed in Figure 4. During the daytime, four sites (Carnide, 70.6%; Bairro Alto, 61.6%; Monsanto, 58.3%; and Saldanha, 50.5%) presented the highest

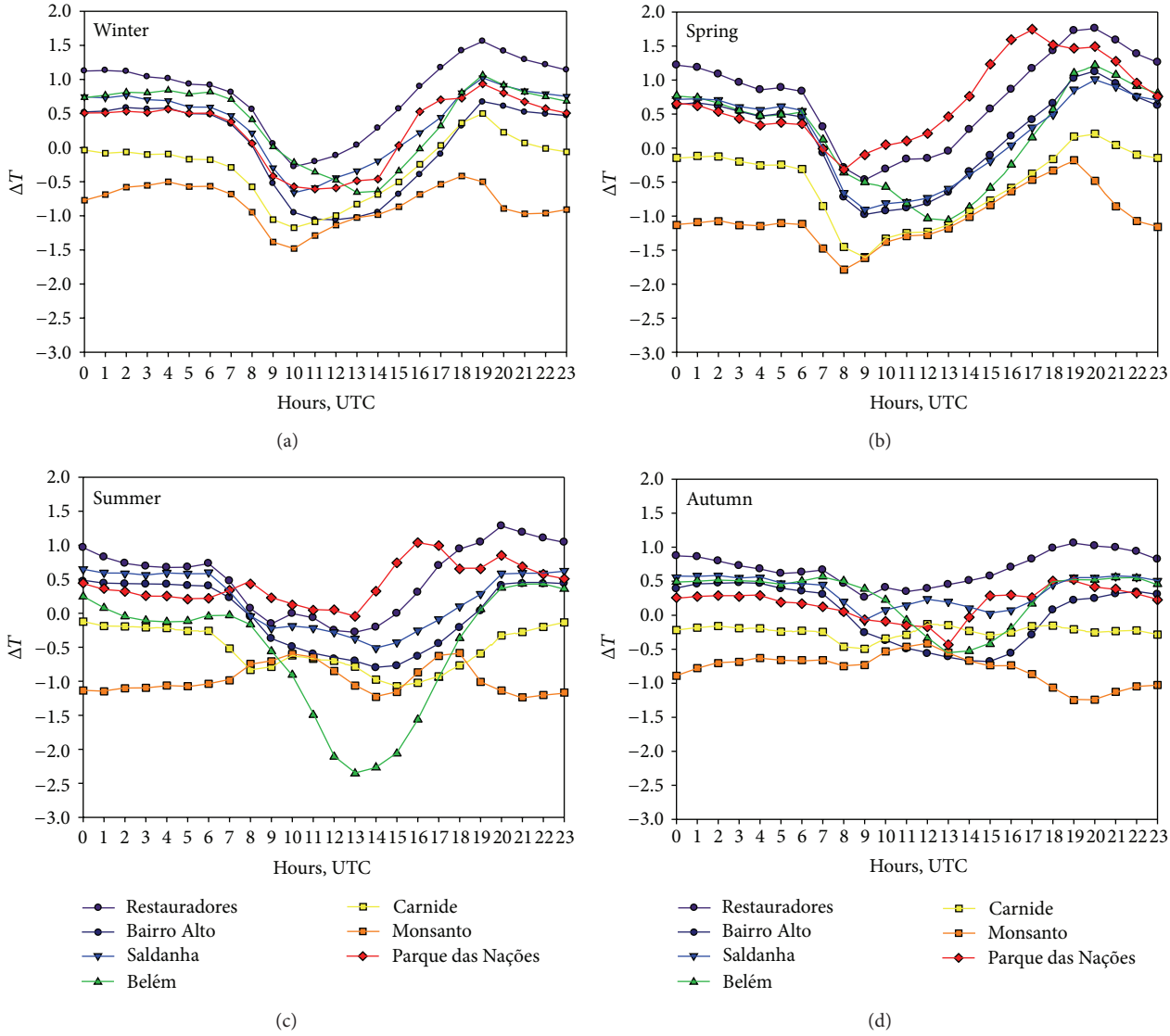

FIGURE 5: Seasonal hourly average deviations between the urban sites of the CEG/CliMA mesoscale network and Lisbon Airport. Winter: DJF; Spring: MAM; Summer: JJA; Autumn SON.

frequency of values between ($-2^{\circ}C < \Delta T < 0^{\circ}C$). During the nighttime and contrasting with the previous values, the class between ($0^{\circ}C < \Delta T < 2^{\circ}C$) is the most frequent in five sites (all, excluding Monsanto and Carnide). A tendency to register values of $\Delta T < 0^{\circ}C$ in Carnide and Monsanto, during day and nighttime, can be clearly observed.

During the daytime, Belém (near the river) and Monsanto (a green park) were the locations where the higher negative intensities ($\Delta T \leq -4^{\circ}C$) were observed (with frequencies of 7.9% and 1.9%, resp.). In the class rage of ($-4^{\circ}C < \Delta T < -2^{\circ}C$) the "air refreshment" effect can also be observed, highlighting the importance of breeze systems and green areas in the improvement of thermal conditions in the city.

Fortunately, the instances when $\Delta T > 4^{\circ}C$ (for which values, serious health problems can occur [14, 23–25], especially during periods of high temperatures) were not frequent.

Figure 5 shows the seasonal mean of ΔT. Monsanto presents a lower ΔT than the other measurement sites, for nearly every season. It is worth mentioning that Monsanto is Lisbon's largest green area having, therefore, the ability to intercept solar radiation, besides cooling the surrounding air by the process of evapotranspiration [26, 27]. In summer, the southwest Tagus breeze reaches Monsanto, which also cools down the atmosphere, although it is stronger and more frequent in Belém. Also during the summer, between 10:00 h and 16:00 h, it was observed that, on average, Belém registered lower temperatures than Monsanto. According to Vasconcelos and Lopes [28] breezes in Lisbon are usually set off during the morning period (10:00 h UTC), when the temperature of the Tagus estuary is cooler than the city. As the continent keeps warming throughout the day, the *Nortada* (north wind) can increase and invalidate the estuarine breeze

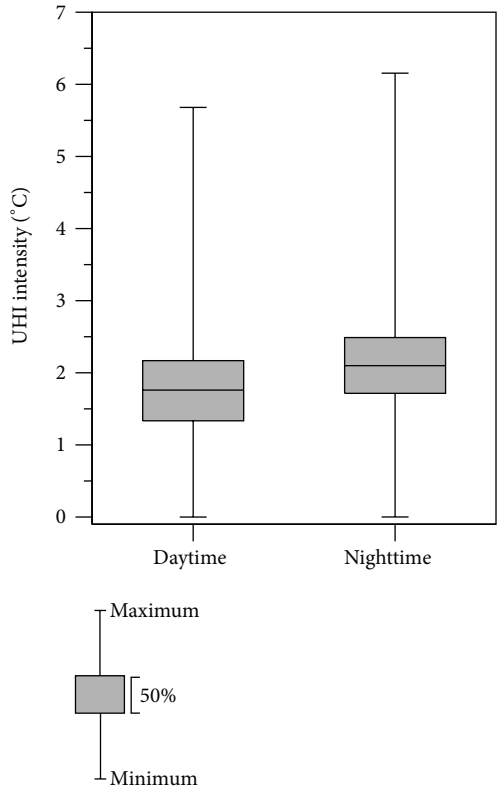

Figure 6: Nighttime and daytime urban heat island intensity (UHII).

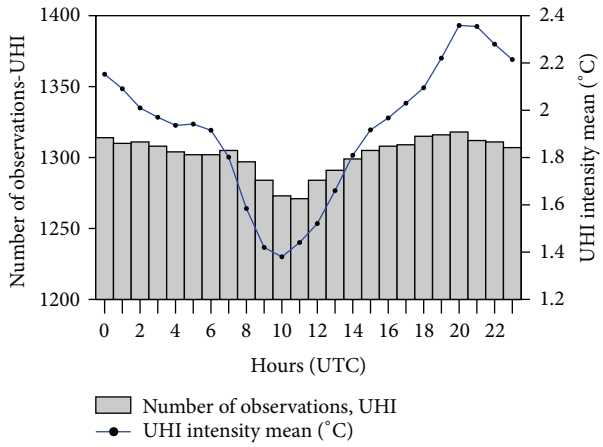

Figure 7: UHII (hourly means) in the period 2004–2012.

[17]. The flow can oppose the Tagus breeze throughout the day. The riverfront may be, on average, 3.5°C cooler than the inner city [28].

In Parque das Nações it was verified that, during the spring and summer, from 9:00 h 17:00 h, ΔT was higher than for the other measurement sites. Despite being a riverbank area that may be affected by the estuarine breezes in the morning, it is not as exposed to the ocean, unlike Belém, which is the first site the cool sea air reaches. Parque das Nações cools down by regional wind flows from northeast or when eastern and south-eastern breezes occur [17, 28].

Restauradores mostly displayed the highest values of ΔT in the mesoscale network, a fact previously observed by Alcoforado et al. [14]. Bairro Alto, and Saldanha alternate as the 2nd and 3rd sites registering highest ΔT. Carnide (urban periphery) was the second site with the lowest ΔT.

3.2. Urban Heat Island Intensity (UHII). According to the above-stated results, the presence of a heat island in Lisbon has been observed and the recent data confirmed the tendencies found in previous research [2, 14, 15] where the temperatures registered in central areas (Saldanha, Restauradores,

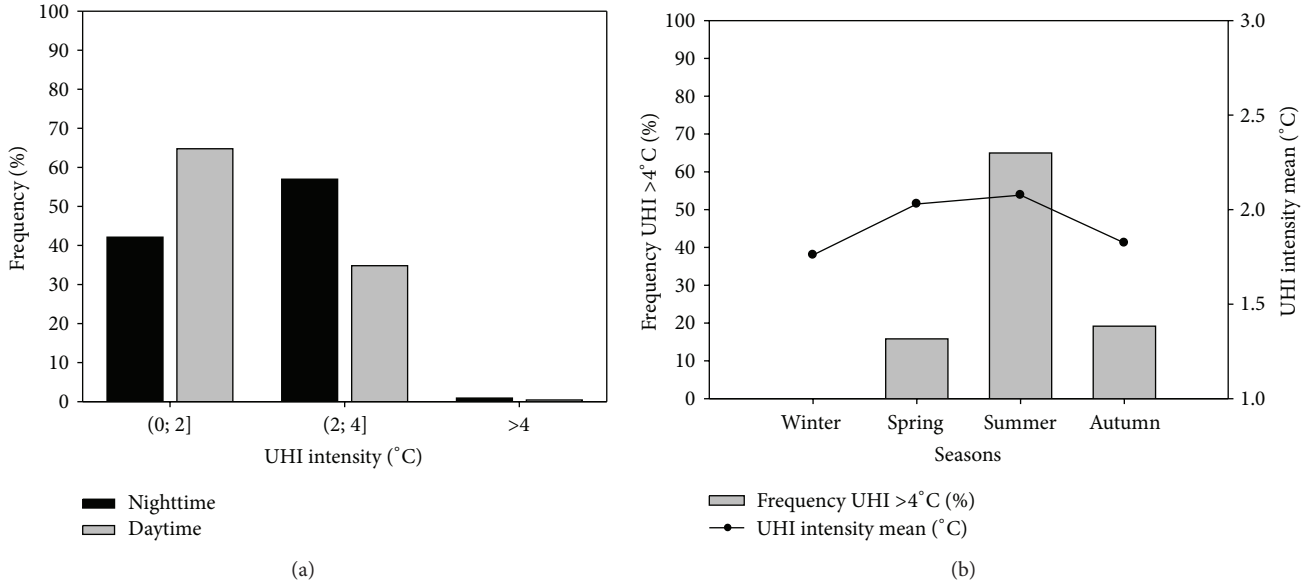

Figure 8: Frequency of the UHII during night- and daytime periods (a) and seasons (b). Winter: DJF; Spring: MAM; Summer: JJA; Autumn SON.

and Bairro Alto) were higher than the temperatures observed in the surrounding sites (Monsanto and Carnide). However, new highlights are now much clearer: Figure 6 shows that during the night 50% of the UHI varies from 1.7 to 2.4°C, whereas during the day it is between 1.3 and 2.2°C. The mean and the median of the nocturnal urban heat island are 2°C, while the diurnal only reaches 1.8°C. The maximum UHII observed was 6.1°C, during the night and 5.7°C during the day (114 cases with UHI > to 4°C were observed). We should note that these values are rare and must be better investigated in future research.

Taking into account all the observations (Figure 7), the rhythm of the average Lisbon UHI becomes clear: more intense at 20:00 h and 21:00 h (2.3°C) and less at 10:00 h (1.4°C).

Figure 8(a) shows that, during the day, the highest frequency of UHII (64.7%), occurred in the *low intensity* class (up to 2°C). During the night, the *medium intensity* class (2 to 4°C) reached the highest frequency (57%), results that confirm the eminently nighttime characteristics of the UHI in Lisbon. This had already been mentioned by [2, 14, 15]. As for the seasonality, UHI occurs in every season. However, the strong UHII > 4°C (Figure 8(b)) was observed more often during the summer (65%, mean is 2.1°C), with only 19.2% in autumn and 15.8% in spring and was never observed in winter (the lowest UHII mean temperature: 1.7°C).

3.3. Lisbon Wind Regimes. Figure 9 displays the seasonal wind regimes from 2004 to 2010. As was mentioned before, the northwestern and northeastern winds prevail in autumn and winter. In spring and summer northwestern winds predominate: the *nortada*, which is characterized by wind speeds above 5 m/s [1, 2, 17], occurs in 45% of the days. Its origin is associated with the strong atmospheric pressure gradient between the thermal low over the Iberian Peninsula and the Atlantic anticyclones [2, 5].

When the *nortada* slows down or ceases, a second (local) ventilation pattern develops in Lisbon; in 30% of summer days estuarine or ocean breezes occur [2, 5, 15, 17].

3.4. The Relationship between Urban Heat Island (UHI) Patterns and Wind. UHI is related to the wind speed, wind direction, and time (hours) [12, 29–31]. Figures 10(a), 10(b), and 10(c) illustrate these relationships. As the wind speed increases, the UHII presents a tendency to decrease (Figure 10(a)). However, unlike other cities, higher frequencies of UHII in Lisbon do not occur during situations of atmospheric calm (as noted by Alcoforado et al. [14]). In fact, the highest frequencies of UHII occur with winds of 2 to 4 m/s (32.6%) and 4 to 6 m/s (29.4%). The strong UHII (>4°C) occurs, more frequently, with winds between 2 to 4 m/s (45%) and 4 to 6 m/s (25%).

However, very strong winds prevent the development of the UHII [31]. Winds of about 6 and 7 m/s are critical values for the existence of the maximum UHII in Seoul (South Korea) and Salamanca (Spain) [32, 33]. In Lisbon, it was observed that from 8 m/s on, strong intensity urban heath islands do not occur (Figure 10(a)). Figure 10(b) demonstrates that UHI occurred with winds in every direction. However, strong UHII occurs more frequently with north and northwestern winds, followed by southwestern and western winds. The considerable number of observations of strong UHII occurred between 21:00 h and 00:00 h (Figure 10(c)).

4. Conclusions

The analysis of the Lisbon mesoscale network data, for the time series between 2004 and 2012, showed a high variability in the urban thermal field. The highest frequencies of $\Delta T >$ 0°C were found in Restauradores, both during the day and at night, especially in the class between 0 and 2°C. In Monsanto, the highest frequency was found in the class

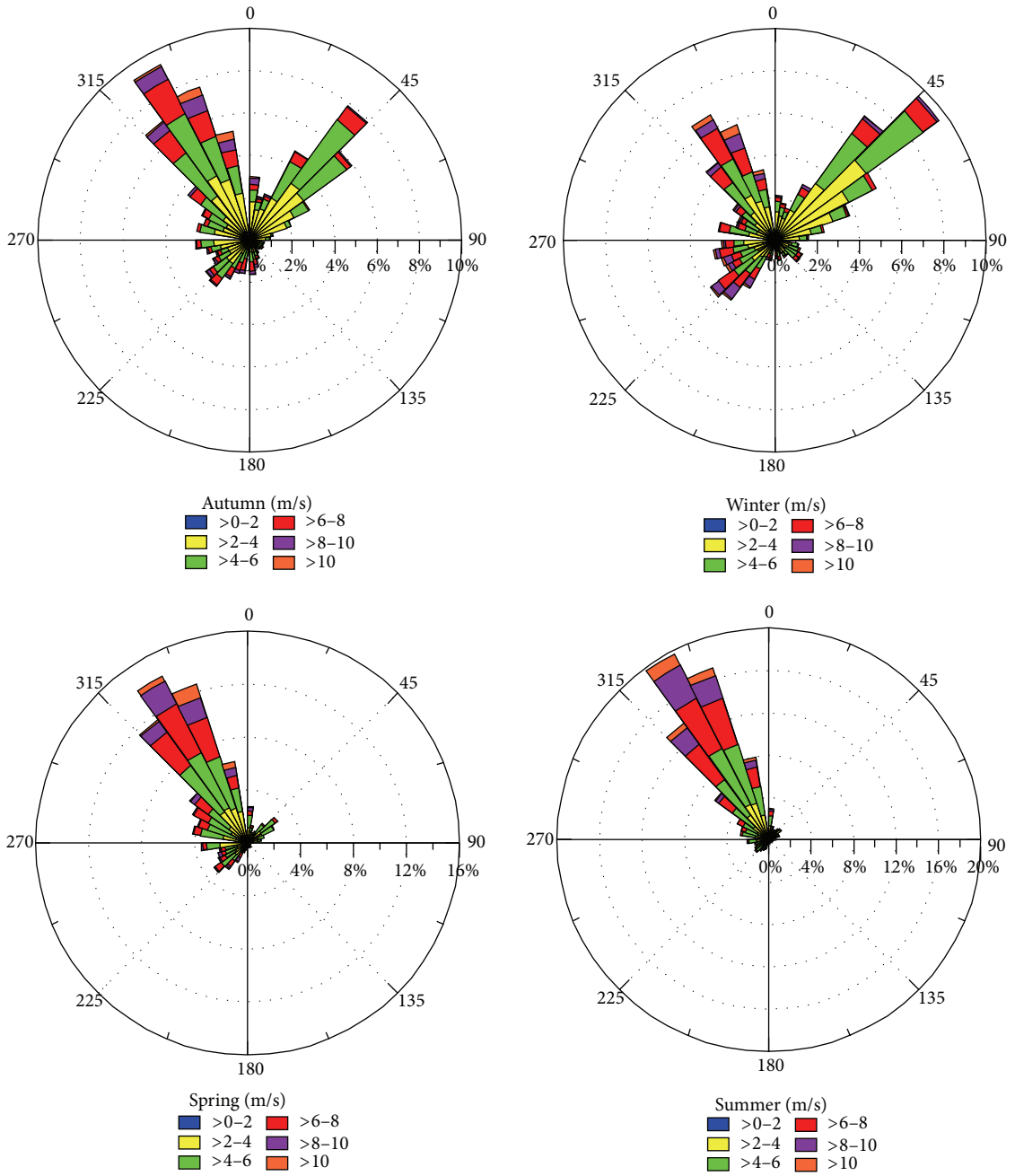

Figure 9: Seasonal regimes of wind speed and direction. Autumn: SON; Winter: DJF; Spring: MAM; Summer: JJA. Data: IPMA.

between −2 and 0°C. In Belém, during the summer, the effect of the breezes was observed, attenuating the air temperature and, consecutively, presenting prevalence of $\Delta T < 0$°C, as observed in the study of Vasconcelos and Lopes [28].

Urban heat islands were observed throughout the year; however, strong UHI (UHII >4°C) occurred more often during the summer, where the highest seasonal difference mean (2.1°C) was also recorded, whereas, in the winter, the lower UHI mean was verified (1.7°C).

The median value of the UHI intensity during the night and day periods were, respectively, 2°C and 1.8°C (this last value is slightly different from the one verified by Alcoforado et al. [14] during the day, 1.6°C). Although the number of extreme positive differences during the night are rare (only 114 cases with temperature > than 4°C), these cases must be investigated in future research because they probably correspond to situations of extreme heat stress, which endanger human health in the city and lead to more energy consumption (the maximum UHII observed was 6.1°C).

In Lisbon, the highest frequencies of UHII took place with winds of 2 to 4 m/s and 4 to 6 m/s, which differs from the atmospheric calm pattern defined by Oke [12], due to the importance of the shelter effect from Northern cold or cool winds. The strong UHI intensity occurred, mainly, with

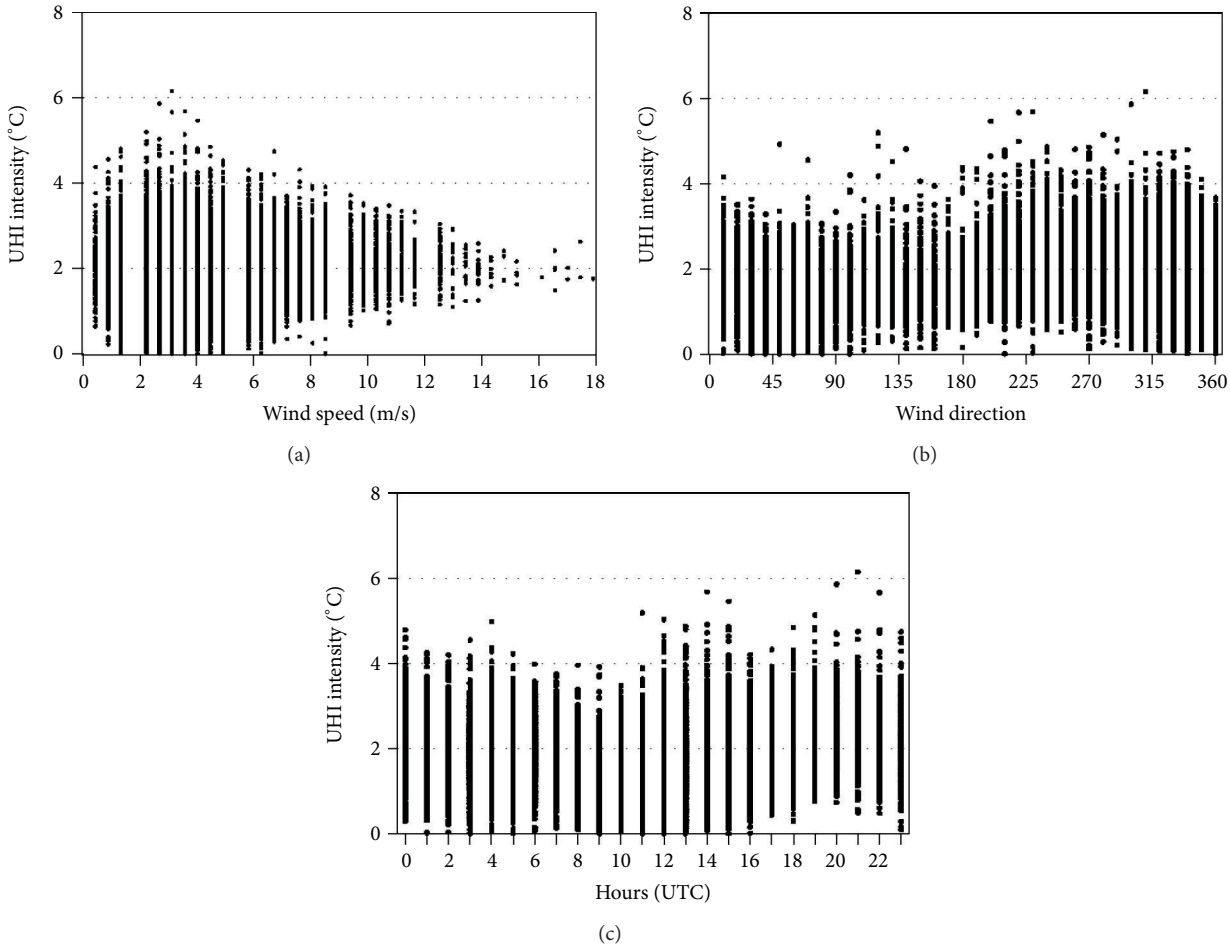

Figure 10: UHII versus wind speed (a), wind direction (b), and time (hours) (c).

north, northwestern, and southwestern winds. Finally, winds blowing above 8 m/s in the Airport area, seem to inhibit the occurrence of strong UHI inside the city.

Conflict of Interests

The authors declare that there is no conflict of interests regarding the publication of this paper.

Acknowledgments

This research was elaborated in memory of the authors' colleague and friend Professor Henrique Andrade (1961–2013), who was the first to implement a temporary meteorological network that would precede the current measurement network. Thanks are due to the colleagues that have worked so hard to keep and improve the mesoscale network, namely, the Ph.D. student Paulo Canário. The network has been financed by the CliMA research group. The authors also thank the São Paulo Research Foundation (FAPESP) for granting the scholarship (grant 12/20598-5) of Elis Dener Lima Alves. The authors are grateful to the anonymous reviewers for providing valuable comments that helped improve the paper.

References

[1] A. Lopes, J. Saraiva, and M. J. Alcoforado, "Urban boundary layer wind speed reduction in summer due to urban growth and environmental consequences in Lisbon," *Environmental Modelling and Software*, vol. 26, no. 2, pp. 241–243, 2011.

[2] M.-J. Alcoforado and H. Andrade, "Nocturnal urban heat island in Lisbon (Portugal): main features and modelling attempts," *Theoretical and Applied Climatology*, vol. 84, no. 1–3, pp. 151–159, 2006.

[3] M. Kolokotroni, Y. Zhang, and R. Watkins, "The London heat island and building cooling design," *Solar Energy*, vol. 81, no. 1, pp. 102–110, 2007.

[4] I. Zoulia, M. Santamouris, and A. Dimoudi, "Monitoring the effect of urban green areas on the heat island in Athens," *Environmental Monitoring and Assessment*, vol. 156, no. 1 4, pp. 275–292, 2009.

[5] M.-J. Alcoforado, H. Andrade, A. Lopes, and J. Vasconcelos, "Application of climatic guidelines to urban planning. the example of Lisbon (Portugal)," *Landscape and Urban Planning*, vol. 90, no. 1-2, pp. 56–65, 2009.

[6] I. Eliasson, "Urban nocturnal temperatures, street geometry and land use," *Atmospheric Environment*, vol. 30, no. 3, pp. 379–392, 1996.

[7] E. Ng, "Policies and technical guidelines for urban planning of high-density cities—air ventilation assessment (AVA) of Hong Kong," *Building and Environment*, vol. 44, no. 7, pp. 1478–1488, 2009.

[8] C. Ren, E. Y. Y. Ng, and L. Katzschner, "Urban climatic map studies: a review," *International Journal of Climatology*, vol. 31, no. 15, pp. 2213–2233, 2011.

[9] H. E. Landsberg, *The Urban Climate*, Elsevier Science, Amsterdam, The Netherlands, 1981.

[10] P. I. Figuerola and N. A. Mazzeo, "Urban-rural temperature differences in Buenos Aires," *International Journal of Climatology*, vol. 18, no. 15, pp. 1709–1723, 1998.

[11] J. P. Montávez, A. Rodríguez, and J. I. Jiménez, "A study of the urban heat island of Granada," *International Journal of Climatology*, vol. 20, no. 8, pp. 899–911, 2000.

[12] T. R. Oke, *Boundary Layer Climates*, Routledge, London, UK, 2nd edition, 1987.

[13] E. D. L. Alves and M. S. Biudes, "Method for determining the footprint area of air temperature and relative humidity," *Acta Scientiarum. Technology*, vol. 35, no. 2, pp. 187–194, 2013.

[14] M. -J. Alcoforado, H. Andrade, A. Lopes, and S. Oliveira, "A ilha de calor em Lisboa. aquisição de dados e primeiros resultados estatísticos para aplicação ao ordenamento urbano," *in Geophilia—O Sentir e Os sentidos da Geografia Homenagem a Jorge Gaspar*, pp. 593–612, 2007.

[15] H. Andrade, *Bioclima humano e temperatura do ar em Lisboa [Ph.D. thesis]*, University of Lisbon, Lisbon, Portugal, 2003.

[16] M. -J. Alcoforado, H. Andrade, A. Lopes, J. Vasconcelos, and R. Vieira, "Observational studies on summer winds in Lisbon (Portugal) and their influence on daytime regional and urban thermal patterns," *Merhavim*, vol. 6, pp. 90–112, 2006.

[17] M. -J. Alcoforado, "Brisas estivais do Tejo e do oceano na região de Lisboa," *Finisterra*, vol. 22, no. 43, pp. 71–112, 1987.

[18] M.-J. Alcoforado, A. Lopes, H. Andrade, and J. Vasconcelos, *Orientações Climáticas Para O Ordenamento Em Lisboa*, Relatório, Centro de Estudos Geográficos, Lisbon, Portugal, 2005.

[19] F. F. García, *Manual de Climatología Aplicada: Clima, Medio Ambiente Y Planificación*, Síntesis Editorial, Madrid, Spain, 1996.

[20] T. R. Oke, "Initial guidance to obtain representative meteorological observations at urban sites," IOM Report 81, WMO/TD. No. 1250, World Meteorological Organization, Geneva, Switzerland, 2006.

[21] H. Andrade, M. J. Alcoforado, and P. Canário, "Estimação da influência antrópica no campo térmico de Lisboa; uma tentativa de modelação estatística," in *Proceedings of the 2nd Workshop Internacional Sobre Clima e Recursos Naturais nos Países de Língua Portuguesa*, pp. 207–214, Bragança, Portugal, 2010.

[22] K. Klysik and K. Fortuniak, "Temporal and spatial characteristics of the urban heat island of Lodz, Poland," *Atmospheric Environment*, vol. 33, no. 24-25, pp. 3885–3895, 1999.

[23] J. Tan, Y. Zheng, X. Tang et al., "The urban heat island and its impact on heat waves and human health in Shanghai," *International Journal of Biometeorology*, vol. 54, no. 1, pp. 75–84, 2010.

[24] K. M. A. Gabriel and W. R. Endlicher, "Urban and rural mortality rates during heat waves in Berlin and Brandenburg, Germany," *Environmental Pollution*, vol. 159, no. 8-9, pp. 2044–2050, 2011.

[25] P. Shahmohamadi, A. I. Che-Ani, I. Etessam, K. N. A. Maulud, and N. M. Tawil, "Healthy environment: the need to mitigate urban heat island effects on human health," in *Proceedings of the 2nd International Building Control Conference (IBCC '11)*, pp. 61–70, Penang, Malaysia, July 2011.

[26] S. Streiling and A. Matzarakis, "Influence of single and small clusters of trees on the bioclimate of a city: a case study," *Journal of Arboriculture*, vol. 29, no. 6, pp. 309–316, 2003.

[27] L. Shashua-Bar, O. Potchter, A. Bitan, D. Boltansky, and Y. Yaakov, "Microclimate modelling of street tree species effects within the varied urban morphology in the Mediterranean city of Tel Aviv, Israel," *International Journal of Climatology*, vol. 30, no. 1, pp. 44–57, 2010.

[28] J. Vasconcelos and A. Lopes, "Recent urban development trends and its implication on the estuarine breezes," in *Proceedings of the 6th International Conference on Urban Climate*, pp. 466–469, Lisbon, Portugal, 2006.

[29] T. R. Oke, "City size and the urban heat island," *Atmospheric Environment*, vol. 7, no. 8, pp. 769–779, 1973.

[30] J. Unger, "Heat island intensity with different meteorological conditions in a medium-sized town: Szeged, Hungary," *Theoretical and Applied Climatology*, vol. 54, no. 3-4, pp. 147–151, 1996.

[31] I. Camilloni and M. Barrucand, "Temporal variability of the Buenos Aires, Argentina, urban heat island," *Theoretical and Applied Climatology*, vol. 107, no. 1-2, pp. 47–58, 2012.

[32] Y. H. Kim and J. J. Baik, "Maximum urban heat island intensity in Seoul," *Journal of Applied Meteorology*, vol. 41, no. 6, pp. 651–659, 2002.

[33] M. S. Alonso, M. R. Fidalgo, and J. L. Labajo, "The urban heat island in Salamanca (Spain) and its relationship to meteorological parameters," *Climate Research*, vol. 34, no. 1, pp. 39–46, 2007.

Hindawi Publishing Corporation
Advances in Meteorology
Volume 2013, Article ID 749270, 10 pages
http://dx.doi.org/10.1155/2013/749270

Research Article

Human-Biometeorological Assessment of Urban Structures in Extreme Climate Conditions: The Example of Birobidzhan, Russian Far East

Jan Paul Bauche,[1] Elena A. Grigorieva,[2] and Andreas Matzarakis[1]

[1] *Chair of Meteorology and Climatology, Albert Ludwigs University Freiburg, Werthmannstraße 10, 79085 Freiburg, Germany*
[2] *Institute for Complex Analysis of Regional Problems, Far Eastern Branch, Russian Academy of Sciences, Birobidzhan 679016, Russia*

Correspondence should be addressed to Jan Paul Bauche; paul@mbauche.de

Received 4 June 2013; Revised 27 August 2013; Accepted 23 September 2013

Academic Editor: Marialena Nikolopoulou

The study shows the effect of urban structures on human thermal comfort indices in the extreme climate region of the Russian Far East, with an annual temperature range of 75°C. The study examines different urban zones in Birobidzhan, the capital city of the Jewish Autonomous Region (JAR). The climate of this region can be characterized as continental monsoon climate. The difference of thermal values for three zones with different vegetation and build-up density shows the influence of urban planning on the local microclimate. The moderating effect of dense build-up and inner city vegetation on extreme thermal conditions becomes clear when comparing all zones. Through the analysis of daily and monthly timelines it was possible to determine preferable times of the day for inner city outdoor activities. From the results derived from PET with a total of 170 days per year with PET values below 0°C Birobidzhan can be considered a region of extreme cold stress. This means that an adaptation based solely on behaviour and clothing is not sufficient, but an adaptation of the urban surroundings and therefore the identification and choice of preferable urban structures is necessary.

1. Introduction

Since the last decades of the 20th century and due to the challenges of climate change, climatological and meteorological parameters have been in the focus of urban planning. Most of those studies assess the standard meteorological parameters associated with human thermal comfort such as air temperature, global radiation, wind velocity, relative humidity, or precipitation. However, if they are assessed just by themselves, the results are taken out of the human context and lose their original purpose. To put them into context, the application of complex and differentiated human bioclimate indices is needed. For the purpose of this study two of these indices haven been applied to the meteorological conditions and the urban structures of Birobidzhan, the capital city of the Jewish Autonomous Region (JAR), at the Russian Far East. In the course of a year this region experiences all facets of extreme meteorological conditions from arid cold to humid warm (Figure 1). This makes the region of the JAR extremely suitable for the purpose of analysing the impact of urban structures on the human thermal comfort assuming an intensification of extreme meteorological conditions in presently moderate climate areas, due to the global climate change. During the last 20 years the interest in the human thermal bioclimate has been rising due to great awareness of the influence of climate on our lives which is strongly connected to the public debate about climate change and its influence on everyday life. As a result of this development regions that are already under the influence of harsh climates are very interesting for analysis of climate change results.

The indices used for this study are the physiologically equivalent temperature (PET) based on the Munich Energy-balance Model for Individuals (MEMI) [1–3], displayed in degrees Celsius (°C) which makes it easy to comprehend and easy to be compared to other indices or measurement, and the universal thermal climate index (UTCI), also displayed in °C, which is based on a multinode human energy balance model for a more adaptive approach to extreme climate conditions

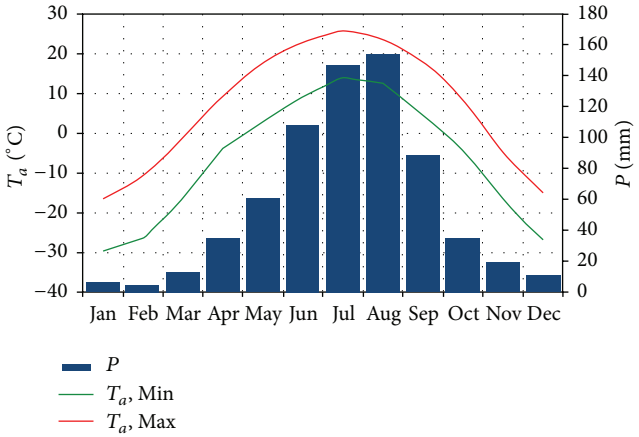

Figure 1: Climate diagram for the Birobidzhan area (data source: http://worldweather.wmo.int/).

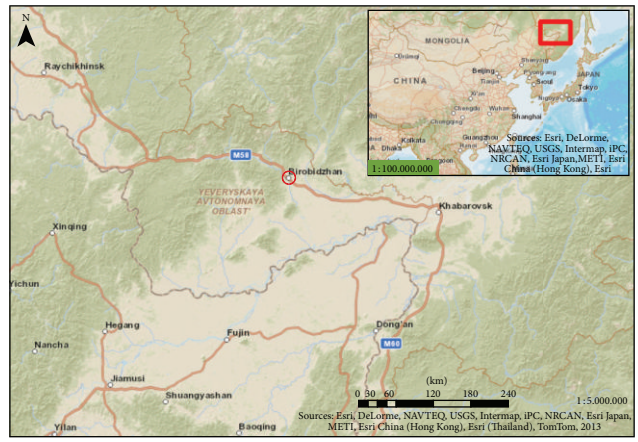

Figure 2: Regional and local position of Birobidzhan.

[4, 5]. A selection of studies conducted in the JAR, and such concerning the topic of the human biometeorology, is displayed to show what has been done so far. Studies on this topic have been published since the late eighties [1, 6]. They show the development and application of PET based on the human energy balance model MEMI [1–3, 7, 8] and the RayMan model [9, 10] and the effect of shading on outdoor comfort [11, 12] as well as the development of UTCI [5, 13, 14] and the underlying multinode model [4, 15–17]. In the following years, papers concerning the bioclimate of the JAR, focusing on the efficiency of agricultural crop growing and outdoor recreation and tourism, were published [18–22]. These works are designed to find preferable outdoor activities or to quantify the influence of the regional climate on crop seasons and are usually based on daily and monthly climate data. This study aims to give an actual and accurate assessment of the human thermal bioclimate and to find preferable city structures or at least preferable inner city locations at any given time of day in the city of Birobidzhan using a high temporal resolution of meteorological data.

2. Area of Investigation

Birobidzhan is located close to the Chinese northern border at 48°N and 132°E (Figure 2) with a mean altitude of 76 m a.sl. and is inhabited about 75,000 people on an area of 169 km^2. Even though the latitude coincides with a moderate climate by the climate in the Jewish Autonomous Region (JAR), of which Birobidzhan is the capital, is far from moderate. Its continental exposition leads to cold winters and warm summers. This effect is intensified by the influence of the summer monsoon and its close proximity to the Siberian high pressure field resulting in an annual variation in air temperature of up to 75°C in the course of six months in extreme cases. Due to this variation the annual course of the meteorological factors in this region shows great variability. From a mean maximum air temperature of about 26°C in July to −29°C in January and a monthly precipitation of 154 mm in August to 5 mm in February all facets of an extreme climate can be experienced.

Table 1: Selected locations (zones) and their respective properties.

Zone	Type	Build-up	Vegetation
1	Residential	Dense	High
2	Street	Medium	Light
3	Square	Light	None

3. Methods

For the assessment of the human thermal bioclimate several indices have been developed over the last 50 years. Two thermal indices were used for this study, namely, the physiologically equivalent temperature (PET) and the universal thermal climate index (UTCI) [4, 15–17], both of which use the unit degrees Celsius and are based on models of human thermal balance. The meteorological data from the Birobidzhan WMO station (WMO index 31713) has been used as input for the calculation of the thermal indices, specifically the data for air temperature, wind velocity, wind direction, relative humidity, and cloud cover as a proxy value for the global radiation. These parameters have been recorded at the climate station in a three-hour interval, resulting in eight measuring points per day, for the 11-year period from 2000 to 2010.

Using this data and the RayMan model the thermal indices can be calculated [9, 10]. Additionally the obstacle parameters at three different locations within the city were put into the model to determine their influence on the human thermal bioclimate. All three locations are highly frequented by the local population, but they are very different in terms of their structural specifications. Information for all three locations is summarised in Table 1. The terms used to describe "Build-up" and "Vegetation" are relative terms meant to compare the zones with each other. Pictures of the selected areas as well as fisheye pictures can be found in the appendix.

The meteorological data were made freely available via http://www.ogimet.com/ and were downloaded for the period from 2000 to 2010 in 3-hour intervals (01:00, 04:00, 07:00, 10:00, 13:00, 16:00, 19:00, and 22:00 local time). The availability of these meteorological measurements at eight points of time per day ensures a good temporal resolution of

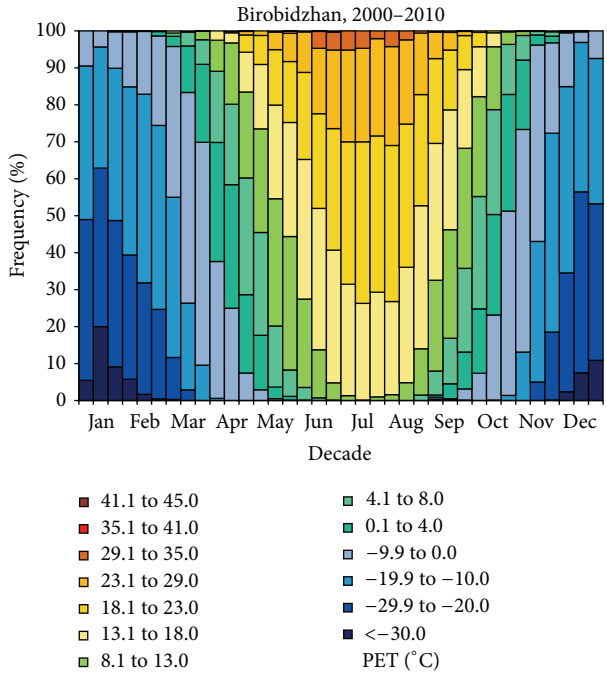

Figure 3: Mean frequency distribution of PET values in Birobidzhan, zone 1, during the year divided into 10-day intervals (decades) for the period 2000–2010.

the data. The data were initially available in SYNOP and had to be decoded to standard meteorological units. This was done using Microsoft Excel. All of the calculations and simulations in this study are based on the meteorological data obtained from this synoptic station and were modified only by the surrounding structures via obstacle files in RayMan which were based on maps of the city and local observation of the buildings. The general assumption for the transfer of the data is that air temperature and air humidity remain the same for the city and the rural station, and only wind speed, which is changed according to roughness, and radiation fluxes, which can be adjusted with the RayMan model, modify the indices.

4. Results

4.1. Physiologically Equivalent Temperature. The following section provides the results of PET in the context of the different building situations. It also includes its daily course for selected months in summer and winter. The overall results showed a great range of PET values being being between summer and winter seasons as well as between the different zones. The general effect of the building situation on PET is visualized in Table 2. The specific dynamics for each zone are discussed in Section 5 of this paper.

Figure 3 shows the mean decadal distribution of PET values in Zone 1 during the year. The lowest values can be found in the time from the end of November to the beginning of March. The highest frequency of extremely low values (PET < −30.0°C) is in the second decade of January with an occurrence frequency of 27.7%. From the end of November until the midst of February PET values were not above 0.0°C as it is a period of constant frost. The highest PET values occur from the midst of June to the end of August. Values between 29.1°C and 41.0°C can be considered a fairly common phenomenon (about 14%). With occurrence frequencies of about 1% values between 41.1°C and 45.0°C occur rather rarely. With about 30.9% the first decade of August shows the highest occurrence frequency of comfortable PET values between 18.1°C and 23.0°C. Spring and autumn generally consist of PET values in the range of slight heat stress to extreme cold stress and require the most flexibility in terms of thermal adaption. In the summer months of July, June, and August PET does not drop to values below 0.0°C.

Figure 4 shows the 2-dimensional daily and monthly courses of PET values in January and July, as an example for winter and summer, respectively. The y-axis shows the days of July and the x-axis shows the time steps according to the legend. The highest PET values can be expected towards the end of July around the 26th day and in general in the time between 13:00 and 16:00. During this time PET reaches values up to the range of 35.0°C to 41.0°C. The coolest times of the day are the ones in the early morning between 4:00 and 7:00. Here PET values range between 13.0°C and 18.0°C. In winter (January) PET drops to values below −30.0°C and in extreme cases even below −40.0°C creating extreme cold stress in terms of the human bioclimate. These extremely low values can be expected in the midst of January (exemplary for winter) in the early morning hours between 4:00 and 7:00. In general the highest PET values in winter do not reach the 0.0°C mark but rather stay considerably lower. They can be expected in the time between 13:00 and 16:00. From 16:00 on, PET drops until it reaches its lowest value in the time around 7:00. During January PET does not vary much, but there is an accumulation of very low values in the time from the 10th to the 17th of January.

Zone 2 is less sheltered from solar radiation than zone 1 and therefore shows a tendency to have more extreme PET values. Since the climate data has been recorded at the same station the yearly change is the same as in zone 1, but its amplitude is different. With 29.4% the frequency of PET values below −30.0°C is about 2% higher than that in zone 1 (Figure 5). Still the winter months from the end of November until the end of February are consistenty below 0.0°C, but the PET values are less extreme. In the summer months the occurrence frequency of comfortable PET values between 18.1°C and 23.0°C drops to 29.8%, that is, 1% lower in comparison to zone 1. The extremely high values that result in moderate to extreme heat stress increase in comparison. The frequency of values above 35.1°C does not increase much in a single-decade but rather occurs in more decades than it does in zone 1. In the summer season zone 2 displayed the same dynamics as zone 1, but there are more days with extreme PET values. Still the range leads up to about 41.0°C in the time between 13:00 and 16:00, but now these values can be found throughout the months. The coldest time of the day during July, used as an example, for summer is 4:00 with PET dropping to values around 10.0°C. The daily course follows the classic pattern with the highest PET values occurring shortly after the sun reaches its zenith. The monthly course

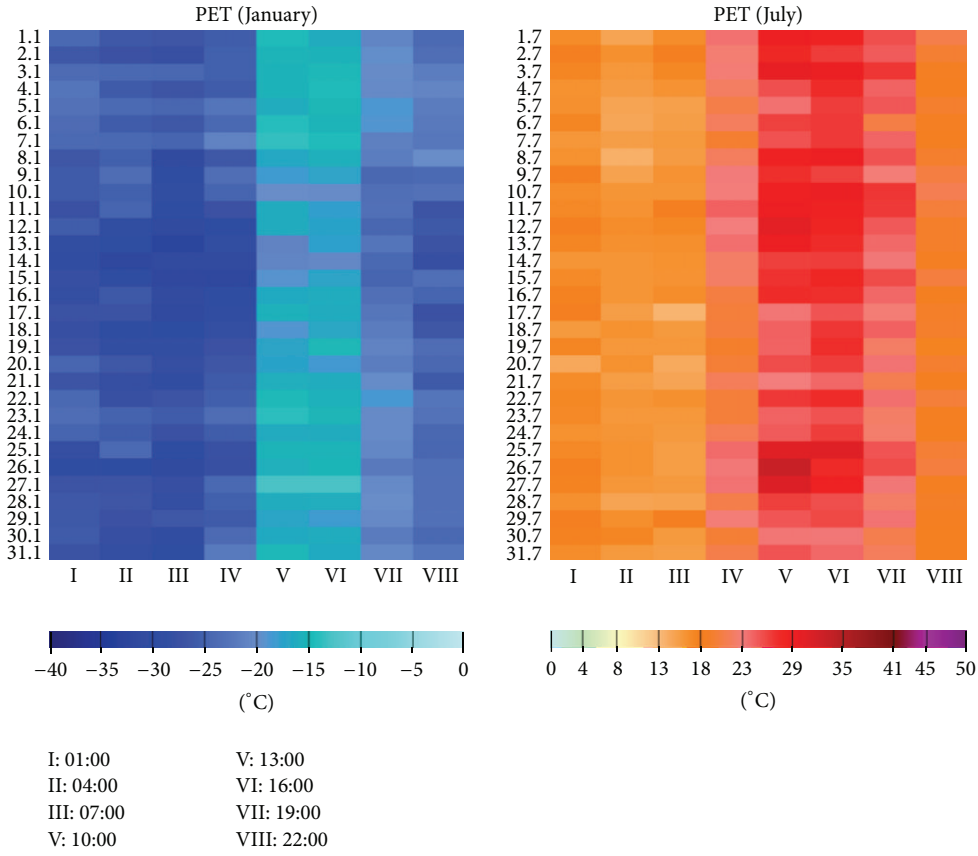

Figure 4: Monthly (along y-axis) and daily (along x-axis) dynamics of thermal comfort in winter (January) and summer (July) calculated with PET for Birobidzhan, zone 1.

Table 2: Mean number of days per year with PET values within a specific class for the 3 zones as well as the climate station in Birobidzhan (2000–2010).

PET (°C)	WMO station	Zone 1	Zone 2	Zone 3
<−30	21.0	12.1	14.9	12.9
<−20	68.3	59.4	63.0	60.5
<−10	117.2	113.0	114.6	113.5
<0	170.1	167.6	168.4	167.7
$(15 \leq X \leq 30)$	65.4	72.3	70.1	72.2
$(18 \leq X \leq 27)$	37.0	42.6	40.5	42.6
>29	19.5	9.9	13.9	10.7
>35	6.0	2.2	3.4	2.4
>41	1.0	0.3	0.6	0.4

does not show a very specific pattern but rather has an even distribution of values over the whole time with a few hotspots especially at 13:00. Winter in zone 2 displays a similar pattern as it does in zone 1, but as in summer the values are more extreme and there are more days with extremely low PET values. The time of the day they occur remains the same at 7:00. The warmest times of day are still the hours after the suns zenith between 13:00 and 16:00. Then the maximum values lie at about −5.0°C. At 22:00 PET starts to drop to values below −30.0°C and reaches its minimum around 4:00 with values close to −40.0°C. A significant monthly pattern is not visible, but there is a cold spot in the second decade of January as it was observed before in the yearly course of PET for zone 2. Since zone 3 is the one with the lowest building density, it has the highest occurrence frequencies of extreme PET values. In Figure 6 the second decade of January showsthat 76.1% of all values are below −20.0°C. As a contrast in the first decade of July 17.8% of all PET values lie above 29.1°C. With 26.1% of all values in the second decade of August situated in between 18.1°C and 23.0°C the maximum frequency of comfortable PET values is the lowest in comparison to the other two zones. The least extreme

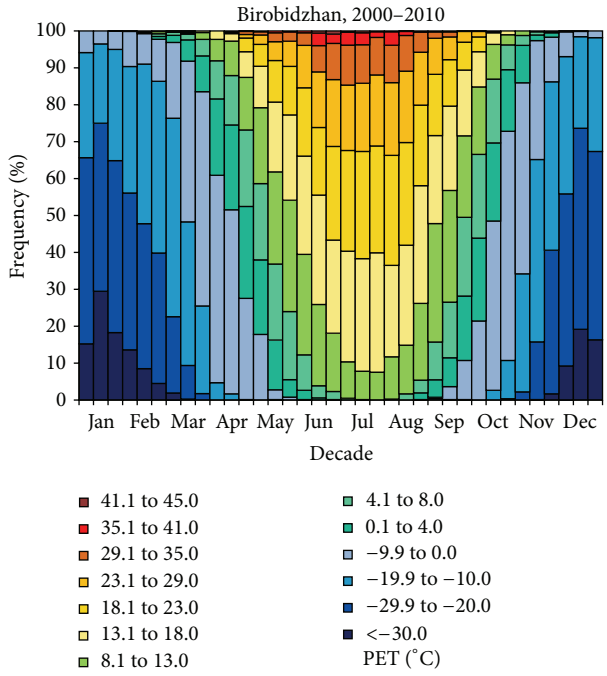

Figure 5: Mean frequency distribution of PET values in Birobidzhan, zone 2, during the year divided into 10-day intervals (decades) for the period 2000–2010.

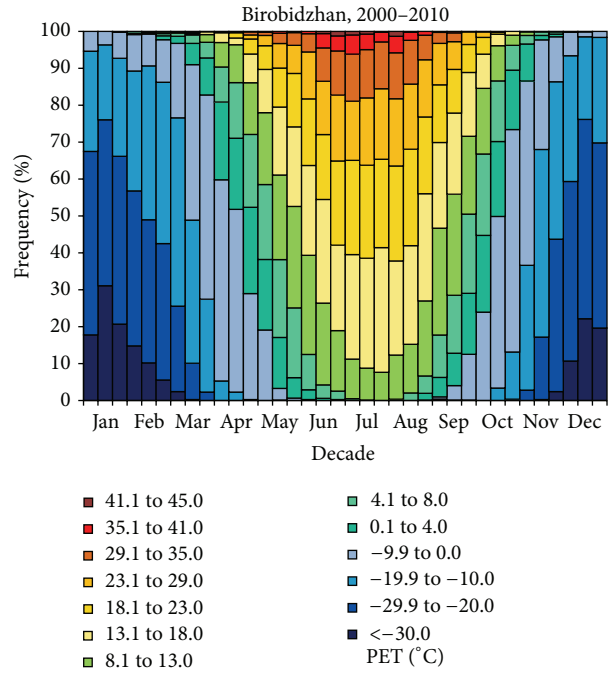

Figure 6: Mean frequency distribution of PET values in Birobidzhan, zone 3, during the year divided into 10-day intervals (decades) for the period 2000–2010.

times marked the end of spring and the beginning of autumn. Still they are not the ones with the highest frequency of comfortable values.

Instead they have a tendency to cold stress with the majority of the values between comfort and strong cold stress. The pattern of maximum and minimum values remains the same in zone 3 since similar meteorological input data were used. However the amplitude of those values reaches its maximum. The hottest time of day was 13:00 with PET values even above 41.0°C. Around 4:00 PET reaches its minimum of about 8.0°C on some days. Usually even then PET does not drop to single digit values but stays in between 13.0°C and 18.0°C. The hottest time of July seems to be the end of the first decade and the beginning of the second. The most comfortable times of the day are the hours from 22:00 to 1:00. At that time most PET values lie in between 18.0°C and 23.0°C. In January the coldest time of day in zone 3 was around 7:00 so about the same time as in zones 1 and 2. The PET values drop below −40.0°C at that time, especially in the ten days from the 8th of January to the 18th of January. The warmest times of the day are still occur between 13:00 and 16:00 making the afternoon and early evening the most pleasant times of the day to be outside on the city square. Still the PET values at that time of day result in extreme cold stress and remain below 0.0°C. Even around 13:00 PET values are closer to −15.0°C than they are to 0.0°C. A day with PET values of single digits below 0.0°C could therefore be considered a comparatively warm day.

4.2. Universal Thermal Climate Index. In general the UTCI values follow the same pattern as the PET values, which is to be expected since both of the indices are based on the human energy budget and are calculated using the same datasets (Table 3).

However the adaptive nature of the UTCI index results in less extreme and more moderate values since clothing and activity are adapted to the surrounding thermal conditions [13]. This presents the opportunity of a more detailed and diverse look at the thermal comfort.

Zone 1 is still the most sheltered and therefore the most comfortable zone. The equivalent temperature calculated with UTCI actually showed more comfortable conditions than that with PET. The adaption of the clothing insulation in combination with the wide range of nonstressful values from 9.0°C to 23.0°C results in a wide range of stress-free UTCI values from spring to autumn with a maximum of comfort in summer. Still the summer months hold more than 30% of moderate to very strong heat stress conditions and winter still remains a time of cold stress varying from extreme to moderate cold stress which makes winter the most stressful time for the human body in terms of the thermal bioclimate. Following the UTCI scale Figure 7 represents the monthly and daily courses of thermal conditions for January and July in zone 1. The warmest time of the day is the time between 13:00 and 16:00, while the lowest values occur between 4:00 and 7:00 although cold stress does not occur. During the warmest time of the day, UTCI reached moderate heat stress values on several occasions. But in general July can be considered a comfortable month. The monthly course showed three phases of high UTCI values with the first being in the beginning of the first decade, the second at the end of the first decade, and the third in the middle of the third decade.

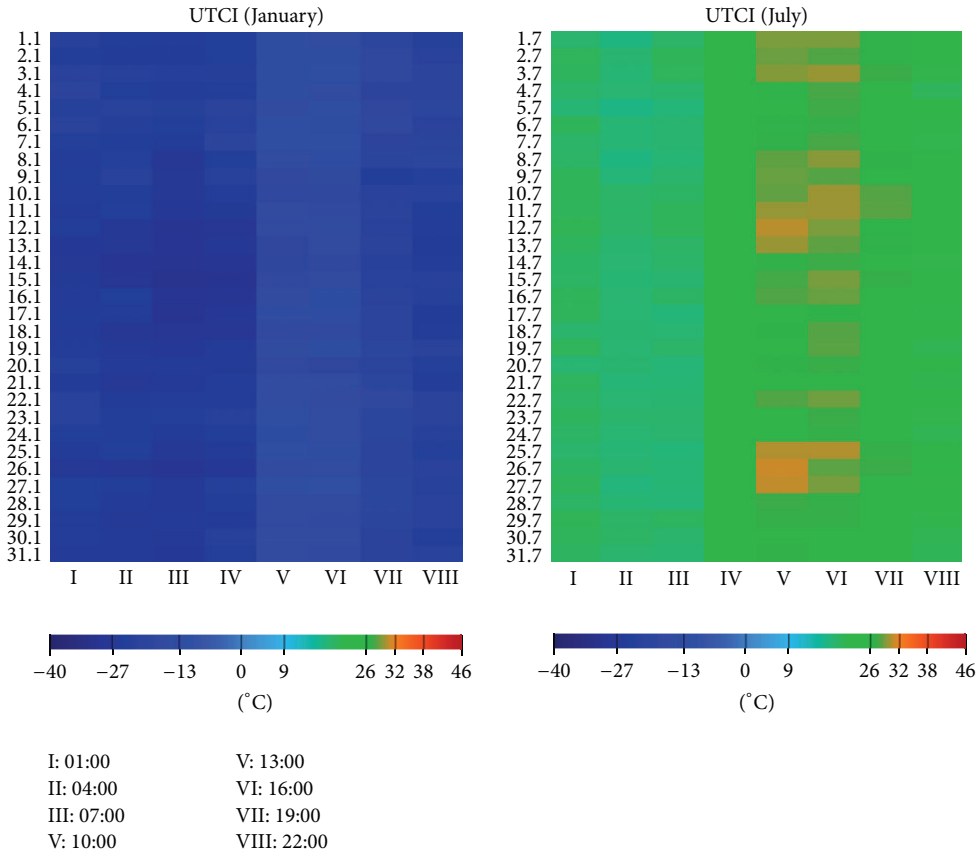

Figure 7: Monthly and daily dynamics of thermal comfort in winter (January) and summer (July) calculated with UTCI for Birobidzhan, zone 1.

Table 3: Mean number of days per year with UTCI values within a specific class for the 3 zones as well as for the climate station in Birobidzhan (2000–2010).

UTCI (°C)	WMO station	Zone 1	Zone 2	Zone 3
<−30	21.0	9.0	10.5	9.4
<−20	68.3	54.8	58.6	55.8
<−10	117.2	108.7	109.6	109.1
<0	170.1	156.1	157.0	156.1
$(15 \leq X \leq 30)$	65.4	91.7	90.6	92.5
$(18 \leq X \leq 27)$	37.0	57.6	55.8	57.8
>29	19.5	10.1	13.5	10.9
>35	6.0	1.1	1.3	1.0
>41	1.0	0.0	0.0	0.0

Winter (exemple in this case January) in zone 1 presents itself to be much less comfortable than summer. The daily course remains the same with the warmest time being between 13:00 and 16:00 and the coldest around 7:00. In contrast to summer there were no periods without thermal stress. Throughout the whole month the body suffers from moderate to very strong cold stress. The highest values lie between 0.0°C and −13.0°C while the coldest are close to −40.0°C. The coldest time of January is in the middle of the second decade from the 12th until the 17th of January, while the highest values occurred at 13:00 between the 23rd and the 27th (Figure 7).

The thermal dynamics in zone 2 were observed to be similar to those in zone 1 but with about 5% more heat stress in the summer months. Comfortable values occurred from the midst of March until the end of October. The month with the most heat stress is July with its second decade being the one with almost 30% of heat stress values. Winter still presented a time of constant cold stress varying in its intensity from extreme to moderate and with the second decade of January as the coldest period of the year. With about 42.1% of all values below −27.0°C this decade showed the highest frequency of very strong cold stress values. The second decade

of December shows 92.4% of all values being below −13.0°C resulting in at least strong cold stress conditions. As in zone 1, the summer months are the ones that present the most comfortable outdoor conditions but also the most heat stress. The thermal dynamics of zone 2 for July were used as an example for the thermal dynamics in summer. The time of the highest thermal stress is the time between 13:00 and 16:00 with UTCI values above 32.0°C. Also around 10:00 and 19:00 the human body can experience slight heat stress on some days. The coldest time of the day is the time between 4:00 and 7:00. During this time the values drop almost to the range of cold stress. In the course of July there are three hot spots. The first two occurr in the first decade while the last hotspot lies in the middle of the third decade. Winter in zone 2 presents itself with constant cold stress. In January the highest values for UTCI occur in the afternoon between 13:00 and 16:00. During this time UTCI lies between 0.0°C and −13.0°C causing moderate to strong cold stress. In the course of the night the values start to drop to reach their minimum values below −27.0°C around 4:00 to 7:00. At this time the human body experiences very strong cold stress. The coldest time of January is between the 10th and the 16th, while the, least cold days are closer to the end of the month.

Since it has the most open space, zone 3 presents itself with the least comfortable thermal conditions. The summer months show the highest frequency of heat stress values, while, in winter the frequency of strong and very strong cold stress is increased. Still summer shows the most comfortable setting with up to 70% of all values being within one decade in the class of 9.0°C to 27.0°C. The highest heat stress occurs in summer around the same time in the middle of July and the beginning of August. In winter the human body experiences exclusively cold stress with 43.9% of all values being between −27.0°C and 39.9°C; the second decade of January shows the most extreme conditions; while the second decade of December can be considered the coldest in general with 92.6% of all values below −13.0°C. Times of no thermal stress occur from the midst of March to the midst of November even though they are very rare at those times. In spring and autumn the range of UTCI covers everything from thermal stress to strong cold stress and in rare cases even heat stress. The warmest time of day in zone 3 in summer is still the time from 13:00 to 16:00, but the occurrence of UTCI values outside the range of no thermal stress around 10:00 and 19:00 is increased. Also the three hotspots in the monthly course that could be observed in zones 1 and 2 are not as prominent because they are closer together and cover more days. From 22:00 to 7:00 the values are the lowest with a minimum around 4:00. Still they do not present any cold stress since they stay quite far above 9°C. In zone 3 the winter season presents itself with the same dynamics as those in the other zones. It shows its coldest period in January from the 8th to the 17th in the monthly course and in general from 4:00 to 7:00 in the daily course. The warmest time of the day is the time between 13:00 and 16:00 but even then the UTCI values do not exceed the range of cold stress. In the coldest hours UTCI values drop far below −27.0°C and get close to −40.0°C.

5. Discussion

The results of the calculations and simulations as well as the measurements of the meteorological parameters show a clear picture of the thermal conditions in terms of the human bioclimate in the JAR. In general it can be concluded that the JAR has a very big gradient of thermal conditions throughout the year not only in the direct thermal parameters such as T_a and T_{mrt} [23, 24] but also in the secondary parameters such as VP and RH. The wind is not so much bound to an annual cycle and therefore influences the thermal conditions in a similar pattern throughout the year. The thermal comfort has been determined with PET and UTCI and they exhibited similar dynamics in the annual course. However they indicate a great difference in their values. While PET shows a lot of very extreme values and only little thermal comfort throughout the year, UTCI shows a lot of nonstressful conditions especially in the summer months. This difference was to be expected since PET has been calculated with the same base parameters for the entire year while UTCI is an adaptive index which results in a less extreme setting. Since it can be assumed that no one is wearing a light business suit (clo = 0.9) in winter in the Russian Far East the adaption of this parameter seems to result in a more realistic assessment. Still the winter season holds a lot of cold stress and in contrast to summer has no comfortable values at all.

In case of cold stress in winter it does not matter whether it is calculated with PET or UTCI. In both cases winter is not comfortable. The only difference is the range of values. While calculated with PET there are more extreme cold stress values, UTCI results strong rather in than extreme cold stress. The thermal conditions in summer, however, differ greatly depending on the applied index. While PET depicts a rather harsh picture of the thermal conditions in summer, UTCI shows a lot of nonstressful values. This difference is the result of the different procedures of calculating the indices as well as the different index classes applied to the definitions of thermal comfort. While PET provides only a narrow window of thermal comfort (18.0°C to 23.0°C), UTCI considers a much wider range (9.0°C to 27.0°C) comfortable or at least not stressful for the human body [2, 3, 5]. The result of this calculation is a very comfortable thermal situation in summer with about 30% of the values resulting in slight to strong heat stress and the remaining 70% being comfortable. PET shows most of the variability in its classed values during summer. It shows little thermal comfort but wide rather a range from extreme heat stress to moderate cold stress. How wide the range of PET or UTCI is and how narrow the window of comfortable values is depend on the surrounding structures as well. The higher the building density is in an area and the more vegetation there is, the more comfortable are outdoor conditions are. In summer this is the result of shading effects and the resulting reduction of T_{mrt} and in winter the high urban density results in a reduction of heat loss due to long wave radiation. As a result the outdoor areas of the residential area (zone 1) can be considered the most comfortable one throughout the year while the city square (zone 3) is the least comfortable due to its high exposure to the elements.

Figure 8: Residential area in Birobidzhan (zone 1).

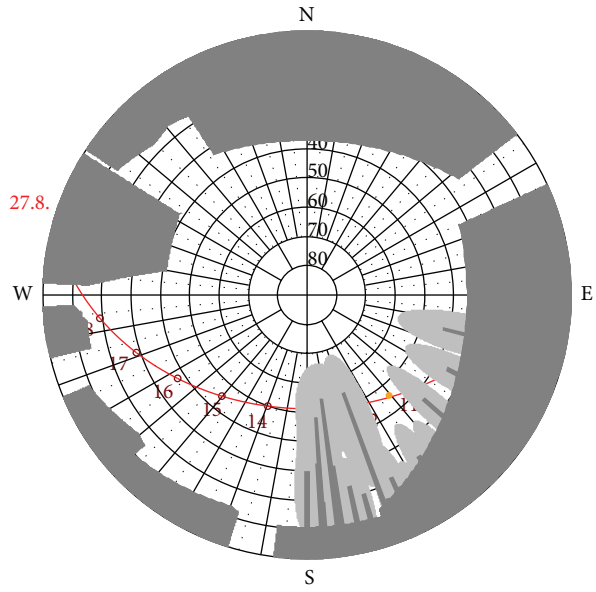

1999–2010 RayMan Pro 2.1

Figure 9: Polar diagram for the sky view factor (zone 1) in Birobidzhan.

The results also show the influence of all the parameters that are part of the calculations of PET. The higher the relative humidity is the more extreme is the thermal impact of T_a and T_{mrt} is. The wind always has a cooling effect (except when the air temperature is higher than the surface temperatures of humans), but its role in this region is very important since the occurrence of high wind velocities is rather rare. The main impact on the human thermal bioclimate in this region lies with the air temperature and the mean radiant temperature. Therefore the best possibilities for human interference lie in the reduction of irradiation. Using wind channelling to reduce T_a in summer seems premature since the same action would lead to even more extreme cold stress during winter. Another way to reduce thermal stress in urban areas of the JAR would be the increase of vegetation.

According to a paper on thermal strain due to a change in locations within the Russian Far East [25] the difference in thermal comfort during the winter months is negligible due to an overall extreme cold stress which makes the results of this study applicable for the whole region in winter. In summer, however, the thermal conditions within the Far East district vary greatly making more localized investigations necessary for a thorough assessment of preferable urban outdoor structures in summer.

On the topic of the change of extreme climate regions due to global climate change it can be assumed that the overall frequency of extremely cold days is reduced in favour of an increase in heat stress days which would lead to an overall increase in thermal comfort for regions of high cold stress [26]. In a region of high gradients of thermal comfort like the JAR, however, the result would rather be a shift in types of thermal discomfort than an increase of comfortable days.

In comparison, Freiburg in south western Germany which lies at the same latitude (48°N) but at a very different longitude (9°E) than Birobidzhan (127°E) has a very different climate setting. In Birobidzhan the annual climate variation is much higher and is based on the summer monsoon or the Siberian high pressure area. In Freiburg climate is much more dependent on the pressure systems in the northern Atlantic especially the Northern Atlantic Oscillation (NAO) and the interaction with the alpine climate system. As a result the climate in Freiburg is much less extreme. In particular in winter the thermal parameters show a much more moderate situation [22, 27, 28]. In summer being located on a wide open space with close to no vegetation Freiburg and Birobidzhan present similar heat stress conditions [27–29]. This difference in climate situations shows a longitudinal dependency of the regional climate that is not at all linked to the classic climate zones which depend on the latitude but rather to its proximity to pressure systems and its location in the path of meteorological phenomena such as a monsoon or El Niño.

6. Conclusions

After analysing the results of measurements and calculations it can be concluded that the JAR is a climatic extreme region with a massive gradient of thermal comfort conditions. However there is a variety of possibilities for adaption to this phenomenon. The first and most simple one is of course to follow the saying "there is no bad weather, just a bad choice of clothing" and to choose the right clothing for the meteorological situation. This action is taken into consideration in the application of UTCI and it shows a significant moderation of the otherwise unpleasant conditions in late spring, summer, and early autumn. In the cold season, however, even clothing does not help much. It moderates the extreme cold stress but it does not suffice to relieve the human body entirely. To gain a maximum of cold stress reduction it is therefore necessary to make sure that one stays outside as little as possible and—if one does stay outside—to choose the location wisely. According to the results of this study the wisest decision would be to avoid wide open spaces and to remain in areas of high urban density. Another important factor is of course the time of the day. While it is advisable to choose the morning and late afternoon hours of the day and to avoid noon and early afternoon for outside chores in summer, the opposite

Figure 10: Main street in Birobidzhan (zone 2).

Figure 12: Square in Birobidzhan (zone 3).

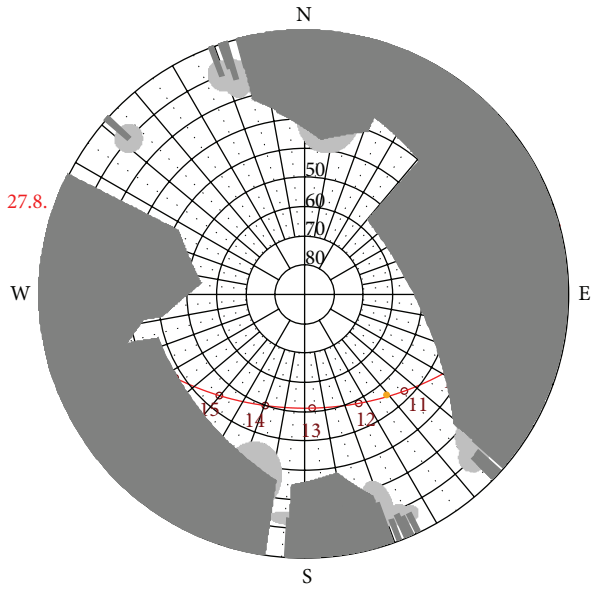

Figure 11: Polar diagram for the sky view factor (zone 2) in Birobidzhan.

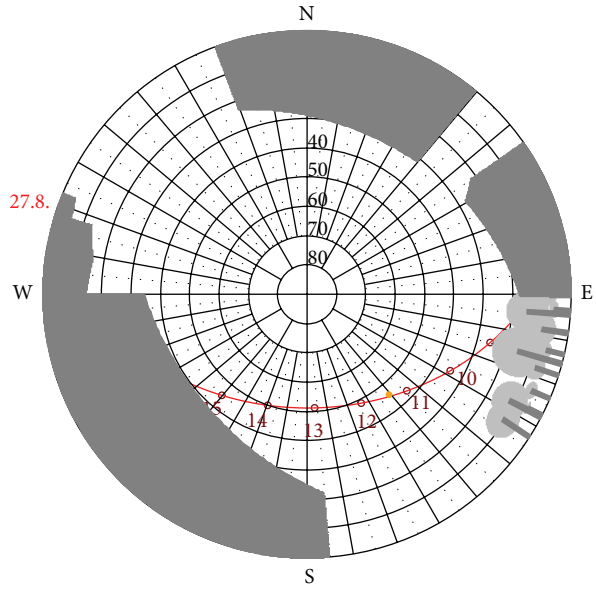

Figure 13: Polar diagram for the sky view factor (zone 3) in Birobidzhan.

can be said about winter. The least thermal stress in winter occurs for all zones in the time between 13:00 and 16:00 which makes it the most pleasant time to be outside. Staying outside at night especially in the hours of early morning around 4:00 would be ill advised since those are the hours of the strongest cold stress.

For planning purposes in this region or regions affected by a similar climate it can be concluded that a high urban density combined with a fair amount of inner city vegetation would be a preferable setting to reduce thermal stress. This measure would be especially preferable for locations that are equally important throughout the year such as public transport stops, train stations, or other points of public interest.

Appendix

See Figures 8, 9, 10, 11, 12, and 13.

References

[1] P. Höppe, *Die Energiebilanz des Menschen [M.S. thesis]*, Wissenschaftliche Mitteilungen des Meteorologischen Instituts Universität München, 1984.

[2] P. Höppe, "The physiological equivalent temperature—a universal index for the biometeorological assessment of the thermal environment," *International Journal of Biometeorology*, vol. 43, no. 2, pp. 71–75, 1999.

[3] A. Matzarakis, H. Mayer, and M. G. Iziomon, "Applications of a universal thermal index: physiological equivalent temperature," *International Journal of Biometeorology*, vol. 43, no. 2, pp. 76–84, 1999.

[4] D. Fiala, G. Havenith, P. Bröde, B. Kampmann, and G. Jendritzky, "UTCI-Fiala multi-node model of human heat transfer and temperature regulation," *International Journal of Biometeorology*, vol. 56, no. 3, pp. 429–441, 2012.

[5] G. Jendritzky, R. de Dear, and G. Havenith, "UTCI-Why another thermal index?" *International Journal of Biometeorology*, vol. 56, no. 3, pp. 421–428, 2012.

[6] H. Mayer and P. Höppe, "Thermal comfort of man in different urban environments," *Theoretical and Applied Climatology*, vol. 38, no. 1, pp. 43–49, 1987.

[7] P. R. Höppe, "Heat balance modelling," *Experientia*, vol. 49, no. 9, pp. 741–746, 1993.

[8] P. Höppe, "Die Wärmebilanzmodelle MEMI und IMEM zur Bewertung der thermischen Beanspruchung am Arbeitsplatz," *Verhandlungen der Deutschen Gesellschaft für Arbeitsmedizin und Umweltmedizin*, vol. 34, pp. 153–158, 1994.

[9] A. Matzarakis, F. Rutz, and H. Mayer, "Modelling radiation fluxes in simple and complex environments—application of the RayMan model," *International Journal of Biometeorology*, vol. 51, no. 4, pp. 323–334, 2007.

[10] A. Matzarakis, F. Rutz, and H. Mayer, "Modelling radiation fluxes in simple and complex environments: basics of the RayMan model," *International Journal of Biometeorology*, vol. 54, no. 2, pp. 131–139, 2010.

[11] R.-L. Hwang, T.-P. Lin, and A. Matzarakis, "Seasonal effects of urban street shading on long-term outdoor thermal comfort," *Building and Environment*, vol. 46, no. 4, pp. 863–870, 2011.

[12] T.-P. Lin, A. Matzarakis, and R.-L. Hwang, "Shading effect on long-term outdoor thermal comfort," *Building and Environment*, vol. 45, no. 1, pp. 213–221, 2010.

[13] K. Blazejczyk, Y. Epstein, G. Jendritzky, H. Staiger, and B. Tinz, "Comparison of UTCI to selected thermal indices," *International Journal of Biometeorology*, vol. 56, no. 3, pp. 515–535, 2012.

[14] A. Psikuta, D. Fiala, G. Laschewski et al., "Validation of the Fiala multi-node thermophysiological model for UTCI application," *International Journal of Biometeorology*, vol. 56, no. 3, pp. 443–460, 2012.

[15] D. Fiala, K. J. Lomas, and M. Stohrer, "A computer model of human thermoregulation for a wide range of environmental conditions: the passive system," *Journal of Applied Physiology*, vol. 87, no. 5, pp. 1957–1972, 1999.

[16] D. Fiala, K. J. Lomas, and M. Stohrer, "Computer prediction of human thermoregulatory and temperature responses to a wide range of environmental conditions," *International Journal of Biometeorology*, vol. 45, no. 3, pp. 143–159, 2001.

[17] D. Fiala, K. J. Lomas, and M. Stohrer, "First principles modeling of thermal sensation responses in steady-state and transient conditions," in *Technical and Symposium Papers Presented at the 2003 Winter Meeting of the ASHRAE*, pp. 179–186, January 2003.

[18] E. Grigorieva and V. Tunegolovets, "Change of climate on the south of the Russian Far East in the second half of the 20th century," *Annalen Der Meteorologie*, vol. 41, pp. 209–212, 2005.

[19] E. Grigorieva and D. Fetisov, "Estimation of climatic resources for summer sport recreation," in *The Jewish Autonomous Region of Russia, Developments in Tourism Climatology*, pp. 87–92, 2007.

[20] E. Grigorieva, "Spatial-temporal dynamics of climate thermal resources for the southern part of the Russian Far East," in *Proceedings of the 18th International Congress of Biometeorology*, p. 121, International Society of Biometeorology, Tokyo, September 2008.

[21] E. Grigorieva, A. Matzarakis, and C. R. de Freitas, "Analysis of growing degree-days as a climate impact indicator in a region with extreme annual air temperature amplitude," *Climate Research*, vol. 42,, pp. 143–154, 2010.

[22] E. Grigorieva and A. Matzarakis, "Physiologically equivalent temperature as a factor for tourism in extreme climate regions in the Russian Far East: preliminary results," *European Journal of Tourism, Hospitality and Recreation*, vol. 3, pp. 127–142, 2011.

[23] P. O. Fanger, *Thermal Comfort*, McGraw-Hill, New York, NY, USA, 1972.

[24] VDI, *Environmental Meteorology, Methods for the Human Biometeorological Evaluation of Climate and Air Quality for the Urban and Regional Planning at Regional Level. Part I. Climate*, VDI/DIN—HandbuchReinhaltung der Luft, Düsseldorf, Germany, 1998.

[25] C. R. de Freitas and E. A. de Grigorieva, "The acclimatization thermal strain index (ATSI): a preliminary study of the methodology applied to climatic conditions of the Russian Far East," *International Journal of Biometeorology*, vol. 53, no. 4, pp. 307–315, 2009.

[26] D. H. W. Li, K. K. W. Wan, L. Yang, and J. C. Lam, "Heat and cold stresses in different climate zones across China: a comparison between the 20th and 21st centuries," *Building and Environment*, vol. 46, no. 8, pp. 1649–1656, 2011.

[27] D. Fröhlich and A. Matzarakis, "Heat stress and city planning—the example of the "Platz der alten synagoge" in Freiburg in Breisgau," *Gefahrstoffe Reinhaltung der Luft*, vol. 71, no. 7-8, pp. 333–338, 2011.

[28] J. Herrmann and A. Matzarakis, "Mean radiant temperature in idealised urban canyons-examples from Freiburg, Germany," *International Journal of Biometeorology*, vol. 56, no. 1, pp. 199–203, 2012.

[29] A. Matzarakis and C. Endler, "Climate change and thermal bioclimate in cities: impacts and options for adaptation in Freiburg, Germany," *International Journal of Biometeorology*, vol. 54, no. 4, pp. 479–483, 2010.

Hindawi Publishing Corporation
Advances in Meteorology
Volume 2013, Article ID 538508, 15 pages
http://dx.doi.org/10.1155/2013/538508

Research Article

One-Day Prediction of Biometeorological Conditions in a Mediterranean Urban Environment Using Artificial Neural Networks Modeling

K. P. Moustris,[1] P. T. Nastos,[2] and A. G. Paliatsos[3]

[1] *Department of Mechanical Engineering, Technological Educational Institute of Piraeus, 250 Thivon and P. Ralli Street, 122 44 Aegaleo, Greece*
[2] *Laboratory of Climatology and Atmospheric Environment, Faculty of Geology and Geoenvironment, University of Athens, Panepistimiopolis, 157 84 Athens, Greece*
[3] *General Department of Mathematics, Technological Educational Institute of Piraeus, 250 Thivon and P. Ralli Street, 122 44 Aegaleo, Greece*

Correspondence should be addressed to K. P. Moustris; kmoustris@yahoo.gr

Received 13 June 2013; Revised 11 August 2013; Accepted 5 September 2013

Academic Editor: Andreas Matzarakis

The present study, deals with the 24-hour prognosis of the outdoor biometeorological conditions in an urban monitoring site within the Greater Athens area, Greece. For this purpose, artificial neural networks (ANNs) modelling techniques are applied in order to predict the maximum and the minimum value of the physiologically equivalent temperature (PET) one day ahead as well as the persistence of the hours with extreme human biometeorological conditions. The findings of the analysis showed that extreme heat stress appears to be 10.0% of the examined hours within the warm period of the year, against extreme cold stress for 22.8% of the hours during the cold period of the year. Finally, human thermal comfort sensation accounts for 81.8% of the hours during the year. Concerning the PET prognosis, ANNs have a remarkable forecasting ability to predict the extreme daily PET values one day ahead, as well as the persistence of extreme conditions during the day, at a significant statistical level of $P < 0.01$.

1. Introduction

The impact of climate and prevailing weather on human thermal comfort discomfort is almost obvious. Environmental conditions affect the heat balance between the human body and the environment and they are the source of possible discomfort conditions. In particular, during the summer period, extreme meteorological conditions have a direct impact on energy consumption of buildings for air-conditioning purposes [1]. It has been reported as an increase of about 800% in annual purchases of air-conditioning units ever since, due to the serious heat waves observed in Greece during 1987–1989 [2].

Human thermal comfort or discomfort conditions may be assessed through a large number of theoretical and empirical indices requiring usually a larger or smaller number of input microclimate parameters such as air temperature, wind speed, and air humidity [4–6]. An important issue, in terms of human health risk assessment, is to predict the microclimate and the associated human thermal comfort-discomfort conditions in the urban environment. Despite the existence of various microclimate models, there are only a few models that are able to deal with human thermal comfort estimations, for example, the RayMan model [7, 8] and the Envi-Met model [9]. These models may be used efficiently in both estimating and predicting human thermal comfort conditions in the urban environment [10–13].

The present study deals with the application of artificial neural networks (ANNs), an alternative modeling technique against common modeling efforts for the evaluation and the prognosis of human thermal comfort conditions in the urban environment. During the last decade, there has been an increasing use of ANNs, in various aspects of the atmospheric environment studies [14–20]. Despite this increasing use

of ANNs and their advantages (generalization properties, capability of handling high dimensional data, and nonlinearities), the number of ANNs model applications in problems related to bioclimatic aspects of human health is, however, still limited (e.g., [21, 22]), whereas in the case of the urban environment studies, those focus only on the microclimate patterns [23]. Specifically, during the last decade, only few researches around the world started to apply the artificial neural networks modeling in order to predict the human thermal comfort-discomfort levels for different purposes.

Gao and Bai [24] proposed an artificial neural network model for the prediction of bioclimatic conditions by the use of back-propagation neural network, giving good results. Wong et al. [25] investigated the predictability of clothing sensory comfort from psychological perceptions by using a feed-forward back-propagation network in an artificial neural network (ANN) system. Results, showing a good correlation between predicted and actual comfort ratings with a significance of $P < 0.01$ for all of the five developed models, indicated that overall comfort performance is predictable with neural networks, particularly models with log sigmoid hidden neurons and pure linear output neurons. Ji et al. [26] examined the possibility of using ANNs to model the relationship between the thermal environmental factors and the residents' thermal reaction in order to predict the environmental thermal comfort. The test results showed that the ANN model had higher precision in prediction than the traditional method-linear regression under steady conditions. Further, under unsteady conditions, the model can also be correctly used to predict the change of the residents' thermal reaction avoiding dealing with the complicated nonlinear relation, while using the regression method. Atthajariyakul and Leephakpreeda [27] presented a practical approach to determine human thermal comfort quantitatively via neural computing. The results showed good agreement between the thermal comfort index calculated from the neural network model in real time and those calculated from the conventional PMV model. Liu et al. [28] examined the relation between the main influencing factors (such as temperature, relative humidity, air velocity, mean radiant temperature, air pressure, and clothing insulation) and human thermal sensation, using ANN. Moreover, back-propagation (BP) neural network evaluation model of human thermal comfort was put forward under low pressure environment and learning algorithm of network was given. Liu et al. [28] concluded that the prediction of network model is closely consistent with experimental results.

Finally, regarding Greece and the prognosis of human thermal comfort-discomfort levels using ANNs models, Mihalakakou et al. [23] applied an intelligent "data-driven" method (ANN) for investigating, analyzing, and quantifying the urban heat island phenomenon in the major Athens region, where hourly ambient air-temperature data are recorded at twenty-three stations. The results were tested with extensive sets of nontraining measurements and it was found that they corresponded well to the real values. Moustris et al. and Vouterakos et al. [29–31] developed ANNs in order to forecast the human thermal comfort-discomfort levels within the Greater Athens Area (GAA), Greece, as well as the number of consecutive hours of thermal discomfort for the next day. Results in all cases showed that ANNs have a good ability to forecast one day ahead the values of the thermal indices used.

The growth of the city of Athens in the last decades and the phenomenon of urbanization obviously have led to the creation of a microclimate with explicit effects on human thermal comfort-discomfort. The knowledge of human thermal comfortdiscomfort levels, predicted for the next days, is very important for suitable actions in order to protect public health [29–31]. The aim of this work is the prognosis of the biometeorological conditions, expressed by the physiologically equivalent temperature (PET), one day ahead within the GAA urban environment, using ANNs modeling techniques.

2. Data and Methodology

2.1. The Monitoring Site. The Greek capital city of Athens is located in an area of about 450 km^2 with a complex topography within the Greater Athens Area-basin. According to the census of 2011, about the 40% of Greece's population lives in the Greater Athens Area (GAA). During the last decades and due to continued population growth, there was an extremely large and rapid spatial and residential growth of the GAA. This development led, according to many scientists, to the heat island effect [32–35]. This phenomenon leads to the creation of microclimates resulting in the configuration of different humans thermal comfort-discomfort conditions even between adjacent regions [32–36].

For the estimation of human thermal comfort-discomfort levels, the physiologically equivalent temperature (PET) in an hourly base was calculated using the RayMan model. Specifically, hourly values of air temperature (°C), wind speed (m/s), relative humidity (%), and global solar irradiation (W/m^2) covering the period 15/06/2005–31/12/2011 (57,384 hours) were used. These data concern the location of Galatsi (GAL) and have been recorded by the Hydrological Observatory of Athens (HOA) operated by the National Technical University of Athens [37]. Figure 1 depicts the monitoring site within the GAA. The monitoring station is sited within the Galatsi water treatment plant installations of the Water Supply and Sewerage Company of Athens (WSSCA). Data completeness of the examined location-monitoring site is found about 98.8%.

2.2. Physiologically Equivalent Temperature. The PET is based on the Munich Energy balance Model for Individuals (MEMI), which describes the thermal conditions of the human body in a physiologically relevant way [38]. PET is defined as the air temperature at which, in a typical indoor setting (without wind and solar radiation), the heat budget of the human body is balanced with the same core and skin temperature under the complex outdoor conditions to be assessed [39, 40]. Table 1 presents the different stress levels and human thermal sensations according to PET value.

For biometeorological purposes, the height of 1.1 m is considered as the mean gravity center of the human body [7]. In order to calculate the hourly values of PET, using

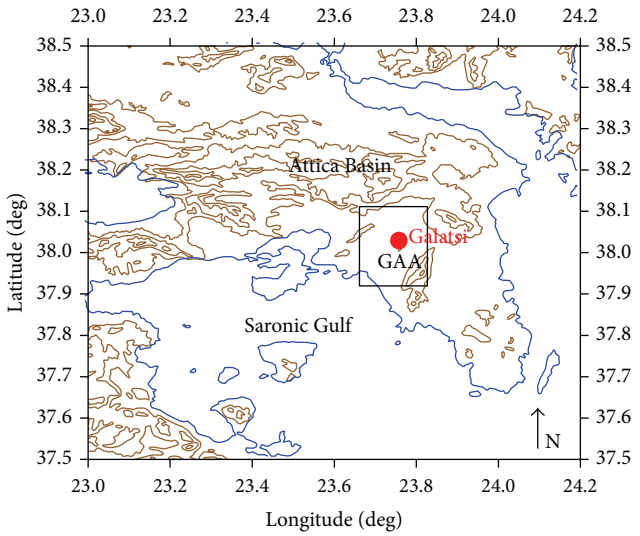

Figure 1: The Greater Athens Area (GAA) along with the examined monitoring site of Galatsi.

Table 1: Physiologically equivalent temperature (PET) for different grades of thermal sensation and physiological stress on human beings (during standard conditions: heat transfer resistance of clothing: 0.9 clo, internal heat production: 80 W) [41].

PET (°C)	Thermal sensation	Physiological stress level
<4	Very cold	Extreme cold stress
8	Cold	Strong cold stress
13	Cool	Moderate cold stress
18	Slightly cool	Slight cold stress
23	Comfortable	No thermal stress
29	Slightly warm	Slight heat stress
35	Warm	Moderate heat stress
41	Hot	Strong heat stress
>41	Very hot	Extreme heat stress

the RayMan model, the hourly values of wind speed at 1.1 m above the ground are necessary. The available wind speed values (56,704 hourly values) derived from an anemometer's recordings, which is mounted on the top of a meteorological mast at a height of 10.0 m above the ground. The meteorological mast is located inside the water treatment plant installations of the WSSCA. It is a flat area without vigorous and high obstacles 150~200 m around the meteorological mast approximately. Figure 2 depicts, (Google Maps-Google Earth), the monitoring site inside the WSSCA area.

For that purpose, the measured hourly values of wind speed at 10.0 m above the ground level had to be recalculated at the high of 1.1 m above the ground level. This parameterization assumes a logarithmic vertical wind profile as it is described in (1) [42, 43]:

$$u(z) = u_{\text{ref}} \cdot \frac{\ln(z/z_0)}{\ln(z_{\text{ref}}/z_0)}, \quad (1)$$

where $u(z)$ is the wind speed at height (z) above the ground level, (z_0) is the aerodynamic roughness length of the surface

Figure 2: Map of the examined monitoring site of Galatsi with its altitude above sea level (from Google Maps-Google Earth).

in meters, and u_{ref} is the measured wind speed by the anemometer at the (z_{ref}) height above the ground level. In our case, $z = 1.1$ m and $z_{\text{ref}} = 10.0$ m. The aerodynamic roughness length of the surface for the given monitoring site was taken as $z_0 = 0.03$ m [44].

Finally, using the hourly values of the air temperature, air relative humidity, wind speed at 1.1 m above the ground, and the corresponding hourly values of global solar irradiance, the hourly values of PET were calculated.

2.3. Artificial Neural Networks. Artificial neural networks are a branch of artificial intelligence developed in the 1950s aiming at imitating the biological brain architecture. They are an approach to the description of functioning of human nervous system through mathematical functions. Typical ANNs use very simple models of neurons. These artificial neurons models retain only very rough characteristics of biological neurons of the human brain [45]. ANNs are parallel distributed systems made of many interconnected nonlinear processing elements (PEs), called artificial neurons [46]. A renewal of scientific interest has grown exponentially since the last decade, mainly due to the availability of appropriate hardware that has made them convenient for fast data analysis and information processing [47].

During the last two decades, more and more scientists around the world have apply ANNs modeling in many different scientific fields. ANNs have a lot of applications in many sectors such as

(i) pattern classification applications,
(ii) control, time series, estimation, prediction, and prognosis,
(iii) optimization,
(iv) environmental applications,
(v) engineering applications,
(vi) financial and commercial applications,
(vii) medical diagnosis,
(viii) management and marketing applications,
(ix) energy cost prediction.

2.3.1. Multilayer Perceptron and Feed-Forward ANNs. The Multilayer Perceptron (MLP) is the most commonly used type of ANNs. Its structure consists of processing elements (PEs) and connections [48]. PEs, which are called neurons, are arranged in layers. The first layer is the input layer, one or more hidden layers follow and the final layer is the output layer. An input layer serves as buffer that distributes input signals to the next layer, which is a hidden layer. Each neuron of the hidden layer communicates with all the neurons of the next hidden layer, if any, having in each connection a typical weight factor. So, each unit-artificial neuron in the hidden layer sums its input, processes it with a transfer function, and distributes the result to the output layer. It is also possible that there are several hidden layers connected in the same fashion. The units-artificial neurons in the output layer compute their output in a similar manner. Finally, the signal reaches the output layer, where the output value from the ANN is compared to the target value and an error is estimated. Thus, the values of weight factors are amended appropriately and the training cycle is repeated until the error is acceptable, depending on the application. Since data flow within the artificial neural network from a layer to the next one without any return path, such kinds of ANNs are defined as feed-forward ANNs. The structure of a feed-forward Multilayer Perceptron artificial neural network can be represented as in Figure 3.

2.3.2. Feed-Forward ANNs Training and the Back-Propagation Training Algorithm. The training-learning process of ANNs can be far from the ensemble optimum in some cases, and the problem can be solved only with a very good database, the best choice of the input configuration for training, or using most powerful learning algorithms [47].

The back-propagation learning algorithm consists of two steps of computation: a forward pass and a backward pass. In the forward pass, an input pattern vector is applied to the sensory nodes of the network, that is, to the units in the input layer. The signals from the input layer are propagated to the units in the first layer and each unit produces an output. The outputs of these units are propagated to the units in the subsequent layers and this process continues until, finally, the signals reach the output layer, where the actual response of the network to the input vector is obtained (Figure 3).

During the forward pass, the synaptic weights of the network are fixed. During the backward pass, on the other hand, the synaptic weights are all adjusted in accordance with an error signal, which is propagated backward through the network against the direction of synaptic connections.

The mathematical analysis of the algorithm is well described by Viotti et al. [47]. It is worthwhile noting that a network architecture having just one hidden layer and activation functions arranged as described above, constitutes a universal predictor and it can theoretically approximate any continuous function to any degree of accuracy. In practice, such degree of flexibility is not achievable because parameters must be estimated from sample data, which are both finite and noisy [49].

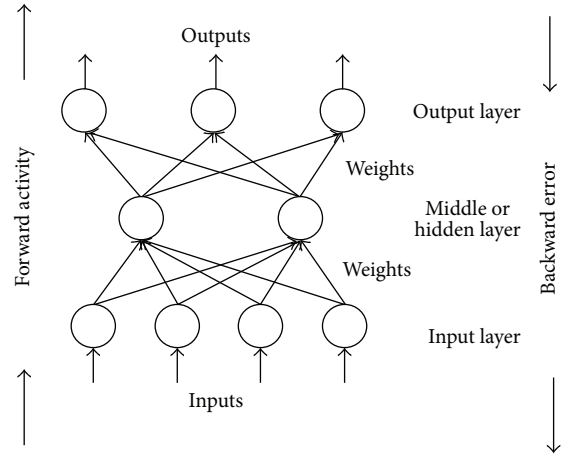

Figure 3: Typical MLP feed-forward artificial neural network structure [3].

The ANNs work on a matrix containing more patterns. Particularly, the patterns represent the rows while the variables are the columns. This data set is a sample. To be more precise, giving the ANN three different subsets of the available sample, we can get the forecasting model; the three subsets concern the training, the validation and the test subsets. These subsets are briefly described as follows:

(i) *training subset*, the group of data with which we train-educate the network according to the gradient descent for the error function algorithm, in order to reach the best fitting of the nonlinear function representing the phenomenon;

(ii) *validation subset*, the group of data, given to the network still in the learning phase, by which the error evaluation is verified, in order to update the best thresholds and weights effectively. Also, the cross validation phase during the model training is used to avoid the models' overtraining. If the model is overtrained, then memorize the problem instead to find a reliable solution;

(iii) *test subset*, one or more sets of new and unknown data for the ANN, which are used to evaluate ANN generalization, that is, to evaluate whether the model has effectively approximated the general function representative of the phenomenon, instead of learning the parameters uniquely.

2.4. Architecture Structure of the Developed ANNs Models. Applying the RayMan model, the hourly values of PET were calculated covering the examined period 15/06/2005–31/12/2011. Then, the daily maximum and minimum PET values from the 24 hourly values were extracted. Further, the numbers of hours during the day where PET is greater than 41.0°C or less than 4.0°C (Table 1) were estimated.

Two different ANN models were developed. The first, ANN no. 1, was trained to forecast 24 hours ahead the daily maximum and minimum PET value, as well as the number of extreme heat stress hours (PET > 41.0°C) during the next

day, for the warm period of the year (May–September) [36]. The second ANN model, ANN no. 2, was trained to forecast 24 hours ahead the daily maximum and the minimum PET value, as well as the number of the extreme cold stress hours (PET < 4.0°C) during the next day, for the cold period of the year (October–April) [36].

In order to estimate the optimal number of previous days that should be taken into account for the appropriate ANNs training, it is important to formulate an appropriate data set and decide how many days prior to the forecasted day should be included in the training data set. For that purpose, the daily maximum and minimum PET values for the studied period have been organized in a superposed epoch analysis (SPEA) illustrations and are depicted in Figure 4 [50, 51].

The "zero" day (D-0) represents the mean daily maximum or minimum PET values for the warm and the cold period of the year, respectively, when an "exceedance" day (PET > 41.0°C or PET < 4.0°C) occurred in the monitoring site, Galatsi. The other days, named as D-1, D-2, and so forth, represent the mean value of the daily maximum or minimum PET values 1, 2, 3, 4, 5, 6, 7, and 8 days before the exceedance day, respectively. In a same manner, the days named D+1, D+2, and so forth, represent the mean value of the daily maximum or minimum PET values 1, 2, 3, 4, 5, 6, 7, and 8 days after the exceedance day, respectively.

The significance of differences between two sample means was investigated applying the t-statistic, in other words, the difference of two-means test [52]. This test requires that we calculate two means and compare them to see if one is greater than the other. Results showed that there is a significant increase of mean daily PET values three days before the "zero" day, $t_{(0.05,1024)} \geq 1.960$, and $t_{(0.05,1330)} \geq 1.960$ for the warm and the cold period of the year, respectively, at a significant statistical level of $P < 0.05$.

The above results are also depicted in Figure 4, which shows that during the warm period of the year (upper graph), there is a significant increase of daily maximum PET values three days before the "zero" day. The same conclusion is extracted for the cold period of the year (lower graph). It seems that three days before the "zero" day, the daily minimum PET value is reduced.

In other words, when an "exceedance" day (PET > 41.0°C or PET < 4.0°C) occurs, there is a significant trend of the daily maximum and minimum values three days earlier. Furthermore, in both warm and cold periods of the year, it appears that the phenomenon is smoothed out three to four days after the onset of the "exceedance" day.

Taking into consideration the SPEA analysis, the appropriate training data set was created, including data concerning the three days, prior to the forecasted day. Initially, the available data were divided in two data files. The first concerns the warm period of the year (May–September) and the second the cold period of the year (October–April). Two different prognostic ANN models were developed, ANN no. 1 for the warm period of the year and ANN no. 2 model for the cold period of the year. In both cases, the available data sets were divided into two subsets. The first subset included data from the period 2005 to 2010 and used for training the ANN model. A portion of this subset (20%) was used for cross validation during the training process. The second subset included data for 2011 and was used as the testing set for the evaluation of the developed ANN no. 1 and ANN no. 2 models.

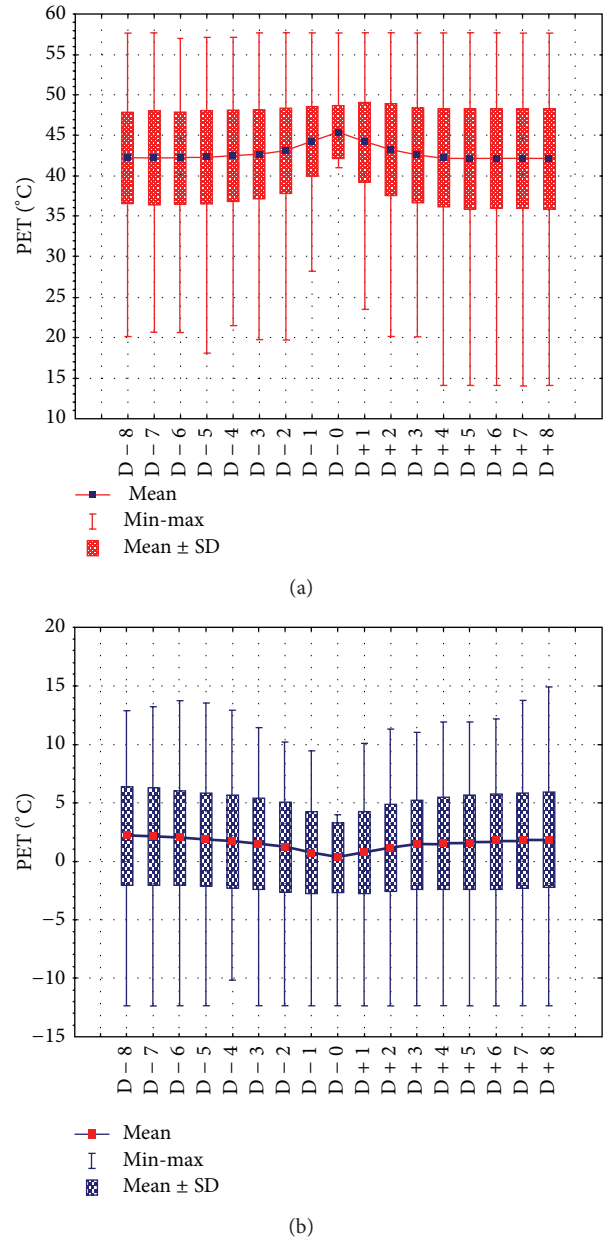

Figure 4: Superposed epoch analysis during the warm period of the year (upper graph) and during the cold period of the year (lower graph).

Table 2 presents the input PEs and the outputs targets for the developed ANN no. 1 and ANN no. 2 forecasting models respectively. The two developed models are feed forward MLP ANNs. They consist of one input layer with 21 PEs, one hidden layer with 4 PEs (hidden neurons) and one output layer with 3 PEs. Also, they have 4 PEs (hidden neurons) in the hidden layer. The transfer function in both ANN no. 1 and ANN no. 2 is the hyperbolic tangent function, and the learning rule in both models is the momentum [31]. The best ANNs structure

Table 2: The input PEs and the output target for the developed ANN no. 1 and ANN no. 2 forecasting models, respectively.

Input Layer (PEs)	Output layer (targets values)
The number of the month (1, 2, 3, . . . , 12)	The maximum and the minimum daily value of PET of the next day, as well as the number of hours during the next day with PET > 41.0°C (ANN no. 1) or PET < 4.0°C (ANN no. 2)
The maximum daily air temperature for each of the three previous days	
The minimum daily air temperature for each of the three previous days	
The maximum daily PET value for each of the three previous days	
The minimum daily PET value for each of the three previous days	
The number of hours with PET > 41.0°C (ANN no. 1) for each of the three previous days or the number of hours with PET < 4.0°C (ANN no. 2) for each of the three previous days	
The persistence factor (PF) for each of the three previous days	
The maximum (ANN no. 1) and the minimum (ANN no. 2) air temperature of the next day (the forecasted day)	

was selected based on a set of exploratory experiments. The aforementioned architecture structure of both ANN no. 1 and ANN no. 2 was selected after the trial-and-error method [53–56].

The persistence factor (PF), which is mentioned in Table 2, is an integer number. The PF is representing the number of consecutive exceedance days (persistence) where the PET value is greater than 41.0°C (warm period of the year) or less than 4.0°C (cold period of the year). For example, PF = 5 means that the given day is the fifth consecutive exceedance day, and PF = 6 means that the given day is the sixth consecutive exceedance day and so on. According to the statistical treatment of the available data, it was found that during the warm period of the year, PF takes values ranging between 1 and 37. This means that 37 consecutive days with daily maximum PET greater than 41.0°C (extreme heat stress) were observed at least one time. During the cold period of the year, PF takes values ranging between 1 and 45, meaning that 45 consecutive days with daily minimum PET less than 4.0°C (extreme cold stress) were observed at least once.

2.5. Statistical Performance Indices. In order to evaluate the results and the predicting performance of the developed models, statistical indices such as the root mean square error (RMSE), the mean bias error (MBE), the coefficient of determination (R^2), and the index of agreement (IA) were used. The coefficient of determination (R^2) provides information about the percentage of the variance that the model is able to explain [57, 58]. The RMSE is a commonly used measure of the differences between the predicted values by a predictable model and the real observed values. The RMSE is used as a single measure that indicates the ability of the model to predict and has the same units as the predicted value. The RMSE is always positive and a zero value is ideal. The MBE provides information on the long-term performance. A low MBE is desirable. Ideally, a zero value of MBE should be obtained. A positive value gives the average amount of overestimation in the calculated values while a negative value underestimates. The coefficient of determination (R^2) is used in cases of statistical models, whose main purpose is the forecast of future outcomes on the basis of other related information. It is the proportion of the variability in a data set that is accounted for, by the statistical model. It provides a measure of how well future outcomes are likely to be predicted by the model. The coefficient values range from zero to one ($0 \leq R^2 \leq 1$). The closer the value is to one, the better and more accurate the prediction is. The index of agreement is a dimensionless measure with values between zero and one ($0 \leq \text{IA} \leq 1$). The IA gives information about how close the predicted values are to the observed ones. When IA = 0, there is no agreement between prediction and observation, while IA = 1 denotes a perfect agreement between prediction and observation.

The accuracy of the proposed prognostic models to predict the "exceedances" days was assessed by using appropriate statistical indices such as the true predicted rate (TPR), the false positive rate (FPR), the false alarm rate (FAR), and the Success Index (SI) [58]. The true predicted rate (TPR) represents the fraction of correct predictions over total exceedances with values from 0.0% to 100.0% and a perfect score equals 100.0%. False positive rate (FPR) represents the fraction of false predictions over total nonexceedances with values from 0.0% to 100.0% and a perfect score equals 0.0%. False alarm rate (FAR) represents the fraction of false predictions over total exceedances with values from 0.0% to 100.0% and a perfect score equals 0.0%. Finally, SI represents the fraction of correct predictions over total predictions with values from 0.0% to 100.0% and a perfect score equals 100.0%.

3. Results and Discussion

Initially, the hourly values of PET during the examined period 15/6/2005–31/12/2005 were calculated applying the RayMan model. Figure 5 depicts the time series of hourly PET values, along with extreme heat (PET > 41°C) and cold stress (PET < 4°C) thresholds, for the period 15/06/2005–31/12/2011.

According to the statistical treatment data analysis and Figure 5, during the warm period of the year, PET > 41.0°C (extreme heat stress) appeared in 10.0% of the examined

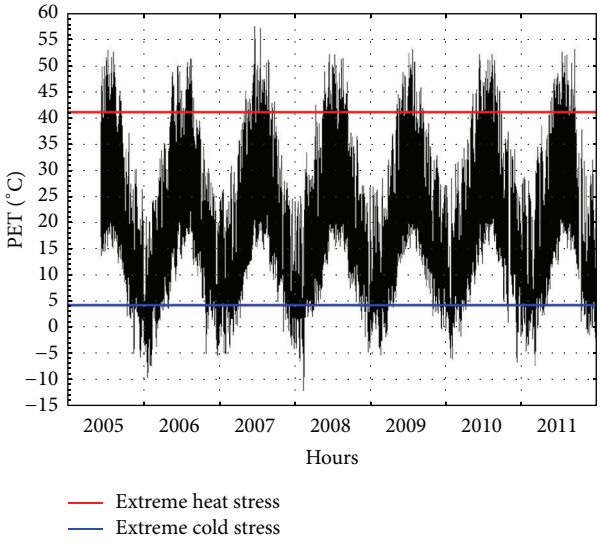

Figure 5: The time series of hourly PET values along with extreme heat (PET > 41°C) and cold stress (PET < 4°C) thresholds, for the period 15/06/2005–31/12/2011.

hours (2,449 of the 24,609 available hours) present, against 22.8% of the hours during the cold period of the year (7,320 of the 32,095 available hours) with PET < 4.0°C (extreme cold stress). Finally, a comfort human thermal sensation appeared in 81.8% of the hours during the years. This indicates that in general, the bioclimatic conditions in the examined monitoring site could be characterized as human healthy comfort conditions.

As mentioned above, the whole data set was divided into two subsets. The first subset concerns the warm period of the year (May–September) and the second one the cold period of the year (October–April). Further below, the results with respect to the warm and cold period of the year are presented and discussed separately.

3.1. Warm Period of the Year (May–September). The data set of the year 2011 was absolutely unknown to the trained ANN model ANN no. 1. Thus, the model was then fed with the appropriate data in order to forecast 24 hours ahead the daily maximum and minimum PET value, as well as the number of hours during the next day when PET is greater than 41.0°C (extreme heat stress). Then, the forecasted values were compared with the observed ones.

Figure 6 depicts the observed versus the predicted daily maximum PET values (a), the scatter plot between the observed versus the predicted daily maximum PET values (b), the differences between the observed and the predicted daily maximum PET values (c), and the histogram with the distribution of the absolute differences between the observed and the predicted daily maximum PET values (d) . Further, Figure 7 illustrates the same as Figure 6, but with respect to daily minimum PET values. Table 3 presents the values of the statistical indices used for the evaluation of the forecasting ability of the developed ANN no. 1 model.

According to Figures 6 and 7 and Table 3, the developed ANN no. 1 prognostic model presents a very good forecasting ability. Specifically, concerning, on one hand, the prediction of the daily maximum PET value, the coefficient of determination equals $R^2 = 0.831$, which means that the model is able to explain 83.1% of the variability of the daily maximum PET 24 hours ahead. On the other hand, $R^2 = 0.910$ with respect to the prediction of the daily minimum PET value, meaning that the model is able to explain 91.0% of the variability of the daily minimum PET, 24 hours ahead. Besides, 70.0% of the absolute differences between the observed and predicted daily maximum PET values range between −3.0°C and +3.0°C, against 98.0% of the absolute differences between the observed and predicted daily minimum PET values. The same conclusions can be derived concerning the prognosis of the number of the hours during the next day when PET is greater than 41.0°C. Figure 8 presents the observed versus the predicted hours with PET > 41.0°C (a), the scatter plot between the observed and predicted hours with PET > 41.0°C (b), the differences between the observed and the predicted hours with PET > 41.0°C (c), and the histogram with the distribution of the absolute differences between the observed and the predicted hours with PET > 41.0°C (d). The coefficient of determination equals $R^2 = 0.796$, meaning that the developed model is able to explain 79.6% of the variability of the hours with extreme heat stress one day ahead. Finally, 96.0% of the absolute differences between the observed and the predicted hours with PET > 41.0°C, range between −3.0 hours and +3.0 hours. All the aforementioned indicate that the developed ANN no. 1 prognostic model, after its appropriate training phase, presents a very satisfactory forecasting ability at a significant statistical level of $P < 0.01$.

Table 3: Statistical indices for the evaluation of the forecasting ability of the developed ANN no. 1 forecasting model. One day ahead prognosis. Warm period of 2011.

	RMSE	MBE	R^2	IA
Maximum PET value (°C)	2.9°C	−0.5°C	0.831	0.950
Minimum PET value (°C)	1.2°C	−0.2°C	0.910	0.975
Hours with PET > 41.0°C	1.3 hrs	−0.3 hrs	0.796	0.938

Table 4 presents the values of the statistical indices for the evaluation of the forecasting ability of the model in order to predict correctly the exceedances days, in other words, the days with daily maximum PET greater than 41.0°C (extreme heat stress). Concerning the ability of the model to forecast whether the next day is going to be a day with extreme heat stress sensation (exceedance day) and according to Table 4, the true predicted rate is TPR = 85.9%, which indicates that the fraction of the correct predictions over total exceedances is forecasted by the model at a rate of 85.9%. Also, FPR = 4.0% which means that the fraction of false predictions over total nonexceedances is quite small. Furthermore, FAR = 4.3%, meaning that the fraction of false predictions over total exceedances is very small. Finally, SI = 90.8%, which indicates that the fraction of correct predictions over total predictions is about 90.8%. In other words, the developed ANN no. 1 model is able to forecast at a rate of 90.8% whether the next day is going to be an exceedance day or not. As far as the hours with extreme heat stress (PET > 41.0°C), one day ahead, are

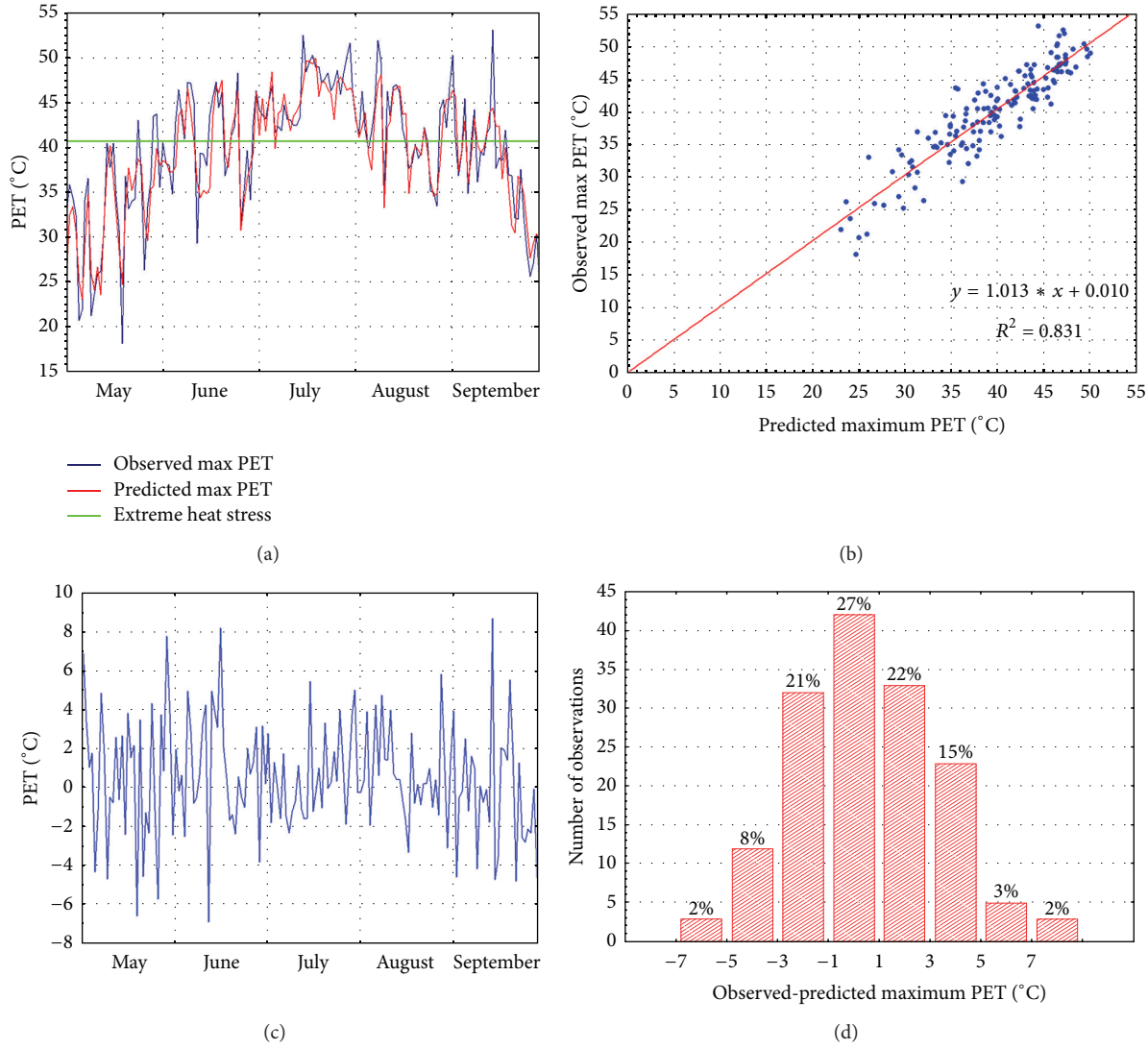

Figure 6: Observed versus predicted daily maximum PET values (a); scatter plot between observed versus predicted daily maximum PET values (b); observed minus predicted daily maximum PET values (c) and histogram with the absolute differences between the observed and the predicted daily maximum PET values (d). One day ahead prognosis. Warm period of 2011.

concerned, SI was found equal to 84.3%, indicating that the fraction of correct predictions over total predictions is about 84.3%.

The findings of the analysis during the warm period of the year revealed that the combination of the prognosis of the daily maximum and minimum PET values with the prognosis of the number of extreme heat stress hours simultaneously, one day ahead, gives the ability for a good monitoring of what is expected to happen during the next day.

3.2. Cold Period of the Year (October–April). Following the same reasoning, the prognostic ability of the developed ANN no. 2 model is presented. The ANN no. 2 model was appropriately trained in order to predict, for the cold period of the year, the daily maximum and minimum PET values, as well as the number of extreme cold stress hours during the next day.

Table 4: Statistical indices for the evaluation of the forecasting ability of the developed ANN no. 1 forecasting model to predict the number of hours during the day when PET > 41.0°C (extreme heat stress). One day ahead prognosis. Warm period of 2011.

	TPR (%)	FPR (%)	FAR (%)	SI (%)
Day with maximum PET > 41.0°C	85.9	4.0	4.3	90.8
Day with extreme heat hours	80.0	9.5	7.7	84.3

Figure 9 depicts, for the cold period of the year, the observed versus the predicted daily maximum PET values (a), the scatter plot between the observed versus the predicted daily maximum PET values (b), the differences between the observed and the predicted daily maximum PET values (c), and the histogram with the distribution of the absolute differences between the observed and the predicted daily

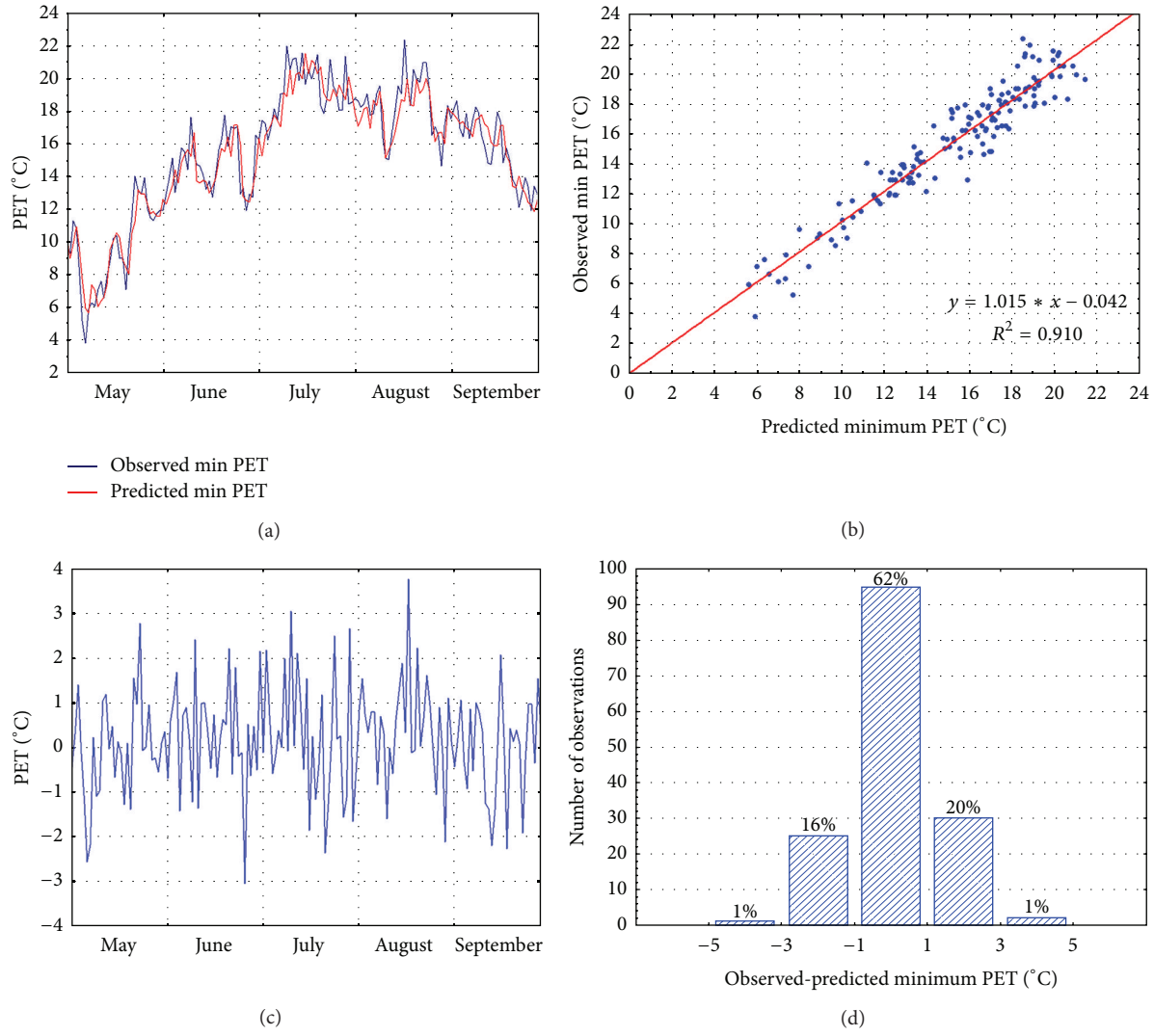

Figure 7: Observed versus predicted daily minimum PET values (a); scatter plot between observed versus predicted daily minimum PET values (b); observed minus predicted minimum daily PET values (c) and histogram with the absolute differences between the observed and the predicted minimum daily PET values (d). One day ahead prognosis. Warm period of 2011.

Table 5: Statistical indices for the evaluation of the forecasting ability of the developed ANN no. 2 forecasting model. One day ahead prognosis. Cold period of 2011.

	RMSE	MBE	R^2	IA
Maximum PET value (°C)	3.7°C	−0.7°C	0.819	0.943
Minimum PET value (°C)	0.9°C	+0.0°C	0.940	0.984
Hours with PET < 4.0°C	2.3 hrs	+0.2 hrs	0.896	0.972

maximum PET values (d). Figure 10 depicts the same as Figure 9, but with respect to daily minimum PET values. Table 5 presents the values of the statistical indices used for the evaluation of the forecasting ability of the developed ANN no. 2 model.

According to Figures 9 and 10 and Table 5, the developed ANN no. 2 prognostic model shows a very good forecasting ability. Concerning the prediction of the daily maximum PET value, during the cold period of the year, the coefficient of determination equals $R^2 = 0.819$, which means that the model is able to explain 81.9% of the variability of the daily maximum PET value, 24 hours ahead. Further, with respect to the prediction of the daily minimum PET value, R^2 equals to 0.940, meaning that the model is able to explain 94.0% of the variability of the daily minimum PET value, 24 hours ahead. Also, 59.7% of the absolute differences between the observed and predicted daily maximum PET values range between −3.0°C and +3.0°C, against 100.0% of the absolute differences between the observed and predicted daily minimum PET values. The same conclusions can be derived concerning the prognosis of the number of the hours during the next day with extreme cold stress (PET < 4.0°C). Figure 11 presents the observed versus the predicted hours with PET < 4.0°C (a), the scatter plot between the observed and predicted hours with PET < 4.0°C (b), the differences between the observed and the predicted hours with PET < 4.0°C (c), and the histogram with the distribution of the absolute differences

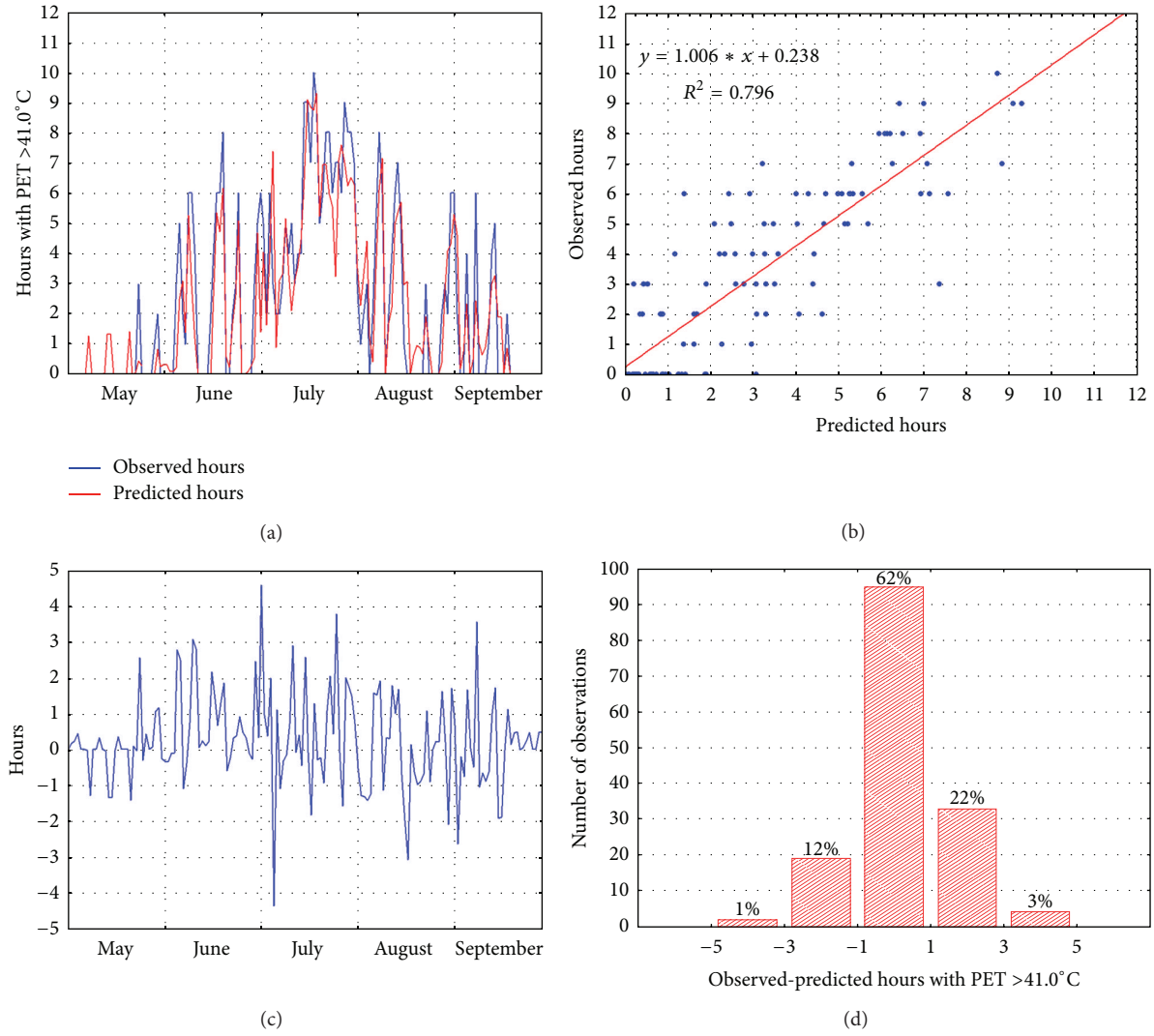

Figure 8: Observed versus predicted hours with PET > 41.0°C (a); scatter plot between the observed and predicted hours with PET > 41.0°C (b); observed minus predicted hours with PET > 41.0°C (c) and histogram with the absolute differences between the observed and the predicted hours with PET > 41.0°C (d). One day ahead prognosis. Warm period of 2011.

between the observed and the predicted hours with PET < 4.0°C (d). The coefficient of determination equals R^2 = 0.896, which means that the developed model is able to explain 89.6% of the variability of the hours with extreme cold stress, one day ahead. Further, 82.6% of the absolute differences between the observed and the predicted hours with PET < 4.0°C range between −3.0 hours and +3.0 hours. All the aforementioned indicate that the developed ANN no. 2 prognostic model, after its appropriate training phase, presents a very satisfactory forecasting ability at a significant statistical level of $P < 0.01$.

Table 6 presents the values of the statistical indices for the evaluation of the forecasting ability of the developed model ANN no. 2, in order to predict correctly the exceedances days, in other words, the days with minimum PET value less than 4.0°C (extreme cold stress hours). Concerning the ability of the model to forecast whether the next day is going to be a day with extreme cold stress (exceedance day) and according to Table 6, the true predicted rate is TPR = 92.8%, which indicates that the fraction of the correct predictions over total exceedances is forecasted by the model at a rate of 92.8%. Also, FPR = 7.9%, which means that the fraction of false predictions over total nonexceedances is quite small.

Table 6: Statistical indices for the evaluation of the forecasting ability of the developed ANN no. 2 forecasting model to predict the number of hours during the day when PET < 4.0°C (extreme cold stress). One day ahead prognosis. Cold period of 2011.

	TPR (%)	FPR (%)	FAR (%)	SI (%)
Day with maximum PET < 4.0°C	92.8	7.9	3.8	92.5
Day with extreme cold hours	98.6	31.7	12.8	89.1

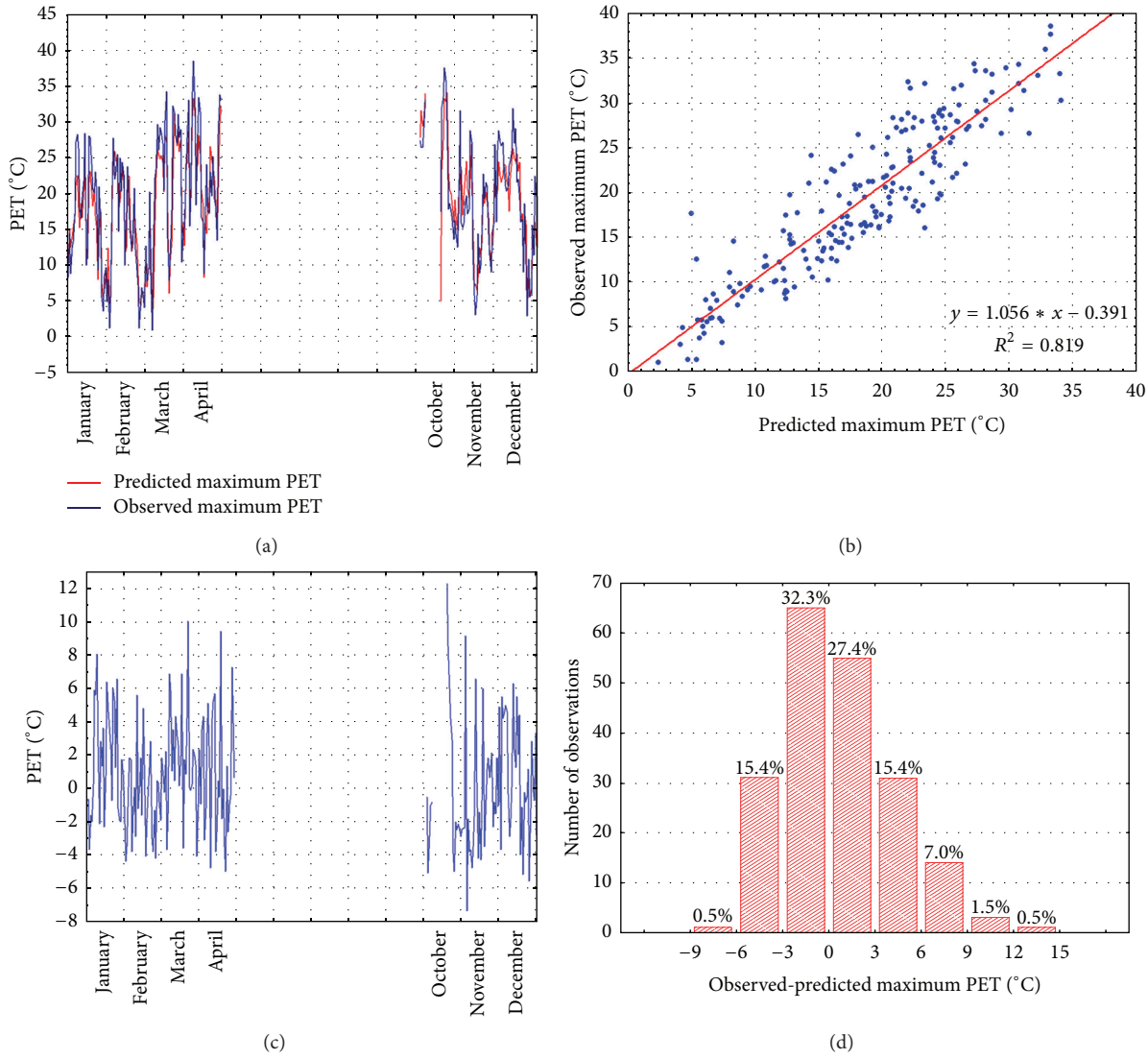

Figure 9: Observed versus predicted daily maximum PET values (a); scatter plot between observed versus predicted daily maximum PET values (b); observed minus predicted daily maximum PET values (c) and histogram with the absolute differences between the observed and the predicted daily maximum PET values (d). One day ahead prognosis. Cold period of 2011.

Furthermore, FAR = 3.8%, meaning that the fraction of false predictions over total exceedances is very small. Finally, SI = 92.5%, which indicates that the fraction of correct predictions over total predictions is about 92.5%. In other words, the developed ANN no. 2 model is able to forecast at a rate of 92.5% whether the next day will be an exceedance day or not. Regarding the hours with extreme cold stress (PET < 4.0°C) for the next day, SI equals to 89.1%, which indicates that the fraction of correct predictions over total predictions is about 89.1%.

From the performed analysis during the cold period of the year, it is concluded that the combination of the prognosis of the daily maximum and minimum PET values with the prognosis of the number of the extreme cold stress hours simultaneously, one day ahead, gives the ability for a good monitoring of what is expected to happen during the next day.

4. Conclusions

The main objective of this work was to develop prognostic models, using the artificial neural networks topology, in order to forecast 24 hours ahead the biometeorological human conditions for both the warm and the cold period of the year. For that purpose, the hourly values of the well-known human thermal index PET were calculated for the time period from 15/06/2005 till 31/12/2011 in an open space area of Galatsi, which is located inside the urban environment of the capital city Athens, Greece. The appropriate calculation of the hourly PET values was carried out using the RayMan model.

Statistical treatment of the available data showed that during the calendar year, both extreme heat and cold stress hours appear. During the warm period of the year, 10.0% of the examined hours present extreme heat stress (PET > 41.0°C). Respectively, 22.8% of the hours during the cold

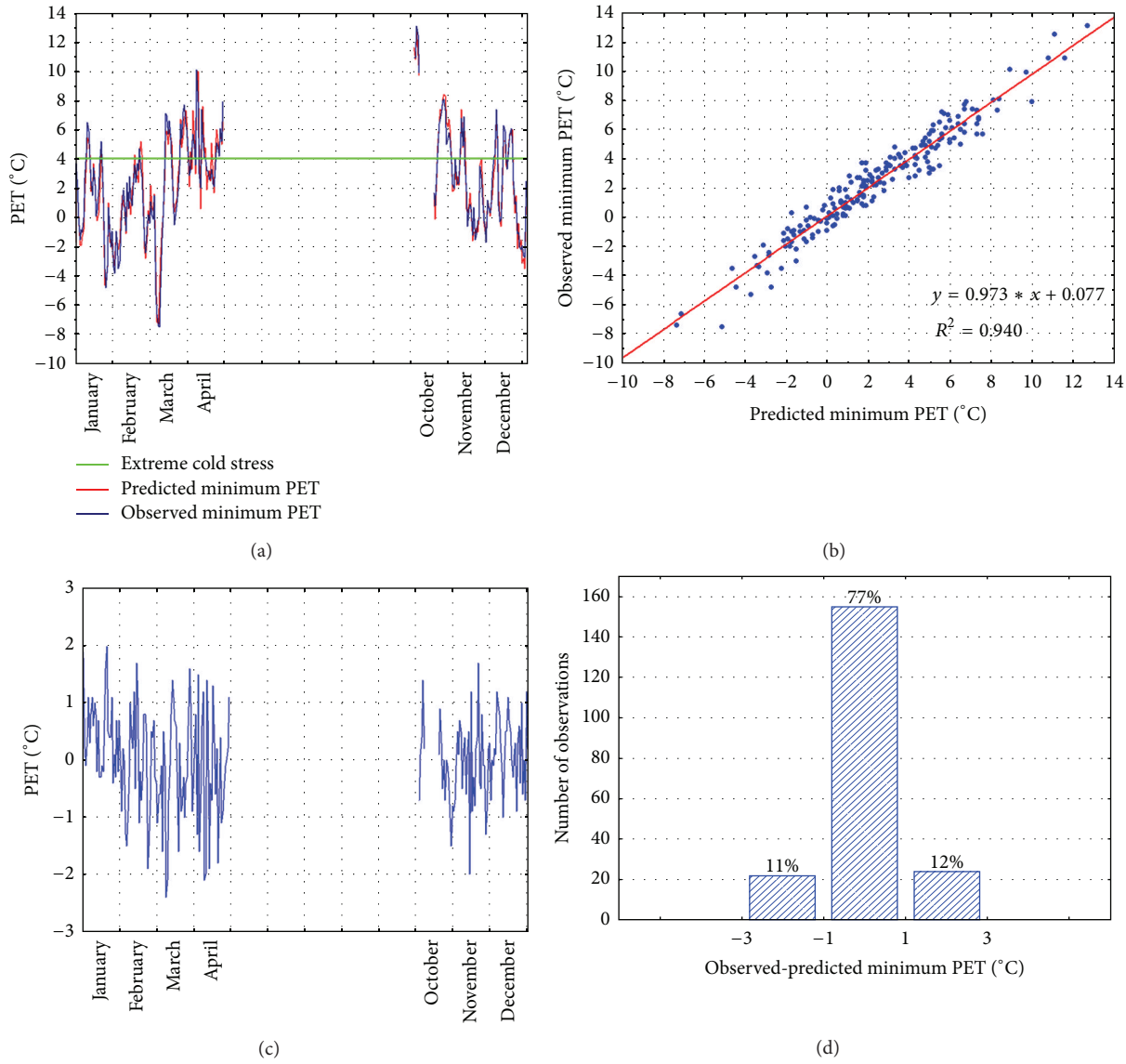

FIGURE 10: Observed versus predicted daily minimum PET values (a); scatter plot between observed versus predicted daily minimum PET values (b); observed minus predicted daily minimum PET values (c) and histogram with the absolute differences between the observed and the predicted daily minimum PET values (d). One day ahead prognosis. Cold period of 2011.

period of the year present extreme cold stress (PET < 4.0°C). Finally, 81.8% of the hours during the calendar year present a comfort human thermal sensation (18.0°C < PET < 29.0°C), indicating that, in general, the bioclimatic conditions in the examined monitoring site are healthy comfort conditions for a humans.

As far as the prognostic ability of the two developed models (ANN no. 1 and ANN no. 2) is concerned, the values of appropriate statistical evaluation indices indicate a very satisfactory forecasting ability at a significant statistical level of $P < 0.01$. The developed ANN models show a satisfactory and sufficient prognostic ability in order to forecast the daily maximum and minimum PET value, as well as the number of extreme heat or cold stress hours for the next day. The innovation of this work consists of the reasons listed below.

(a) The ANNs modeling is applied instead of traditional statistical modeling.

(b) The biometeorological conditions were estimated applying the RayMan model and using the PET index, a modern index which can describe very precisely the human thermal comfort-discomfort conditions.

(c) The developed forecasting models seem to be able to forecast 24 hours ahead not only the human thermal comfort-discomfort levels but also the persistence of extreme heat or cold stress, depending on the period of the year. Thus, in an operational form, it will be a very important tool for the state to take the appropriate measures to avoid negative results

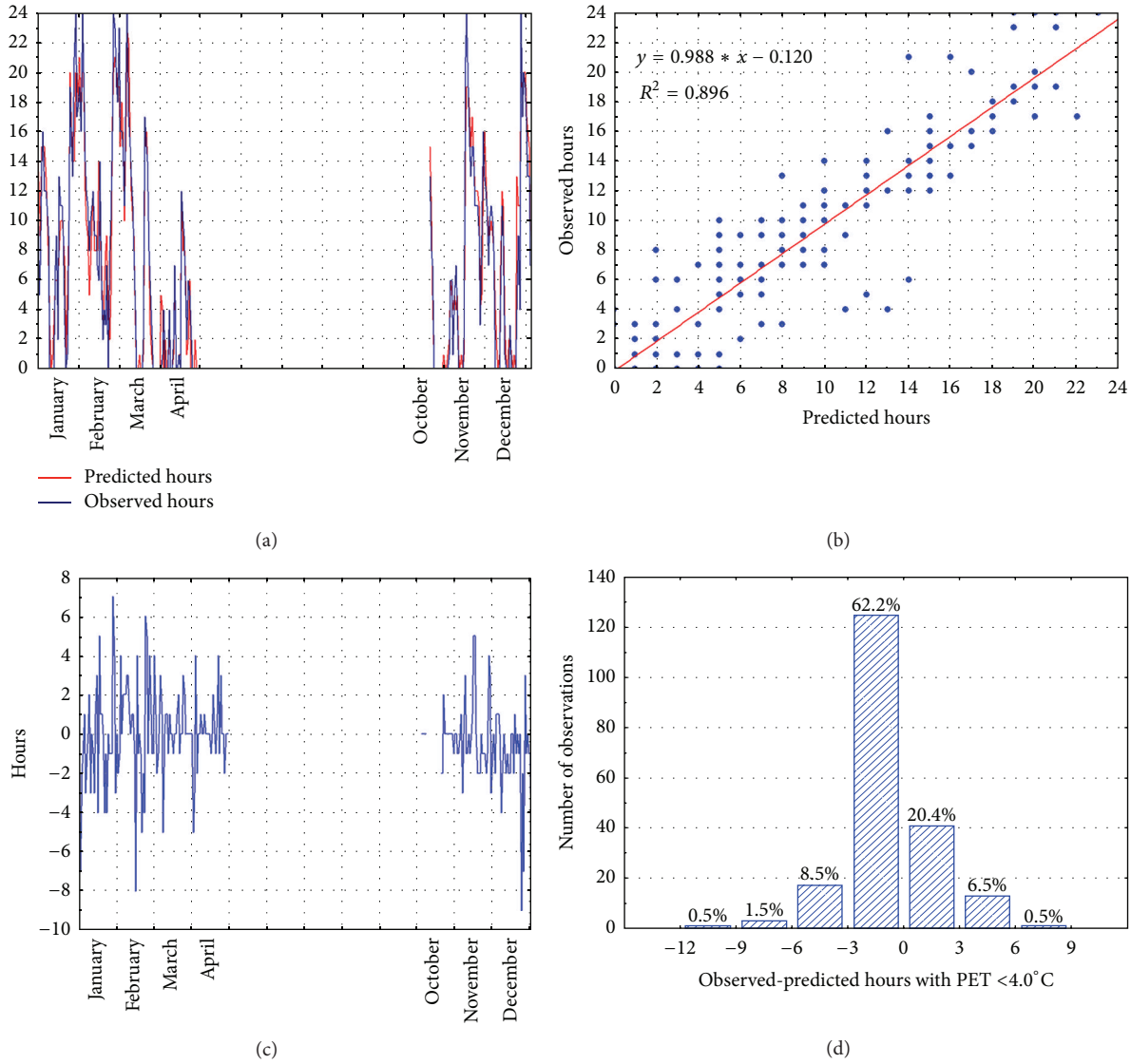

Figure 11: Observed versus predicted hours with PET < 4.0°C (a); scatter plot between the observed and predicted hours with PET < 4.0°C (b); observed minus predicted hours with PET < 4.0°C (c) and histogram with the absolute differences between the observed and the predicted hours with PET < 4.0°C (d). One day ahead prognosis. Cold period of 2011.

for the population due to extreme meteorological circumstances.

(d) Finally, the developed ANN models (ANN no. 1 and ANN no. 2) are able to forecast the extreme (maximum and minimum) daily values of PET, as well as the persistence of the phenomenon simultaneously, providing real time prognosis.

According to authors' opinion, furthermore investigation is necessary in order to increase the prognostic ability of the proposed ANN models, as well as to extend the prediction time at 48 or 72 hours ahead. In that way, a forecasting and a protection monitoring network for the public health would be developed. Also, the state would obtain prior warning of extreme energy demand due to extreme heat waves within the warm period of the year.

References

[1] I. Tselepidaki, M. Santamouris, C. Moustris, and G. Poulopoulou, "Analysis of the summer discomfort index in Athens, Greece, for cooling purposes," *Energy and Buildings*, vol. 18, no. 1, pp. 51–56, 1992.

[2] M. Santamouris, "Natural cooling techniques," in *Proceedings of the Passive Cooling Conference*, EEC, DG, Ispra, Italy, 1990.

[3] M. Caudill and C. Butler, *Understanding Neural Networks*, MIT Press, Cambridge, Mass, USA, 1992.

[4] B. Givoni, *Climatic Considerations in Building and Urban Design*, Van Nostrond Reinholds, New York, NY, USA, 1998.

[5] S. Becker, O. Potchter, and Y. Yaakov, "Calculated and observed human thermal sensation in an extremely hot and dry climate," *Energy and Buildings*, vol. 35, no. 8, pp. 747–756, 2003.

[6] S. Conti, P. Meli, G. Minelli et al., "Epidemiologic study of mortality during the Summer 2003 heat wave in Italy," *Environmental Research*, vol. 98, no. 3, pp. 390–399, 2005.

[7] A. Matzarakis, H. Mayer, and M. G. Iziomon, "Applications of a universal thermal index: physiological equivalent temperature," *International Journal of Biometeorology*, vol. 43, no. 2, pp. 76–84, 1999.

[8] I. Charalampopoulos, I. Tsiros, A. Chronopoulou-Sereli, and A. Matzarakis, "Analysis of thermal bioclimate in various urban configurations in Athens, Greece," *Urban Ecosystems*, vol. 16, no. 2, pp. 217–233, 2013.

[9] M. Bruse and H. Fleer, "Simulating surface-plant-air interactions inside urban environments with a three dimensional numerical model," *Environmental Modelling & Software*, vol. 13, no. 3-4, pp. 373–384, 1998.

[10] A. Matzarakis, F. Rutz, and H. Mayer, "Modelling radiation fluxes in simple and complex environments—application of the RayMan model," *International Journal of Biometeorology*, vol. 51, no. 4, pp. 323–334, 2007.

[11] R. Emmanuel, H. Rosenlund, and E. Johansson, "Urban shading—a design option for the tropics? A study in Colombo, Sri Lanka," *International Journal of Climatology*, vol. 27, no. 14, pp. 1995–2004, 2007.

[12] A. Matzarakis, M. De Rocco, and G. Najjar, "Thermal bioclimate in Strasbourg—the 2003 heat wave," *Theoretical and Applied Climatology*, vol. 98, no. 3-4, pp. 209–220, 2009.

[13] S. Muthers, A. Matzarakis, and E. Koch, "Summer climate and mortality in Vienna—a human-biometeorological approach of heat-related mortality during the heat waves in 2003," *Wiener Klinische Wochenschrift*, vol. 122, no. 17-18, pp. 525–531, 2010.

[14] F. Benvenuto and A. Marani, "Neural networks for environmental problems: data quality control and air pollution nowcasting," *Global Nest Journal*, vol. 2, no. 3, pp. 281–292, 2000.

[15] D. Melas, I. Kioutsioukis, and I. C. Ziomas, "Neural network model for predicting peak photochemical pollutant levels," *Journal of the Air & Waste Management Association*, vol. 50, no. 4, pp. 495–501, 2000.

[16] I. X. Tsiros and I. F. Dimopoulos, "A preliminary study of the application of some predictive modeling techniques to assess atmospheric mercury emissions from terrestrial surfaces," *Journal of Environmental Science and Health, Part A*, vol. 38, no. 11, pp. 2495–2508, 2003.

[17] I. F. Dimopoulos, I. X. Tsiros, K. Serelis, and A. Chronopoulou, "Combining neural network models to predict spatial patterns of airborne pollutant accumulation in soils around an industrial point emission source," *Journal of the Air & Waste Management Association*, vol. 54, no. 12, pp. 1506–1515, 2004.

[18] P. Perez and J. Reyes, "An integrated neural network model for PM10 forecasting," *Atmospheric Environment*, vol. 40, no. 16, pp. 2845–2851, 2006.

[19] D. Wang and W.-Z. Lu, "Forecasting of ozone level in time series using MLP model with a novel hybrid training algorithm," *Atmospheric Environment*, vol. 40, no. 5, pp. 913–924, 2006.

[20] K. I. Chronopoulos, I. X. Tsiros, I. F. Dimopoulos, and N. Alvertos, "An application of artificial neural network models to estimate air temperature data in areas with sparse network of meteorological stations," *Journal of Environmental Science and Health, Part A*, vol. 43, no. 14, pp. 1752–1757, 2008.

[21] J. A. Sánchez Mesa, C. Galán, and C. Hervás, "The use of discriminant analysis and neural networks to forecast the severity of the Poaceae pollen season in a region with a typical Mediterranean climate," *International Journal of Biometeorology*, vol. 49, no. 6, pp. 355–362, 2005.

[22] A. Grinn-Gofroń and A. Strzelczak, "Artificial neural network models of relationships between Alternaria spores and meteorological factors in Szczecin (Poland)," *International Journal of Biometeorology*, vol. 52, no. 8, pp. 859–868, 2008.

[23] G. Mihalakakou, M. Santamouris, N. Papanikolaou, C. Cartalis, and A. Tsangrassoulis, "Simulation of the urban heat island phenomenon in Mediterranean climates," *Pure and Applied Geophysics*, vol. 161, no. 2, pp. 429–451, 2004.

[24] L. Gao and H. Bai, "The prediction of PMV index based on neural networks," in *Proceedings of the International Conference on Energy and the Environment*, vol. 2, pp. 1306–1309, December 2003.

[25] A. S. W. Wong, Y. Li, P. K. W. Yeung, and P. W. H. Lee, "Neural network predictions of human psychological perceptions of clothing sensory comfort," *Textile Research Journal*, vol. 73, no. 1, pp. 31–37, 2003.

[26] Y.-Z. Ji, G.-B. Tu, and X.-J. Wang, "Feasibility of artificial neural network on thermal comfort research," *Journal of Tianjin University Science and Technology*, vol. 37, no. 4, pp. 331–335, 2004.

[27] S. Atthajariyakul and T. Leephakpreeda, "Neural computing thermal comfort index for HVAC systems," *Energy Conversion and Management*, vol. 46, no. 15-16, pp. 2553–2565, 2005.

[28] G. Liu, J. Zhou, G. Wang, S. Hu, and R. Liu, "Human thermal comfort assessment model under lower-pressure environment based on BP network," in *Proceedings of the International Conference on Information Engineering and Computer Science (ICIECS '09)*, Wuhan, China, December 2009.

[29] K. P. Moustris, I. C. Ziomas, and A. G. Paliatsos, "24 hours in advance forecasting of thermal comfort-discomfort levels during the hot period of the year at representative locations of Athens city, Greece," *Fresenius Environmental Bulletin*, vol. 18, no. 5, pp. 601–608, 2009.

[30] K. P. Moustris, I. X. Tsiros, I. C. Ziomas, and A. G. Paliatsos, "Artificial neural network models as a useful tool to forecast human thermal comfort using microclimatic and bioclimatic data in the great Athens area (Greece)," *Journal of Environmental Science and Health, Part A*, vol. 45, no. 4, pp. 447–453, 2010.

[31] P. A. Vouterakos, K. P. Moustris, A. Bartzokas, I. C. Ziomas, P. T. Nastos, and A. G. Paliatsos, "Forecasting the discomfort levels within the greater Athens area, Greece using artificial neural networks and multiple criteria analysis," *Theoretical and Applied Climatology*, vol. 110, no. 3, pp. 329–343, 2012.

[32] B. D. Katsoulis and G. A. Theoharatos, "Indications of the urban heat island in Athens, Greece," *Journal of Climate & Applied Meteorology*, vol. 24, no. 12, pp. 1296–1302, 1985.

[33] I. Livada, M. Santamouris, K. Niachou, N. Papanikolaou, and G. Mihalakakou, "Determination of places in the great Athens area where the heat island effect is observed," *Theoretical and Applied Climatology*, vol. 71, no. 3-4, pp. 219–230, 2002.

[34] G. Mihalakakou, H. A. Flocas, M. Santamouris, and C. G. Helmis, "Application of neural networks to the simulation of the heat island over Athens, Greece, using synoptic types as a predictor," *Journal of Applied Meteorology*, vol. 41, no. 5, pp. 519–527, 2002.

[35] M. Santamouris, K. Paraponiaris, and G. Mihalakakou, "Estimating the ecological footprint of the heat island effect over Athens, Greece," in *Proceedings of the International Conference Passive and Low Energy Cooling for the Built Environment*, pp. 113–116, Santorini, Greece, 2005.

[36] K. P. Moustris, G. T. Proias, I. K. Larissi, P. T. Nastos, and A. G. Paliatsos, "Bioclimatic and air quality conditions in the greater

Athens area, Greece, during the warm period of the year: trends, variability and persistence," *Fresenius Environmental Bulletin*, vol. 21, no. 8, pp. 2368–2374, 2012.

[37] "The Hydrological Observatory of Athens," 2012, http://hoa.ntua.gr/.

[38] P. T. Nastos and A. Matzarakis, "The effect of air temperature and human thermal indices on mortality in Athens, Greece," *Theoretical and Applied Climatology*, vol. 108, no. 3-4, pp. 591–599, 2012.

[39] H. Mayer and P. Höppe, "Thermal comfort of man in different urban environments," *Theoretical and Applied Climatology*, vol. 38, no. 1, pp. 43–49, 1987.

[40] P. Höppe, "The physiological equivalent temperature—a universal index for the biometeorological assessment of the thermal environment," *International Journal of Biometeorology*, vol. 43, no. 2, pp. 71–75, 1999.

[41] A. Matzarakis and H. Mayer, "Another kind of environmental stress: thermal stress," *WMO Newsletter*, vol. 18, pp. 7–10, 1996.

[42] M. A. Nelson, M. D. Williams, D. Zajic, E. R. Pardyjak, and M. J. Brown, "Evaluation of an urban vegetative canopy scheme and impact on plume dispersion," in *Proceedings of the 89th American Meteorological Society Annual Meeting*, Phoenix, Ariz, USA, 2009.

[43] R. W. Macdonald, "Modelling the mean velocity profile in the urban canopy layer," *Boundary-Layer Meteorology*, vol. 97, no. 1, pp. 25–45, 2000.

[44] "Estimate wind speed at a height above your measurement height," 2013, http://www.baranidesign.com/wind-height/.

[45] W. S. McCulloch and W. Pitts, "A logical calculus of the ideas immanent in nervous activity," *The Bulletin of Mathematical Biophysics*, vol. 5, no. 4, pp. 115–133, 1943.

[46] R. Hect-Nielsen, *Neurocomputing*, Addison-Wesley, Reading, Mass, USA, 1990.

[47] P. Viotti, G. Liuti, and P. Di Genova, "Atmospheric urban pollution: applications of an Artificial Neural Network (ANN) to the city of Perugia," *Ecological Modelling*, vol. 148, no. 1, pp. 27–46, 2002.

[48] R. Hect-Nielsen, *Neurocomputing*, Addison-Wesley, Reading, Mass, USA, 1991.

[49] G. Corani and S. Barazzeta, "First results in the prediction of particulate matter in the Milan area," in *Proceedings of the 9th International Conference on Harmonisation within Atmospheric Dispersion Modelling for Regulatory Purposes*, vol. 1, pp. 365–369, Garmisch-Partenkirchen, Germany, 2004.

[50] H. A. Panofsky and G. W. Brier, *Some Applications of Statistics to Meteorology*, Pennsylvania State University, University Park, Pa, USA, 1968.

[51] Y. P. Singh and B. Badruddin, "Statistical considerations in superposed epoch analysis and its applications in space research," *Journal of Atmospheric and Solar*, vol. 68, no. 7, pp. 803–813, 2006.

[52] D. W. Zimmerman, "Correcting two-sample z and t tests for correlation: an alternative to one-sample tests on difference scores," *Psicológica*, vol. 33, pp. 391–418, 2012.

[53] G. Spellman, "An application of artificial neural networks to the prediction of surface ozone concentrations in the United Kingdom," *Applied Geography*, vol. 19, no. 2, pp. 123–136, 1999.

[54] A. Elkamel, S. Abdul-Wahab, W. Bouhamra, and E. Alper, "Measurement and prediction of ozone levels around a heavily industrialized area: a neural network approach," *Advances in Environmental Research*, vol. 5, no. 1, pp. 47–59, 2001.

[55] R. S. Ettouney, F. S. Mjalli, J. G. Zaki, M. A. El-Rifai, and H. M. Ettouney, "Forecasting of ozone pollution using artificial neural networks," *Management of Environmental Quality*, vol. 20, no. 6, pp. 668–683, 2009.

[56] A. Mahapatra, "Prediction of daily ground-level ozone concentration maxima over New Delhi," *Environmental Monitoring and Assessment*, vol. 170, no. 1–4, pp. 159–170, 2010.

[57] M. Kolehmainen, H. Martikainen, and J. Ruuskanen, "Neural networks and periodic components used in air quality forecasting," *Atmospheric Environment*, vol. 35, no. 5, pp. 815–825, 2001.

[58] K. P. Moustris, I. C. Ziomas, and A. G. Paliatsos, "3-day-ahead forecasting of regional pollution index for the pollutants NO_2, CO, SO_2, and O_3 using artificial neural networks in Athens, Greece," *Water, Air, & Soil Pollution*, vol. 209, no. 1–4, pp. 29–43, 2010.

Hindawi Publishing Corporation
Advances in Meteorology
Volume 2013, Article ID 964904, 7 pages
http://dx.doi.org/10.1155/2013/964904

Research Article

Pedestrian Exposure to Air Pollution in Cities: Modeling the Effect of Roadside Trees

Jorge Humberto Amorim, Joana Valente, Pedro Cascão, Vera Rodrigues, Cláudia Pimentel, Ana I. Miranda, and Carlos Borrego

CESAM & Department of Environment and Planning, University of Aveiro, 3810-193 Aveiro, Portugal

Correspondence should be addressed to Jorge Humberto Amorim; amorim@ua.pt

Received 3 May 2013; Revised 28 August 2013; Accepted 2 September 2013

Academic Editor: Panagiotis Nastos

The exposure of students to traffic-emitted carbon monoxide (CO) in their daily walk to school is evaluated, with a particular emphasis on the effect of trees and route choice. The study is focused on the city centre of Aveiro, in central Portugal. Time evolution of the georeferenced location of an individual is tracked with a GPS for different alternative walking routes to a school. Spatial distribution of CO concentration is simulated with a computational fluid dynamics (CFD) model. An exposure model is developed that associates the georeferenced location of the student with the computed air quality levels (at an average breathing height) for that specific grid cell. For each individual, the model calculates the instantaneous exposure at each time frame and the mean value for a given period. Results show a general benefit induced by the trees over the mean exposure of the student in each route. However, in the case of instantaneous exposure values, this is not consistent along the entire period. Also, the variability of the estimated exposure values indicates the potential error that can be committed when using a single value of air quality as a surrogate of air pollution exposure.

1. Introduction

According to the United Nations Environment Programme (UNEP) information in 2009 [1], at least 1 billion people are exposed to outdoor air pollution that exceeds the air quality standards of the World Health Organization (WHO). Poor air quality in urban areas, mainly associated with the transportation sector, has been directly linked to almost 0.8 million premature deaths annually, especially in sensitive groups as children [1].

In urban areas, motor vehicles are a significant source of air pollution, and, despite the achieved technological progress in reducing motor emissions, there is a continuous growth in the world's motor-vehicle fleet and consequently an increase in the total traffic-related emissions. Motor vehicles emit large quantities of air pollutants (such as carbon monoxide (CO), hydrocarbons (HC), nitrogen oxides (NO_x), particulate matter (PM), benzene, formaldehyde, and acetaldehyde) that have a negative impact on human health and contribute to the formation of by-products such as ozone (O_3) and secondary aerosols. Noncombustion emissions from these vehicles should also be taken into account since road dust, tire, and break wear contain chemical compounds that may pose risk to human health. Due to the high amount of air pollutants released by traffic and the difficulty in quantifying them, taking all into account, it is common to use traffic-pollutant surrogates such as CO, NO_2, or benzene in exposure studies [2].

Since the 1990s numerous studies have demonstrated the association between air pollutants concentration and the occurrence of health related problems [3–6]. In particular, some authors [7–10] have found associations between exposure to traffic and adverse health effects, such as hypertension, myocardial infarction, stroke, atherosclerosis, heart disease, and mortality. The majority of the studies on health effects from traffic exposure mostly rely on associations between hospital records and data from air quality monitoring stations, considered as representative of exposure in a large geographical area. Nevertheless, the health effects of air pollution are the result of a sequence of events, which include

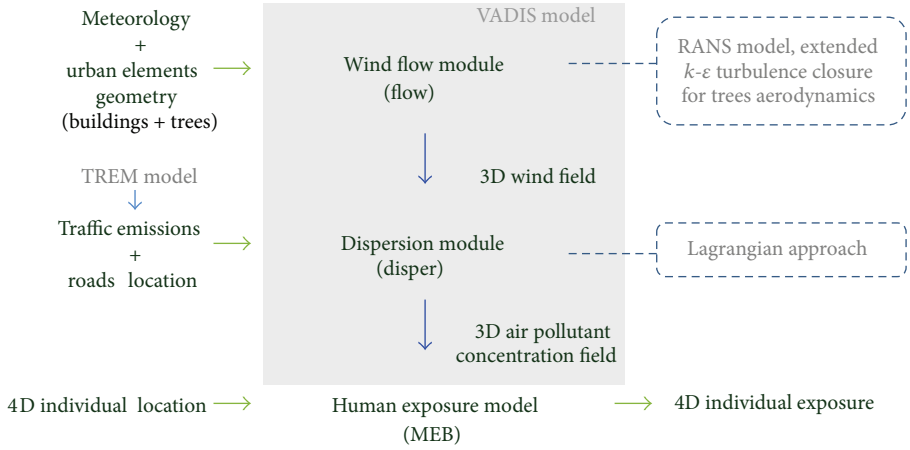

Figure 1: Schematic representation of modeling system architecture.

the release of pollutants, their transport and dispersion in the atmosphere, and their contact and uptake by humans. These events should be taken into account when performing a complete and correct assessment of human exposure. For that, one of the possible approaches is the use of numerical air quality models, which allow estimating spatial and temporal distribution of air pollutants [11], together with a microenvironment approach [12], for exposure estimation.

Although generally associated with environmental benefits, the presence of trees can also cause unwanted and unexpected outcomes on local air quality. It has been shown by field campaigns [13], wind-tunnel experiments [14], and numerical modeling [15, 16] that the complexity of the wind flow inside a given street-canyon is significantly increased by the presence of urban vegetation. The mechanisms behind the action of trees are based on the modification of the number and arrangement of vortical structures that characterize the turbulent recirculating flow between buildings, disrupting the vertical exchange rate of pollutants with the upper level atmosphere. Nevertheless, to the best of the authors' knowledge, the effect on the exposure of pedestrians resulting from perturbed air pollution dispersion induced by urban trees has not been addressed in the scientific literature.

This paper aims to evaluate the exposure of students to traffic-emitted CO in their daily walk to school and how it relates with the effect of trees and route choice.

2. Model Development and Application

2.1. Modeling System Description. With the purpose of evaluating the air pollution exposure of students in their morning walk to school, a local scale modeling system was used. This system (see Figure 1) includes two main models, one for simulating air quality and the other for estimating the individual exposure with time.

2.1.1. Air Quality Modeling. Local scale air quality modeling was carried out using the computational fluid dynamics (CFD) model VADIS [17]. In this model, the 3D wind flow is simulated by an RANS prognostic model with a standard k-ε turbulence closure. For the dispersion, VADIS uses a Lagrangian approach. This model incorporates also the urban vegetation canopy module, URVE [18], which is intended for the simulation of the effect of vegetation over the wind flow and air pollutant dispersion. The main concept behind URVE involves the extension of the standard mean flow and turbulence equations, through the inclusion of additional source terms when coupled to a CFD model, allowing it to mathematically represent the effect of leaves and branches on the wind field. Consequently, the dispersion of the emitted air pollutants is conditioned by the disturbed wind flow, with effects that depend, most of all, on the characteristics of the vegetation itself and of the prevailing airflow. The loss of wind speed due to pressure and viscous drag forces exerted by the leaves an branches is accounted in the model as a source term that is added to the momentum conservation equation, which is dependent on the leaf area density (LAD) of each individual tree. Similarly, the turbulent interaction between the airflow and the plant canopy is addressed by including additional source terms in the transport equations of the turbulent kinetic energy and its dissipation. Model validation can be found in Section 3.1. For more details see Amorim et al. [18].

Road traffic emissions were estimated applying the transport emission model for line sources (TREM) [17], using detailed data on vehicles counting. Due to the short time and spatial scales of the analysis, CO can be considered as a nonreactive chemical species. Also, the CO removal by the canopy was neglected due to its insignificance (approximately 0.0015% of the CO concentration in ambient air according to Nowak et al. [19]).

2.1.2. Exposure Modeling. It is important to distinguish between the concepts of concentration and exposure. While the first is a physical characteristic of the environment at a given place and time, the latter quantifies the interaction between the polluted atmosphere and the person [20]. MEB [21], the exposure model used in this research, was developed with the objective of providing an estimate of the exposure of an individual to air pollution and being able to be used in both outdoor and indoor environments.

Table 1: General description of the trees in the domain.

Species	LAD ($m^2 \cdot m^{-3}$)	Crown height range (m)
Acer pseudoplatanus and *Quercus robur*	1.08	6–10

The MEB core is the calculation of personal exposure through the following general expression (which is a simplification from the microenvironment approach of Hertel et al. [12] since in this case only one microenvironment, outdoors, exists):

$$\exp_i = C_j \times t_{i,j}, \quad (1)$$

where $\exp_i$ is the total exposure of the person i over the specified period of time; C_j is the pollutant concentration in a given location j; and t_i is the time spent by the person i in that specific location. As a result, the exposure value is expressed in concentration × time (e.g., $\mu g \cdot m^{-3} \cdot min$) and thus can be interpreted as the mean pollutant concentration value to which the individual has been exposed during a given period of time.

The input data for this model is the following:

(i) the temporal variation of the individual location: this information was provided by a GPS equipment with a predefined temporal resolution (as it will be analysed in the following section);

(ii) the spatial distribution of concentrations at an average inhalation height for a given period of time.

By matching, in each time-step, the georeferenced position of the individual with the corresponding concentration, the model tracks the time evolution of the exposure. The output data produced by MEB are both instant and mean exposure values.

2.2. Model Application. This research was carried out in Aveiro, a medium sized town located in central Portugal, and is focused in the High School of "José Estêvão," including one of its most important traffic lanes, the "25 de Abril" avenue, in front of the school.

The study domain has an area of approximately 0.4 × 0.2 km^2. The 3D configuration of the buildings and trees was virtually created in VADIS and the resulting computational domain is shown in Figure 2. The dimensions of the computational domain and the boundary conditions were defined following the recommendations from COST Action 732 [22] for the simulation of urban flows with multiple buildings. For more details on the air quality simulations see Amorim et al. [18].

Table 1 summarizes the information collected on trees. The LAD value was obtained from Lalic and Mihailovic [23].

A field campaign was carried out on May 5, 2004, which included meteorological measurements at the school front yard and road traffic counting in the main avenue ("25 de Abril") and in four other roads. CO concentrations were obtained from an "urban traffic" air quality monitoring station (AQS) of the national Portuguese network [24] that is located also in the school yard.

Table 2: Walking routes parameters (obtained from GPS tracking): maximum distance travelled; average walking speed; and the range of heights above mean sea level.

Route	Distance (m)	Mean speed ($km \cdot h^{-1}$)	Elevation range (m)
A	300	4.4	10–12
B	315	4.9	12–15
C	217	5.8	12–14
D	333	5.0	9–12

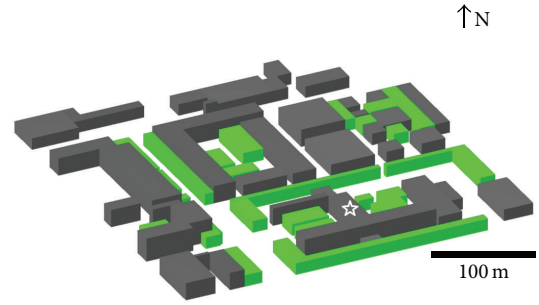

Figure 2: Computational domain generated by VADIS for the set of buildings (in grey) and trees (in green). The star indicates the location of the school.

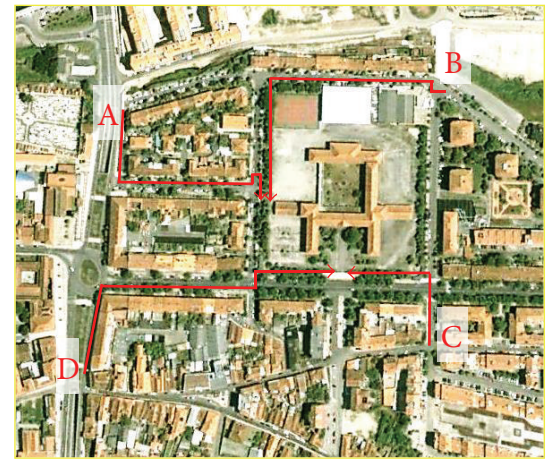

Figure 3: Tracked walking routes to school for exposure calculation.

Four different walking routes to the school were defined (see Figure 3) and then tracked with a GPS equipment with a 10-second time resolution. This procedure allowed to account for realistic walking speeds for each pathway and for the effect of potential delays caused by, for example, traffic lights in road traversing.

Table 2 characterizes the different routes according to the total distance covered by each individual, average walking speed, and elevation range.

With a mean speed of 5 $m \cdot s^{-1}$ (std. dev.: 0.6 $m \cdot s^{-1}$) and a mean distance of 291 m (std. dev.: 51 m), no significant differences exist between the four routes, except for the traffic volume of each road.

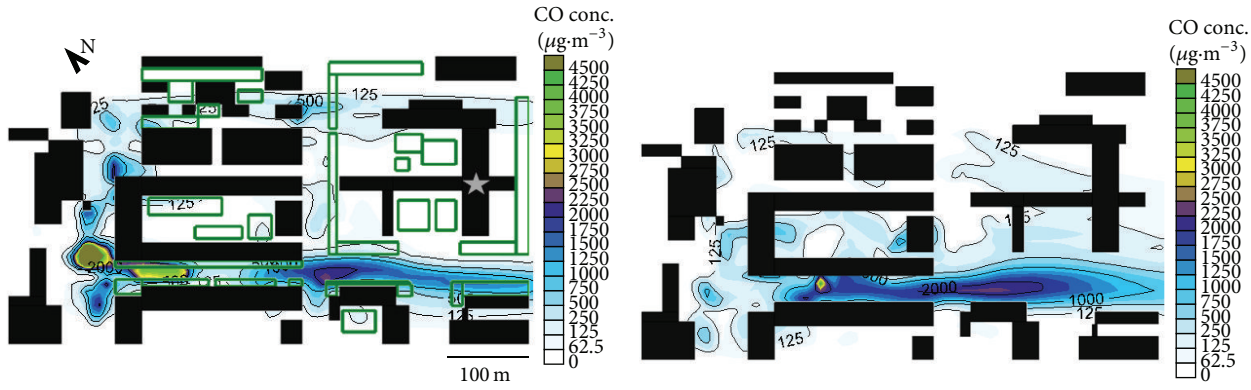

Figure 4: Comparison of 3 m high horizontal CO concentration fields with (a) and without (b) the effect of trees (in green) for the period between 8 and 9 a.m. The star indicates the location of the school.

In order to evaluate the effects induced by the vegetation canopy, the modeling system shown in Figure 1 was applied with the URVE module activated and deactivated. Simulations correspond to the hourly period between 8 and 9 a.m., which comprises the start of classes in the morning.

3. Results and Discussion

Results are analysed in the following sections in terms of local air quality and individual exposure attained on each route.

3.1. Air Quality. In order to validate the modeling results, we have compared the simulated hourly averaged values of CO concentration and wind velocity against the observed data for the period between 5 p.m. on May 4 and 12 p.m. of the next day. For this entire period, the normalized mean squared error (NMSE) obtained was 0.04 and the correlation coefficient was 0.9. All the statistical metrics calculated fulfill the model acceptance criteria defined by Chang and Hanna [25] for air quality model assessment. The modeling uncertainty was 19%, fulfilling the data air quality objective established by the Directive 2008/50/CE. We have also concluded that the model performance increased when the effect of trees was taken into account. Additional details on the validation of the air quality simulations can be found in Amorim et al. [18].

In an inhomogeneous urban canopy the magnitude of the effect of trees on air quality is mostly determined by the characteristics of buildings and trees and by the angle between the prevailing wind and the street-canyons. This heterogeneous role of trees leads to specific areas benefiting from their action over the wind flow and dispersion while others have their ventilation capacity diminished (thus, promoting the formation of air pollution hot-spots). These effects are evident in the CO concentration patterns shown in Figure 4.

Figure 4(a) shows that the CO emitted by traffic in the "25 de Abril" avenue is partially "contained" by the rows of trees in the sidewalks, causing an air quality improvement at the school front yard. On the contrary, without the windbreak action induced by trees the pollutant is more easily dispersed into the school, as shown in Figure 4(b). It should be noted that as a consequence of the "barrier effect" shown in Figure 4(a), a clear hot-spot is formed on the left end of the avenue, highlighting the strong spatial heterogeneity of the impacts of trees on urban air quality.

3.2. Human Exposure. In Figure 5, the evolution of the CO exposure is presented for the considered walking routes.

The differences in the magnitude of the exposure shown in Figure 5 are notorious, revealing that the individuals approaching the school from north (A and B) are exposed to much lower levels of CO than the others, which is a direct consequence from the lower traffic levels in the northern area.

Opposite effects of trees are found in routes C and D. The inflection points (corresponding to instant 55 s after departure in C and 115 s in D) correspond to the arrival of child C at the main avenue and to the moment in which child D, after entering the avenue, leaves the hot-spot at its left end (shown in Figure 4(a)). This allows to conclude that the presence of vegetation has no linear effect on the exposure values. This result is, in fact, consistent with the conclusion drawn from the comparative analysis of the air quality fields (in Figure 4), where no absolute tendency was observed.

As it can be seen from Figure 5, the values of the individual exposure to CO vary significantly with route and time, ranging from values close to zero to nearly 260 $\mu g \cdot m^{-3} \cdot min$. From this fact it can be concluded that even in a small domain, a significant error can occur if a mean air quality value is used as a proxy for the exposure of the individuals that use that space.

A comparison between the different profiles is shown in the box plot of Figure 6. In all routes the trees promote a decrease of the mean exposure value. Except in D, peak values are also decreased by the vegetation.

Additionally, Figure 7 shows the variation rate of the mean exposure that is induced by trees. The results shown in Figure 7 indicate a consistent decrease in exposure caused by trees. As can be seen by the comparison with Figure 6, maximum differences are found for lower exposure levels.

4. Conclusions

As shown by the CFD simulations, the individual exposure of pedestrians (which is closely linked with the local air quality)

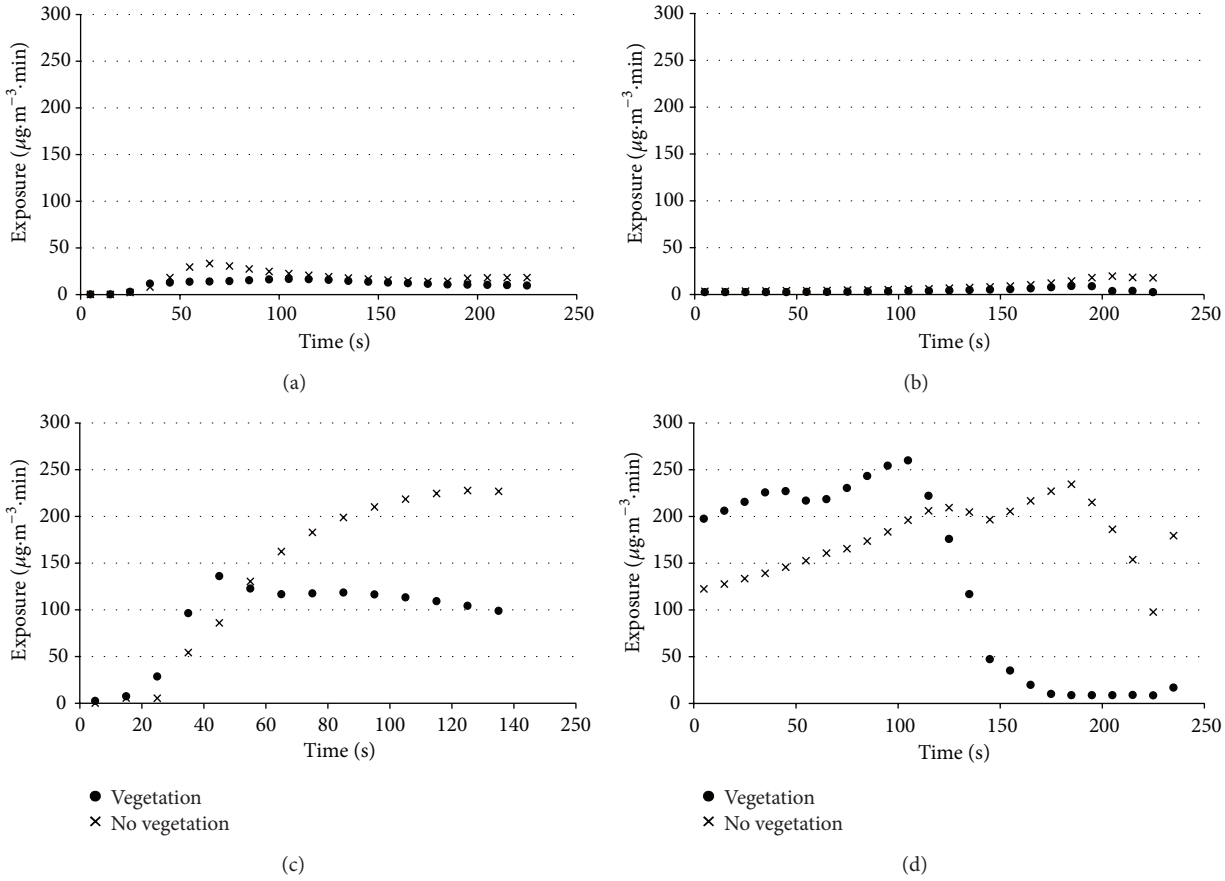

Figure 5: Time evolution of the individual exposure (μg·m^{-3}·min) to CO for each of the four considered pathways, with and without the presence of trees.

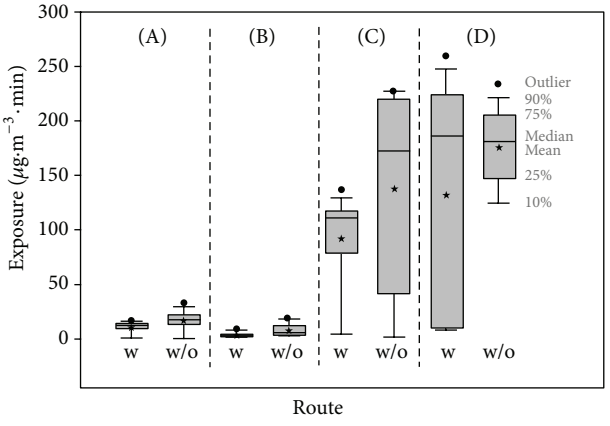

Figure 6: Box plot of the simulated exposure values for each route, comparing the results obtained with (w) and without (w/o) the influence of trees.

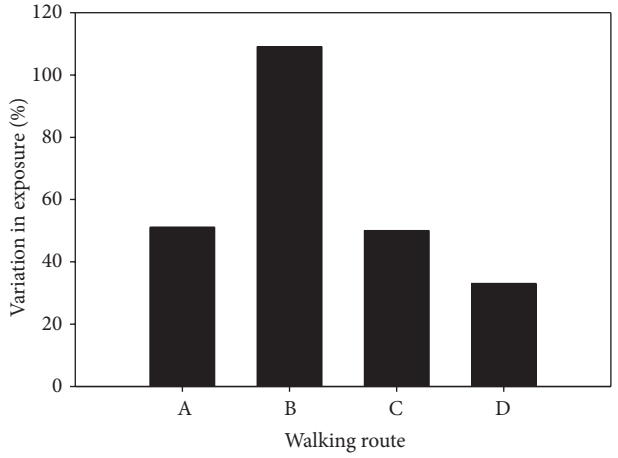

Figure 7: Comparison of the effect of trees on the personal exposure in each walking route. The variation in exposure was calculated as follows: $[(EXP_{notrees} - EXP_{trees})/EXP_{trees}] \times 100$, where $EXP_{notrees}$ is the average exposure calculated without the effect of trees and EXP_{trees} is the average exposure with the presence of trees.

is strongly dependent on the synergies between the meteorological conditions, the three-dimensional configuration of the street-canyons, and the presence of vegetation. The effect of the urban canopy (as a mosaic of buildings and trees) on the dispersion of air pollutants, and resulting exposure, was shown to be complex and highly spatially dependent. The variability of the exposure results obtained in this study indicates the potential error that can be committed when

a single value of air quality is used as a surrogate of air pollution exposure. This conclusion is valid for a small domain, such as the one studied in this work, and it can be easily concluded that the error may be significantly higher when larger domains are considered.

The fact that the presence of vegetation may have opposite effects on air quality, and consequently on pedestrian exposure, clearly indicates that, aiming at the improvement of public health, exposure studies are worth to be developed when a planning intervention is envisioned. The simulation of different planning alternatives, where the position and type of vegetation are explored in terms of its effect on air quality and exposure, should be supported by tools, as CFD models, that allow an enhanced understanding of the symbiosis between the city morphology and the citizen dynamics. This is a needed step towards healthier and sustainable future cities.

Acknowledgments

The authors would like to acknowledge the financial support of the 3rd European Framework Program and the Portuguese Ministry of Science, Technology and Higher Education, through the Foundation for Science and Technology (FCT), for the Postdoc grants of Jorge Humberto Amorim (SFRH/BPD/48121/2008) and Joana Valente (SFRH/BPD/78933/2011) and for the funding of research project INSPIRAR (PTDC/AAC-AMB/103895/2008), supported in the scope of the Competitiveness Factors Thematic Operational Programme (COMPETE) of the Community Support Framework III and by the European Community Fund FEDER. This work was also partly supported by COST Action FP1204 "Green Infrastructure approach: linking environmental with social aspects in studying and managing urban forests."

References

[1] UNEP, *Concept Paper for Workshop on Partnership for Clean Fuels and Vehicles for East Asia*, United Nations Environment Programme, and Regional Resource Center for Asia and Pacific, 2009.

[2] HEI Panel on the Health Effects of Traffic-Related Air Pollution, "Traffic-related air pollution: a critical review of the literature on emissions, exposure, and health effects," HEI Special Report 17, Health Effects Institute, Boston, Mass, USA, 2010.

[3] A. Seaton, W. MacNee, K. Donaldson, and D. Godden, "Particulate air pollution and acute health effects," *The Lancet*, vol. 345, no. 8943, pp. 176–178, 1995.

[4] J. M. Samet, F. Dominici, F. C. Curriero, I. Coursac, and S. L. Zeger, "Fine particulate air pollution and mortality in 20 U.S. cities, 1987–1994," *The New England Journal of Medicine*, vol. 343, no. 24, pp. 1742–1749, 2000.

[5] WHO, *Development of WHO Guidelines for Indoor Air Quality*, Report on a Working Group Meeting, World Health Organization Regional Office for Europe, 2007.

[6] C. A. Pope III and D. W. Dockery, "Health effects of fine particulate air pollution: lines that connect," *Journal of the Air and Waste Management Association*, vol. 56, no. 6, pp. 709–742, 2006.

[7] M. M. Finkelstein, M. Jerrett, and M. R. Sears, "Traffic air pollution and mortality rate advancement periods," *The American Journal of Epidemiology*, vol. 160, no. 2, pp. 173–177, 2004.

[8] G. Hoek, B. Brunekreef, S. Goldbohm, P. Fischer, and P. A. van den Brandt, "Association between mortality and indicators of traffic-related air pollution in the Netherlands: a cohort study," *The Lancet*, vol. 360, no. 9341, pp. 1203–1209, 2002.

[9] B. Hoffmann, S. Moebus, S. Möhlenkamp et al., "Residential exposure to traffic is associated with coronary atherosclerosis," *Circulation*, vol. 116, no. 5, pp. 489–496, 2007.

[10] C. Tonne, S. Melly, M. Mittleman, B. Coull, R. Goldberg, and J. Schwartz, "A case-control analysis of exposure to traffic and acute myocardial infarction," *Environmental Health Perspectives*, vol. 115, no. 1, pp. 53–57, 2007.

[11] C. Borrego, O. Tchepel, A. M. Costa, H. Martins, J. Ferreira, and A. I. Miranda, "Traffic-related particulate air pollution exposure in urban areas," *Atmospheric Environment*, vol. 40, no. 37, pp. 7205–7214, 2006.

[12] O. Hertel, F. A. A. M. de Leeuw, O. Raaschou-Nielsen et al., "Human exposure to outdoor air pollution (IUPAC technical report)," *Pure and Applied Chemistry*, vol. 73, no. 6, pp. 933–958, 2001.

[13] A. Kikuchi, N. Hataya, A. Mochida et al., "Field study of the influences of roadside trees and moving automobiles on turbulent diffusion of air pollutants and thermal environment in urban street canyons," in *Proceedings of the 6th International Conference on Indoor Air Quality, Ventilation and Energy Conservation in Buildings (IAQVEC '07)*, pp. 137–144, Sendai, Japan, October 2007.

[14] C. Gromke and B. Ruck, "On the impact of trees on dispersion processes of traffic emissions in street canyons," *Boundary-Layer Meteorology*, vol. 131, no. 1, pp. 19–34, 2009.

[15] A. Mochida, Y. Tabata, T. Iwata, and H. Yoshino, "Examining tree canopy models for CFD prediction of wind environment at pedestrian level," *Journal of Wind Engineering and Industrial Aerodynamics*, vol. 96, no. 10-11, pp. 1667–1677, 2008.

[16] R. Buccolieri, C. Gromke, S. Di Sabatino, and B. Ruck, "Aerodynamic effects of trees on pollutant concentration in street canyons," *Science of the Total Environment*, vol. 407, no. 19, pp. 5247–5256, 2009.

[17] C. Borrego, O. Tchepel, A. M. Costa, J. H. Amorim, and A. I. Miranda, "Emission and dispersion modelling of Lisbon air quality at local scale," *Atmospheric Environment*, vol. 37, no. 37, pp. 5197–5205, 2003.

[18] J. H. Amorim, V. Rodrigues, R. Tavares, J. Valente, and C. Borrego, "CFD modelling of the aerodynamic effect of trees on urban air pollution dispersion," *Science of the Total Environment*, vol. 461-462, pp. 541–551, 2013.

[19] D. J. Nowak, D. E. Crane, and J. C. Stevens, "Air pollution removal by urban trees and shrubs in the United States," *Urban Forestry and Urban Greening*, vol. 4, no. 3-4, pp. 115–123, 2006.

[20] W. R. Ott, "Concepts of human exposure to air pollution," *Environment International*, vol. 7, no. 3, pp. 179–196, 1982.

[21] A. I. Miranda, J. H. Amorim, V. Martins et al., "Modelling the exposure of firefighters to smoke based on measured data," in *Proceedings of the 3rd International Conference on Modelling, Monitoring and Management of Forest Fires*, 2011.

[22] J. Franke, A. Hellsten, H. Schlünzen, and B. Carissimo, *Best Practice Guideline for the CFD Simulation of Flows in the Urban Environment*, COST Action 732, Quality Assurance and Improvement of Microscale Meteorological Models, COST Office, 2007.

[23] B. Lalic and D. T. Mihailovic, "An empirical relation describing leaf-area density inside the forest for environmental modelling," *Journal of Applied Meteorology*, vol. 43, no. 4, pp. 641–645, 2004.

[24] APA, *Air Quality Data for Portuguese Monitoring Stations*, APA, Lisbon, Portugal, 2011, http://www.qualar.org/.

[25] J. C. Chang and S. R. Hanna, *Technical Descriptions and User's Guide for the BOOT Statistical Model Evaluation Software Package*, version 2.0, 2005.

Hindawi Publishing Corporation
Advances in Meteorology
Volume 2013, Article ID 549096, 12 pages
http://dx.doi.org/10.1155/2013/549096

Research Article

Effects of Urban Configuration on Human Thermal Conditions in a Typical Tropical African Coastal City

Emmanuel Lubango Ndetto[1,2] and Andreas Matzarakis[1]

[1] *Chair of Meteorology and Climatology, Albert-Ludwigs University of Freiburg, Werthmannstrasse 10, 79085 Freiburg, Germany*
[2] *Department of Physical Sciences, Sokoine University of Agriculture, P.O. Box 3038, Morogoro, Tanzania*

Correspondence should be addressed to Emmanuel Lubango Ndetto; ndettoel3@yahoo.co.uk

Received 14 May 2013; Revised 12 August 2013; Accepted 22 August 2013

Academic Editor: Panagiotis Nastos

A long-term simulation of urban climate was done using the easily available long-term meteorological data from a nearby synoptic station in a tropical coastal city of Dar es Salaam, Tanzania. The study aimed at determining the effects of buildings' height and street orientations on human thermal conditions at pedestrian level. The urban configuration was represented by a typical urban street and a small urban park near the seaside. The simulations were conducted in the microscale applied climate model of RayMan, and results were interpreted in terms of the thermal comfort parameters of mean radiant (T_{mrt}) and physiologically equivalent (PET) temperatures. PET values, high as 34°C, are observed to prevail during the afternoons especially in the east-west oriented streets, and buildings' height of 5 m has less effect on the thermal comfort. The optimal reduction of T_{mrt} and PET values for pedestrians was observed on the nearly north-south reoriented streets and with increased buildings' height especially close to 100 m. Likewise, buildings close to the park enhance comfort conditions in the park through additional shadow. The study provides design implications and management of open spaces like urban parks in cities for the sake of improving thermal comfort conditions for pedestrians.

1. Introduction

Dar es Salaam is a hot, humid tropical city situated along the Tanzanian coast on the Western Indian Ocean coast. It enjoys the sea-land breezes system which is observed to be more organised during the months of March, April, September, and October [1, 2]. On the other hand, sultriness is not uncommon particularly during the December–February (DJF) season. Such sultry conditions bring an undesirable thermal discomfort especially to pedestrians and street vendors. Most biometeorological studies done elsewhere have revealed the effects of street orientation and height to width ratio on the variation of local thermal comfort at an urban canyon level [3–6].

Although the human thermal comfort is influenced by four meteorological parameters of air temperature, humidity, wind speed, and radiation flux (usually quantified in terms of mean radiant temperature), it is the wind speed and mean radiant temperature which can be significantly varied by changing the street orientation and height to width ratio [7]. A past urban climate research in Dar es Salaam has suggested that the observed sea-land breeze effect could improve the thermal comfort at high ground places in the city like at the university of Dar es Salaam campus which is about 12 km to the west from the city centre [1]. Moreover, various methods have been applied elsewhere in order to deepen the understanding of the effect of street geometry and orientation on urban thermal comfort especially at pedestrian level. For instance, from the field-measurements in an east-west urban canyon during cloudless summer weather in 2003, it was found that thermal stress is mostly attributable to solar exposure, and the study suggested further field investigations to be done in other locations and climatic conditions in order to verify the generality of such thermal observations in street canyons [3].

In Fez, Morocco, measurements were carried out during the hot summer and cool winter seasons where the deep canyons were found considerably cooler in day than

the shallow canyons [8]. Effects of urban configuration on urban thermal climate have also been recently explored through series of field measurements in many cities including Tokyo, Japan [9] Athens, Greece [4] Constantine [5], Colombo [10, 11]. In some of the cities situated within the coastal environments, influence of sea breezes on urban thermal climate was also investigated [10, 12, 13].

Likewise, numerical simulation also offers a valuable method to understanding the effects of urban geometry and street orientation. In Ghardaia, Algeria, numerical simulations were done using the three-dimensional numerical model, ENVI-met, for a typical summer day, and results showed contrasting patterns of thermal comfort between shallow and deep urban streets as well as between various orientations [6]. In studying the impact of street geometry on ambient temperatures and on daytime pedestrian comfort levels, two approaches involving field measurements and urban climate simulations using the ENVI-met were carried out in downtown of Curitiba, Brazil [14]. Having observed that maximum daily temperature within street canyons in Colombo, Sri Lanka, decreases with increasing height to width (H/W) ratio and that sea breezes exert a cooling effect, simulations done in ENVI-met model were initiated by data obtained from a synoptic weather station located at the airport (approximately 24 km north of the measurement location) for the purpose of understanding the effect of different urban design options on air and surface temperatures, as well as on outdoor thermal comfort [15]. Similarly, long-term thermal comfort at the University Campus in Taiwan was predicted by using long-term meteorological data collected from a nearby station, and simulations were performed in RayMan model [7]. This suggests that with modern advances in urban climatology especially through continuous improvement on the available microscale models, assessment of thermal conditions in urban places could then be sufficiently studied where simulations could deliver helpful results. Besides, most field studies examining outdoor thermal comfort merely clarify characteristics measured on a particular day; hence, such studies may not represent annual thermal conditions accurately.

Due to its coastal location and proximity to the equator, Dar es Salaam seems to be a perfect location of understanding the effects of urban geometry on human thermal comfort at pedestrian level in the low latitudes. Long-term analysis of urban thermal climate in Dar es Salaam is therefore of paramount importance in understanding the tropical urban climate in a typical African city.

The current study, therefore aimed at quantifying the effects of the buildings' height and orientation on radiation fluxes in a typical urban canyon and an urban park in a tropical African city. In order to optimise thermal comfort through modified urban configurations, human thermal index of physiologically equivalent temperature (PET) was used in visualizing the changes in terms of thermal comfort classes after every modification. Simulations were performed using the microscale model of RayMan [16, 17]. The model is reputed to be easy to use. Recent research done in a midlatitude city found that RayMan can even deliver more accurate results at high sun elevations [18], and this underpins it as

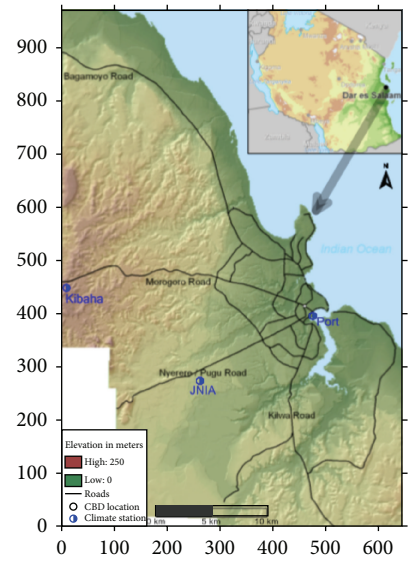

(a)

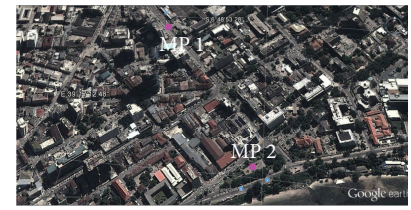

(b)

Figure 1: (a) Location of measurement stations and area of study. Source: modified from Hill and Lindner (2010). (b) A satellite picture as obtained from Google Earth, locating the simulation points, MP1 (typical urban street) and MP2 (urban park), in a part of Dar es Salaam city, Tanzania.

an ideal microscale model to study urban climate in the low latitude cities including Dar es Salaam where, as elsewhere in the world, the afternoons are usually the most thermal stressful times [1, 2]. Simulating the optimal configurations for thermal comfort in Dar es Salaam is of utmost importance in advancing the science of urban climate in low latitudes and urban planning of cities in developing countries. Dar es Salaam is an important economic centre in eastern Africa due to its harbour services, and it has recently been observed to expand rapidly. Better understanding of its urban climate is significant for its future urban planning and well-being of the increasing population.

2. Methods

Dar es Salaam (Figure 1(a)) is located at 6°51′S, 39°18′E along the south western coast of the Indian ocean, covering an area of 1350 km^2 of which about 1000 km^2 is a land area [19, 20]. Dar es Salaam is generally a lowland area with its altitude ranging from the sea level at the coast to an approximately 250 m in the south-west along the Pugu hills situated about 25 km from the city centre [21]. The climate is typically hot-humid, referred to as *tropical wet/dry climate (Aw)* according

to the Köppen classification system [22, 23]. The climate is mainly influenced by the northeast monsoon which prevails from March to October and the southeast monsoon between October and March [19]. This is in response to the passage of the Intertropical convergence zone (ITCZ). Local winds are generally high up to 13 m/s during the afternoons particularly from August to November.

Usually, the relative humidity in Dar es Salaam ranges between 67 and 96% in a year, and the annual rainfall is about 1050 mm with peaks in April and December. April is however the wettest month, and the rain seasons are usually described as short rains (October–December season) with an average of 75 to 100 mm and long rains (March–May season) with a monthly average of 150 to 300 mm of rainfall [24]. The mean annual air temperature is about 30°C with a slight seasonal change due to its proximity to the equator. The mean daily sunshine duration is about 10–12 hours.

The study area comprised of two urban resort places (Figure 1(b)). The first area (MP1) is along the typical street (width of 24.5 m) in the downtown area of Dar es Salaam. One side of the street there is a tall building of 21 storeys (about 93 m high), and the other side is a waiting area for boarding public transport. The second area of simulation (MP2) is on a small urban park (locally called as a Posta garden) overlooking the sea to the south. It also serves as the bus waiting and recreation place. The street is originally orientated in a northwest-southeast direction (i.e., about 45° from the north in an anticlockwise direction) while the park takes the triangle-like shape measuring 156 m × 140 m × 60 m with its hypotenuse facing the sea. There are few trees of mainly Ashoka type along the street whereas the park has many trees with different species, but notably the leaf trees of Neem species, grass, and a concrete floor at the centre. Although the park overlooks the sea, the presence of two lines of trees may act as an obstacle to the sea breezes at low levels or near the ground level. Simulations were therefore done by rotating the orientation every 15° and by increasing the buildings' height by 5 m up to 50 m, and 100 m was taken as the maximum height of the current highest building in the city.

The input meteorological data used for the long-term simulation were based on the available meteorological data collected at a synoptic station located at the Julius Nyerere International Airport (JNIA) (see Figure 1(a)). These data were from the year 2001 to 2012. The airport station usually does meteorological observations at every synoptic hour. However, the available data used in this study had a three-hour frequency period, with observation times at 0 LST (local standard time), 3 LST, 6 LST, 9 LST, 12 LST, 15 LST, 18 LST, and 21 LST. These include air temperature, wind speed, relative humidity, and amount of cloud cover. Cloud cover was used to estimate the radiation flux as there are only daily measurements of radiation at the synoptic station. The airport datasets were used on the assumption that they form a continuous long-term dataset as required in long-term climatic analysis, unlike the datasets from the other two stations. The urban effect at MP1 and MP2 locations was considered to affect the wind speed which was then estimated from the readings at the airport station using equation provided in [25] and applied in [26]:

$$\mathrm{ws}_{1.1} = \mathrm{ws}_h\left(\frac{1.1}{h}\right)^{\propto}, \quad \propto = 0.12z_0 + 0.18, \tag{1}$$

where ws_h is the wind speed (ms^1) at a height of h (10 m), $\propto$ is an empirical exponent that depends on the surface roughness, and z_0 is the roughness length. Due to slight differences in terrain features at MP1 (a densely built-up city area) and MP2 (partly wooded areas with buildings and open to sea), z_0 were taken to be 1.5 and 1.3, respectively, though both areas are within the inner city.

Table 1: Climate measuring stations in Dar es Salaam.

Meteorological station	Grid reference	Altitude (m)	Approximate distance to area of study (km)
JNIA	06°52′S, 39°12′E	53.0	11.2
Port	06°50′S, 39°18′E	18.0	0.8
Kibaha	06°50′S, 38°58′E	167.0	35.2

Source: Tanzania meteorological agency.

Additional meteorological datasets of air temperature (including maximum and minimum) and relative humidity were also obtained from other two stations located at the harbour (Port) and at the Kibaha Sugarcane Research Institute (Kibaha) (see Figure 1(a) and Table 1). The air temperature datasets from the two stations were from the year 2001 to 2011, whereas relative humidity data spanned for the period March–September 2005 was only collected at the Port station. These additional datasets were compared with the corresponding datasets from the airport station in order to establish the rationale of using long-term synoptic data to simulate urban bioclimatic conditions. Comparison between the weather elements from the three weather stations was examined using the rank correlation of Kendall tau correlation at a 0.05 significance level. The Kendall tau is a bivariate measure of correlation/association usually used for the rank-order data [27].

The simulated bioclimatic conditions at pedestrian level were interpreted using PET and T_{mrt}. PET evaluates the thermal conditions in a human physiological manner and uses a commonly known unit of degree Celsius. PET is defined as the air temperature at which the human energy budget for the assumed indoor conditions is balanced by the same skin temperature and sweat rate as under the actual complex outdoor conditions to be assessed [28–30]. On the other hand, the mean radiant temperature is defined as the uniform temperature of an imaginary enclosure in which the radiant heat transfer from the human body equals the radiant heat transfer in the actual nonuniform enclosure [31]. T_{mrt} is one of the meteorological parameters that govern human thermal energy balance hence affecting the human thermal comfort [32].

As the aim of the study was to determine the optimal urban configuration for the urban thermal comfort in Dar es Salaam at pedestrian level, long-term simulation would give reliable and comprehensive information as opposed to short

field measurements. Field studies examine outdoor thermal comfort that merely expound characteristics measured on a particular day and would not accurately represent the annual thermal conditions. Besides, the lack of urban meteorological stations with continuous measurements in many tropical cities including Dar es Salaam lead to many urban climate studies in such cities to rely on the easily available long-term meteorological data from nearby stations [7, 15, 33–35]. For instance, climatic changes in temperature conditions in Nairobi city were investigated using data collected from weather stations situated about 4 kilometres from the city centre [33], and in Taiwan, long-term thermal environment was simulated using meteorological data of a 10-year period collected from a nearby station [7]. However, altitude is acknowledged as a determinant factor for the spatial variation of weather and climate, and winds are experienced to decrease in urban areas [36]. Taking into consideration such observations, variation of weather in Dar es Salaam due to altitude could be assumed insignificant as the synoptic station lies at an altitude of 53 m above sea level while the city centre is at about 11 m above sea level. Theoretically, air temperature varies by 0.6°C for every 100 m high. Furthermore, mean climatic conditions of Dar es Salaam are defined using data from the airport station.

The assumptions that guided the use of the available synoptic meteorological data as input in the simulations thus base on the fact that Dar es Salaam lies within the coastal lowland terrain, and a weather change due to altitude is insignificant within few horizontal distances. A robust and plausible long-term urban thermal characteristic can be attained by using long-term and continuous meteorological data. Although differences exist in some atmospheric parameters between the simulation points in the city and the synoptic weather station, the attributed changes in thermal indices generated by the simulation model are relatively small and can be neglected. Therefore, the simulated results provide a precise representation of the thermal conditions within the city environment.

3. Results and Discussion

3.1. Local Urban Micrometeorological Variations. The intraurban variation of local meteorological conditions in Dar es Salaam was investigated in order to determine to what extent does the local meteorological conditions change in spatial and temporal scales. Analysis was done only in terms of relative humidity and air temperature due to availability of these meteorological parameters in the three weather stations. Spatial variability in cloud cover could be understood to be within the allowable limits as the observation at the synoptic station is considered to span a horizontal distance of nearly 30 km from the observation point for the horizontal visibility and consequently cloud cover. This analysis was of course considered necessary and of utmost importance to understand the variability of the local weather, and hence, how reliable can the weather parameters at the synoptic weather station be considered representative of the city's climate. Further, variability analysis of weather parameters

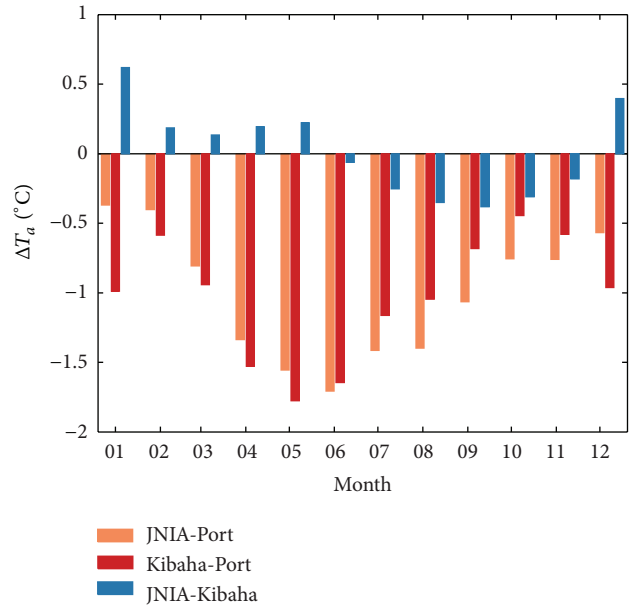

Figure 2: Intraurban air temperature differences as depicted by the long-term mean monthly differences between the three weather stations.

was also considered as an important step to establish a rationale of using the meteorological data from the synoptic station as the representative input parameter in the long-term urban climate simulation.

The results, therefore, suggested that the variation of the local micrometeorological conditions in Dar es Salaam could be highly influenced by its proximity to the sea. Places close to the sea could be slightly warmer than those far away from the sea as suggested by the analysis of air temperature from the three stations. Figure 2 depicts the long-term mean monthly air temperature differences (ΔT_a) where air temperature at the Port station could be on average 1.5°C or higher than the readings at the airport and Kibaha stations. The monthly mean air temperature differences between JNIA and Port varied from −0.4°C in February to −1.7°C in June and between Port and Kibaha ranged from 0.3°C in October to 1.8°C in May. Between JNIA and Kibaha, the intraurban monthly mean air temperature differences were up to 0.6°C from December to May, warm at JNIA and cold by nearly 0.5°C during June–November season. The intraurban air temperature differences were observed to be more consistent in terms of the mean daily air temperatures in a sense that it is warmer near the seaside (Port station) than inland of the coast (see Figure 2).

The relationship between the evolutions of temperature profiles among the three measuring stations as determined by the Kendall tau coefficient was found to be as low as 0.25 and 0.27 between the maximum air temperature at the Port and that of other stations, respectively (Table 2). On the contrary, the correlation coefficients for the mean and minimum air temperature between the three stations was high as 0.6 suggesting a similar evolution of temperature at the stations. Usually, the maximum temperature is reached at 15 LST

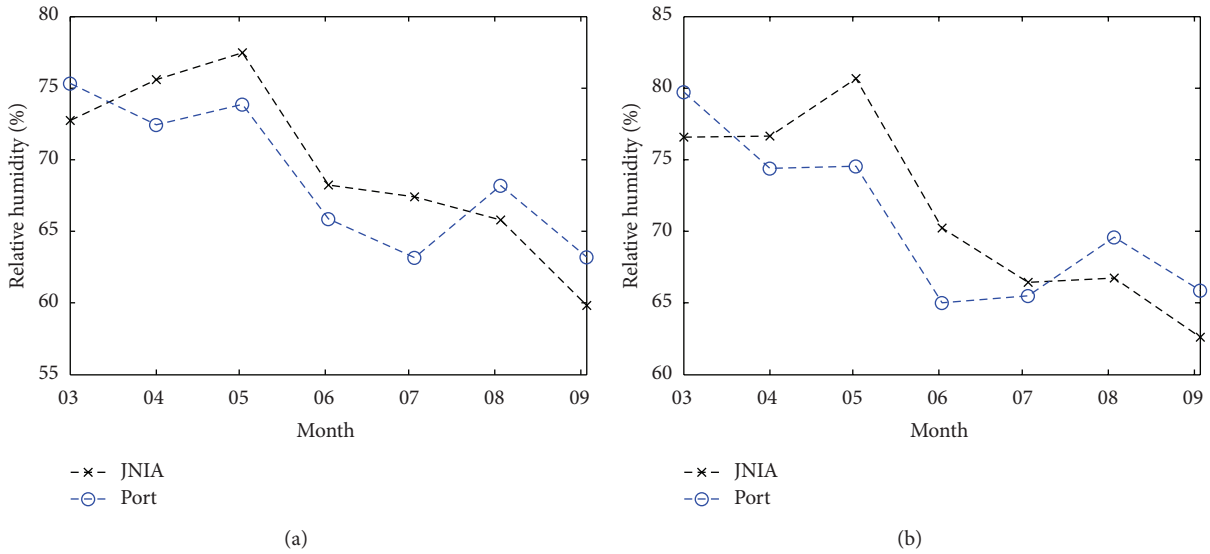

Figure 3: Mean monthly relative humidity at JNIA and Port (a) and its corresponding mean relative humidity at 15 LST (lowest relative humidity for the day) (b), for the period March–September 2005.

Table 2: Kendall's tau correlation coefficients at a significant level of 0.05 for intra-urban temperature and relative humidity differences between the three stations.

	JNIA-Port	Kibaha-Port	JNIA-Kibaha
T_a maximum	0.25	0.27	0.72
T_a minimum	0.87	0.86	0.87
T_a mean	0.70	0.60	0.67
RH mean	0.49	—	—
RH at 15 LST	0.43	—	—

where the surface receives much of the solar insolation. The low correlation coefficients between the seaside station and the inland stations during the maximum temperature could be explained by the differences in terrain at the measuring stations. While Port is near to the sea, terrain features at the inland stations is mostly consisted by green vegetation, usually short grass at the airport (JNIA) and scattered trees at Kibaha. It could be suggested that the differences in thermal capacity between the mostly vegetated terrain station and the station near the large water body is pronounced during the daytime. Other studies also found a trend towards a greater difference between annual mean of daily maximum and that of minimum temperatures from the coast to inland stations [37].

Relative humidity is always high along the eastern Africa coast, but our analysis for relative humidity was limited by availability of data in Dar es Salaam area. Although two of the stations (JNIA and Port) can do observation of relative humidity, available data at Port station were limited to six months of the year 2005. This cannot give a conclusive spatial distribution of relative humidity in Dar es Salaam. With such shortcomings, the current analysis, however, surprisingly indicated that relative humidity is slightly higher at the airport station than at a seaside station especially from April to July (Figure 3). The significant correlation coefficients between readings of relative humidity at the port and the airport stations for the mean monthly and at 15 LST (time of lowest relative humidity) are given in Table 2. The relative humidity climatology of Dar es Salaam as observed from previous studies indicates that relative humidity along the coast usually reach it daily maximum during the night at 90–95% throughout the year, and greater variations are experienced during the daily minimum period at 15 LST [37]. While the seaside station is very close to the city and despite the presence of a large water body, relative humidity readings can as well be influenced by the impervious surface of the urban on the other side. The airport station is well within a short-grass vegetation area. Furthermore, the months of April and May are usually rainy months in Dar es Salaam, and perhaps the proportion difference in terrain features and rain events can influence high humidity in many places not necessarily being close to the sea. However, a good picture of intraurban relative humidity variation in Dar es Salaam could be comprehensive with more datasets with good spatial resolution.

3.2. Simulation Results in the Street. The simulations of varying the street orientation and height of buildings were done at two popular urban places in Dar es Salaam for a purpose of quantifying the effects of street orientation and buildings' height on the human thermal comfort at pedestrian level. This section therefore describes the results of the simulation performed at the street and at the urban park.

In its original orientation of a northwest-southeast direction and settings of one side with tall buildings, pedestrians at the street can experience thermal stress during the afternoons. The temporal distribution of T_{mrt} as depicted in Figure 4 indicates high values of about 45°C occurring at around 12 LST from the end of November through

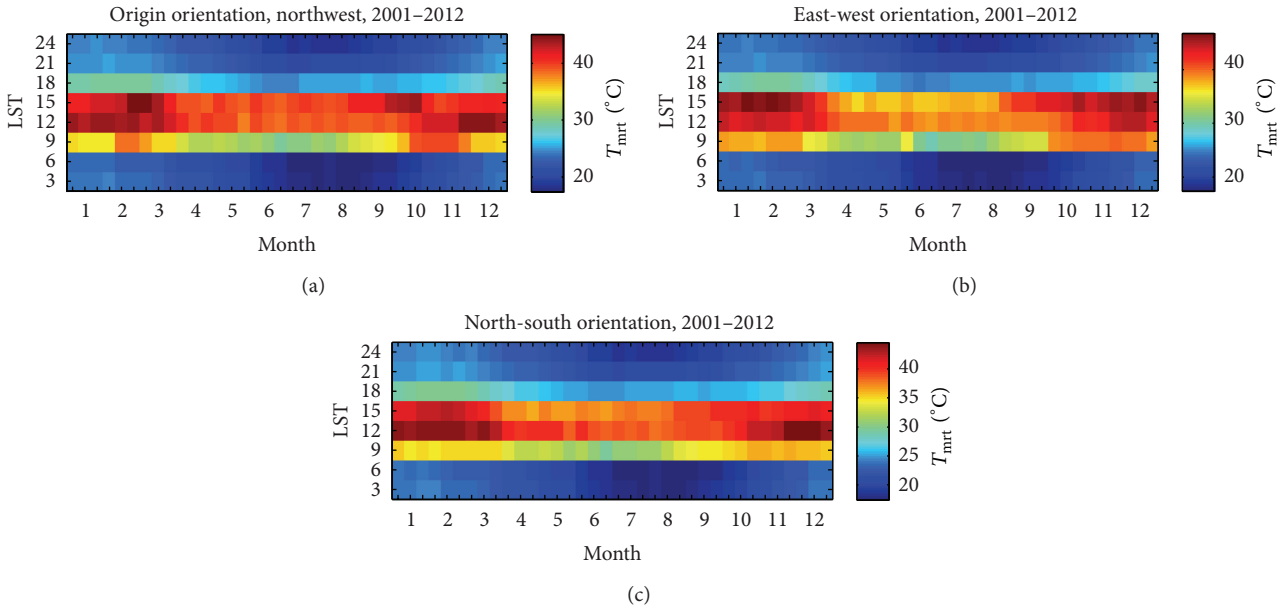

Figure 4: The temporal distribution of T_{mrt} at the urban street in its origin orientation of a northwest-southeast direction (a), east-west orientation (225°) (b) and north-south orientation (315°) (c).

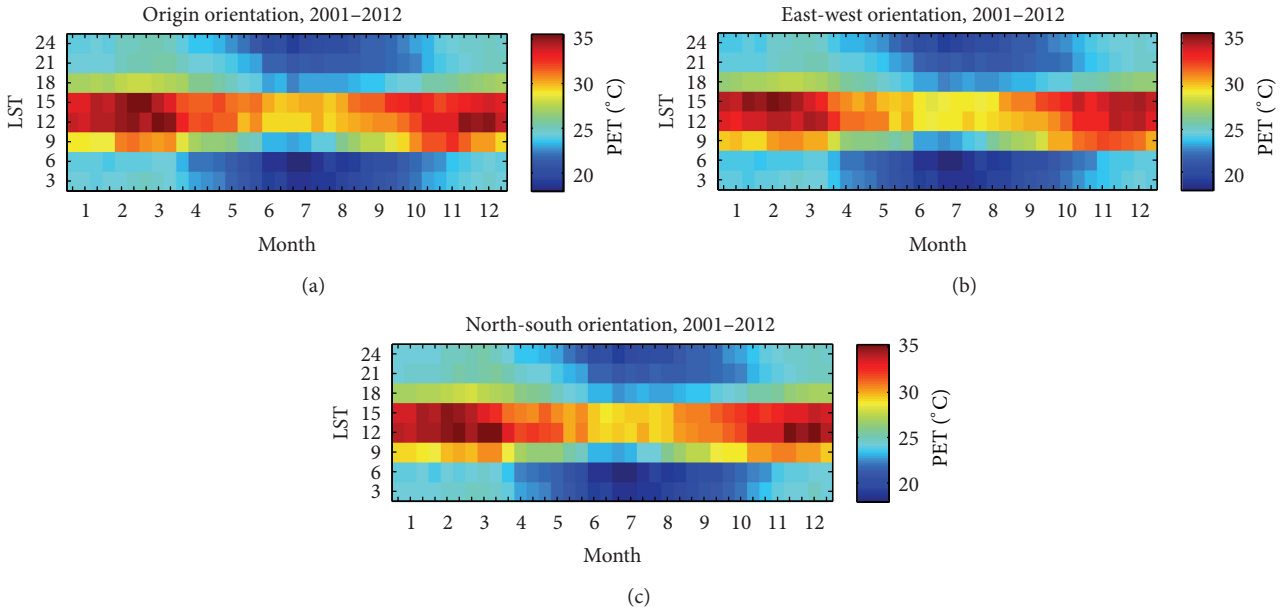

Figure 5: The temporal distribution of thermal comfort conditions in terms of PET index at the urban street in its origin orientation of a northwest-southeast direction (a), east-west orientation (225°) (b), and north-south orientation (315°) (c), suggesting a high prevalence of human thermal stress between 12 and 15 LST particularly from late October to early April.

the beginning of January as well in March. When reoriented in the west-east direction, the highest values of T_{mrt} above 45°C became prevalent at 15 LST in October and from late January to early March while in the north-south reorientation, high values of T_{mrt} of more than 45°C prevailed at noon time from late November to early March.

The corresponding situation in terms of human thermal comfort was analysed using PET index and depicted in Figure 5. The temporal distribution then indicated that high value of PET as 34°C was prevalent between 12 and 15 LST in the months of February, March, November, and December. Further, in an east-west reorientation, high PET values of about 34°C could frequently occur between 12 and 15 LST in March and November whereas in the north-south reorientation similar high values would be experienced in February, March, November, and December in the same hours of the day. The same period was also indentified in the earlier studies as the most thermal stress period in Dar es Salaam

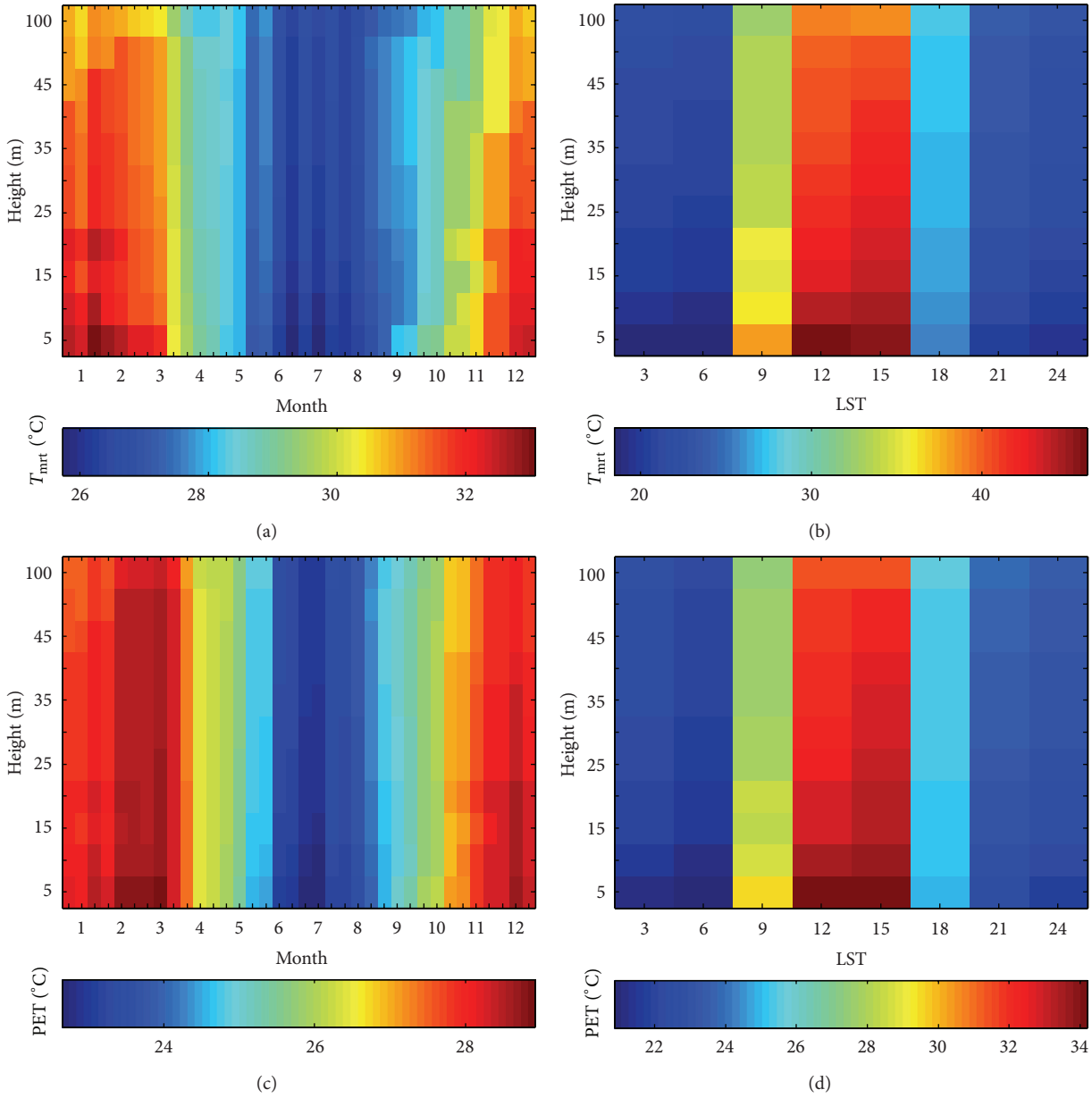

FIGURE 6: Effects of increasing buildings' height on the temporal distribution of T_{mrt} at the urban street as depicted in the annual cycle (a) and the diurnal cycle (b). The corresponding thermal comfort distribution is shown in terms of PET index ((c) and (d)).

even without considering urban obstacles in calculating the thermal indices [1, 2]. Thus, in order to visualize the thermal comfort characteristics in Dar es Salaam, an idealized urban canyon was considered in further analysis.

An idealized urban canyon with equal heights of buildings on each side was then formulated based on the settings of the original street, and simulations were done by varying the orientation and height of buildings. It is important to note that the new city master plan strategize on densification of the central business district (CBD) of Dar es Salaam through erecting buildings of more than 10 storeys while leaving most of the streets' widths unchanged. Results in this setting are described in Figures 6 and 7 in terms of the annual and diurnal cycles of evolution of T_{mrt} and its corresponding thermal comfort condition in terms of PET index.

From Figure 6, effect of buildings' height is described in terms of the annual and diurnal distribution of T_{mrt} ((a) and (b)) and its corresponding PET index ((c) and (d)). It could then be evidently observed that a significant reduction of T_{mrt} and PET values just at the buildings' height of 20 m can be attained and more reduction at the height of 100 m. Whereas, effect of street orientation is illustrated by keeping the buildings at a height of 5 m (Figures 7(a) and 7(b)) and at a height of 25 m. Although significant differences could not be easily discerned at the 5 m buildings' height (Figures 7(a) and 7(b)), it is evident that street orientation particularly on

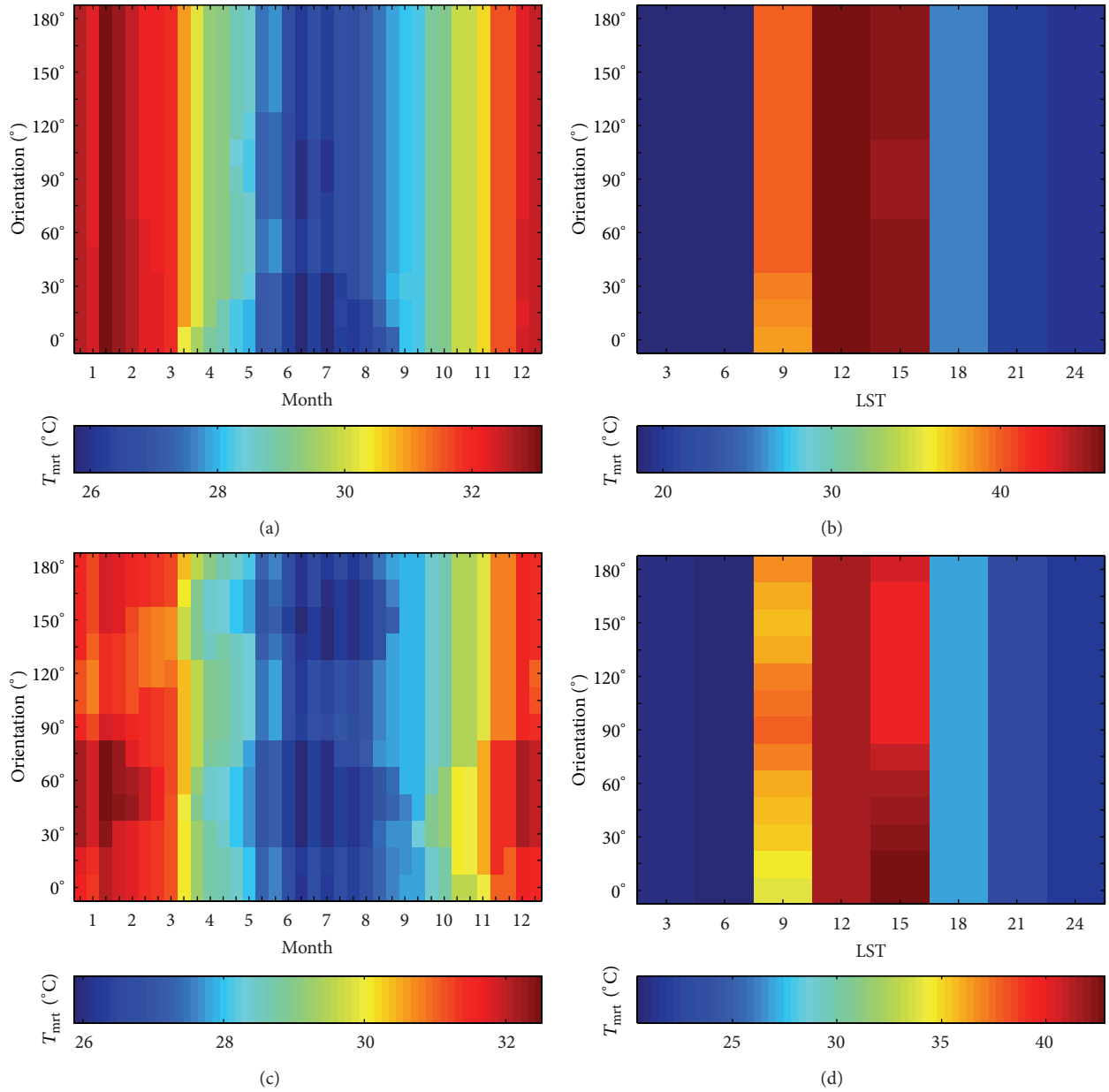

FIGURE 7: Effects of orientation on the temporal distribution of T_{mrt} at the urban street when the buildings' height was kept at 5 m, depicted in terms of the annual cycle of T_{mrt} (a) and the diurnal cycle (b). ((c) and (d)) show the corresponding effects when the buildings' height was kept at 25 m high.

the east-west direction (i.e., 45° in the figure) influences the calculated thermal comfort parameters as it can be observed in Figures 7(c) and 7(d). For this case, in Dar es Salaam, the east-west oriented street could be an undesirable street orientation for pedestrian thermal comfort condition. Other studies have attributed such an orientation to be prone to solar access [3, 6]. Otherwise, the north-south oriented streets (i.e., 120–135° in the figure) could present a good scenario for pedestrian thermal comfort in Dar es Salaam based on both annual and diurnal temporal distributions of T_{mrt}.

3.3. Simulation Results in the Urban Garden. Perhaps one of the reasons of doing simulation at the urban park is the understanding that many of the urban parks in Tanzanian cities including Dar es Salaam are relatively small in size but are also very close to surrounding buildings. The close buildings to such parks could potentially impose some significant effects on the thermal comfort in a garden or park (see MP2 in Figure 1) especially when buildings' height is too high. Figure 8, therefore, describes the effects of buildings' height on a small urban garden while the effect of orientation is illustrated in Figure 9.

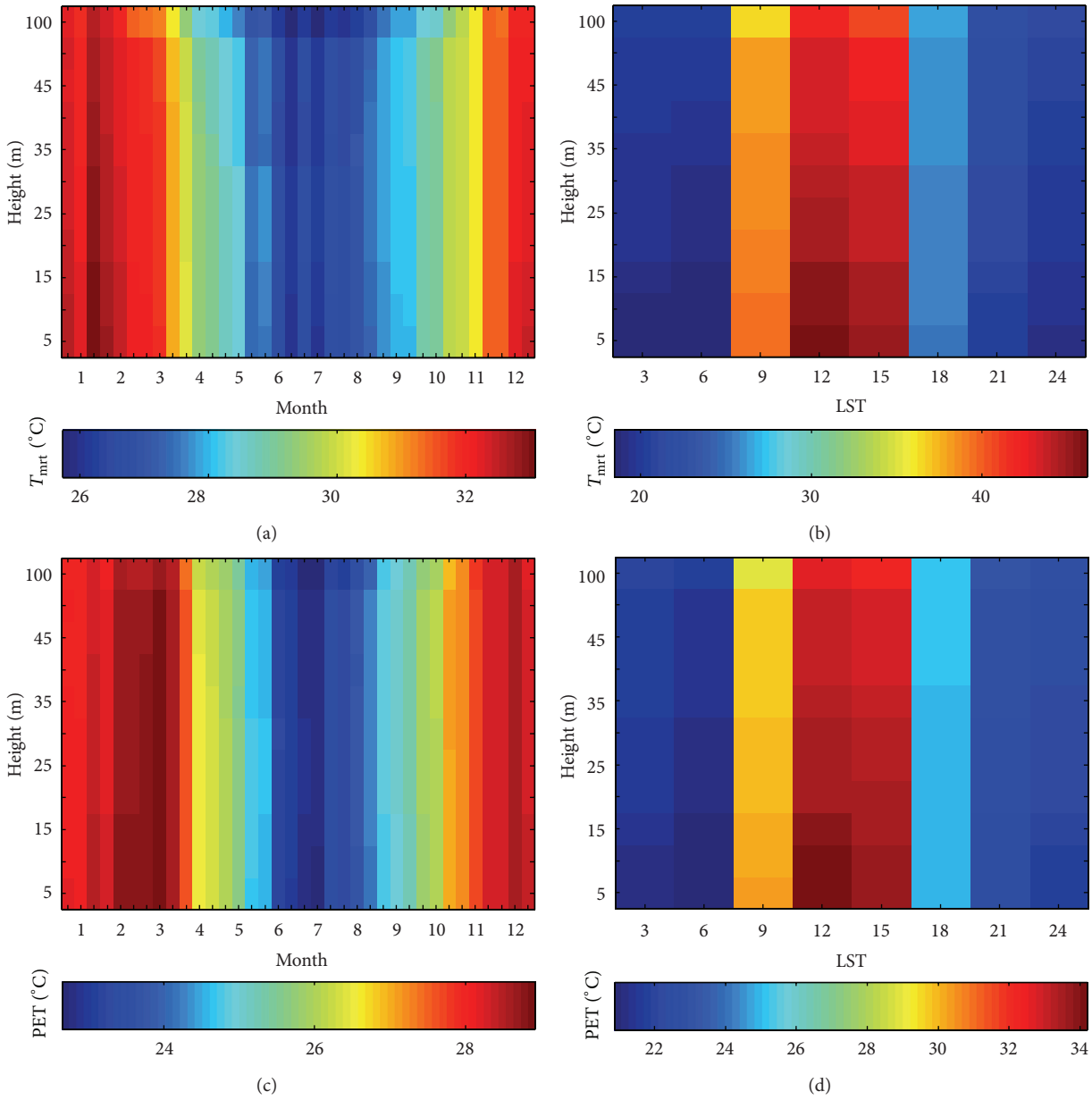

FIGURE 8: Effects of increasing buildings' height on the temporal distribution of T_{mrt} at the urban park as depicted in terms of the annual cycle (a) and diurnal cycle (b). The corresponding thermal comfort distribution is shown in terms of PET index ((c) and (d)).

The simulations results at the urban park suggested that buildings close to the park could significantly affect the thermal comfort at pedestrian level (i.e., human beings resting in an urban park), and the effects become clear as the height of the buildings increases. For instance, at a building height of 100 m, both T_{mrt} and PET values were observed to be significantly reduced (Figure 8). In order to visualize the buildings effect on the park thermal comfort, the park setup was also idealized and rotated every 15°. It should be noted that the buildings surrounding the urban parks are not usually uniformly located around the park as the case here. Results in this simulation are therefore illustrated in Figure 9.

In Figures 9(a) and 9(b), the buildings surrounding the park were kept at 5 m high, and it is clear that a significant reduction of T_{mrt} values could be reached when most of the buildings are located to the south-western side of the park (60° and 105° in the figure). In the diurnal distribution, this reduction could be revealed clearly at 9 LST. When the buildings' height was increased to 100 m, still the situation where most of them are located to the southwest side favours the significant reduction of T_{mrt} (Figures 9(a) and 9(b)). Due to the increased height of the buildings, the effect can also be observed at 15 LST on the diurnal cycle.

The simulations of varying the heights of surrounding buildings and rotating the urban park in order to determine

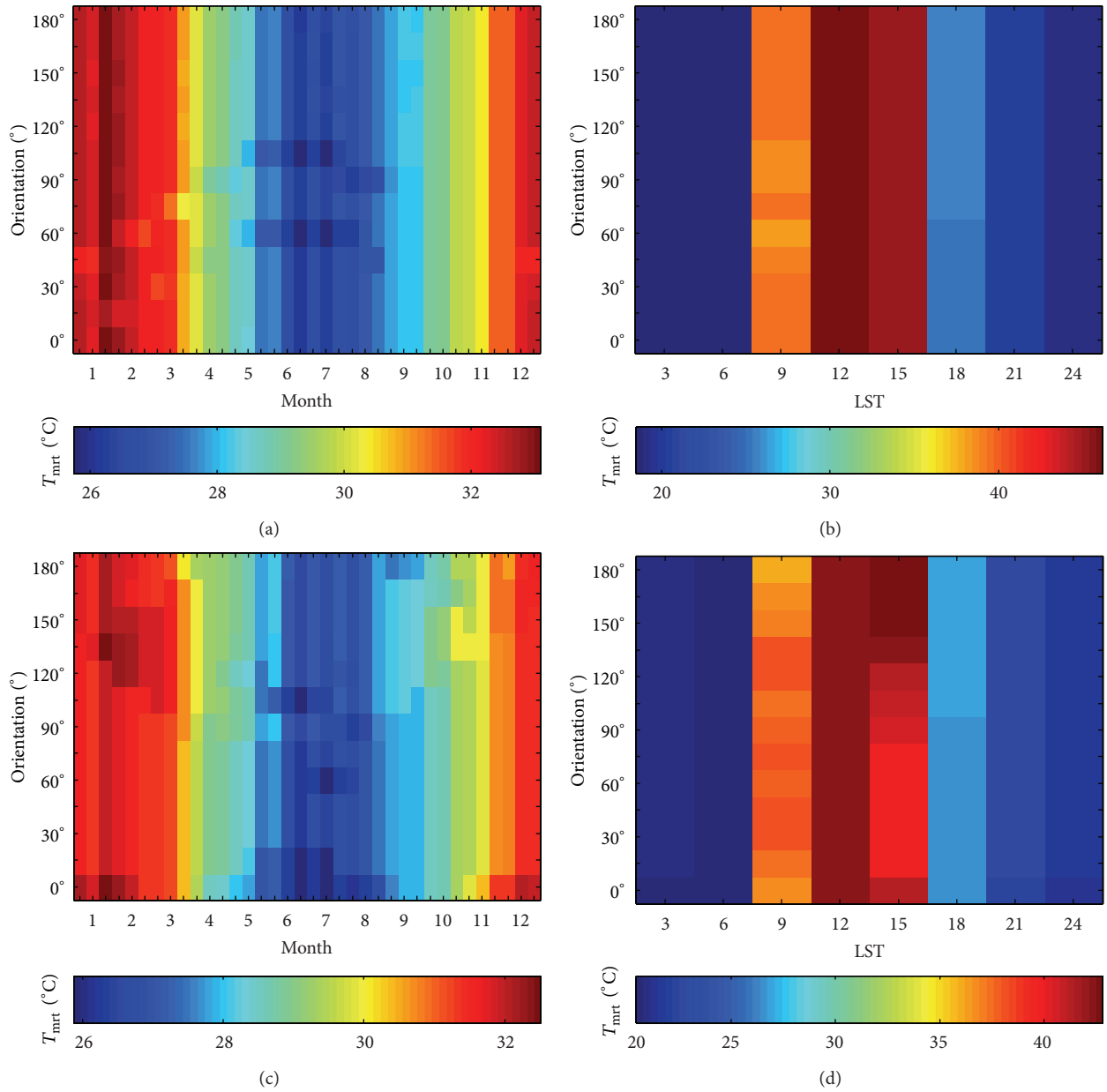

FIGURE 9: Effects of orientation on the temporal distribution of T_{mrt} at the urban park in terms of annual and diurnal cycles ((a) and (b)) with buildings' height kept at 5 m. Corresponding effect when buildings' height was increased to 100 m high ((c) and (d)).

the effect on thermal comfort at pedestrian level seems to be of a novelty in urban climate simulation studies. Many studies have concentrated on simulation of an urban canyon [3, 6, 11, 15, 38], and most of the studies suggested that at pedestrian level, the extreme cases in terms of thermal comfort parameters could be observed at the east-west and north-south orientations [3, 6, 38]. This situation was also observed in this study although with some slight differences which could be attributed to the latitudinal location of the cities which slightly affects the solar path of a particular place.

Simulation of thermal comfort for open spaces is very important especially in realizing the thermal comfort and recreation potential for the parks. Information like this has potential impact on design implications in cities particularly in developing countries where open spaces in cities might be considerably few. It can also help in management of urban parks in the sense that optimal comfort conditions within the urban park could be attained through shading effects of plants within the park itself and the influence of nearby buildings. In this study, buildings' height was particularly observed to exert a decisive role in altering the thermal comfort parameter values. Although, generally the increase in buildings' height was observed to favour reduction in thermal comfort parameters mainly through altering the solar access, this could also have an effect on the wind flow as already discussed in [15]. For Dar es Salaam example, any design

affecting the city open spaces should consider taking the advantage of the sea breezes too.

4. Conclusion

Due to its economic importance in eastern and central Africa, Dar es Salaam city is growing fast. There are increasingly many tall buildings especially in the central business district. Although there are no continuous measurements of urban climate, simulation of urban climate especially to quantify the effects of building and street orientation at pedestrian level using the easily available synoptic data is important and could provide applicable information in terms of urban planning in developing countries. Simulation of urban climate at pedestrian level is also of crucial impact in tropical cities since most of the activities are outdoors. For instance, in Dar es Salaam, there are lot of street vendors who spend most of their daytime hours outside in streets. Thus, the results provided in this study could help in redesigning the streets that ensure thermal comfort at pedestrian level through the variation of buildings' height and orientation.

The simulations performed in this study shows that the thermal comfort parameters (T_{mrt} and PET) at both the urban street and the park can be significantly affected by the urban configuration. Optimal reduction of T_{mrt} and PET values could particularly be obtained on the north-south reoriented streets and with increased buildings' heights. Additionally, the results from the simulations undertaken on a small urban park provided a novelty in design implications and management of open spaces in many cities in the developing countries including Dar es Salaam. These should also help planners understand the potential of open spaces on improving the microclimates in urban areas. The results of this study could also ultimately assist planners in determining appropriate configuration in urban growth areas of Tanzania and elsewhere. Further urban spatial modelling of open spaces in Dar es Salaam is also suggested involving more microscale models for the sake of having robust and firm bioclimatic information to assist in urban planning and management of open spaces.

Acknowledgments

The meteorological data used in the study were obtained from the Tanzania Meteorological Agency and from http://www.ogimet.com/. Emmanuel L. Ndetto would like to acknowledge the financial support granted from the joint scholarship program of Tanzania and Germany through the Germany Academic Exchange Service and Ministry of Education and Vocational Training (DAAD-MOEVT) for his stay in Freiburg, Germany.

References

[1] S. Nieuwolt, "Breezes along the Tanzanian East Coast," *Archiv für Meteorologie Geophysik und Bioklimatologie B*, vol. 21, no. 2-3, pp. 189–206, 1973.

[2] E. L. Ndetto and A. Matzarakis, "Basic analysis of climate and urban bioclimate of Dar es Salaam, Tanzania," *Theoretical and Applied Climatology*, 2013.

[3] F. Ali-Toudert and H. Mayer, "Thermal comfort in an east-west oriented street canyon in Freiburg (Germany) under hot summer conditions," *Theoretical and Applied Climatology*, vol. 87, no. 1–4, pp. 223–237, 2007.

[4] I. Charalampopoulos, I. Tsiros, A. Chronopoulou-Sereli, and A. Matzarakis, "Analysis of thermal bioclimate in various urban configurations in Athens, Greece," *Urban Ecosystems*, vol. 16, no. 2, pp. 217–233, 2013.

[5] F. Bourbia and F. Boucheriba, "Impact of street design on urban microclimate for semi arid climate (Constantine)," *Renewable Energy*, vol. 35, no. 2, pp. 343–347, 2010.

[6] F. Ali-Toudert and H. Mayer, "Numerical study on the effects of aspect ratio and orientation of an urban street canyon on outdoor thermal comfort in hot and dry climate," *Building and Environment*, vol. 41, no. 2, pp. 94–108, 2006.

[7] T.-P. Lin, A. Matzarakis, and R.-L. Hwang, "Shading effect on long-term outdoor thermal comfort," *Building and Environment*, vol. 45, no. 1, pp. 213–221, 2010.

[8] E. Johansson, "Influence of urban geometry on outdoor thermal comfort in a hot dry climate: a study in Fez, Morocco," *Building and Environment*, vol. 41, no. 10, pp. 1326–1338, 2006.

[9] H. Sugawara, A. Hagishima, K. Narita, H. Ogawa, and M. Yamano, "Temperature and wind distribution in an EW-oriented urban street canyon," *Scientific Online Letters of the Atmosphere (SOLA)*, vol. 4, pp. 53–56, 2008.

[10] R. Emmanuel and E. Johansson, "Influence of urban morphology and sea breeze on hot humid microclimate: the case of Colombo, Sri Lanka," *Climate Research*, vol. 30, no. 3, pp. 189–200, 2006.

[11] E. Johansson and R. Emmanuel, "The influence of urban design on outdoor thermal comfort in the hot, humid city of Colombo, Sri Lanka," *International Journal of Biometeorology*, vol. 51, no. 2, pp. 119–133, 2006.

[12] A. Lopes, S. Lopes, A. Matzarakis, and M. J. Alcoforado, "The influence of the summer sea breeze on thermal comfort in funchal (Madeira). A contribution to tourism and urban planning," *Meteorologische Zeitschrift*, vol. 20, no. 5, pp. 553–564, 2011.

[13] S. Ahmad, N. M. Hashim, Y. M. Jani, and N. Ali, "The impacts of sea breeze on urban thermal environment in tropical coastal area," *Advances in Natural and Applied Sciences*, vol. 6, no. 1, pp. 71–78, 2012.

[14] E. L. Krüger and F. A. Rossi, "Effect of personal and microclimatic variables on observed thermal sensation from a field study in southern Brazil," *Building and Environment*, vol. 46, no. 3, pp. 690–697, 2011.

[15] R. Emmanuel, H. Rosenlund, and E. Johansson, "Urban shading—a design option for the tropics? A study in Colombo, Sri Lanka," *International Journal of Climatology*, vol. 27, no. 14, pp. 1995–2004, 2007.

[16] A. Matzarakis, F. Rutz, and H. Mayer, "Modelling radiation fluxes in simple and complex environments—application of the RayMan model," *International Journal of Biometeorology*, vol. 51, no. 4, pp. 323–334, 2007.

[17] A. Matzarakis, F. Rutz, and H. Mayer, "Modelling radiation fluxes in simple and complex environments: basics of the RayMan model," *International Journal of Biometeorology*, vol. 54, no. 2, pp. 131–139, 2010.

[18] S. Thorsson, F. Lindberg, I. Eliasson, and B. Holmer, "Different methods for estimating the mean radiant temperature in an outdoor urban setting," *International Journal of Climatology*, vol. 27, no. 14, pp. 1983–1993, 2007.

[19] P. Jonsson, C. Bennet, I. Eliasson, and E. Selin Lindgren, "Suspended particulate matter and its relations to the urban climate in Dar es Salaam, Tanzania," *Atmospheric Environment*, vol. 38, no. 25, pp. 4175–4181, 2004.

[20] S. E. Mbuligwe and G. R. Kassenga, "Automobile air pollution in Dar es Salaam City, Tanzania," *Science of the Total Environment*, vol. 199, no. 3, pp. 227–235, 1997.

[21] A. Hill and C. Lindner, *Modelling Informal Urban Growth Under Rapid Urbanisation: A CA-Based Land-Use Simulation Model for the City of Dar Es Salaam, Tanzania*, Technische Universität Dortmund, Dortmund, Germany, 2010.

[22] F. R. Fosberg, B. J. Garnier, and A. W. Küchler, "Delimitation of the humid tropics," *Geographical Review*, vol. 51, no. 3, pp. 333–347, 1961.

[23] M. Roth, "Review of urban climate research in (sub)tropical regions," *International Journal of Climatology*, vol. 27, no. 14, pp. 1859–1873, 2007.

[24] C. Howorth, I. Convery, and P. O'Keefe, "Gardening to reduce hazard: urban agriculture in Tanzania," *Land Degradation and Development*, vol. 12, no. 3, pp. 285–291, 2001.

[25] W. Kuttler, "Stadtklimain," in *Handbuch der Umweltveränderungen und Ökotoxologie*, R. Guderian, Ed., pp. 420–470, Springer, Berlin, Germany.

[26] A. Matzarakis, M. Rocco, and G. Najjar, "Thermal bioclimate in Strasbourg-the 2003 heat wave," *Theoretical and Applied Climatology*, vol. 98, no. 3-4, pp. 209–220, 2009.

[27] M. G. Kendall, "A new measure of rank correlation," *Biometrika*, vol. 30, no. 1/2, pp. 81–93, 1938.

[28] A. Matzarakis, H. Mayer, and M. G. Iziomon, "Applications of a universal thermal index: physiological equivalent temperature," *International Journal of Biometeorology*, vol. 43, no. 2, pp. 76–84, 1999.

[29] H. Mayer and P. Höppe, "Thermal comfort of man in different urban environments," *Theoretical and Applied Climatology*, vol. 38, no. 1, pp. 43–49, 1987.

[30] P. Höppe, "The physiological equivalent temperature—a universal index for the biometeorological assessment of the thermal environment," *International Journal of Biometeorology*, vol. 43, no. 2, pp. 71–75, 1999.

[31] D. J. Wessel, *Ashrae Fundamentals Handbook 2001*, ASHRAE, Atlanta, Ga, USA, 2001.

[32] A. Matzarakis, F. Rutz, and H. Mayer, "Modelling radiation fluxes in simple and complex environments—application of the RayMan model," *International Journal of Biometeorology*, vol. 51, no. 4, pp. 323–334, 2007.

[33] G. L. Makokha and C. A. Shisanya, "Trends in mean annual minimum and maximum near surface temperature in Nairobi City, Kenya," *Advances in Meteorology*, vol. 2010, Article ID 676041, 6 pages, 2010.

[34] O. Akinbode, A. Eludoyin, and O. Fashae, "Temperature and relative humidity distributions in a medium-size administrative town in southwest Nigeria," *Journal of Environmental Management*, vol. 87, no. 1, pp. 95–105, 2008.

[35] R. Emmanuel, "Thermal comfort implications of urbanization in a warm-humid city: the Colombo Metropolitan Region (CMR), Sri Lanka," *Building and Environment*, vol. 40, no. 12, pp. 1591–1601, 2005.

[36] C. Grimmond, S. Potter, H. Zutter, and C. Souch, "Rapid methods to estimate sky-view factors applied to urban areas," *International Journal of Climatology*, vol. 21, no. 7, pp. 903–913, 2001.

[37] N. D. Burgess and G. P. Clarke, *Coastal Forests of Eastern Africa*, IUCN, Gland, Switzerland, 2000.

[38] J. Herrmann and A. Matzarakis, "Mean radiant temperature in idealised urban canyons-examples from Freiburg, Germany," *International Journal of Biometeorology*, vol. 56, no. 1, pp. 199–203, 2012.

Hindawi Publishing Corporation
Advances in Meteorology
Volume 2013, Article ID 287934, 10 pages
http://dx.doi.org/10.1155/2013/287934

Research Article

Microclimate Variations between Semienclosed and Open Sections of a Marathon Route

Paulina Wong,[1] Poh-Chin Lai,[1] and Melissa Hart[1,2]

[1] *Department of Geography, The University of Hong Kong, Pokfulam Road, Pokfulam, Hong Kong*
[2] *Australian Research Council Centre of Excellence for Climate System Science, Climate Change Research Centre, The University of New South Wales, Sydney, NSW 2052, Australia*

Correspondence should be addressed to Paulina Wong; paulinaw@hku.hk

Received 22 July 2013; Accepted 24 August 2013

Academic Editor: Andreas Matzarakis

The Hong Kong Standard Chartered Marathon, held annually, is one of the most popular international marathon events. Its primarily urban environmental setting characterized by high-density urban areas, semienclosed tunnels, and suspension bridges, together with the herds of runners, has an influence on the microclimate along the marathon course. This study focused on assessing and comparing variations in temperature and vapour pressure (vis-à-vis relative humidity) against the crowd of runners, or the herd effects, in two different environmental settings along the marathon course: semienclosed (a tunnel) versus open space (a suspension bridge). A series of small iButtons were deployed at strategic locations along the course to undertake minute-by-minute measurements of temperature and relative humidity. It was found that herd effects of varying degrees were present in both semienclosed and open settings. Various environmental differences also played a role in ameliorating or amplifying the climatological effects of the herd of runners. Our study suggests that microclimate variations in different environmental settings and crowd conditions could have an impact on runners. This new knowledge can inform the design of marathon routes. It also establishes the feasibility of employing the iButton logging sensors for widespread deployment and monitoring of meteorological situations.

1. Introduction

More than 500 marathons are held annually around the world, with competitors ranging from elite marathon runners to recreational athletes [1]. Each marathon is challenging by the way of its course design and the environment through which the route passes. The increased popularity of marathons has prompted research on the effects of weather conditions on runners. Previous studies have been mainly based on statistical analyses of past marathon data by quantifying effects of weather conditions on the performance or completion times of the runners [2–6].

The most noticeable human effect is in the microclimates found in the heavily built-up areas, and this localised microclimate may become more pronounced when runners are tightly bunched in moving packs or "herds" [7, 8]. In addition to anthropogenic impacts on the microclimate from the herds of runners, course terrain, landscape, urban configurations, and meteorological conditions will contribute to the microclimate along a marathon route [9], which may influence level of human thermal comfort [10] and performance of each individual runner. However, there is a lack of studies exploring possible impacts of microclimatic variation along marathon courses, particularly in events held in such challenging conditions as in the Hong Kong urban area.

The Hong Kong Standard Chartered Marathon, one of the signature international sporting events of Hong Kong, is held annually with recorded entrants growing from 1,000 in 1997 to 70,000 in 2012 [11]. The event route is confined to urban areas passing through various types of urban morphology and topography. The route passes through commercial areas with high building density and many built structures which do not usually have pedestrian access, such as enclosed tunnels, divided highways, and overhead bridges.

It is well known that warmer temperatures and higher humidity levels have a negative effect on the runners due to

the reduction of heat loss and the corresponding increase in the body temperature [8, 12]. During warm conditions, marathon runners' control of their thermoregulation may be reduced [5, 13], and heat loss of runners would physiologically worsen by a parallel increase in the metabolic heat production from exercising under a relatively high ambient temperature. Febbraio [14] suggested that the intramuscular temperature would rise in proportion to the increase of work load and that metabolism rate would also amplify during exercise and under thermal stress. It is common for runners to suffer from heat exhaustion, heat stress, and other heat-related illnesses [15, 16]. A few young runners collapsed in the middle of the 2012 Hong Kong Marathon run, and one was reported dead [17]. In addition to heating up when exercising, metabolic heat emissions from surrounding people when in a crowd can also affect levels of thermal comfort and/or stress [7].

Blows [7] established the "penguin effect" to illustrate physiological changes on people in overcrowded situations. He argued that overcrowding would reduce the heat loss ability of an individual exercising in a crowd and that the physiological heat stress would amplify if the crowd was to engage in physical or emotionally heightened activities. He also claimed that heat would transfer from people to the environment. A similar study conducted by De Freitas et al. [18] quantified and modelled heat loads brought about by running in a herd. It became evident that the heat load for a runner in an exercising crowd would increase a great deal compared to those running solo. Furthermore, Montain et al. [8] recognised that slower or casual runners compared to elite runners would suffer further performance deprivation in warmer weather. They argued that slower runners would be exposed longer to the environment and would be more likely to run in close proximity to other runners. The situation would mean that they would be running in a microclimate that tended to be warmer than the indicated weather conditions. In this paper, the effects of heat retention on an individual in a moving crowd are described as the "herd effect" which is unlike the "penguin effect" which describes the effects of heat retention on an individual in a stationary crowd.

In view of the likelihood of thermal heat stress arising from exercising in high ambient temperatures and the adverse health impacts caused by excessive heat retention of an individual in a crowd, this study focuses on assessing the above phenomena in semienclosed and open spaces. It offers empirical evidence of the "herd effect" on the microclimate in different environmental settings along a marathon route.

2. Materials and Method

2.1. Background and Study Area. Hong Kong has a humid subtropical climate (Köppen classification Cwa) with hot and humid summers and mild winters. Most summer days have high humidity with warm air coming from the southwest, creating local thermal discomfort. The Hong Kong Standard Chartered Marathon is usually held in late winter or early spring to minimise runner discomfort. The full marathon follows its famed urban route starting at Nathan Road in Tsim Sha Tsui and finishing at the Victoria Park in Causeway Bay [11] (Figure 1). The course follows major highways and passes through three tunnels (Nam Wan, Cheung Tsing, and Western Harbour) and three bridges (Stonecutters, Tsing Ma, and Ting Kau). In 2012, the marathon was held on 5th February from 0530 to 1300. The weather on that day was calm with light north-easterly winds and warmer than average air temperature and vapour pressure ranging from 16°C to 22°C and 13.6 hPa to 25.1 hPa, respectively, as reported by the Hong Kong Observatory [19]. Average daily temperatures in February range between 15.0°C to 18.9°C, and mean daily vapour pressure is 15.4 hPa [19].

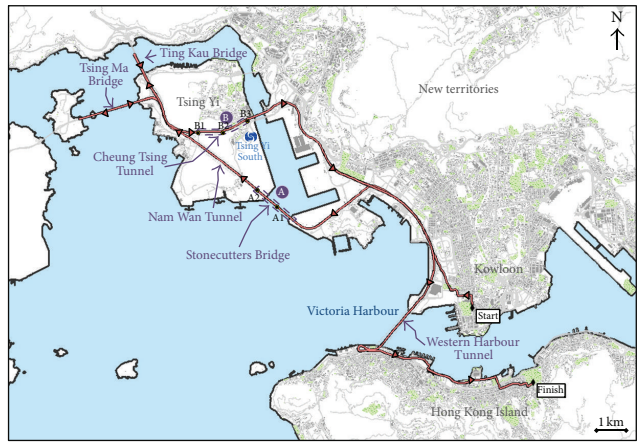

Figure 1: The 2012 Hong Kong Standard Chartered Marathon Route with study sites and sampling locations indicated.

Two study locations representing an open area (Site A) and a semienclosed space (Site B) (Figure 1 and Table 1) were used to examine variability in thermal environment and microclimate conditions along the marathon course. A camera with a fish-eye lens was employed to take photos at both sites to calculate their sky view factors (SVF) using the RayMan model developed by Matzarakis et al. [20]. Site A is the Stonecutters Bridge, a suspension bridge above water located 8 km along the marathon route. It is totally exposed without vegetation coverage (SVF = 0.97 for visible sky, Table 1). Site B is the Cheung Tsing Tunnel, 24 km into the marathon route; the site is a borne tunnel through solid granite of Tsing Yi Island. The 1.6 km long semienclosed tunnel (SVF = 0 for no visible sky, Table 1) carries three lanes of dual carriageway and is connected by an overpass at one end and a bridge at the other [21].

Two types of data were collected at these sites: meteorological data and runner counts.

2.2. Meteorological Data. To monitor microclimatic conditions, dry-bulb temperature and relative humidity were monitored using a wireless temperature measuring system, the Thermochrons iButton (type DS1923; Maxim/Dallas Semiconductor Corp., USA). The iButton is a small and durable temperature/humidity sensor equipped with a data logger

Table 1: Urbanisation characteristics of the sampling sites with respect to the marathon route.

	Site A	Site B
(a) Characteristic	Open area	Semienclosed area
(b) Location	Stonecutters Bridge	Cheung Tsing Tunnel
(c) Specifications	(i) 1.60 km length (ii) Dual three-lane high-level cable-stayed bridge	(i) 1.60 km length (ii) Dual three-lane twin-borne tunnel
(d) Width of marathon course	3 to 4 m (single lane)	3 to 4 m (single lane)
(e) Distance from starting point	Approximately 8 km	Approximately 24 km
(f) Location of iButtons		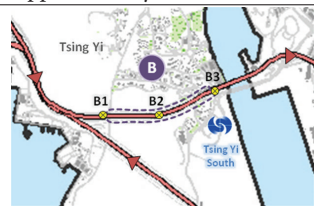
(g) Orthophotograph	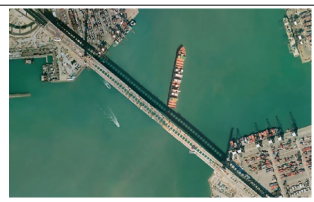	
(h) Snapshot		
(i) Sky view factor (SVF)	 SVF = 0.97	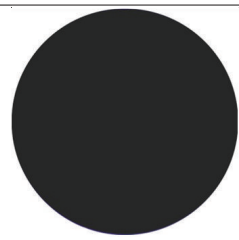 SVF = 0

(Figure 2(a)). The thermal and relative humidity accuracy stated by its manufacturer are ±1°C with thermal response time of 130 seconds and ±5% with a 30-second response time, respectively. All iButtons have been calibrated and tested in house, utilizing ice and warm water baths to assure that all of the iButtons were within ±1°C accuracy. Notably, most of them were within ±0.5°C, which was well within the stated accuracy. Two iButtons (A1 and A2) were installed at Site A. A1 is at the middle of the bridge which is an entirely open area above water (Figure 3(A1)). A2, on the other hand, is on the landward side and partially surrounded by high-rise buildings on both sides (Figure 3(A2)). Due to the complexity of the semienclosed tunnel microclimate, three iButtons (B1, B2, and B3) were placed at Site B. B1 is at the entrance of the tunnel with lush vegetation alongside the overpass (Figure 3(B1)), site B2 is located in the middle of the tunnel (Figure 3(B2)), and site B3 is located near the exit of the tunnel leading to a suspension bridge which was entirely exposed (Figure 3(B3)). There are jet fans installed along the ceiling of the tunnel for longitudinal ventilation.

Each of the iButtons was housed in an Onset HOBO RS3 solar radiation shield and installed on a standard one-metre high traffic cone (Figure 2(b)). The sensors were set to measure air temperature and relative humidity at one-minute intervals. In addition, one-minute meteorological data were obtained from the nearby Tsing Yi South automatic weather station (see Figure 1). The weather station is managed by the Hong Kong Observatory (HKO) and was classified by Siu

(a) (b)

Figure 2: Temperature and relative humidity measurement and logging equipment: (a) iButton in solar radiation shield and (b) iButton in solar radiation shield installed on a traffic cone.

(A1) The 1.6 km long Stonecutters Bridge is a suspension bridge surrounded by open water on both sides

(A2) Exit of the Stonecutters Bridge is surrounded by buildings on both sides before approaching a tunnel

(B1) Entrance to the Cheung Tsing Tunnel is surrounded by green vegetation on both sides

(B2) The 1.6 km long Cheung Tsing Tunnel is equipped with jet-fan longitudinal ventilation

(B3) Exit of the Cheung Tsing Tunnel leads to a suspension bridge that is totally exposed

Figure 3: Photographs and descriptions of each of the sampling locations (A1, A2, B1, B2, and B3).

and Hart [22] as open-set blocks (BCZ5) using the Local Climate Zones (LCZ) landscape classification system [23]. These official measurements were used as a control against data collected by the iButtons.

2.3. Runner Counts. There were a total of 12,105 recorded entrants for the full marathon in 2012 [11]. Staggered start times at 0645 and 0715 were used to manage the large number of runners. Several timing mats were positioned

by the marathon organisers at split or turning points to track runners throughout the race. The temporal accounts of individual runners were used to model the herds of runners at various junctures to correlate with microclimate data at the corresponding time intervals.

2.4. Method of Analysis. One-minute temperature (T_{IB}) and humidity (RH_{IB}) readings collected by iButton sensors at Site A (open space) and Site B (semienclosed space) were compared against the corresponding one-minute HKO meteorological data measured at the Tsing Yi South weather station (T_{HKO} and RH_{HKO}) to develop the temperature differences ($\Delta T = T_{IB} - T_{HKO}$). The temperature differences of each location were then plotted across the temporal scale at a one-minute interval. The herds of runners for the same time period were modelled from the time records of individual runners based on the available runner counts data. With the aid of global positioning system devices, the runner counts were mapped against the temporal scale to examine the herd effects at each site, which have two very different environmental settings.

The humidity readings were used to compute vapour pressure (VP), an absolute measure of atmospheric moisture that is not temperature dependent. The computed vapour pressures were compared across the computed official HKO data to develop the vapour pressure differences ($\Delta VP = VP_{IB} - VP_{HKO}$). The vapour pressure differences of each site were plotted across the temporal scale of per-minute interval and correlated with the herd of runners to examine the herd effects on atmospheric moisture level under the different environmental settings.

Microclimatic conditions (temperature and vapour pressure) at the two sites were also compared for two groups, herd and no herd, using Student's t-test for further verification of the herd effect on microclimatic conditions. Temporal intervals with more than 10 runners (arbitrarily set for this study) were put into the group with herd and the remaining into the group with no herd. This grouping effectively preempted the few elite runners and the very slow runners from skewing the results.

3. Results

3.1. Site A—Stonecutters Bridge (Open Space). The marathon commenced at 0645 with runners coming through the measurement sites at Stonecutters Bridge (8 km from the starting point) from 0717 to 0830 (Figure 3). Figure 4 illustrates the temperature difference between the iButton readings (T_{IB}) and the official temperature readings (T_{HKO}) from the Tsing Yi South weather station. Sites A1 (orange line) and A2 (green line), located at the middle and near one end of the 1.6 km long suspension bridge, respectively, experienced similar trends, with A2 experiencing, on average, a 0.2°C higher temperature difference to the control site. Figure 4 also shows two batches of full marathon runners with staggered start times peaking at the Stonecutters Bridge site at 0730 and 0810. Between 0723 and 0740 and 0800 and 0817, the herds of runners crossing the bridge amounted to more than

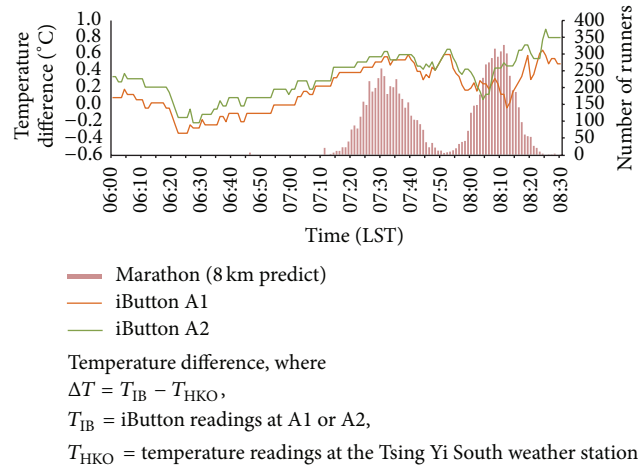

Figure 4: Minute-by-minute temperature difference and runner counts at the Stonecutters Bridge (Site A: open space).

100 per minute. The temperature difference was on average 0.5°C when the first herd of runners were crossing the bridge; this difference narrows after the sun had risen at 0700. The temperature difference for the second herd of runners was less with an average of 0.3°C.

The microclimatic conditions at the Stonecutters Bridge were examined under two scenarios: herd and no herd. As defined in Section 2.4, temporal intervals with more than 10 runners were added to the "herd" group, and the remaining intervals fell into the group "no herd". The results of Student's t-test in Table 2 reveal significant temperature differences ($P = 0.00$) in the microclimate of both sites when runners pass by. Both A1 and A2 reported mean temperature differences of 0.2°C higher, during times the herd was passing by.

Figure 5 shows the minute-by-minute vapour pressure differences derived with relative humidity readings from the iButtons (VP_{IB}) and the Tsing Yi South weather station (VP_{HKO}). The line graphs of both A1 (orange line) and A2 (green line) at the middle and exit of the suspension bridge, respectively, displayed similar fluctuations. However, vapour pressure difference at A2 was on average 0.4 hPa higher than A1. During the times the first herd of runners crossed Stonecutters Bridge the vapour pressure difference was more pronounced at A2, with an average difference of 0.5 hPa, compared to 0.1 hPa at A1 when the first herd of runners crossed the bridge. The vapour pressure difference for both A1 and A2 rose sharply (an average of 0.5 hPa and 0.8 hPa, resp.) when the second herd passed.

Results of Student's t-test, shown in Table 2, revealed significant vapour pressure differences as the herd passed at A2 ($P = 0.00$), which is situated at one end of the suspension bridge, but not at A1 ($P = 0.05$) which is located in the middle of the 1.6 km long crossing. A mean vapour pressure difference of 0.2 hPa higher with herd was observed at A2 (the landward side) compared with 0.1 hPa at A1 (in the middle of the bridge) indicating the ameliorating effects of open-air circulation.

Table 2: Statistical results (Student's t-test) of temperature and vapour pressure differences for conditions with and without herd effects at each of the sampling locations.

Site	Sampling location	Type	Effect	N	Mean	Std. deviation	Std. error mean	t	df	Sig. (2-tailed)	Mean difference	Std. error difference	95% confidence interval Lower	95% confidence interval Upper
A	A1	ΔT	Herd	66	0.4	0.1	0.02	5.1	43.9	0.00	0.2	0.1	0.1	0.3
			No herd	33	0.1	0.2	0.04							
	A2	ΔT	Herd	66	0.5	0.1	0.02	5.8	48.1	0.00	0.2	0.04	0.1	0.2
			No herd	33	0.3	0.2	0.03							
	A1	ΔVP	Herd	66	0.2	0.3	0.03	2.0	97.0	0.05	0.1	0.06	0.0	0.2
			No herd	33	0.04	0.3	0.04							
	A2	ΔVP	Herd	66	0.6	0.2	0.02	4.3	97.0	0.00	0.2	0.04	0.1	0.3
			No herd	33	0.4	0.2	0.03							
B	B1	ΔT	Herd	125	1.0	0.4	0.03	5.6	109.6	0.00	0.3	0.05	0.2	0.3
			No herd	27	0.8	0.2	0.03							
	B2	ΔT	Herd	125	1.7	0.4	0.04	4.8	75.8	0.00	0.3	0.05	0.2	0.4
			No herd	27	1.4	0.2	0.04							
	B3	ΔT	Herd	125	2.4	0.6	0.05	8.4	106.8	0.00	0.6	0.07	0.4	0.7
			No herd	27	1.9	0.2	0.04							
	B1	ΔVP	Herd	125	1.0	0.3	0.03	0.3	150.0	0.80	0.01	0.1	−0.10	0.1
			No herd	27	1.0	0.2	0.05							
	B2	ΔVP	Herd	125	3.1	1.6	0.14	14.0	149.2	0.00	2.1	0.2	1.8	2.4
			No herd	27	1.0	0.3	0.06							
	B3	ΔVP	Herd	125	1.1	0.3	0.03	−2.1	150.0	0.04	−0.1	0.1	−0.3	−0.01
			No herd	27	1.2	0.2	0.04							

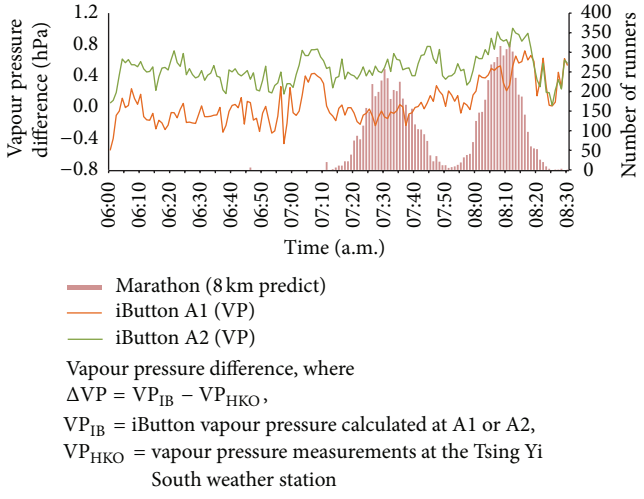

Figure 5: Minute-by-minute vapour pressure difference and runner counts at the Stonecutters Bridge (Site A: open space).

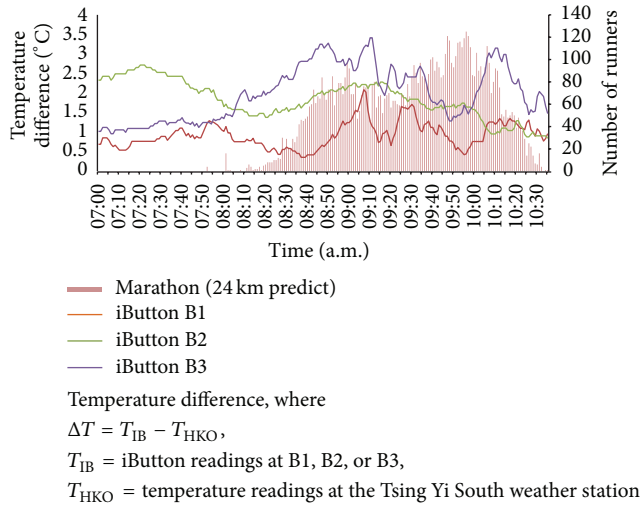

Figure 6: Minute-by-minute temperature difference and runner counts at the Cheung Tsing Tunnel (Site B: semienclosed space).

3.2. Site B—Cheung Tsing Tunnel (Semienclosed Space). The iButtons B1, B2, and B3 were located at the entrance, centre, and exit of the Cheung Tsing Tunnel as shown in Table 1. The iButton measurements commenced from 0700 until 1030. Figure 6 shows the minute-by-minute temperature difference between the iButtons (T_{IB}) and official temperature (T_{HKO}) readings from the Tsing Yi South weather station. The three lines (red for B1, green for B2, and purple for B3) registered dissimilar trends with B3, at the exit point of the tunnel, measuring the highest temperature difference (average = 2.3°C), compared to an average of 1.6°C for B2 at the centre of the tunnel and 1.0°C for B1 at the entrance of the tunnel. Figure 6 shows that two herds of runners passed through the Cheung Tsing Tunnel, showing the influence of the staggered start times. It was also evident that, between 0915 and 0935, some runners from the first herd had begun to slow down to merge with the faster runners of the second herd; the tunnel is more than half way (24 km) into the 42 km full marathon run. Time intervals with herds of runners exceeding 100 per minute appeared intermittently between 0945 and 1005.

Given that the Cheung Tsing Tunnel has jet fans installed along the tunnel ceiling for longitudinal ventilation [21, 24], temperature differences at the centre of the tunnel (B2) displayed a decreasing trend in the presence of runners to indicate that the ventilation system may have done its job in regulating the airflow. The jet fans regulate airflow along one direction to evacuate air pollutants and heat to the end of the tunnel [25]. The situation was quite different at the ends of the tunnel. Before the first herd of runners approached the tunnel starting from 0750, the temperature difference at the centre of the tunnel (B2) was on average 1.4°C higher than those at the two ends (B1 and B3). The entrance to the tunnel (B1), unlike the exit (B3), experienced a drop in temperature for the first 40 minutes when total runners per minute stayed below 40. Thereafter, the temperature differences for both entrance (B1) and exit (B3) fluctuated in the same patterns, with B3 on average 1.0°C higher than B1. The temperature differences appeared to oscillate with the number of runners for the major part of the marathon, except around the second peak of runner counts. We attribute this anomaly to the ventilation control in the tunnel that could have ventilated the airflow to this end and disrupted the herd effect.

The microclimatic conditions in the Cheung Tsing Tunnel were examined under two scenarios: herd and no herd. Results in Table 2 confirmed significant temperature differences ($P = 0.00$) at all three sites during times with herd and no herd. When the sites were under the influence of the herd effect, mean temperature differences of 0.3°C, 0.3°C, and 0.6°C higher were observed for B1, B2, and B3, respectively.

Figure 7 illustrates that the vapour pressure differences for all three sampling sites (B1 at the entrance, B2 at the centre, and B3 at the exit) of the tunnel exhibited similar trends and values before the first herd of runners approached the tunnel. Site B2, at the centre of the tunnel, measured a steady increase in vapour pressure as the first herd of runners entered the tunnel at around 0830. The vapour pressure difference continued to rise for 25 minutes from 1.5 hPa to the maximum of 6.0 hPa. The vapour pressure declined thereafter as the second herd of runners were leaving the tunnel. Comparable differences with average values of 0.9 hPa and 1.0 hPa higher than the official readings were found at both ends of the tunnel at B1 and B3. There was no remarkable fluctuation at B1 and B3 in the presence of runners.

The results of the t-test in Table 2 confirmed that there were significant differences in vapour pressure with herd and no herd at B2 ($P = 0.00$) and B3 ($P = 0.04$) located at the centre and exit of the tunnel, with a mean difference in vapour pressure of 2.1 and −0.1 hPa, respectively. No significant difference was observed at B1 located at the entrance of the tunnel, with mean vapour pressure differences of 0.01 hPa ($P = 0.80$), with herd.

4. Discussion

Our study offers empirical evidence about the microclimatic differences between semienclosed and open sections

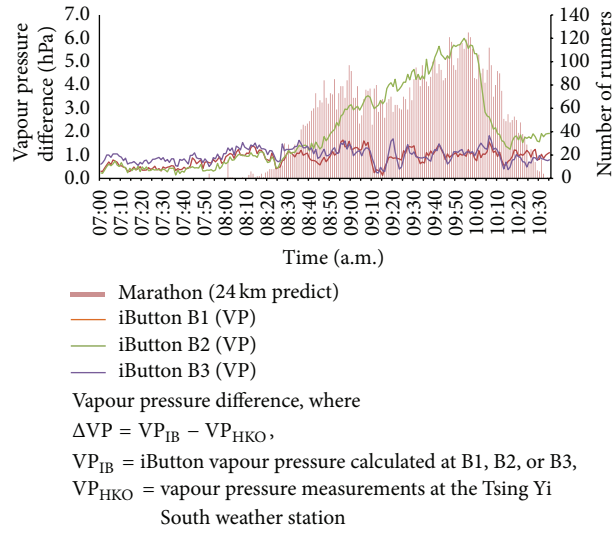

Figure 7: Minute-by-minute vapour pressure difference and runner counts at the Cheung Tsing Tunnel (Site B: semienclosed space).

of a marathon route. Herd effects were felt in both settings, with the effects in the semienclosed setting interrupted by controlled ventilation in the tunnel. It does appear that environmental differences have an impact on ameliorating or amplifying the herd effects. For Site A, representative of the entirely open sections of the route (as illustrated in Figures 4 and 5), both temperature and vapour pressure differences for the site located at the end of the bridge (A2) were higher compared to those at Site A1, located at the middle of the bridge. A1 at the middle of the Stonecutter Bridge is an entirely open area above water and has abundant air circulation to offset the herd effects (Figure 3(A1)). A2, on the other hand, is partially surrounded by high-rise buildings to compromise wind ventilation (Figure 3(A2)). Herd effects were, therefore, more pronounced at A2 than A1. In other words, sufficient wind ventilation and proximity to a large water body (serving as a cool sink) effectively reduce both microclimatic urbanisation effects at pedestrian level [26] and herd impacts on the runners.

The situation of B3 at the exit of the semienclosed tunnel (Figure 3(B3)) is comparable to that of A2 near the end of the overhead bridge. Figures 6 and 7 showed that temperature and vapour pressure differences at B3 were always above those at B1 (entrance of the tunnel). The former led to a suspension bridge which was entirely exposed (Figure 3(B3)), while the latter had lush vegetation alongside the motorway (Figure 3(B1)), demonstrating cooling effects of vegetation on the microclimate [27, 28]. It is also interesting to note that the ventilation system of the tunnel may have played a role in moderating temperature differences but not in reducing vapour pressure arising from the herds, as illustrated in Figures 6 and 7. The increased airflow from the ventilation system may have caused evaporative cooling of the initial warm, moist air mass brought into the tunnel by the herd of runners. Ventilation systems of this type are designed to evacuate air pollutants (traffic emissions) and heat within the tunnel as means of air quality and fire safety measure [25]. During normal traffic conditions in tunnels of this kind, the airflow from the ventilation fans flows in the direction of prevailing traffic, and the system may occasionally switch off to self-ventilate by taking advantage of traffic-induced piston effects [24]. One major limitation of this study is that we were unable to gain explicit information on the operation of the system during the event, making it difficult to quantify the exact effects of the ventilation system on the herd.

Our study also confirms the practical utility of the small and low-cost iButtons for widespread deployment. The affordable iButtons offer reliable measurement and consistent performance when compared against official readings from a nearby HKO weather station. Similar to a study by Cheung et al. [29], the accuracy of iButtons in our study was well within ±1°C as listed by the manufacturer.

We note a few methodological drawbacks in our study. Firstly, we made use of meteorological data from a nearby weather station managed by the HKO to compute microclimate differences. However, we were unable to separate clearly herd effects from the diurnal warming effects after sunrise at 0700. Secondly, we modelled runner counts from temporal accounts of individual runners. The derived values might not be entirely accurate as 27.8% of full marathon runners were miscounted for various reasons. For instance, some runners started after the cutoff time, or they did not step on the timing mats properly, or they pulled at the event at some point along the course. In addition, the modelling procedure for runner counts at one-minute time interval assumed that individual runners ran at steady speeds without provisions for stopping for replenishment or relaxation. And finally, the lack of information available to us on the operation of the ventilation system in the tunnel during the event makes it difficult to quantify its impact on the herd of runners; future studies of this kind would benefit from the incorporation of wind speed and wind direction measurements at sampling locations. Despite these limitations, results of our study did suggest that environmental factors and herd effects will affect the microclimate of a marathon course, which may detrimentally impact marathon runners although the error limits of the iButton temperature sensors (±1°C) should be taken into account during the interpretation of the results.

5. Conclusion

This study presented empirical evidence of the "herd effect" on marathon runners and contrasted the microclimate variations of herd effects in two different environmental settings along a full marathon course: open-space suspension bridge (Site A) versus semienclosed vehicle tunnel (Site B).

The microclimate differences at both sites, in terms of temperature and vapour pressure, with and without the influence of the herd of runners were statistically significant. Comparatively, the microclimate differences appeared to be more pronounced at the exits of both sites (A2 and B3). Environmental factors such as greenery, wind ventilation, water body, urban morphology, and mesoscale flows also play a role in impacting the magnitude of the herd effect.

Although our findings on herd effects may not be exact, the study is the first of its kind to examine association between microclimate differences and crowding of runners. It also demonstrates methodological feasibility for bulk installation of an economical monitoring device for temperature and humidity measurements. Our findings also provide guidance to marathon organisers about design considerations for an optimum marathon course and the need for crowd control to minimise the impact of herd effects.

Conflict of Interests

The authors declare that there is no conflict of interests regarding the publication of this paper.

Acknowledgments

The authors would like to acknowledge support from organisers of the Hong Kong Standard Chartered Marathon and the Hong Kong Amateur Athletic Association (HKAAA). Thanks are also extended to the Hong Kong Observatory (HKO). This paper was funded through the University of Hong Kong Hui Oi Chow Trust Fund-General Award (Project no. 201103172004) and the General Research Fund (Project no. 746210) from the Research Grants Council of Hong Kong.

References

[1] D. M. D. Webner, "Study Done In Marathon Runners Gets National Recognition," The Journal of Crozer-Keystone Healthplex, 2012, http://www.crozerkeystone.org/news/Publications/The-Journal/2012/december/study-done-in-marathon-runners-gets-national-recognition/.

[2] M. R. Ely, S. N. Cheuvront, and S. J. Montain, "Neither cloud cover nor low solar loads are associated with fast marathon performance," *Medicine and Science in Sports and Exercise*, vol. 39, no. 11, pp. 2029–2035, 2007.

[3] M. R. Ely, S. N. Cheuvront, W. O. Roberts, and S. J. Montain, "Impact of weather on marathon-running performance," *Medicine & Science in Sports & Exercise*, vol. 39, no. 3, pp. 487–493, 2007.

[4] L. M. Trapasso and J. D. Cooper, "Record performances at the Boston marathon: biometeorological factors," *International Journal of Biometeorology*, vol. 33, no. 4, pp. 233–237, 1989.

[5] T. Vihma, "Effects of weather on the performance of marathon runners," *International Journal of Biometeorology*, vol. 54, no. 3, pp. 297–306, 2010.

[6] Z. Suping, M. Guanglin, W. Yanwen, and L. Ji, "Study of the relationships between weather conditions and the marathon race, and of meteorotropic effects on distance runners," *International Journal of Biometeorology*, vol. 36, no. 2, pp. 63–68, 1992.

[7] W. T. Blows, "Crowd physiology: the 'penguin effect'," *Accident and Emergency Nursing*, vol. 6, no. 3, pp. 126–129, 1998.

[8] S. J. Montain, M. R. Ely, and S. N. Cheuvront, "Marathon performance in thermally stressing conditions," *Sports Medicine*, vol. 37, no. 4-5, pp. 320–323, 2007.

[9] I. Charalampopoulos, I. Tsiros, A. Chronopoulou-Sereli, and A. Matzarakis, "Analysis of thermal bioclimate in various urban configurations in Athens, Greece," *Urban Ecosystems*, vol. 16, no. 2, pp. 217–233, 2013.

[10] A. Matzarakis, H. Mayer, and M. G. Iziomon, "Applications of a universal thermal index: physiological equivalent temperature," *International Journal of Biometeorology*, vol. 43, no. 2, pp. 76–84, 1999.

[11] HKAAA, "Standard Chartered Hong Kong Marathon," 2012, http://www.hkmarathon.com/marathon/eng/home.

[12] Y. Kobayashi, Y. Ando, and S. Takeuchi, "Effects of heat acclimation of distance runners in a moderately hot environment," *European Journal of Applied Physiology and Occupational Physiology*, vol. 45, no. 2-3, pp. 189–198, 1980.

[13] N. El Helou, M. Tafflet, G. Berthelot, J. Tolaini, A. Marc et al., "Impact of environmental parameters on marathon running performance," *PLoS One*, vol. 7, no. 5, Article ID e37407, 2012.

[14] M. Febbraio, "Alterations in energy metabolism during exercise and heat stress," *Sports Medicine*, vol. 31, no. 1, pp. 47–59, 2001.

[15] E. Law, "Marathon runners urged to watch step on health," The Standard, 2011, http://www.thestandard.com.hk/news_detail.asp?pp_cat=11&art_id=108182&sid=31326326&con_type=1&d_str=20110217&isSearch=1&sear_year=2011.

[16] A. M. Porter, "Marathon running and adverse weather conditions: a miscellany," *British Journal of Sports Medicine*, vol. 18, no. 4, pp. 261–264, 1984.

[17] A. So, "Tragic End. The Standard," 2012, http://www.thestandard.com.hk/news_detail.asp?pp_cat=30&art_id=119402&sid=35310569&con_type=3&d_str=20120206&isSearch=1&sear_year=2012.

[18] C. R. De Freitas, N. J. Dawson, A. A. Young, and W. J. Mackey, "Microclimate and heat stress of runners in mass participation events," *Journal of Climate & Applied Meteorology*, vol. 24, no. 2, pp. 184–191, 1985.

[19] HKO, "The Hong Kong Observatory Official Website," 2012, http://www.hko.gov.hk/contente.htm.

[20] A. Matzarakis, F. Rutz, and H. Mayer, "Modelling radiation fluxes in simple and complex environments—application of the RayMan model," *International Journal of Biometeorology*, vol. 51, no. 4, pp. 323–334, 2007.

[21] A. Tam, "Construction of the cheung ching tunnel," *Tunnels and Tunnelling*, vol. 29, no. 6, pp. 25–26, 1997.

[22] L. W. Siu and M. Hart, "Quantifying urban heat island intensity in Hong Kong SAR, China," *Environmental Monitoring and Assessment*, vol. 185, no. 5, pp. 4383–4398, 2013.

[23] I. D. Stewart and T. R. Oke, "Local climate zones for urban temperature studies," *Bulletin of the American Meteorological Society*, vol. 93, no. 12, pp. 1879–1900, 2012.

[24] J. S. M. Li and W. K. Chow, "Vehicular tunnel ventilation design and application of CFD Air Distribution in Rooms," in *Proceedings of the 7th International Conference on Air Distribution in Rooms, Ventilation for Health and Sustainable Environment*, 2000.

[25] S. Li, *Analysis on the fire safety aspects for tunnels in Hong Kong with mathematical models [Ph.D. thesis]*, The Hong Kong Polytechnic University, Hong Kong, 2005.

[26] E. Ng, "Policies and technical guidelines for urban planning of high-density cities-air ventilation assessment (AVA) of Hong Kong," *Building and Environment*, vol. 44, no. 7, pp. 1478–1488, 2009.

[27] T. Fung and W.-L. Siu, "A study of green space and its changes in Hong Kong using NDVI," *Geographical and Environmental Modelling*, vol. 5, no. 2, pp. 111–122, 2001.

[28] S. S. Lau, P. Lin, and H. Qin, "A preliminary study on environmental performances of pocket parks in high-rise and high-density urban context in Hong Kong," *International Journal of Low-Carbon Technologies*, vol. 7, no. 3, pp. 215–225, 2012.

[29] H. K. Cheung, G. J. Levermore, and R. Watkins, "A low cost, easily fabricated radiation shield for temperature measurements to monitor dry bulb air temperature in built up urban areas," *Building Services Engineering Research and Technology*, vol. 31, no. 4, pp. 371–380, 2010.

Hindawi Publishing Corporation
Advances in Meteorology
Volume 2013, Article ID 976510, 8 pages
http://dx.doi.org/10.1155/2013/976510

Research Article

Human Bioclimatic Conditions, Trends, and Variability in the Athens University Campus, Greece

Panagiotis T. Nastos[1] and Andreas Matzarakis[2]

[1] *Laboratory of Climatology and Atmospheric Environment, Department of Geography and Climatology, Faculty of Geology and Geoenvironment, University of Athens, Panepistimioupolis, 15784 Athens, Greece*
[2] *Meteorology and Climatology, University of Freiburg, Germany*

Correspondence should be addressed to Panagiotis T. Nastos; nastos@geol.uoa.gr

Received 18 July 2013; Accepted 13 August 2013

Academic Editor: Tzu-Ping Lin

The objective of this work is the assessment of human thermal bioclimatic conditions in the Athens University Campus (AUC), including the Faculties and their respective Departments of the largest state institution of higher learning in Greece, and among the largest universities in Europe. The analysis of bioclimate was carried out, using the physiologically equivalent temperature (PET), which is based on the energy balance model of the human body. The meteorological data required for the calculation of PET concern hourly values of air temperature, relative humidity, wind speed and total solar radiation, for the time period 1999–2007. The recorded data sets were obtained from the meteorological station of the Laboratory of Climatology and Atmospheric Environment of the University of Athens. The results revealed the hours of the day in which thermal comfort or stress prevails, as well as the trends and variability of PET, for the studied period. Finally, the intense heat waves occurred during summer 2007 along with extreme cold conditions during December 2003-February 2004 were analyzed in terms of PET classes and compared to the respective average bioclimatic conditions of the study period.

1. Introduction

Analysis of the human thermal environment is subject of special investigation among scientists serving at different disciplines such as climatologists, urban planners, architects, biologists, and physicians. A lot of human bioclimatic research has been carried out recently, indicating the impact of urban bioclimate on human morbidity [1–3], mortality [1–8], tourism potential and decision making [9–12], and urban planning [13–15]. Although a heat/cold wave is a meteorological event, it cannot be assessed without reference to its impacts on humans. An analysis of weather elements should always include the assessment of the human sensation of heat/cold [12]. Many thermal indices have been used, such as among others the Effective Temperature [16], the Discomfort Index by Thom [17] and the Cooling Power index [18, 19]. Since 1938, Buttner [20] found that the total effects of all thermal components and not of a single meteorological parameter should be taken into account, in order to assess the thermal effect of environment on the human body. The necessity of modeling the human thermal balance led to the development of bioclimatic models, which are widely applied in bioclimatic studies, known as KLIMA-MICHEL-MODEL [21, 22] and MEMI [23]. Driscoll [24] refers to eleven independent indices, and, since then, Kalkstein and Valimont [25] and Höppe [26] have proposed further analysis. Following this effort, remarkable research has been carried out in order to formulate a reliable and user-friendly index for the assessment of the physiological thermal response of the human body to climatic conditions [27], but only Physiologically Equivalent Temperature (PET) and Universal Thermal Climate Index (UTCI) seem to meet these requirements. PET is recommended for the evaluation of the thermal component of different climates by VDI Guideline 3787 [28]. PET is based on the Munich Energy-balance Model for Individuals (MEMI), which describes the thermal conditions of the human body in a physiological relevant way [29, 30]. The UTCI equivalent temperature for a particular set of wind,

radiation, humidity, and air temperature parameters is then defined as the air temperature of the reference environment which produces the same strain index value as the actual conditions [31, 32].

The climate is already changing, and the intensity and frequency of extreme weather events, such as floods, heatwaves, and cold spells, may change in the future. Recent extreme weather events caused serious health and social problems in Europe, particularly in urban areas. These events will continue to pose additional challenges to health risk management and to the reliability of the power supply and other infrastructure. This demands a proactive and multidisciplinary approach by governments, agencies, and international organizations and improved interaction on all levels from local to international [33]. Europe experienced a deadly summer in 2003, when average summer temperatures were about 3°C higher than the long-term mean, and in major cities of Europe, the daily maximum temperature exceeded 35°C for more than a week, causing about 70,000 excess deaths in parts of southern, western, and central Europe [34–36]. This is the reason that the German Weather Service, within the framework of the EuroHeat project [37], has developed a climate information decision support tool with medium-term heat forecasting, which maps the probability of a forthcoming heat-wave over Europe (http://www.euroheat-project.org/dwd/).

The purpose of the present study is the assessment and interpretation of human bioclimatic conditions in Athens University Campus, during the 1999–2007 period, based on PET human thermal index, which is irrespective of clothing and metabolic activity. Further, the heat waves occurred in summer 2007, and the cold spells during winter 2003/2004 were also analyzed and compared to the mean bioclimatic conditions.

2. Data and Methodology

The performed human biometeorological analysis in the Athens University Campus (AUC) was considered by the authors of great importance due to the large number of people involved in the AUC, during the entire year. National and Kapodistrian University of Athens is the largest state institution of higher learning in Greece and among the largest universities in Europe. With a student body of about 125000 undergraduate and postgraduate students, over 2000 members of academic staff, and approximately 1300 administrative and secretarial staff and specialized personnel, the University of Athens aims at excellence in both teaching and research in a significantly varied range of disciplines. Regarding the time distribution during the year of the mentioned crowd in the university campus, there are two semesters within the year, the first begins in September and ends in January and the second from February to July. During August, the university is closed due to summer holidays. Official holidays concern the Christmas and Easter holidays from December 24 to January 7 and fifteen days in April or May, respectively. Further, there are a few sparse individual days off, due to national celebrations such as October 28 and March 25. Thus, in general, the campus is not crowded fifteen days in winter, fifteen days in spring, and the whole August.

The meteorological data used in the study were acquired from the meteorological station of the Laboratory of Climatology and Atmospheric Environment, University of Athens (latitude: 37°58′N, longitude: 23°47′E, and altitude: 257 m) and concern hourly values of air temperature, relative humidity, total solar radiation, and wind speed for the period 1999–2007. In this point we have to remark that the time series of the meteorological data had been interrupted after 2007 for long consecutive spells, due to technical reasons. This is why we considered the 9-year period as the one with the most reliable meteorological data sets for the performed analysis. The location of the meteorological station in AUC along with a satellite image of the greater Athens area is depicted in Figure 1.

For bioclimatic purposes, the wind speed was adjusted according to the following formula [38]:

$$\mathrm{WS}_{1.1} = \mathrm{WS}_h * \left(\frac{1.1}{h}\right)^{\alpha} \quad \alpha = 0.12 * z_0 + 0.18, \tag{1}$$

where WS_h is the wind speed ($\mathrm{m\,s^{-1}}$) at the anemometer height (h, usually 10 m a.g.l.), α is an empirical exponent, depending on the surface roughness, and z_0 is the roughness length. Wind velocity was estimated at 1.1 m, which is the center of gravity of the human body and builds the reference level for human biometeorological studies. In this study, the value of roughness length $z_0 = 0.25$ was applied, depending on the landscape around the examined station. The aforementioned value of roughness length for a specific terrain was derived from the European Wind Atlas [39].

The quantification of human bioclimatic conditions was achieved using the Physiologically Equivalent Temperature (PET), at a given place (outdoors or indoors). It is equivalent to the air temperature at which—in a typical indoor setting (without wind and solar radiation)—the heat balance of the human body (work metabolic rate 80 W of light activity, that should be added to the basic metabolic rate 86.5 W, [40]; heat resistance of clothing 0.9 clo, which is the reference clothing insulation value used for the formulation of PET) is maintained with core and skin temperatures equal to those of the under assessment conditions [26, 41]. The following assumptions are made for indoor reference climate: mean radiant temperature equals air temperature ($T_{\mathrm{mrt}} = T_a$). Air velocity is set to 0.1 m/s. Water vapour pressure is set to 12 hPa (approximately equivalent to relative humidity of 50% at $T_a = 20$°C). The PET assessment scale (Table 1) is derived by calculating Fanger's [29] PMV for varying air temperatures in the reference environment using the settings for the PET reference person (height: 1.75 m, weight: 75 kg, age: 35 yrs, and sex: male; work metabolic rate 80 W of light activity, that should be added to the basic metabolic rate and heat resistance of clothing 0.9 clo) [42]. According to Höppe [26], the assumption of constant values for clothing and activity in the calculation of PET was made in order to define an index independent of individual behavior.

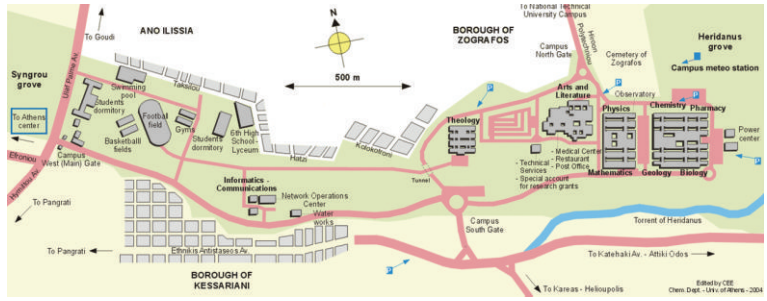

(a)

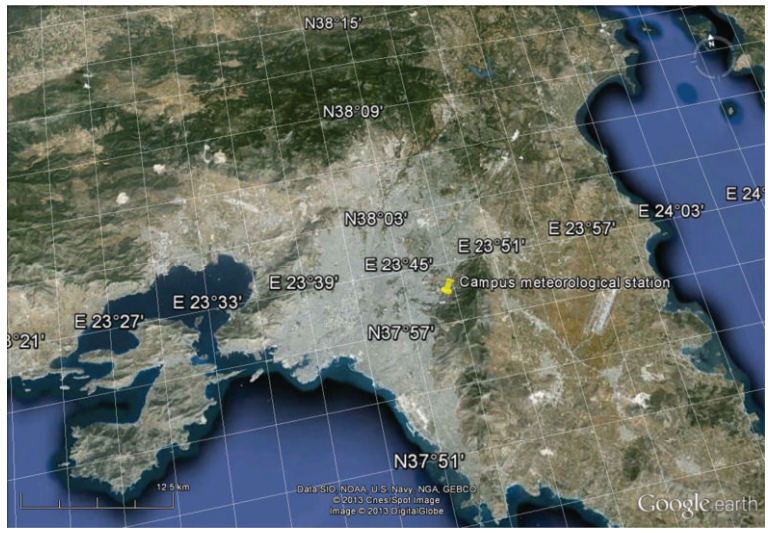

(b)

Figure 1: Athens University Campus (a) and satellite image of the wider Athens area (b) with the marked site of the campus meteorological station.

Table 1: Physiologically Equivalent Temperature (PET) for different grades of thermal sensation and physiological stress on human beings [42].

PET (°C)	Thermal sensation	Physiological stress level
<4	Very cold	Extreme cold stress
4–8	Cold	Strong cold stress
8–13	Cool	Moderate cold stress
13–18	Slightly cool	Slight cold stress
18–23	Comfortable	No thermal stress
23–29	Slightly warm	Slight heat stress
29–35	Warm	Moderate heat stress
35–41	Hot	Strong heat stress
>41	Very hot	Extreme heat stress

PET was calculated using "RayMan" model, appropriate to calculate radiative heat transfer and human biometeorological indices [42, 43]. The "RayMan" model, developed according to Guideline 3787 of the German Engineering Society [28], calculates the radiative heat transfer in both simple and complex environments. Finally, the use of pivot diagrams was considered necessary to demonstrate the frequency (%) of PET classes, in order to interpret the bioclimatic patterns prevailing in different time scales. The time used in the analysis concerns local time, thus UTC + 2h.

3. Results and Discussion

3.1. Human Bioclimatic Conditions in Athens University Campus. The mean PET within the examined period (1999–2007) was found 14.6°C, while the absolute maximum PET was 54.8°C in June 24, 2007, at 15:00, and the absolute minimum PET was −15.5°C in February 14, 2004, at 07:00. These high/low figures of PET characterize the extreme heat stress, appeared during the heat waves in summer 2007 and the extreme cold stress in the very cold winter 2004, respectively. In addition, the mean frequency of days, within the examined period, with strong and extreme heat stress (PET > 35°C), thermal comfort and slight heat stress (18°C < PET < 29°C), and strong and extreme cold stress (PET < 8°C) was calculated, and the results are presented in Table 2.

The daily minimum figures of PET, occurring at night, were taken into account in order to estimate the frequency of days with strong and extreme cold stress against daily maximum PET for the other classes of PET. About 50% of

Table 2: Mean frequency (days) of characteristic thresholds of PET, within the period 1999–2007.

	PET < 8°C	18°C < PET < 29°C	PET > 35°C
Frequency (days)	187.1	98.5	114.3

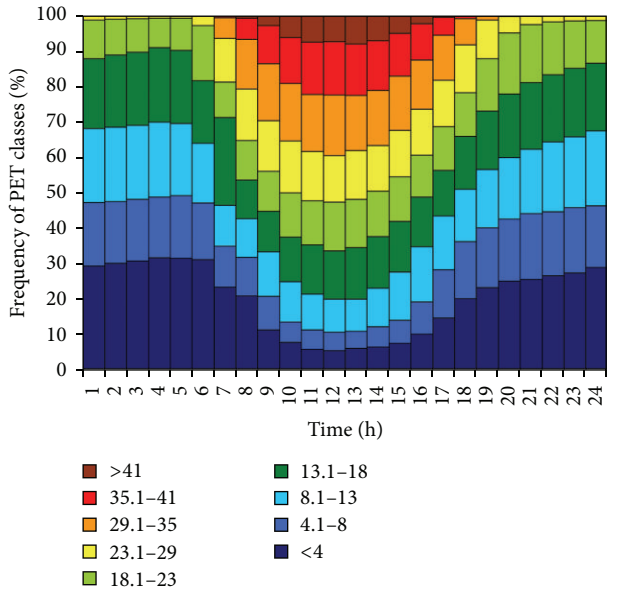

Figure 2: Bioclimatic diagram for Athens University Campus for the period 1999–2007; frequencies (%) of the nine PET classes for each hour of the mean day.

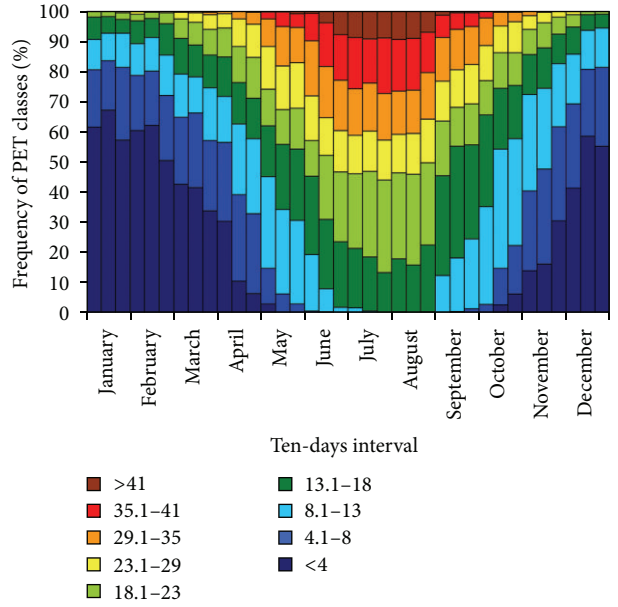

Figure 3: Bioclimatic diagram for Athens University Campus for the period 1999–2007; frequencies (%) of the nine PET classes for 10-day period of the mean year.

the nights of the year were related to strong/extreme cold bioclimatic conditions, which is very likely due to AUC which is lying out of the urbanized area and on the foothills of Hymettus Mountain. Approximately 30% of the days of the year were associated with strong/extreme heat stress and thermal comfort or slight heat stress appeared in almost 27% of the days.

The human bioclimatic conditions are presented in terms of PET classes (%) for each hour of the day (Figure 2) and for 10-days period (Figure 3) in the respective diagrams. These bioclimatic diagrams provide very clear and in a simple way the bioclimatic information for the area concerned. Figure 2 reveals that approximately 45%–65% of days, from 08:00 in the morning to 17:00 in the afternoon, depict PET greater than 18°C (thermal comfort). Further, for about 13%–23% of days, the environment is characterized by strong/extreme heat stress from 09:00 in the morning till 16:00 in the afternoon. Regarding the strong/extreme cold stress, it appears for almost 50% of days from midnight to early morning hours (06:00).

The frequency distribution of PET classes in 10-day period is depicted in Figure 3. Here, it should be noted that the results shown in the diagram concern mean daily figures of PET. Since the first 10 days of June up to the second 10 days of September, 45%–85% of the days within the examined period are associated with PET greater than 18°C (threshold for thermal comfort). Regarding the strong/extreme heat stress (PET > 35°C), it appears in almost 20%–25% of the days from the third 10 days of June to the third 10 days of August.

PET index has been used widely in the assessment of human bioclimatic conditions. More specifically, Thorsson et al. [15] and Gulyás et al. [44] have applied PET in urban built-up area with complex shading patterns and generated accurate predictions of thermal environments. Outdoor thermal environment is impacted by the built environment, for example, anthropogenic heat, evaporation and evapotranspiration of plants, shading by trees and man-made objects [45], and ground surface covering, such as natural grass and artificial pavement. However, Lin [46] concluded that in hot and humid regions few people visit squares or other public spaces when the thermal index is high. The largest numbers of people who visit squares are when the thermal condition is close to their thermal comfort range. Svensson et al. [47] presented the PET distribution map of Goteborg using the geographic information system. Gulyás et al. [44] evaluated thermal comfort in Szeged, Hungary. Bouyer et al. [48] evaluated the thermal comfort in two stadia (Stade de France, Paris, and the Atatürk olympic stadium, Istanbul), using wind tunnel experiments and PET.

Further to the above discussion, we must acknowledge a constraint related to the PET assessment scale. We used the PET scale for western/middle European countries taking into consideration that the greater Athens area has a temperate climate, not significantly different from the climate of western/middle European countries. Thus, the use of the PET assessment scale for western/middle European countries is almost acceptable, while a future work for the determination of PET assessment scale in Athens, Greece, is already in progress. A recent study by Cohen et al. [49] confirms our

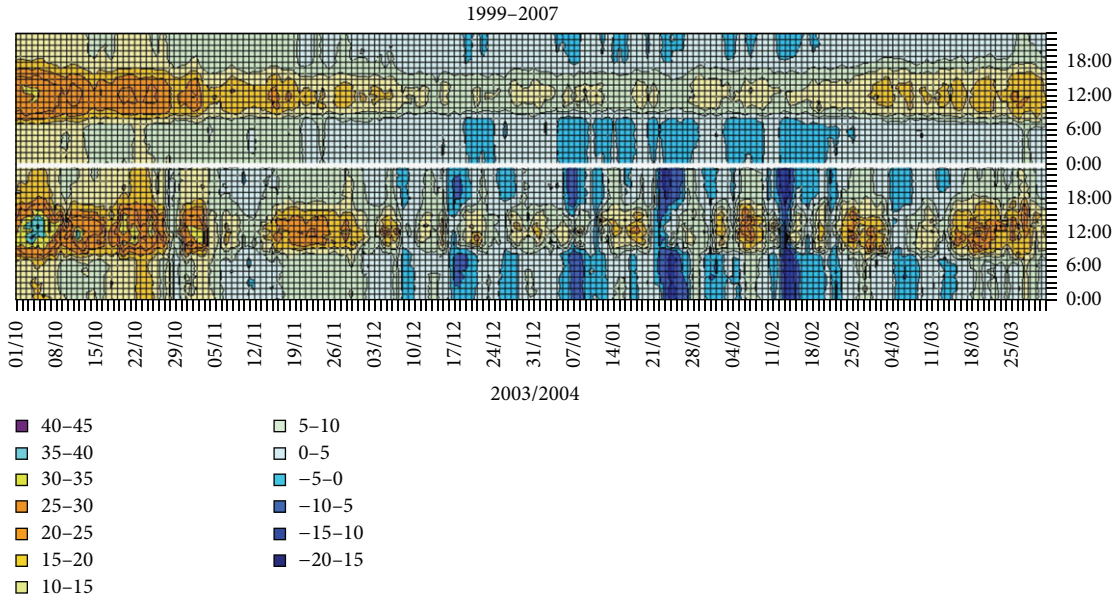

Figure 4: Composite mean hourly variability of PET within the cold period 1999–2007 (upper graph), along with the hourly variability of PET within the cold period 2003-2004 (lower graph).

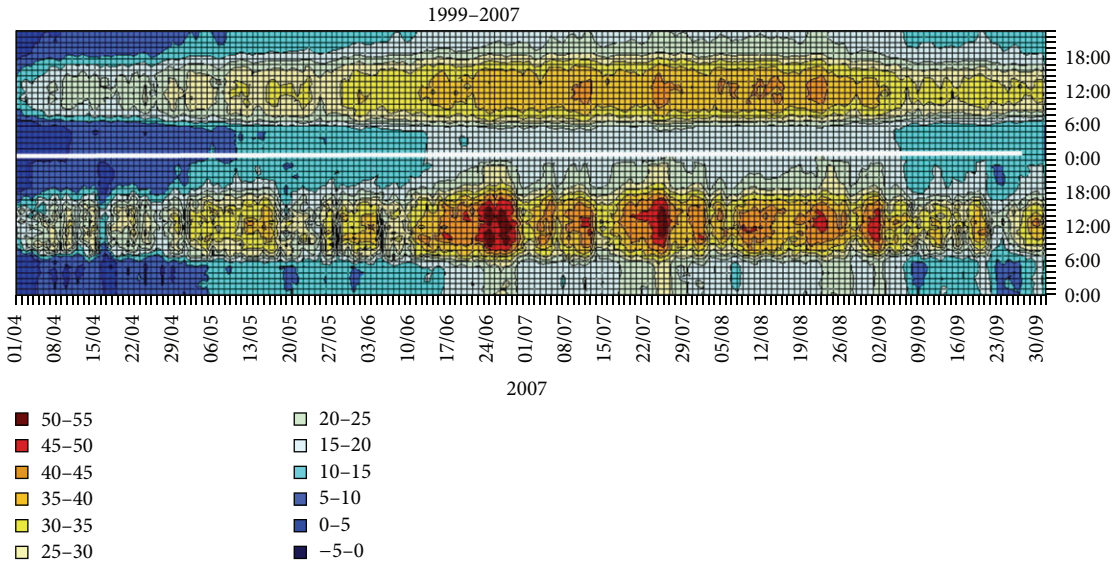

Figure 5: Composite mean hourly variability of PET within the warm period 1999–2007 (upper graph), along with the hourly variability of PET within the warm period 2007 (lower graph).

assumption, revealing that the acceptable comfort range of PET for the Mediterranean climate of Tel Aviv is 19–26°C, against 18–23°C for the acceptable comfort range of PET for western/middle European countries. Besides, the assessment scale [42] is frequently used in international literature to estimate bioclimatic conditions in different places, such as Istanbul and Paris [48], Goteborg [47], Szeged [44], Matsudo (a satellite city near Tokyo), Japan [15], and Far-Eastern Federal District of the Russian Federation (temperate monsoon climate zone, which is characterized by an extreme continental regime of annual temperatures) [50].

3.2. Warm and Cold Periods of the Year-Heat Waves and Cold Spells. We analyzed on one hand the composite mean hourly variability of PET within the cold (October–March) and warm (April to September) periods of the year during 1999–2007, and on the other hand we compared these two composite periods with the corresponding periods of extremes, which appeared within the examined period, namely, the cold period 2003/2004 with the occurrence of two extreme cold spells and the warm period 2007, associated with three extreme heat waves. The results of the analysis are depicted in Figures 4 and 5.

As far as the composite cold period is concerned, the bioclimatic conditions appeared to be cool to slightly warm from 08:00 in the morning until 17:00 in the afternoon, and this is evident from early October until late November and in March, as well. The thermal sensation was classified in cool to cold during the day, while the midnight hours were usually characterized by strong/extreme cold stress, from December to February (Figure 4, upper graph). Comparing the composite mean cold period with the corresponding cold period 2003-2004 (Figure 4, lower graph), the two extreme cold spells (January 22–24, 2004, and February 13-14, 2004) are obvious, and one could remark the very extreme low PET figures (−20°C to −15°C), appeared even during the whole day (this is the case of total frost).

During the composite warm period, the environment was characterized by strong/extreme heat stress from 08:00 in the morning until 17:00 in the afternoon, against thermal comfort to slightly heat stress for the rest of the day (Figure 5, upper graph). Analyzing the extreme warm period appeared in 2007, the three cells corresponding to three extreme heat waves were revealed, which were recorded in June 24–28, July 19–27 and August 22–24, in descending order of intensity, respectively. The thermal stress was very extreme (PET: 50°C–55°C), and it was evident from 08:00 in the morning to 15:00 in the afternoon, especially for the first two heat waves (Figure 5, lower graph). It should be remarked here the duration of the heat waves concerning 8, 6, and 3 consecutive days, respectively, as well as the prevailing calm against the development of Etesian winds, which is normal event during summer in Greece. These winds are periodical winds of the north section established over the Aegean Sea, when a high pressure center in the central and south Europe is combined with the Indian low pressure system over Asia Minor and the Eastern Mediterranean Sea [51]. A characteristic effect of the Etesians regime is summer droughts and uniform weather conditions in Greece [52]. This prevailing weather type (cool and dry winds over the Aegean Sea) in summer moderates the intensity of heat stress affecting the population mainly living in urban areas.

3.3. Trends and Variability. In order to examine the variability and trends of PET extremes, the annual number of days with PET values above or below certain thresholds was estimated. The results are presented in Figure 6 and should be only considered as indicative of the PET variability, due to the short record of observations. The time series of annual number of days with PET > 41°C (extreme heat stress) shows a statistically significant increasing trend ($P < 0.05$), which when combined with the projected climate change allows us to consider that the human bioclimatic conditions in the study area are likely to get worse. Further, the time series of annual number of days with PET < 4°C (extreme cold stress) showed similar statistically significant increasing trend ($P < 0.05$), indicating that the human bioclimatic conditions tend to become more extreme with respect to the cold component of thermal sensation. The time series of annual number of days with strong cold/heat stress did not show significant trends. Matzarakis and Nastos [53] have

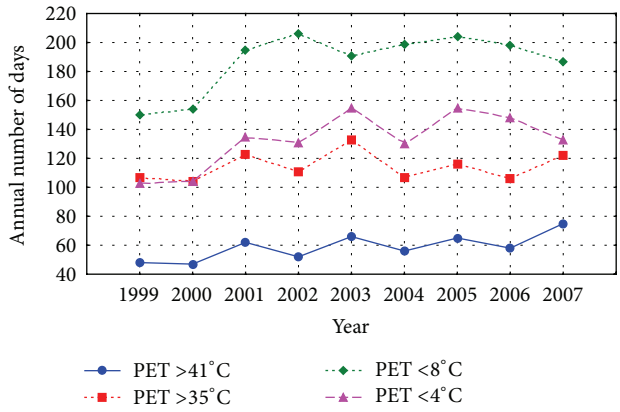

Figure 6: Annual number of days with PET > 41°C, PET > 35°C, PET < 8°C, and PET < 4°C.

revealed that the human thermal bioclimatic conditions are expected to change rapidly in summer, based on A1F scenario. The forthcoming changes concern increases in more than two or three heat stress classes for the summer, within the greater Athens area, while in winter, the expected changes are likely to range between one and two classes of heat stress.

4. Conclusions

The conducted analysis for the assessment of PET in the Athens University Campus, using bioclimatic diagrams, revealed the following findings.

(i) About 50% of the nights of the entire year were related to strong/extreme cold bioclimatic conditions, against almost 30% of the days associated with strong/extreme heat stress. Thermal comfort or slight heat stress appeared in almost 27% of the days.

(ii) The outdoor thermal environment was characterized by strong/extreme heat stress from 09:00 in the morning till 16:00 in the afternoon for approximately 13%–23% of days. Regarding strong/extreme cold stress, it appears for almost 50% of days from midnight to early morning hours (06:00).

(iii) The outdoor thermal environment remains above thermal comfort (PET > 18°C) for approximately 45%–65% of days, from 08:00 in the morning to 17:00 in the afternoon.

(iv) The period from the beginning of June until the middle of September is characterized by PET > 18°C concerning 45%–85% of the days, while strong/extreme heat stress (PET > 35°C) appeared in almost 20%–25% of the days from the end of June to the end of August.

(v) During the warm period of the year, the thermal environment was characterized by strong/extreme heat stress from 08:00 in the morning until 17:00 in the afternoon, while during the cold period of the year, the bioclimatic conditions appeared to be cool to

slightly warm from 08:00 in the morning until 17:00 in the afternoon, and this is evident from early October until late November and in March.

The trend analysis of PET extremes indicated increasing trends for both extreme heat/cold stress. Besides, taking into consideration the extreme heat waves in summer 2007 and extreme cold spells in winter 2003-2004, the authors are aware that the application of human biometeorological indices against single meteorological parameters in the assessment of heat/cold waves would contribute more effectively in addressing and mitigating such extreme circumstances. This is very crucial in crowded areas, where outdoor activities are imposed daily, and this is the case of Athens University Campus.

Acknowledgment

This research has been partially funded by the Special Account for Research Grants of the University of Athens.

References

[1] J. Schwartz, J. M. Samet, and J. A. Patz, "Hospital admissions for heart disease: the effects of temperature and humidity," *Epidemiology*, vol. 15, no. 6, pp. 755–761, 2004.

[2] P. T. Nastos and A. Matzarakis, "Weather impacts on respiratory infections in Athens, Greece," *International Journal of Biometeorology*, vol. 50, no. 6, pp. 358–369, 2006.

[3] P. Michelozzi, U. Kirchmayer, K. Katsouyanni et al., "Assessment and prevention of acute health effects of weather conditions in Europe, the PHEWE project: background, objectives, design," *Environmental Health*, vol. 6, article 12, 2007.

[4] F. C. Curriero, K. S. Heiner, J. M. Samet, S. L. Zeger, L. Strug, and J. A. Patz, "Temperature and mortality in 11 cities of the eastern United States," *American Journal of Epidemiology*, vol. 155, no. 1, pp. 80–87, 2002.

[5] A. Analitis, K. Katsouyanni, A. Biggeri et al., "Effects of cold weather on mortality: results from 15 European cities within the PHEWE project," *American Journal of Epidemiology*, vol. 168, no. 12, pp. 1397–1408, 2008.

[6] M. Baccini, A. Biggeri, G. Accetta et al., "Heat effects on mortality in 15 European cities," *Epidemiology*, vol. 19, no. 5, pp. 711–719, 2008.

[7] S. P. Almeida, E. Casimiro, and J. Calheiros, "Effects of apparent temperature on daily mortality in Lisbon and Oporto, Portugal," *Environmental Health*, vol. 9, no. 1, article 12, 2010.

[8] P. T. Nastos and A. Matzarakis, "The effect of air temperature and human thermal indices on mortality in Athens, Greece," *Theoretical and Applied Climatology*, vol. 108, no. 3-4, pp. 591–599, 2012.

[9] C. R. De Freitas, "Tourism climatology: evaluating environmental information for decision making and business planning in the recreation and tourism sector," *International Journal of Biometeorology*, vol. 48, no. 1, pp. 45–54, 2003.

[10] E. A. Didaskalou and P. T. Nastos, "The role of climatic and bioclimatic conditions in the development of health tourism product," *Anatolia*, vol. 14, no. 2, pp. 107–126, 2003.

[11] J. M. Hamilton and M. A. Lau, "The role of climate information in tourist destination choice decision-making," in *Proceedings of the 17th International Congress of Biometeorology*, pp. 608–611, 2005.

[12] A. Matzarakis and P. T. Nastos, "Analysis of tourism potential for Crete Island, Greece," *Global Nest Journal*, vol. 13, pp. 141–149, 2011.

[13] M. Nikolopoulou and S. Lykoudis, "Thermal comfort in outdoor urban spaces: analysis across different European countries," *Building and Environment*, vol. 41, no. 11, pp. 1455–1470, 2006.

[14] S. Thorsson, M. Lindqvist, and S. Lindqvist, "Thermal bioclimatic conditions and patterns of behaviour in an urban park in Göteborg, Sweden," *International Journal of Biometeorology*, vol. 48, no. 3, pp. 149–156, 2004.

[15] S. Thorsson, T. Honjo, F. Lindberg, I. Eliasson, and E. M. Lim, "Thermal comfort and outdoor activity in Japanese urban public places," *Environment and Behavior*, vol. 39, no. 5, pp. 660–684, 2007.

[16] B. Givoni, *Man, Climate and Architecture*, Elsevier, Amsterdam, Netherlands, 1969.

[17] E. Thom, "The discomfort index," *Weatherwise*, vol. 12, pp. 57–60, 1959.

[18] P. A. Siple and C. F. Passel, "Measurements of dry atmospheric cooling in subfreezing temperatures," *Proceedings of the American Philosophical Society*, vol. 89, pp. 177–199, 1945.

[19] A. S. Tzenkova, I. M. Kandjov, and J. N. Ivancheva, "Some biometeorological aspects of urban climate in Sofia," in *Proceedings of 5th International Conference on Urban Climate*, vol. 2, pp. 103–106, Lodz, Poland, 2003.

[20] K. Buttner, *Physikalische Bioklimatologie*, Akademische Verlagsgesellschaft, 1938.

[21] P. O. Fanger, *Thermal Comfort*, McGraw-Hill, New York, NY, USA.

[22] G. Jendritzky, "Bioklimatische Bewertungsgrundlage zur Beschreibung des thermischen Milieus in der Stadt- und Landschaftsplanung," ARL Beitrdge 128, 1990.

[23] P. Höppe, *Die Energiebilanz des Menschen*, vol. 49, Meteorologisches Institut, Universitat Munchen, 1984.

[24] D. M. Driscoll, "Human health," in *Handbook of Applied Meteorology*, D. D. Houghton, Ed., pp. 778–814, John Wiley and Sons, 1985.

[25] L. S. Kalkstein and K. M. Valimont, "An evaluation of summer discomfort in the United States using a relative climatological index," *Bulletin of American Meteorological Society*, vol. 67, no. 7, pp. 842–848, 1986.

[26] P. Höppe, "The physiological equivalent temperature—a universal index for the biometeorological assessment of the thermal environment," *International Journal of Biometeorology*, vol. 43, no. 2, pp. 71–75, 1999.

[27] F. R. d'Ambrosio Alfano, B. I. Palella, and G. Riccio, "Thermal environment assessment reliability using temperature-humidity indices," *Industrial Health*, vol. 49, no. 1, pp. 95–106, 2011.

[28] VDI, *VDI, 3787, Part I: Environmental Meteorology, Methods for the Human Biometeorological Evaluation of Climate and Air Quality for the Urban and Regional Planning at Regional Level. Part I: Climate*, Beuth, Berlin, Germany, 1998.

[29] P. O. Fanger, *Thermal Comfort*, McGraw-Hill, New York, NY, USA, 1972.

[30] P. Höppe, "Heat balance modeling," *Experentia*, vol. 49, pp. 741–746, 1993.

[31] G. Jendritzky, G. Havenith, P. Weihs, E. Batchvarova, and R. de Dear, "The universal thermal climate index UTCI—goal and state of COST action 730 and ISB commission 6," in *Proceedings of the 18th International Congress of Biometeorology (ICB '08)*, Tokyo, Japan, Septembe 2008.

[32] D. Fiala, G. Havenith, P. Bröde, B. Kampmann, and G. Jendritzky, "UTCI-Fiala multi-node model of human heat transfer and temperature regulation," *International Journal of Biometeorology*, vol. 56, no. 3, pp. 429–441, 2012.

[33] WHO Regional Office for Europe, Budapest Declaration, 2004, http://www.euro.who.int/document/e83335.pdf.

[34] J. M. Robine, S. L. K. Cheung, S. Le Roy et al., "Death toll exceeded 70,000 in Europe during the summer of 2003," *Comptes Rendus*, vol. 331, no. 2, pp. 171–178, 2008.

[35] C. Schär, P. L. Vidale, D. Lüthi et al., "The role of increasing temperature variability in European summer heatwaves," *Nature*, vol. 427, no. 6972, pp. 332–336, 2004.

[36] S. Vandentorren, P. Bretin, A. Zeghnoun et al., "August 2003 heat wave in France: risk factors for death of elderly people living at home," *European Journal of Public Health*, vol. 16, no. 6, pp. 583–591, 2006.

[37] WHO, "Improving public health responses to extreme weather/heat-waves—EuroHEAT," Technical Summary, 2009.

[38] W. Kuttler, "Stadtklima," in *Handbuch der Umweltveränderungen und Ökotoxologie. Band 1B: Atmosphäre (Hrsg.)*, R. Guderian, Ed., pp. 420–470, Springer, 2000.

[39] I. Troen and E. L. Petersen, *European Wind Atlas*, Risø National Laboratory, Roskilde, Denmark, 1989.

[40] J. A. J. Stolwijk and J. D. Hardy, "Control of body temperature," in *Handbook of Physiology, Section 9, Reactions to Environmental Agents*, H. K. Douglas and M. D. Bethesda, Eds., pp. 45–69, American Physiological Society, 1977.

[41] H. Mayer and P. Höppe, "Thermal comfort of man in different urban environments," *Theoretical and Applied Climatology*, vol. 38, no. 1, pp. 43–49, 1987.

[42] A. Matzarakis, H. Mayer, and M. G. Iziomon, "Applications of a universal thermal index: physiological equivalent temperature," *International Journal of Biometeorology*, vol. 43, no. 2, pp. 76–84, 1999.

[43] A. Matzarakis, F. Rutz, and H. Mayer, "Modelling radiation fluxes in simple and complex environments: basics of the RayMan model," *International Journal of Biometeorology*, vol. 54, no. 2, pp. 131–139, 2010.

[44] Á. Gulyás, J. Unger, and A. Matzarakis, "Assessment of the microclimatic and human comfort conditions in a complex urban environment: modelling and measurements," *Building and Environment*, vol. 41, no. 12, pp. 1713–1722, 2006.

[45] T. P. Lin, A. Matzarakis, and R. L. Hwang, "Shading effect on long-term outdoor thermal comfort," *Building and Environment*, vol. 45, no. 1, pp. 213–221, 2010.

[46] T. P. Lin, "Thermal perception, adaptation and attendance in a public square in hot and humid regions," *Building and Environment*, vol. 44, no. 10, pp. 2017–2026, 2009.

[47] M. K. Svensson, S. Thorsson, and S. Lindqvist, "A geographical information system model for creating bioclimatic maps—examples from a high, mid-latitude city," *International Journal of Biometeorology*, vol. 47, no. 2, pp. 102–112, 2003.

[48] J. Bouyer, J. Vinet, P. Delpech, and S. Carré, "Thermal comfort assessment in semi-outdoor environments: application to comfort study in stadia," *Journal of Wind Engineering and Industrial Aerodynamics*, vol. 95, no. 9–11, pp. 963–976, 2007.

[49] P. Cohen, O. Potchter, and A. Matzarakis, "Human thermal perception of Coastal Mediterranean outdoor urban," *Applied Geography*, vol. 37, pp. 1–10, 2012.

[50] E. Grigorieva and A. Matzarakis, "Physiologically equivalent temperature as a factor for tourism in extreme climate regions in the Russian Far East: preliminary results," *European Journal of Tourism, Hospitality and Recreation*, vol. 3, pp. 127–142, 2011.

[51] D. A. Metaxas and A. Bartzokas, "Pressure covariability over the Atlantic, Europe and N. Africa. application: centers of action for temperature, winter precipitation and summer winds in Athens, Greece," *Theoretical and Applied Climatology*, vol. 49, no. 1, pp. 9–18, 1994.

[52] P. T. Nastos, C. M. Philandras, and C. C. Repapis, "Application of canonical analysis to air temperature and precipitation regimes over Greece," *Fresenius Environmental Bulletin*, vol. 11, no. 8, pp. 488–493, 2002.

[53] A. Matzarakis and P. T. Nastos, "Heat waves in Athens," in *Proceedings of the 8th Hellenic Conference on Meteorology, Climatology and Atmospheric Physics*, vol. 3, pp. 153–160, Athens, Greece, May 2006.

Hindawi Publishing Corporation
Advances in Meteorology
Volume 2013, Article ID 640473, 8 pages
http://dx.doi.org/10.1155/2013/640473

Research Article

Thermal Comfort for Urban Parks in Subtropics: Understanding Visitor's Perceptions, Behavior and Attendance

Chuang-Hung Lin,[1] Tzu-Ping Lin,[2] and Ruey-Lung Hwang[1]

[1] *Department of Architecture, National United University, 1 Lienda, Miaoli 360, Taiwan*
[2] *Department of Architecture, National Cheng Kung University, 1 University Road, Tainan 701, Taiwan*

Correspondence should be addressed to Ruey-Lung Hwang; rueylung@nuu.edu.tw

Received 23 February 2013; Revised 27 July 2013; Accepted 6 August 2013

Academic Editor: Marialena Nikolopoulou

The paper is an effort toward thermal comfort assessment for urban parks under the climatic conditions of Taiwan to help architects achieve better climatic design. Field interviews, observations, and micrometeorological measurements were conducted in this study. The WBGT was used as the thermophysiological index to investigate the effects of thermal conditions on visitor's thermal perception and adaptive behavior in outdoor urban spaces. In this study, behavioral adaptations used by visitors as a means of achieving comfort were evaluated. Observational results showed that the overall attendance was influenced by sun and thermal conditions. There was a robust relationship between thermal sensation votes, as well as thermal acceptability, and thermal environment, in terms of WBGT. The upper and lower limits of 80% acceptability are 26°C WBGT and 20°C WBGT, respectively.

1. Introduction

Ensuring acceptable thermal comfort conditions in outdoor spaces is always one of the considerations of landscape design, since thermal environmental conditions greatly affect individual moods and activities in the outdoors as well as the usage of the outdoor spaces. In densely populated cities, with the continuously growing emphasis on the importance of quality of life, the public attaches greater value to the quality of thermal comfort in outdoor urban spaces. At the same time, with the expansion of cities, the urban heat island effect is increasingly significant, and the trend of urban microclimate change is not optimistic. Hence, the architects or landscape designers must seriously consider the actions required for outdoor space design to support comfortable conditions. In recent years, the thermal comfort of outdoor spaces has become an important issue, attracting a considerable number of articles to analyze and discuss outdoor thermal comfort through field surveys, for example, Spagnolo and de Dear in Australia [1], Ahmed in Bangladesh [2], Nakano and Tanabe in Japan [3], Nikolopoulou and Lykoudis in European countries [4], Oliveira and Andrade [5] and Andrade et al. [6] in Portugal, Cheng et al. in Hong Kong [7], Kariminia et al. in Iran [8], and Lin [9], Hwang et al. [10], and Lin et al. [11] in Taiwan.

Many of the research studies have generally used a thermophysiological index in outdoor thermal condition analysis. Some of the indices, for example, physiological equivalent temperature (PET), standard new effective temperature (SET*), universal thermal climate index (UTCI), and so forth, are based on comprehensive energy-balance models for the human body to describe outdoor thermal conditions. The outdoor thermal comfort investigations conducted in Taiwan [9–12] found that the thermal comfort characteristics of a population adapted to hot and humid climate were different from residents living in temperate climates. Meanwhile, it was also found that thermo-physiological indices, based on energy-balance model, cannot fully explain subjective perceptions or preferences of people due to the impacts of their personal psychological and behavioral adjustments [12]. In addition, thermo-physiological indices based on energy-balance model are general complex in calculation and result in difficulties in application for those architects or landscape designers who are unfamiliar with energy-balance modeling. In this sense, our research question is, can simpler and directly measurable indices, which correlate well with human

Figure 1: Photograph of investigated Wen-Xin Park in Taichung, Taiwan.

responses and thus enable reliable predictions to be made, be used to replace such complex indictors to help architects achieve better climatic design? Thus, the objectives of this study were to select a thermo-physiological index that can be determined from simple readings to analyze outdoor thermal comfort and to discuss the relationship between the public's outdoor adaptive behaviors and the selected index.

2. Materials and Methods

2.1. Description of Study Park. This study was based on questionnaire surveys and weather measurements performed simultaneously in Taichung City, the third largest city of Taiwan (longitude 120°40′E; latitude 24°09′N), which is located in central Taiwan and has approximately 1,200,000 inhabitants. The city has a hot and humid climate, with mild winters and hot and humid summers.

The field investigations were conducted in the open area of Wen-Xin Park (see Figure 1), which is one of the three metropolitan parks in downtown Taichung City. This park is used for leisure and sport activities, such as lying, sitting, promenading, jogging, and kite flying, particularly during weekends and holidays. The surveyed area has paved sidewalks and green areas, with about 80% of the total area covered by grass. There are a few benches facing the green areas along the sidewalks; however, most people use the grass areas. The trees that provide shade are around the sidewalk in the middle of the surveyed area and cover about 20% of the area.

2.2. Instrumentations and Microclimatic Measurements. A combination of portable equipment, which complies with the requirements of instruments for measuring physical quantities in ISO 7726 [13], was assembled to allow monitoring of the microclimate during questionnaire interviews. Data Logger Center 314 was used to collect measurements of dry-bulb temperature, globe temperature, and relative humidity. The globe thermometer is a standard black-painted matte globe. The dry-bulb temperature and relative humidity sensor were shielded from radiation by a highly reflective aluminized top film but were subject to free-flowing ventilation. Air speed was monitored with a separate data logger, the omnidirectional anemometers Delta HD 2103. Metabolic rate and the insulation of clothing [14] were estimated based on the answers to the questionnaire. The thermo-physiological index WBGT was calculated in order to evaluate the combined effects of atmospheric variables on thermal sensation votes (TSV). The wet-bulb temperature was obtained by substituting the measured dry-bulb temperature and relative humidity into the equations in the Chapter of Psychometrics, ASHRAE Handbook of Fundamentals [15]. Besides the measurements of condition nearby the respondents, two sets of instruments were installed in sunlit and tree-shaded area for continuous measurements on fieldwork days. Meteorological data were also obtained from a nearby local official weather station, which is located in another downtown metropolitan park about 4 km away from the study park.

2.3. Questionnaire Interviews and Observation. A team of three research assistants performed the questionnaire interviews and observations every fieldwork day: two of them were responsible for questionnaire interviews, and the remaining assistant for observations. The interviews were performed in Chinese and required 15 minutes to complete. The questionnaires used in this study were created by modifying those deployed in earlier studies [9–11], divided into two parts, namely, BACKGROUND and PERCEPTION.

BACKGROUND covered questions regarding demographics, current clothing garments, metabolic activities, living or working in the neighborhood of park, the reason for being in the park, and the frequency and duration of time spent in the park.

PERCEPTION had questions concerning the subject's assessment of their immediate thermal environment at that point in time. The subjects were asked to report their sensations of thermal environment through a 7-point scale and of air movement through a 5-point scale. The thermal sensation scale was the ASHRAE 7-point scale, ranging from cold (−3) to hot (+3), with neutral (0) in the middle. The subjects assessed the wind sensation on a 5-point scale: still (−2), weak (−1), moderate (0), strong (+1), and very strong (+2). The final question in the PERCEPTION part asked subjects whether, or not, they considered the weather of the fieldwork day suitable for leisure outdoor activities. The protocol for each interview was as follows: (1) two research assistants approach subject, ask if time is convenient, and present the questionnaire; (2) one of them gives the subject a brief explanation about the aim and the context of questionnaire, while the other settles the instrumentations nearby to measure thermal environmental variables; (3) subject completes questionnaire survey; (4) during the survey, a 15-minute sample of the thermal environment is made; and (5) subject leaves and the assistants seek the next subject. 60–120 subjects were surveyed daily on fieldwork days.

The number of visitors and their activities within the study area were investigated by observations on fieldwork days. Observations on each day were performed every 30

Table 1: Climatic characterization of fieldwork days.

Fieldwork date	Daily average values				Maximum DB temperature	ΔT_{max} †
	DB	RH	Wind speed	Solar radiation		
	˚C	%	m/s	MW/m^2	˚C	˚C
Sep. 19	27.4	74.5	1.3	1.56	31.2	−2.8
Sep. 26	28.1	76.0	1.0	1.65	32.4	−1.6
Oct. 03	28.1	75.5	1.5	1.22	30.7	−1.9
Oct. 10	28.2	71.4	0.8	1.38	32.1	−0.5
Oct. 17	27.9	69.1	1.0	1.44	32.3	−0.3
Oct. 24	27.1	73.3	1.1	1.58	30.8	−1.8
Oct. 31	21.2	61.4	2.6	1.83	26.2	−6.4
Nov. 07	24.4	77.3	2.0	1.30	28.0	−0.1
Nov. 28	21.5	68.0	0.8	1.42	26.4	−1.7
Dec. 05	23.1	67.3	1.0	1.34	28.4	0.0
Dec. 12	19.7	72.4	0.9	1.36	27.0	−1.4
Dec. 19	18.2	65.5	0.6	1.39	24.3	−4.1
Jan. 09	16.6	73.6	2.9	1.34	20.0	−2.9
Jan. 16	10.3	68.5	2.8	0.55	11.5	−11.4

† Difference between daily maximum temperature on fieldwork day and monthly maximum temperature.

minutes from 10:00 am to 5:00 pm, for a daily total of 15 observations. The numbers of people in different subspaces were observed according to the observation protocol. Field investigations were conducted on Saturday or Sunday from September 2010 to January 2011. All fieldwork days were sunny and no festival celebrations held in the park.

3. Results of Key Survey Questions

3.1. Descriptions of the Weather on Fieldwork Days. Table 1 summarizes the weather conditions on the fieldwork days. The data in Table 1 are from the local weather station. The differences between maximum air temperatures of fieldwork days and monthly maximum temperature are also shown for comparison. The mean dry-bulb temperature varies between 10.3˚C and 28.2˚C. Mean relative humidity and mean wind speeds are in the ranges of 61.4–77.3% and 0.6–2.9 m/s, respectively.

3.2. Characterization of Subjects. The fieldwork team invited 759 visitors to take part in the questionnaires. Of the questionnaire responses, 43% were from male visitors of the park and 57% were from female visitors. Of the respondents, 51% live or work in neighborhood of the park, and 49% are from other regions. The profile of subjects' age is 20% teenagers, 75% in the range of 20–50 years, and 5% older than 50 years.

The result of the question regarding how often the subjects visit this park shows 9% visit more than 10 times, 17% visit 5–10 times, and 35% visit 1–5 times per month, respectively. There are 27% of subjects seldom visiting this park and 13% visiting this park for the first time. Regarding the question "How long are you going to spend in this park?" 37% answered more than two hours, 33% answered 1-2 hours, 23% answered 0.5–1 hour, and the remaining 7% answered less than 0.5 hour. Regarding the question "For what purpose do you visit this park?" and 69% said for the special reason of sport, relaxing, or meeting other(s), 31% said for other reasons, such as being on the way to other places. Based on the results of observations, the frequency distribution of visitors' activities shows that 32% of the visitors observed were engaged in light activities, such as seating relaxed, reading, sun bathing, and picnicking; 39% were taking a walk; 16% were jogging; and 14% were playing ball, flying a Frisbee, flying a kite, and so forth. In addition, it was observed that visitors prefer to use this park after 3:00 pm, as the solar radiation at that time would not annoy them.

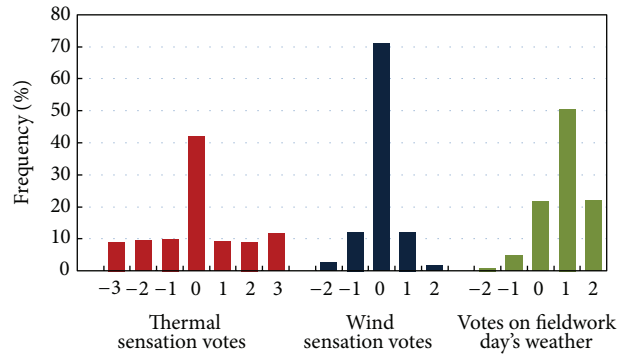

Figure 2

3.3. Assessment of the Thermal Environment. The subjects were asked to report their thermal and wind sensations according to a 7-point and a 5-point scale, respectively. Figure 2 shows, the relative frequency distribution for thermal sensation votes while being surveyed; 42% of the subjects felt the thermal conditions to be thermal neutral; 28% felt slightly cool, cool, and cold; and 30% felt slightly warm, warm, and hot. Figure 2 also shows the distribution for wind

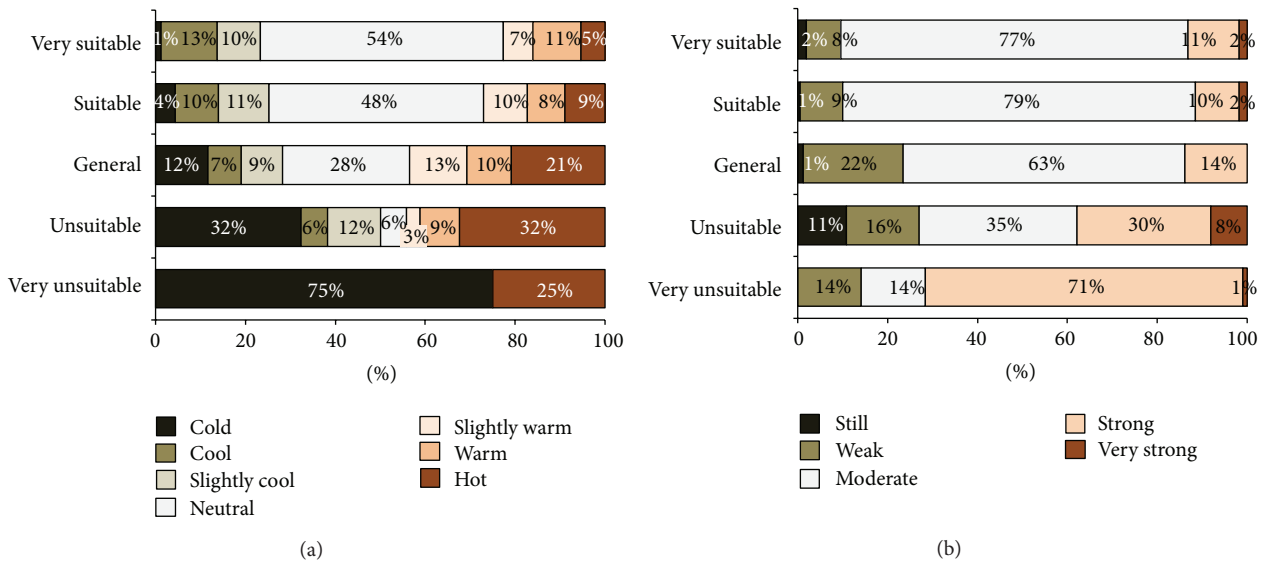

FIGURE 3: (a) Thermal sensation votes versus votes on fieldwork day's weather, (b) wind sensation votes versus votes on fieldwork day's weather.

sensation votes. In wind assessment, the majority of subjects (72%) assessed the wind conditions as being moderate; 14% as still or weak, and 14% as strong or very strong. As shown in Figure 2, the majority of subjects considered the weather of fieldwork days as suitable for outdoor leisure activities; 22% chose very suitable, 51% suitable, 22% general, 5% unsuitable, and 1% as very unsuitable.

Patterns of thermal or wind sensation votes, versus fieldwork day weather, are examined in more detail in Figure 3. As shown in Figure 3(a), when feeling the weather as suitable or very suitable for outdoor leisure activity, about 70% of subjects were also satisfied with the thermal conditions at the site, with their votes falling in the three central categories (TSV = −1, 0 and +1) of the thermal sensation scale, whereas 30% were unsatisfied by voting extreme thermal sensations (TSV = ±2, ±3). Of the people feeling unsuitable or very unsuitable, 80% to 100% were not satisfied with the thermal conditions at the site. In Figure 3(b), the distributions of cross-examinations between wind sensation and votes on the weather fieldwork days revealed the same trend; however, when subjects felt "unsuitable" or "very unsuitable," 35% and 14% felt the wind was moderate, respectively.

4. Thermal Perception Analysis

4.1. Thermal Sensation versus Thermal Environment. The relationship between thermal sensation and thermal environment was examined using linear regressions between thermal sensation votes and the thermo-physiological index. WBGT was selected as the thermal index in this study. Provided in ISO 7243 [16], as a simplified version of ET* for the assessment of hot environments, the WBGT for outdoor environments with solar radiation is determined from three single readings, namely, wet-bulb temperature, globe temperature, and dry bulb temperature. As explained in the introduction, the WBGT seems suitable for practical use by those unskilled in energy-balance modeling of the human body, which is the reason this study decided to test WBGT as the basis for all subsequent analyses. The WBGT index combines temperature, humidity, radiation, and wind into a single index, which is determined as follows:

$$\mathrm{WBGT} = 0.7 \times t_{\mathrm{wb}} + 0.2 \times t_g + 0.1 \times t_a, \quad (1)$$

where t_{wb} is normal meteorological wet bulb temperature shown by a wet bulb thermometer; t_a is dry bulb temperature; and t_g is 150 mm diameter black globe temperature.

In the regression analysis, the mean thermal sensation votes in each temperature interval were used, rather than actual individual votes, in order to eliminate the influence of individual differences. Thus, all thermal sensation votes of the subjects were sorted in ascending order according to WBGT and are binned into 1.0°C intervals of WBGT. The R^2 of the model can be interpreted as an index of goodness of fit. The regression of the mean thermal sensation vote against WBGT is shown in Figure 4. Thermal sensation votes correlate strongly with WBGT; thus, the WBGT index is considered by this study as a suitable index without elaborate procedures of calculations.

4.2. Thermal Acceptability. Generally, the votes equal to "slightly cool," "neutral", and "slightly warm" are considered to be of those who consider the thermal conditions surrounding them acceptable. Thus, for each 1°C interval of the WBGT, the percentage of thermal acceptability could be determined from counting the total number of votes and the number of votes falling into the three categories of "slightly cool", "neutral", and "slightly warm." Figure 5 shows the histogram of the distribution of the acceptable votes as well as the percentage of unacceptability, due to coldness or hotness. The percentage of hot unacceptability in each interval of the WBGT is derived from dividing the number of votes falling into the categories of "warm" and "hot" by the total

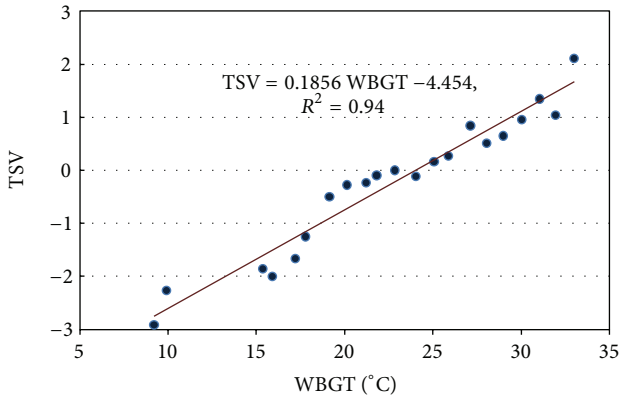

Figure 4

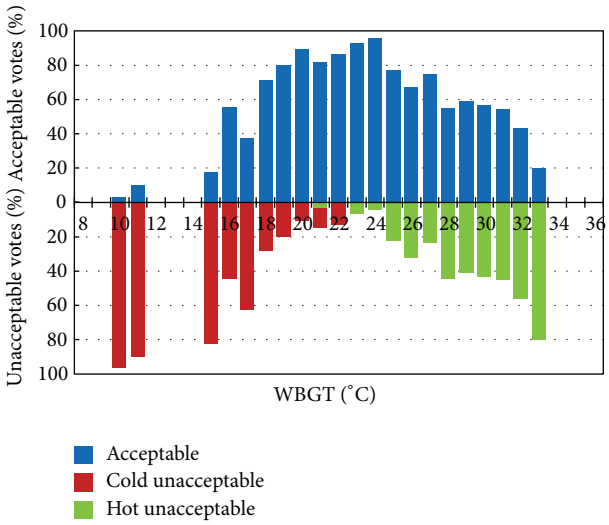

Figure 5

number of votes, while the percentage of cold unacceptability is derived from dividing the number of votes falling into the categories of "cool" and "cold" by the total number of votes. It appears that the distribution of thermal acceptability rate and the distribution of thermal unacceptability rate depend on WBGT.

The sigmoid distribution of unacceptability rates due to hotness or coldness suggests that the resulting percentages within each interval could be subjected to the probit analysis [17, 18]. The resulting models are depicted in Figure 6. The maximum likelihood probit models for the percentages of unacceptability due hotness and coldness are given in (2) and (3), respectively.

For hotness,

$$\text{probit } p_{\text{hot}} = 4.38 \times \text{WBGT} + 29.2R^2 = 0.89. \quad (2)$$

For coldness,

$$\text{probit } p_{\text{cold}} = -4.11 \times WBGT + 16.6R^2 = 0.93. \quad (3)$$

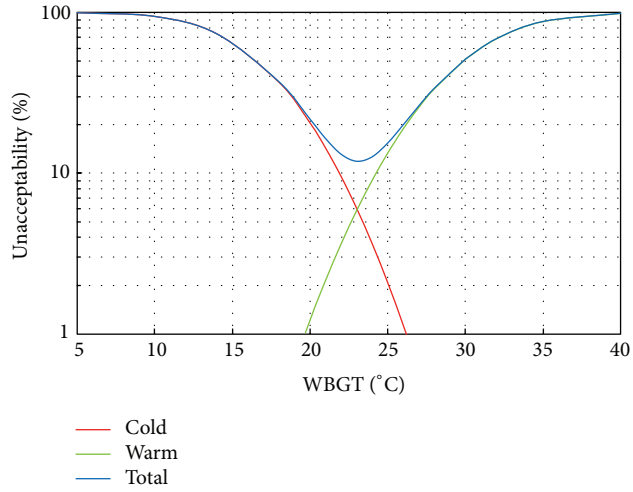

Figure 6

Then, the sum of the probabilities of unacceptability due to hotness and coldness is the total percentage of unacceptability, with respect to a specific WBGT. By inspecting the curve of total unacceptability, it can be noticed that the distribution of thermal unacceptability is approximately symmetrical around the ideal comfort temperature. For WBGT between 20°C and 26.0°C, there are less than 20% of subjects voting unacceptable, that is, more than 80% of subjects voting acceptable. An ideal comfort condition, at which the minimum value of thermal unacceptability occurs, is at the point of 23.2°C WBGT.

5. Behavioral Adaptation

According to the adaptive principle, "If a change occurs, and produces discomfort, people react in ways that tend to restore their comfort" [19]. For the case of this study, the behavioral adaptations of clothing adjustments and metabolic rates were evaluated. The air velocity and attendance of visitors were used as means to measure the methods subjects used to achieve comfort.

5.1. Clothing Level. Adjusting clothing is the most important personal behavioral adaptation to restore thermal comfort at different temperatures. By plotting the value of clothing insulation worn by the subjects, it is easy to determine the correlation between the clo value and the outdoor thermal condition. Figure 7 shows how the clo value varies among the fieldwork days. The scattered clo value was observed from a minimum of 0.3 clo on hot days to a maximum of 1.5 clo on cold days. The regression in (4) shows that the correlation between average clothing insulation and average WBGT on a fieldwork days is robust:

$$\text{clo} = -0.039 \times \text{WBGT} + 1.54R^2 = 0.96. \quad (4)$$

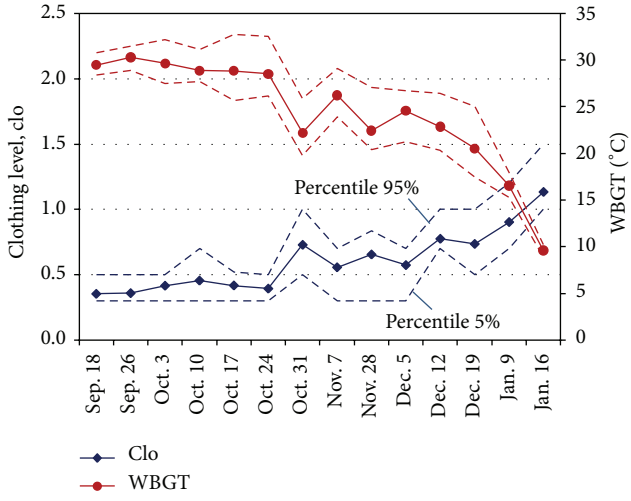

Figure 7

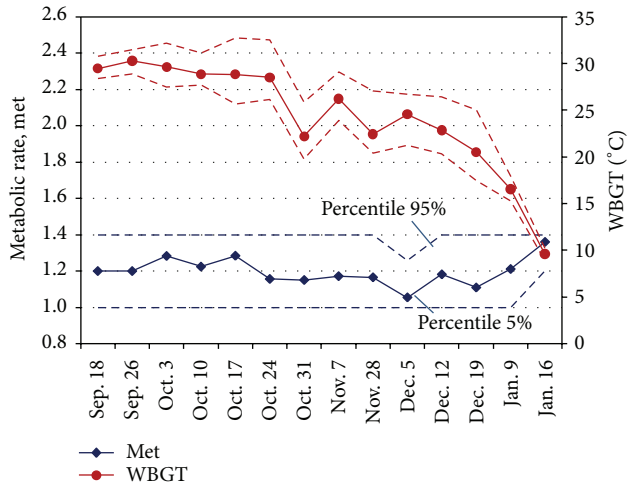

Figure 8

A similar regression was conducted between the clothing and the instantaneous WBGT during interviews. The linear regression gives

$$\text{clo} = -0.031 \times \text{WBGT} + 1.50 R^2 = 0.93. \quad (5)$$

Results from the field studies demonstrate that individuals use changes in clothing levels to try and achieve comfort and that a correlation exists between the clothing and the WBGT.

5.2. Activity Level. The plot of the activity levels of visitors on fieldwork days shows that the corresponding metabolic rate is nearly horizontal, between 1.0 and 1.5 met, Figure 8. This indicates that the visitor's activity level is independent of the value of the WBGT.

5.3. Air Movement. Figure 9 shows the average wind speed and percentage of wind sensation votes in "still" and "weak"

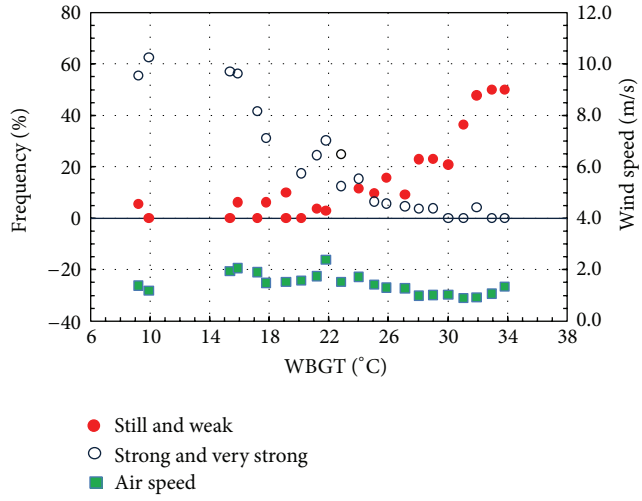

Figure 9

categories or "strong" and "very strong" categories as a function of WBGT. In warmer-than-neutral conditions (WBGT ≧ 24.0°C), the percentage of subjects feeling the wind speed to be "still" or "weak" increases dramatically from 10% at 24.0°C WBGT to 52% at 34.0°C WBGT, even though the mean air speed varies in a narrow range of 0.9–1.5 m/s. A possible explanation is that subjects who exposed to high WBGT perceived the wind to be weak based on their experience that lower wind speed may contribute to hot condition. That is, they think stronger wind may release their uncomfortable feeling so they might vote the wind speed as "still" and "weak" to reflect their subconscious uncomfortable perception. The sharp rise in wind discomfort votes without a significant change in wind speed and in accordance with the respective thermal conditions indicates that wind is actually perceived as a component of the thermal environment rather than as a separate environmental factor. It should be noted that the wind speed measured in this park is not strong due to the high density urban forms in Taiwan and tall buildings surrounding. The subjects may express a reasonable perception equivalent to actual wind speed once the wind speed is relatively high (e.g., >10 m/s).

5.4. Avoidance of the Sun. Thorsson et al. [20] conducted a fieldwork study in Japan, where the ideal beauty is fair skin, and found that 80% of the visitors in the urban public places sought shade at temperatures higher than 20°C. A counterpart study done in Sweden [21], where the ideal beauty includes a suntan, showed that only 14% of park visitors sought shade at temperatures higher than 20°C. With respect to attitudes toward the sun, this study demonstrates the relationship between the thermal environment, in terms of the temperature difference ($t_g - t_a$) between globe temperature and dry-bulb temperature, and the usage as shown Figure 10. Rather than the percentage of visitors in shade, total attendance is used in Figure 10, which results from the limited amount of shade in the park. As shown in Figure 10, the maximum of people in the park was observed at a situation

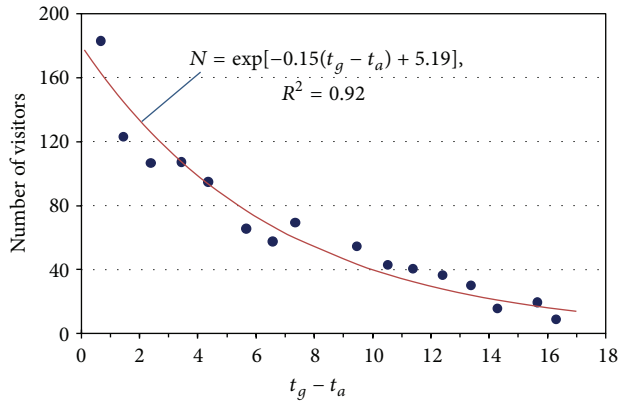

Figure 10

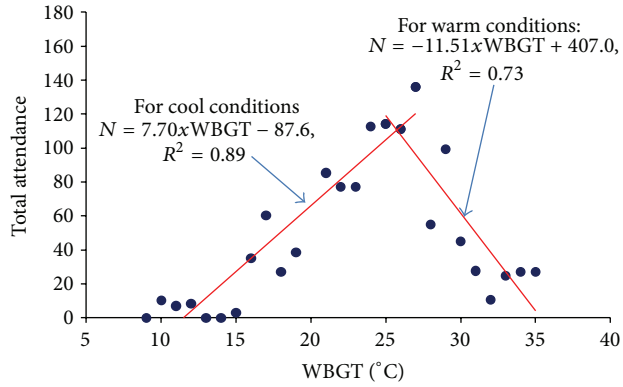

Figure 11

where the temperature difference was less than 1.0°C. As the $t_g - t_a$ increases, the total attendance presents an exponential decay. The best-fitted regression equation is superposed in Figure 10. The $R^2 = 0.92$ indicates a robust relation exists. This demonstrates that strong solar radiation intensity result in people in Taiwan, where the ideal beauty is also fair skin, tends to avoid the sun to a notable extent.

5.5. Relation between Total Attendance and Thermal Conditions. Figure 11 shows the relation between thermal environments in terms of WBGT and the average total attendance. This distribution of total attendance against WBGT is a single peak model. When the park's thermal condition is moderate, there are more than 120 people remaining in the study area of the park, and the total attendance in the park decreases considerably, to a level of less than 20 people staying in the study area. The number of people decreases more rapidly with WBGT in hot conditions than in cool conditions. Linear regression analysis is used to fit the relation between thermal conditions and total attendance, as shown in Figure 11. The relation is found to be significant, which indicates that the more comfortable the perceived thermal environment is, the higher the usage rate of the park will be.

6. Conclusions

Urban outdoor thermal environmental evaluation is of great significance in guiding the public's outdoor activities, the design of comfortable outdoor environments, and the improvement of urban climate. Based on the data from field surveys, this study used the WBGT as the thermophysiological index to analyze outdoor thermal comfort. The major achievements of this study are as follows.

According to the respondents' thermal perceptions, WBGT, as an index of the outdoor thermal conditions, has statistical significance relationship with the thermal perception of the respondents. This suggested the reliability of its application for analyzing outdoor thermal comfort. According to that relationship, the lower and upper limits of comfort acceptability for 80% of acceptability were 20°C WBGT and 26°C WBGT. This study also found that the temperature, corresponding to the lowest thermal unacceptable value, is 23.2°C WBGT.

The results regarding the adjustment behaviors and thermal environments suggested that the amount of clothing was significantly correlated to WBGT. However, the activity was not significantly correlated to WBGT. When the WBGT increases, expectations for high wind speed rise rapidly. When the WBGT decreases, expectations for low wind speed rise rapidly. The research found that Taiwan's residents had the apparent characteristics of avoiding sunlight. With rising or falling of WBGT, the number of visitors in the park would decline accordingly. The WBGT range of most visitors was approximately consistent with the outdoor thermal comfortable zone.

Acknowledgment

The authors offer their sincere appreciation for assistance in grant to the National Science Council of Taiwan (Project no. NSC-99-2221-E-239-028-MY2).

References

[1] J. Spagnolo and R. J. de Dear, "A field study of thermal comfort in outdoor and semi-outdoor environments in subtropical Sydney Australia," *Building and Environment*, vol. 38, no. 5, pp. 721–738, 2003.

[2] K. S. Ahmed, "Comfort in urban spaces: defining the boundaries of outdoor thermal comfort for the tropical urban environments," *Energy and Buildings*, vol. 35, no. 1, pp. 103–110, 2003.

[3] J. Nakano and S. Tanabe, "Thermal comfort and adaptation in semi-outdoor environments," *ASHRAE Transactions*, vol. 110, pp. 543–553, 2004.

[4] M. Nikolopoulou and S. Lykoudis, "Thermal comfort in outdoor urban spaces: analysis across different European countries," *Building and Environment*, vol. 41, no. 11, pp. 1455–1470, 2006.

[5] S. Oliveira and H. Andrade, "An initial assessment of the bioclimatic comfort in an outdoor public space in Lisbon," *International Journal of Biometeorology*, vol. 52, no. 1, pp. 69–84, 2007.

[6] H. Andrade, M.-J. Alcoforado, and S. Oliveira, "Perception of temperature and wind by users of public outdoor spaces:

relationships with weather parameters and personal characteristics," *International Journal of Biometeorology*, vol. 55, no. 5, pp. 665–680, 2011.

[7] V. Cheng, E. Ng, C. Chan, and B. Givoni, "Outdoor thermal comfort study in a sub-tropical climate: a longitudinal study based in Hong Kong," *International Journal of Biometeorology*, vol. 56, no. 1, pp. 43–56, 2012.

[8] S. Kariminia, S. Sh Ahmad, N. Ibrahim, and M. Omar, "Outdoor thermal comfort of two public squares in temperate and dry region of Esfahan, Iran," in *Proceedings of the International Conference on Science and Social Research (CSSR '10)*, pp. 1266–1271, Kuala Lumpur, Malaysia, December 2010.

[9] T.-P. Lin, "Thermal perception, adaptation and attendance in a public square in hot and humid regions," *Building and Environment*, vol. 44, no. 10, pp. 2017–2026, 2009.

[10] R.-L. Hwang, T.-P. Lin, M.-J. Cheng, and J.-H. Lo, "Adaptive comfort model for tree-shaded outdoors in Taiwan," *Building and Environment*, vol. 45, no. 8, pp. 1873–1879, 2010.

[11] T.-P. Lin, R. de Dear, and R.-L. Hwang, "Effect of thermal adaptation on seasonal outdoor thermal comfort," *International Journal of Climatology*, vol. 31, no. 2, pp. 302–312, 2011.

[12] T.-P. Lin, A. Matzarakis, and R.-L. Hwang, "Shading effect on long-term outdoor thermal comfort," *Building and Environment*, vol. 45, no. 1, pp. 213–221, 2010.

[13] ISO, *ISO, 7726: Ergonomics of the Thermal Environment-Instruments for Measuring Physical Quantities*, International Standards Organization, Geneva, Switzerland, 2003.

[14] ISO, *ISO, 7730: Ergonomics of the Thermal Environment-Analytical Determination and Interpretation of Thermal Comfort Using Calculation of the PMV and PPD Indices and Local Thermal Comfort Criteria*, International Standards Organization, Geneva, Switzerland, 2005.

[15] ASHRAE, *ASHRAE Handbook Fundamentals (SI)*, American Society of Heating, Refrigerating and Air Conditioning Engineering, Atlanta, Ga, USA, 2005.

[16] ISO, *ISO, 7243: Hot Environments-Estimation of the Heat Stress on Working Man, Based on the WBGT-Index (Wet Bulb Globe Temperature)*, International Standards Organization, Geneva, Switzerland, 2003.

[17] E. R. Ballantyne, R. K. Hill, and J. W. Spencer, "Probit analysis of thermal sensation assessments," *International Journal of Biometeorology*, vol. 21, no. 1, pp. 29–43, 1977.

[18] J. F. Nicol and M. A. Humphreys, "A stochastic approach to thermal comfort, occupant behaviour and energy use in buildings," *ASHRAE Transactions*, vol. 110, no. 2, pp. 554–568, 2004.

[19] M. A. Humphreys and J. F. Nicol, "Understanding the adaptive approach to thermal comfort," *ASHRAE Transactions*, vol. 104, no. 1, pp. 991–1004, 1988.

[20] S. Thorsson, T. Honjo, F. Lindberg, I. Eliasson, and E.-M. Lim, "Thermal comfort and outdoor activity in Japanese urban public places," *Environment and Behavior*, vol. 39, no. 5, pp. 660–684, 2007.

[21] I. Eliasson, I. Knez, U. Westerberg, S. Thorsson, and F. Lindberg, "Climate and behaviour in a Nordic city," *Landscape and Urban Planning*, vol. 82, no. 1-2, pp. 72–84, 2007.

Hindawi Publishing Corporation
Advances in Meteorology
Volume 2013, Article ID 251586, 10 pages
http://dx.doi.org/10.1155/2013/251586

Research Article

Application of Microclimate Modelling and Onsite Survey in Planning Practice Related to an Urban Micro-Environment

Lilla Andrea Égerházi, Attila Kovács, and János Unger

Department of Climatology and Landscape Ecology, University of Szeged, P.O. Box 653, Szeged 6701, Hungary

Correspondence should be addressed to Lilla Andrea Égerházi; egerhazi@geo.u-szeged.hu

Received 2 May 2013; Revised 12 July 2013; Accepted 31 July 2013

Academic Editor: Andreas Matzarakis

Numerical simulations of human thermal comfort conditions were carried out by means of the urban microclimate model ENVI-met in a popular children's playground located in Szeged, Hungary. Bioclimatic conditions were quantified by the Physiologically Equivalent Temperature (PET). Based on the PET values, thermal stress maps were created in two different periods of typical summer and autumn days. The study aims to reveal the seasonal and diurnal spatial patterns of the simulated thermal conditions and thus the degree of heat stress in different parts of the playground. Furthermore, we analysed the momentary spatial distributions of the visitors triggered by the microclimatic conditions of the area. According to the simulation, remarkable differences in the thermal conditions were found depending on the sun elevation and the resulting shaded conditions as well as the radiation of the heated surfaces. The spatial distribution of the visitors seems to be highly influenced by the patterns of the thermal conditions but the location and the preference of the children's playground equipment also affects it. In order to reveal the possible causes of the people's behaviour, an onsite questionnaire survey was conducted on their opinions and possible modification requirements related to the design of the playground.

1. Introduction

Due to accelerated urbanization, more than half of the Earth's population live in urbanized areas and this ratio may continue to increase in the future [1]. This also means that the number of people affected by the hazards of their housing and working environments such as air and light pollution and noise and thermal load (heat stress) is growing rapidly. In addition to urbanization, the trends of climate change, particularly the increasing frequency and intensification of extreme heat waves [2], increase the importance of urban bioclimatological research.

Urban bioclimatology examines the physiological impacts of the urban climate on the human health and the thermal comfort requirements. In urban environments, climate parameters are modified compared to the rural areas and even microscale climatic conditions change rapidly which have great influence on the thermal sensations and thermal stress levels of the residents and visitors. The microclimatic aspects of an area substantially determine the behavioural reactions as well as the subjective judgments of the visitors related to the area design, and ultimately area usage.

In the last years, numerous prominent urban bioclimate research projects were carried out in order to reveal the microclimatic conditions of open spaces (streets, squares, and parks) with different designs and also the visitors' behavioural reactions (e.g., RUROS [3], UCS [4, 5], and KLIMES [6]). A number of further studies conducted in the field of outdoor thermal comfort have attempted to contribute to encouraging sustainable urban development in various climates around the world. These studies focus on the thermal effects of urban microenvironments based on different methods. Several studies analyze the thermal environment-dependent area usage and the involuntary human reactions (mainly the clothing and solar exposure of visitors) triggered by these environments based on observations, for example, in Cambridge [7], Göteborg [8], Athens [9] as well as in Taichung City [10]. Numerous studies focus on revealing subjective assessments directed towards the thermal sensations, perceptions, and preferences of outdoor thermal factors based on structured

onsite interviews (e.g., [11–14]). Cultural and psychological characteristics and differences in subjective reactions to the thermal environment are also frequently analyzed [15–17].

Recent papers have emphasized the role and importance of urban planning processes in the thermal comfort investigations [18]. The design of an urban space is determined primarily by aspects of architecture but it would be desirable that urban planners and architects create also thermally comfortable and enjoyable microscale climatic conditions taking into account the health and well-being of the citizens. Mainly due to the large role of urban planning, considerable efforts have been put into analyzing the microclimate perception of people in urban environments through cognitive mapping [19], the shading effects of the vegetation, and buildings on outdoor thermal comfort (e.g., [20–23]) as well as the thermal performance and effects of natural and artificial materials used in outdoor urban spaces (e.g., [24, 25]). Extensive research has also been conducted emphasizing the role of microclimate simulations in urban planning.

The application of urban microscale models provides an opportunity to predict the different thermal stress conditions in high spatial and temporal resolution. Simulation results can give useful information for the architects and urban planners already before a construction process begins, therefore, they can estimate its possible thermal impacts and consequences. In case of existing places, thermally comfortable or critical areas can be identified by a modelling approach, and, if necessary, possible goals in relation to the area design can be determined. Nowadays, there are studies dealing with microclimate simulation in planning using the models RayMan [26–28], ENVI-met [19, 29], or their combination [30, 31].

In Szeged, Hungary, several public places (squares, playgrounds, and a pedestrian street) have been evaluated in terms of thermal conditions and the resulting human reactions in the framework of a long-term urban bioclimate project. The applied methods consisted of, for example, onsite questionnaire surveys related to the subjective thermal sensations, perceptions and preferences of the visitors as well as their opinions about the design of the areas [13]. In addition, the momentary attendance of the places was observed [32]. In the second part of the project, the investigation was extended with a microclimate modelling approach performed by means of the models RayMan [33] and ENVI-met [34]. In summer 2011, one of the most modern children's playgrounds of Szeged was included in the thermal comfort studies.

Children's playgrounds have a significant influence on the social life of their neighbourhood and provide recreational activity and enjoyment to the visitors of the area. Typically, the groups most affected by heat stress are the young children and the older adults who often take care of them [35]. Therefore, the thermal comfort examination of these types of public places is a particularly important research topic and can provide valuable information to architects and urban planners as well as decision makers.

The main objective of the study is to identify different microclimatic areas with various thermal stress levels in the above-mentioned popular playground of Szeged according to the results of an urban microscale model simulation. In this context, we also analyze the momentary spatial distributions of the visitors triggered by these different microclimatic conditions. In order to reveal the possible causes of the visitors' behaviour, they were asked to evaluate the design of the area in an onsite questionnaire survey.

The paper is organized as follows. In Section 2, the study area and the methodology are introduced. In Section 3, the results of the model simulation, area usage, and the questionnaire survey are presented. We also propose some possible solutions to improve the thermal conditions in the area. Finally, in Section 4, we summarize the results.

2. Materials and Methods

2.1. Study Area. The examined playground is located in Szeged (46°N, 20°E, 82 m above sea level), a medium-sized city in the southeastern part of Hungary, having a population of 160,000 and an area of 40 km^2. The city belongs to the climatic region Cfb according to Köppen's classification (temperate warm climate with uniform annual distribution of precipitation) or to the climatic region D.1 according to Trewartha's classification (continental climate with a long warm season) [36].

The study area is one of the most popular and attended playgrounds in the city with an area of approximately 3,300 m^2. Children can choose from several playground equipments such as jungle gyms, swings, and slides; moreover a cottage in the western part of the area provides an opportunity to play in comfortable, shaded conditions and also in the case of bad weather (Figure 1). The surface of the area is primarily covered by light-coloured gravel; however, in the immediate vicinity of the playhouse, paving stone can be found. A large number of deciduous trees (about 60) are planted mainly at the boundaries of the playground; however, in the middle parts of the area, there are only a few trees (about 20), moreover they are too young to provide shade yet. Therefore, in the morning and early afternoon hours, a considerable part of the area is exposed to direct sunlight which can adversely affect the thermal conditions in summer, though the shading of the trees would be a decisive way to control heat stress, especially in summer.

2.2. Applied Methods: Model Simulation, Area Usage, and Questionnaire Survey. In order to examine the microbioclimatic conditions of the area, a modelling approach was applied in the study. We used the model ENVI-met which is a three-dimensional nonhydrostatic climate model and is capable to simulate the interactions in the surface-atmosphere-vegetation system with relatively high temporal (10 min) and spatial (0.5–10 m) resolution [37, 38]. The simulation required two groups of model input data: the configuration file (cf) contains the basic settings and the necessary initial meteorological parameters of the simulation while the area input file (.in) includes the morphological elements (buildings, vegetation, land covers, etc.) of the area. ENVI-met needs initialization time, therefore it is suggested to start the simulation at midnight or at sunrise.

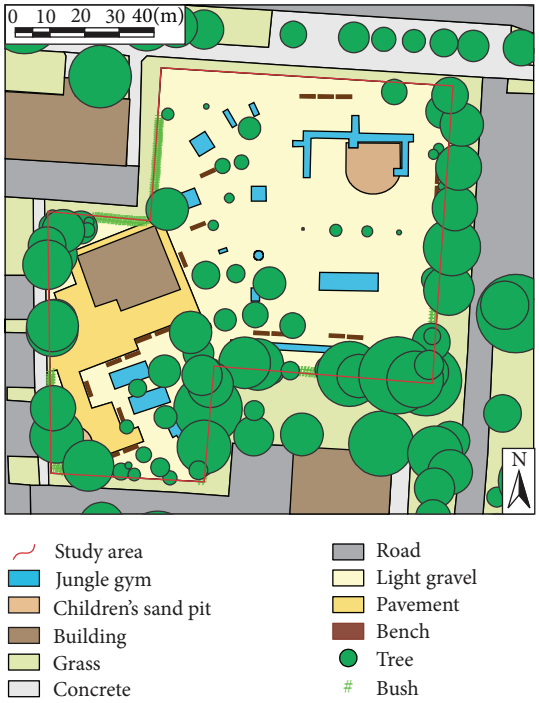

Figure 1: Spatial design and surface cover of the examined playground.

The morphological characteristics of the study area were previously assessed during field surveys. In the model the vegetation (trees and bushes) was divided into six groups based on their heights. Then a default type of tree selected in the model was modified layer by layer according to our groups. This method was applied also in case of the bushes. The model was run with a spatial resolution of 1.5 m, and the results refer to 1.2 m. The simulation had a stabilization time of 24 hours and then results for the period from 9 a.m. to 6 p.m. CEST (in accordance with the opening hours of the playground) were applied for a hot summer day (12th July 2011) and a temperate autumn day (3rd October 2011), both typical in terms of the average climatic conditions of Szeged. We tried to select relatively windless and sunny days so that the thermal conditions could develop clearly in the study area. The necessary initial meteorological data for the model on both days were air temperature, relative humidity (both at 12 a.m.), wind speed (average of the ten-minute measurements in the period from 9 a.m. to 6 p.m.), the most frequent wind direction (from 9 a.m. to 6 p.m.), and specific humidity (sounding measurements at 0 UTC). These necessary meteorological parameters were obtained from the meteorological station of the Hungarian Meteorological Service at a distance of about 6 km from the playground. The specific humidity was derived from [39]. The value at 2500 m necessary for modelling was obtained by interpolation (Table 1).

The simulated thermal conditions were quantified by a widely used thermal comfort index which is the Physiologically Equivalent Temperature (PET). It is defined as the air temperatures at which, in a typical indoor setting, the heat budget of the body is balanced with the same core and skin temperature as those under the prevailing complex outdoor conditions [40, 41]. The PET value ranges were defined according to different Central European thermal sensations and physiological stress levels [42] (Table 2).

Table 1: Basic initial meteorological input parameters of the simulation on both investigated days.

Meteorological parameters	12th July	3rd October
Air temperature at 2 m (K)	294	285
Relative humidity at 2 m (%)	75	70
Wind speed at 10 m (ms^{-1})	3.3	1.3
Wind direction (°)	10	60
Spec. humidity at 2500 m (gkg^{-1})	4	2

Table 2: Categories of the PET values (°C) for different grades of thermal sensation and physiological stress level [42].

PET categories (°C)			
Thermal sensation	Very hot	>41	Extreme heat
	Hot	35–41	Strong heat
	Warm	29–35	Moderate heat
	Slightly warm	23–29	Slight heat
	Neutral	18–23	No stress
	Slightly cool	13–18	Slight cold
	Cool	8–13	Moderate cold
	Cold	4–8	Strong cold
	Very cold	<4	Extreme cold
			Physiological stress level

After the modelling process, hourly thermal stress maps, that is, spatial distributions of the simulated PET, were created with the software Surfer 8 from 9 a.m. to 6 p.m. for the selected days. Surfer is able to visualize accurately microscale model results. Maps in two distinct times of the days (11 a.m. and 4 p.m.) were analyzed. The momentary spatial patterns of visitors in the area (at 11 a.m. and 4 p.m.) are also illustrated on the maps and analyzed in terms of the actual thermal conditions.

Additionally, an onsite questionnaire survey was conducted for 12 days (each day from 10 a.m. to 6 p.m.) related to the subjective evaluation of the design of the playground. The survey was carried out during the summer of 2011 and 2012 (226 interviewees) and the autumn of 2011 (329 interviewees); the dataset from each season comprises 6 days. The responses are fairly well representative of the population regularly visiting the playground.

Table 3 informs about the dates of the surveys and also the overall climatic conditions. The meteorological parameters were obtained from the above-mentioned meteorological station. The data were averaged for the period from 10 a.m. to 6 p.m. for all parameters.

The questionnaires took about 5 minutes to be completed. The first part collected information on the degree of the satisfaction with the design of the area marked in a seven-point semantic differential scale (from −3 very unpleasant to +3 very pleasant). Then subjects were asked to identify more than one preference and deficiency related to the area design. In the last part, we were interested in their possible modification requirements in the area. At first, we asked

Table 3: The dates of the questionnaire surveys and the basic climatic conditions. The parameters are marked in bold in case of the dates considered for simulations.

Campaign	Meteorological parameters			
	Temperature (°C)	Relative humidity (%)	Wind speed (m/s)	Global radiation (W/m^2)
Summer of 2011				
12/07/2011	**29.4**	**43.9**	**3.2**	**767.8**
04/08/2011	25.8	51.2	3.4	467.7
Summer of 2012				
07/06/2012	25.6	45.9	2.8	756.6
08/06/2012	27.6	49.7	5.1	749.3
02/07/2012	34.5	33.6	4.1	697.4
02/08/2012	n/a	n/a	n/a	n/a
Autumn of 2011				
12/09/2011	30.2	38.8	4.6	540.8
19/09/2011	29.4	32.3	8.4	474.9
26/09/2011	25.0	39.0	1.6	445.3
03/10/2011	**22.8**	**34.1**	**1.3**	**445.6**
10/10/2011	13.3	47.7	3.1	412.4
17/10/2011	9.8	32.8	2.6	399.3

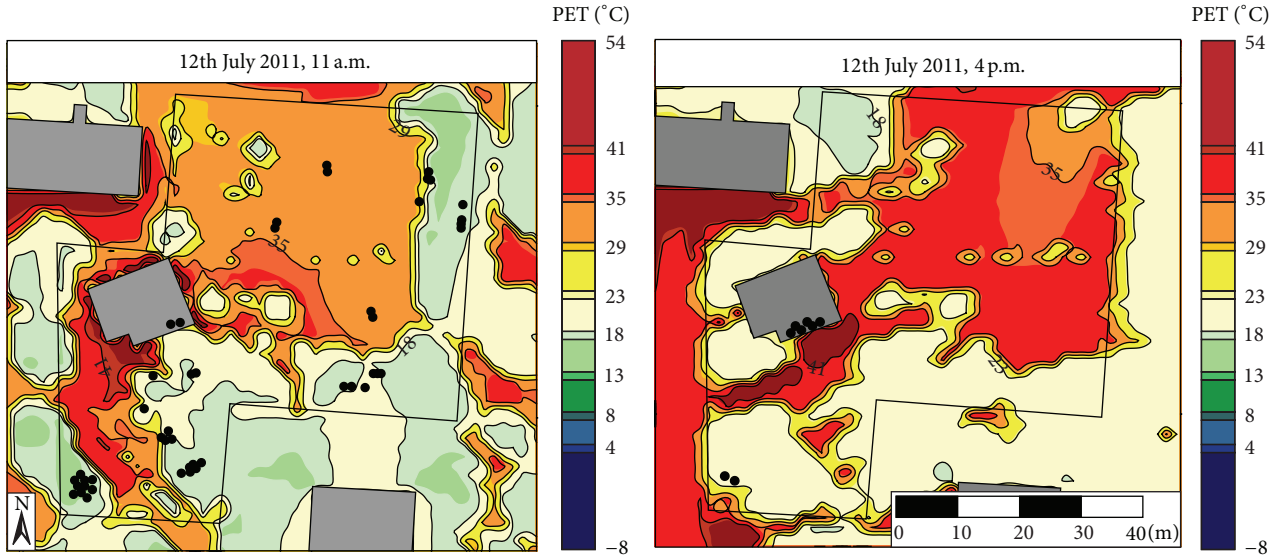

Figure 2: Thermal stress map (PET) and spatial pattern of visitors (black dots) at 11 a.m. (a) and 4 p.m. (b) CEST, 12th July 2011. The thick black line indicates the border of the playground.

them to indicate the degree of their modification demand according to three categories: significant, slight, or none. Then they could give up to three concrete proposals for solutions from a list of six predefined factors (e.g., "construct shade structures", "plant trees", and "construct fountain"), and they also had the option to mention other proposals according to their individual ideas.

3. Results and Discussion

3.1. Simulated Thermal Conditions and the Momentary Spatial Distributions of Visitors. According to the methods described in Section 2, the heat stress conditions expressed by the spatial distribution of PET values and their relationship with the momentary area usage of the playground are examined. The thermal stress maps indicate remarkable differences between summer (Figure 2) and autumn (Figure 3) and also between the investigated times.

The heat load was more dominant in the summer day in the whole area than in autumn. In summer, in the morning (Figure 2(a)), the highest heat load appeared around the playhouse where PET values exceeded 41°C denoting extreme heat stress (very hot thermal sensation). This can be explained by the strong heat radiation of the pavement (see Figure 1)

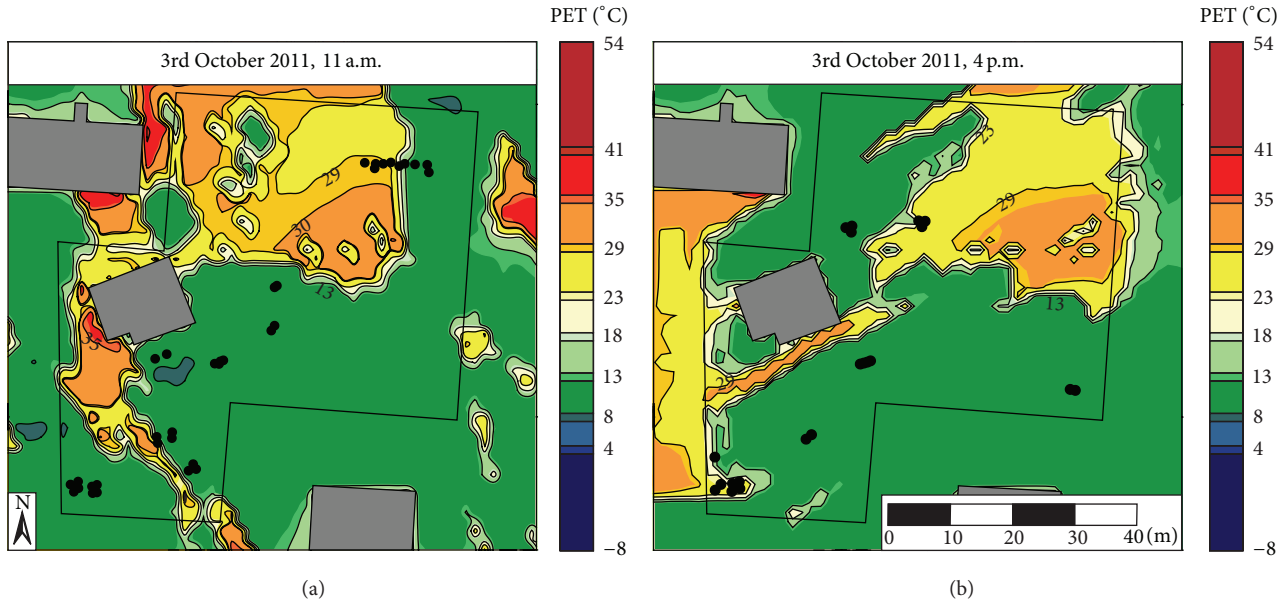

Figure 3: Thermal stress map (PET) and spatial pattern of visitors (black dots) at 11 a.m. (a) and 4 p.m. (b) CEST, 3rd October 2011. The thick black line indicates the border of the playground.

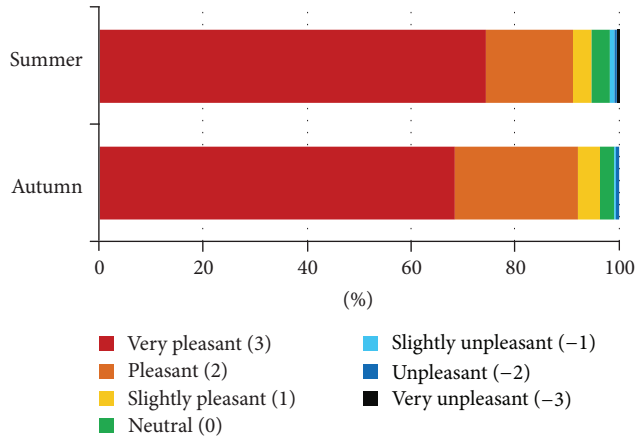

Figure 4: Percentage distribution of the visitors' general satisfaction with the playground.

which was strongly heated by the direct solar radiation. In the middle and northern parts of the playground, slightly more moderate thermal conditions can be found, but even so, mainly warm and hot thermal sensations (29–41°C) occurred. In the immediate vicinity of the single trees, thermal stress was negligible. Due to the shading effect of the dense foliage, thermal conditions were much more pleasant near the southern and eastern boundaries of the area; however, slight cold stress was still present (13–18°C). Although the spatial distribution of the visitors can be highly influenced by the location and the preference of the playground equipment, it also has some connections with the patterns of the thermal conditions. Some visitors spent their time at the playground equipments exposed to the direct sunlight. Seemingly they did not care about the existing heat load too much. However, most people preferred the comfortable southern and eastern spaces protecting themselves from the direct sunlight.

In the afternoon (Figure 2(b)), despite the lower sun elevation, there were more unpleasant thermal conditions in the places exposed to the sunlight compared to those in the morning. Besides the direct radiation, this might be related to the strong radiation from the heated surfaces. The most unpleasant conditions corresponding to hot and very hot thermal sensations (PET of above 35°C) were in the sunny middle and eastern parts of the area as well as on the southern side of the house. Similarly to the situation at 11 a.m., comfortable conditions prevailed in the southern shaded area. However, due to the altered shading conditions of the trees, the thermal sensation on the western part of the playground became also comfortable. The attendance followed the spatial pattern of the thermal conditions, that is, people were not exposed to the direct sunlight at all. Nevertheless, there were much less people in the playground at this time compared to the morning. The more stressful thermal load and, as a consequence, the increasing number of sun-heated equipments may play a role in this phenomenon.

The selected autumn day can be characterized with lower thermal load (Figure 3). At this time, cold stress also appeared in large areas. In the morning (Figure 3(a)), similarly to the summer day, warm load prevailed primarily in the northern parts (corresponding to slight and moderate heat stress, i.e., 23–35°C). Additionally, moderate and strong heat stress conditions (29–41°C) occurred on the western side of the house even in autumn. In these places, there was practically nothing to protect the people from the direct radiation. Due to the lower sun elevation in autumn, greater parts of the area were shaded by the southern vegetation and the buildings. The PET decreased there below 13°C which

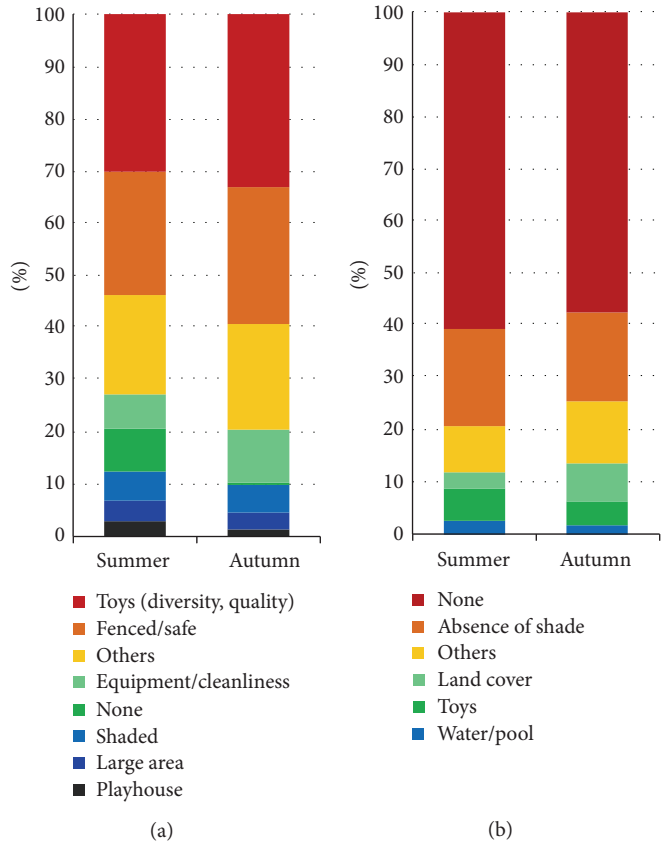

Figure 5: Preferences (a) and deficiencies (b) according to the opinions of the respondents (a person could mention more than one assessment).

already indicates cool conditions (moderate cold stress). It can be therefore concluded that areas with comfortable conditions were negligible, thus people could only choose places with thermal stress. Most people favoured the shady, cold conditions (Figure 3(a)) which can be considered to be a real human reaction in autumn, after a hot summer period. However, several children enjoyed their time on the jungle gym partly exposed to the direct sunlight.

Regarding the late afternoon period of the autumn day (Figure 3(b)), cool thermal sensation (PET of below 13°C) occurred in large parts of the area since they became shady. The heat stress zone (23–35°C) shifted to the northeast compared to that of the morning hour due to the western position of the sun. The number of people was lower at this time and their distribution did not follow strictly that of the thermal conditions; the locations of the playground equipment had rather greater influence on the patterns of the visitors.

The thermal stress maps indicate appropriately the spatial differences in thermal conditions in such a small area. However, the results of ENVI-met should be interpreted with caution due to inaccuracies in simulations, which have been also discussed in [19, 31]. The model gives inaccurate results in certain situations as near the large buildings at the edges of the maps clearly seen in Figures 2 and 3. There is an overestimation of radiation fluxes and thus PET in these spaces, therefore they were excluded from the analysis. It should be noted, however, that the results of ENVI-met entirely outline the adversely thermal effects of the pavement around the playhouse in the studied area (Figures 1–3).

3.2. Questionnaire Survey Related to the Design of the Playground. According to the results analyzed in Section 3.1, the creation of more comfortable conditions becomes particularly important which can be achieved by some modifications in the design of the area reflecting the visitor's opinions and requirements. In this section, the onsite seasonal evaluation of the visitors' answers pertaining to the area design is analyzed.

The first question concerns their general satisfaction with the area was marked in a seven-point semantic differential scale (from −3 very unpleasant to +3 very pleasant) (Figure 4). The vast majority of the votes correspond to the "pleasant" categories (+1–3): 94.6% in summer and 96.4% in autumn, respectively. Moreover, more than two-thirds of the respondents were fully satisfied (+3): 74.3% and 68.4% in the two seasons.

We then surveyed the possible positive or negative judgments of the visitors about the area design (Figure 5) in order to reveal the causes of their satisfaction or dissatisfaction. A person could mention more issues at this question.

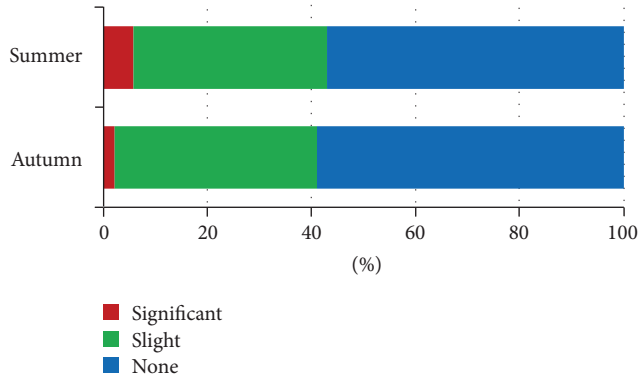

Figure 6: Degree of the modification requirements of the visitors related to the design of the area.

The differences between the seasons are found to be small. As a positive factor, most people emphasized the diversity and high quality of the playground toys as well as the closure and security of the area. Many people found the park to be clean and well equipped. The large size of the area, the amount of shady places, and the existence of the playhouse were also mentioned a few times (Figure 5(a)). The high level of satisfaction is reflected by the fact that 58.3% (in summer) and 57.1% (in autumn) of the interviewees did not mention any problem (Figure 5(b)). As a negative factor, however, the absence or small amount of shade was pointed out by several people (18.7% and 16.9%, resp.). In addition, a few people emphasized the type of the dominant land cover (gravel instead of grass) and the absence of a (drinking) fountain or a pool (Figure 5(b)).

The dissatisfaction of the visitors could be reduced even more by creating more pleasant and comfortable thermal conditions in the area. To facilitate this complex process, finally the possible modification requirements in the area were surveyed where a person could mark more factors. In accordance with the overall satisfaction (Figure 4) and the few deficiencies found (Figure 5(b)), about 60% of the people would not change anything in the design in both seasons and only a few percent of them would modify it significantly (Figure 6). The most frequently marked modification requirements are tree planting and the construction of shade structures which reflect the main deficiency (absence of shade), that is, most people would prefer shady conditions in both seasons (Figure 7). The shade structures would be more desired in summer probably due to human thermal aspects, that is, the intense summer heat load. However, more plants are desired in autumn which may have a primarily aesthetic facet because of the decline of vegetation in autumn. Further important demands are the placement of a fountain and change in land cover (grass instead of gravel) which has both aesthetic and thermal aspects.

3.3. Planning Proposals for Solutions to Improve Thermal Comfort. In the case of the presented playground, it would be highly desirable to ensure suitable shading conditions in order to reduce the heat load of the children and the accompanying adults (often elderly people). This requirement is clearly reflected in the demands of the visitors according to the questionnaire survey described in Section 3.2. The most obvious and natural solution may be to plant trees because of their shading and aesthetic qualities. Although there are some trees in the most uncomfortable middle parts of the studied area, they are too young to provide shade and will remain like this for a long time. It could be a good option to plant adult trees, but we think that it is not economical to replace the existing young trees in the playground with adult trees. Moreover, the thermal effects of adult trees strongly vary by season since they can reduce hot thermal conditions in summer; however, shading is not really required in autumn [43]. Another natural solution may be to create some green roofs, however it is not really possible in the study area. Maybe greening of the southern and eastern walls of the playhouse would be appropriate for this purpose. Thus the most practical option is to construct artificial and temporary shade structures in the unpleasant areas. These devices are to effectively reduce the amount of direct sunlight in the period of high heat stress (in summer, around noon) but allow it to reach the ground in cooler times of the year. Another advantage is to allow for cross-ventilation below.

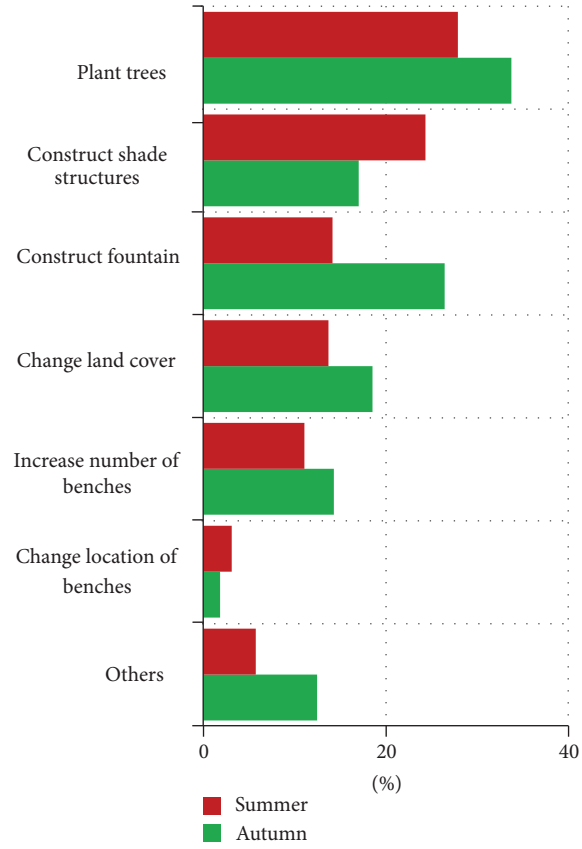

Figure 7: Modification requirements of the respondents related to the area design (a person could mark more factors).

Such structures can be, for example, temporary shade sails (Figures 8(a) and 8(b)) or large shade umbrellas (Figure 8(c)) and might be placed at least above the most

(a) (b)

(c) (d)

Figure 8: Proposals for solutions to reduce heat stress by shade structures during summer: (a) and (b) shade sails [44, 45], (c) shade umbrella [46], and (d) artificial shade canopy [photo: N. Kántor].

exposed parts of the area during summer heat, especially above the most frequently used jungle gym system (in the northeast, see Figure 1). There are examples of using artificial shade canopies (Figure 8(d)) which consist of small resistant plastic items that do not prevent air movement below, but properly protect from strong sunlight around midday due to their adjusted inclination. Additionally, it would be desirable to construct a fountain in the studied area which could improve both thermal and aesthetic conditions.

4. Conclusion

In the studied playground, many children and adults spend their time most of the year and are often exposed to thermal stress conditions which are highly influenced by the design of the area. It is particularly necessary to manage these microclimatically different areas and therefore to provide information to the responsible decision makers and urban planners to make the best choices from the thermal comfort point of view.

According to the analysis of the simulated thermal conditions, remarkable microclimatic differences were found in the two examined seasons and times. The most unpleasant areas were in the middle and northern parts of the area as well as around the playhouse in summer. The shady southern areas had favourable microclimate even in the summer afternoon. However, in autumn, cool conditions already appeared in these places. The detected thermal comfort differences depend on the sun elevation and the resulting shaded conditions caused by the vegetation and the surrounding buildings. Besides the direct sunlight, the radiation of the heated surfaces can greatly contribute to the thermal stress conditions.

The thermal conditions prevailing in the playground highly influence the thermal perception of humans. This is clearly reflected in the involuntary behaviour of visitors altering their spatial distribution depending on the momentary thermal conditions. For example, most people were not exposed to the direct solar radiation in the summer day and preferred comfortable spaces. However, it is important to point out that the location and the preference of the playground equipment also have significant impact on the patterns in both seasons, and it can increase the probability of exposure to stress conditions.

In order to reduce the unpleasant effects of heat load on the visitors, it would be desirable to construct artificial and temporary shade structures especially above the most frequently used toys. This demand, as well as tree planting and placement of a fountain, is clearly supported by the conducted onsite survey and it would be a significant step forward in providing more liveable microclimatic conditions in the area. As a negative factor, most people emphasized the absence or small amount of shade. However, most interviewees were fully satisfied and would not change anything in the design or only slight changes are required. More than half of the respondents did not mention any problem and pointed out the diversity and high quality of the playground equipment and the cleanliness as well as the closure and security of the area.

The methods applied in the study (modelling and onsite surveys) can contribute to encouraging sustainable and climate-friendly urban development and can be generally

applicable to other similar situations. The ENVI-met simulations can be a useful tool to reveal thermal differences in microscale spaces, but the results should be considered with some caution. Due to its high complexity, the model computation is slow especially in case of low spatial resolution (1 m or less) making it slightly difficult to apply in planning practice. However, the model takes also the thermal effects of surface cover into account which makes it beneficial in practice.

Application of microclimate models in urban planning is suggested together with adequate onsite measurements reflecting the real microclimatic conditions in order to validate the outcomes of the simulations. There is a need for a generic microclimate model which takes the effects of all factors influencing thermal conditions (vegetation, buildings, and surface cover) into consideration. By means of such a complex model, the onsite measurements can be eliminated before a construction process begins. Our further study will be directed to compare the results with those from other microclimate models (e.g., RayMan) as well as from onsite measurements.

Acknowledgment

Special thanks are due to N. Kántor and Á. Takács for their tireless participation and coordination in the onsite questionnaire survey. Thanks to E. Tanács for proofreading of the paper.

References

[1] UNFPA, "The state of world population 2011," Report of the United Nations Population Fund, New York, NY, USA, 2011.

[2] IPCC, "Contribution of working groups I, II and III to the fourth assessment report of the intergovernmental panel on climate change," in *Climate Change 2007: Synthesis Report*, R. K. Pachauri and A. Reisinger, Eds., IPCC, Geneva, Switzerland, 2007.

[3] M. Nikolopoulou and S. Lykoudis, "Thermal comfort in outdoor urban spaces: analysis across different European countries," *Building and Environment*, vol. 41, no. 11, pp. 1455–1470, 2006.

[4] I. Eliasson, I. Knez, U. Westerberg, S. Thorsson, and F. Lindberg, "Climate and behaviour in a Nordic city," *Landscape and Urban Planning*, vol. 82, no. 1-2, pp. 72–84, 2007.

[5] S. Thorsson, "Urban climate spaces—a multi- and interdisciplinary research project," in *Urban Climate News*, vol. 30, pp. 11–13, 2008.

[6] H. Mayer, "KLIMES—a joint research project on human thermal comfort in cities," *Berichte Des Meteorologischen Instituts Der Albert-Ludwigs-Universität Freiburg*, vol. 17, pp. 101–117, 2008.

[7] M. Nikolopoulou, N. Baker, and K. Steemers, "Thermal comfort in outdoor urban spaces: understanding the Human parameter," *Solar Energy*, vol. 70, no. 3, pp. 227–235, 2001.

[8] S. Thorsson, M. Lindqvist, and S. Lindqvist, "Thermal bioclimatic conditions and patterns of behaviour in an urban park in Göteborg, Sweden," *International Journal of Biometeorology*, vol. 48, no. 3, pp. 149–156, 2004.

[9] M. Nikolopoulou and S. Lykoudis, "Use of outdoor spaces and microclimate in a Mediterranean urban area," *Building and Environment*, vol. 42, no. 10, pp. 3691–3707, 2007.

[10] T. Lin, "Thermal perception, adaptation and attendance in a public square in hot and humid regions," *Building and Environment*, vol. 44, no. 10, pp. 2017–2026, 2009.

[11] J. Spagnolo and R. de Dear, "A field study of thermal comfort in outdoor and semi-outdoor environments in subtropical Sydney Australia," *Building and Environment*, vol. 38, no. 5, pp. 721–738, 2003.

[12] S. Oliveira and H. Andrade, "An initial assessment of the bioclimatic comfort in an outdoor public space in Lisbon," *International Journal of Biometeorology*, vol. 52, no. 1, pp. 69–84, 2007.

[13] N. Kántor, L. A. Égerházi, and J. Unger, "Subjective estimation of thermal environment in recreational urban spaces—part 1: investigations in Szeged, Hungary," *International Journal of Biometeorology*, vol. 56, no. 6, pp. 1075–1088, 2012.

[14] E. Krüger, P. Drach, R. Emmanuel, and O. Corbella, "Urban heat island and differences in outdoor comfort levels in Glasgow, UK," *Theoretical and Applied Climatology*, vol. 112, pp. 127–141, 2013.

[15] M. Nikolopoulou and K. Steemers, "Thermal comfort and psychological adaptation as a guide for designing urban spaces," *Energy and Buildings*, vol. 35, no. 1, pp. 95–101, 2003.

[16] I. Knez and S. Thorsson, "Influences of culture and environmental attitude on thermal, emotional and perceptual evaluations of a public square," *International Journal of Biometeorology*, vol. 50, no. 5, pp. 258–268, 2006.

[17] I. Knez, S. Thorsson, I. Eliasson, and F. Lindberg, "Psychological mechanisms in outdoor place and weather assessment: towards a conceptual model," *International Journal of Biometeorology*, vol. 53, no. 1, pp. 101–111, 2009.

[18] I. Eliasson, "The use of climate knowledge in urban planning," *Landscape and Urban Planning*, vol. 48, no. 1-2, pp. 31–44, 2000.

[19] S. Lenzholzer, "Research and design for thermal comfort in Dutch urban squares," *Resources, Conservation and Recycling*, vol. 64, pp. 39–48, 2012.

[20] L. Shashua-Bar, D. Pearlmutter, and E. Erell, "The cooling efficiency of urban landscape strategies in a hot dry climate," *Landscape and Urban Planning*, vol. 92, no. 3-4, pp. 179–186, 2009.

[21] J. He and A. Hoyano, "Measurement and evaluation of the summer microclimate in the semi-enclosed space under a membrane structure," *Building and Environment*, vol. 45, no. 1, pp. 230–242, 2010.

[22] M. F. Shahidan, M. K. M. Shariff, P. Jones, E. Salleh, and A. M. Abdullah, "A comparison of *Mesua ferrea* L. and *Hura crepitans* L. for shade creation and radiation modification in improving thermal comfort," *Landscape and Urban Planning*, vol. 97, no. 3, pp. 168–181, 2010.

[23] T. Lin, A. Matzarakis, and R. Hwang, "Shading effect on long-term outdoor thermal comfort," *Building and Environment*, vol. 45, no. 1, pp. 213–221, 2010.

[24] A. Chudnovsky, E. Ben-Dor, and H. Saaroni, "Diurnal thermal behavior of selected urban objects using remote sensing measurements," *Energy and Buildings*, vol. 36, no. 11, pp. 1063–1074, 2004.

[25] L. Doulos, M. Santamouris, and I. Livada, "Passive cooling of outdoor urban spaces. The role of materials," *Solar Energy*, vol. 77, no. 2, pp. 231–249, 2004.

[26] Á. Gulyás, J. Unger, and A. Matzarakis, "Assessment of the microclimatic and human comfort conditions in a complex urban environment: Modelling and measurements," *Building and Environment*, vol. 41, no. 12, pp. 1713–1722, 2006.

[27] A. Matzarakis, F. Rutz, and H. Mayer, "Modelling radiation fluxes in simple and complex environments—application of the RayMan model," *International Journal of Biometeorology*, vol. 51, no. 4, pp. 323–334, 2007.

[28] L. Shashua-Bar, I. X. Tsiros, and M. Hoffman, "Passive cooling design options to ameliorate thermal comfort in urban streets of a Mediterranean climate (Athens) under hot summer conditions," *Building and Environment*, vol. 57, pp. 110–119, 2012.

[29] F. Ali-Toudert and H. Mayer, "Effects of asymmetry, galleries, overhanging facades and vegetation on thermal comfort in urban street canyons," *Solar Energy*, vol. 81, no. 6, pp. 742–754, 2007.

[30] Á. Szűcs, "Wind comfort in a public urban space—case study within Dublin Docklands," *Frontiers of Architectural Research*, vol. 2, pp. 50–66, 2013.

[31] D. Fröhlich and A. Matzarakis, "Modeling of changes in thermal bioclimate: examples based on urban spaces in Freiburg, Germany," *Theoretical and Applied Climatology*, vol. 111, no. 3-4, pp. 547–558, 2013.

[32] L. A. Égerházi and N. Kántor, "Area usage of two outdoor public places with regard to the thermal conditions—observation-based human thermal comfort study in the centre of Szeged," *Acta Climatologica et Chorologica Universitatis Szegediensis*, vol. 44-45, pp. 73–81, 2011.

[33] L. A. Égerházi, N. Kántor, Á. Takács, and J. Unger, "Patterns of attendance and thermal conditions on a pedestrian street," in *Proceedings of the 8th International Conference on Urban Climate*, 2012, paper 169.

[34] L. A. Égerházi, N. Kántor, and T. Gál, "Evaluation and modelling the micro-bioclimatological conditions of a popular playground in Szeged, Hungary," *International Review of Applied Sciences and Engineering*, vol. 4, no. 1, pp. 57–61, 2013.

[35] C. Koppe, S. Kovats, G. Jendritzky, and B. Menne, "Heat-waves: risks and responses," in *Health and Global Environmental Change, Series No. 2*, World Health Organization, WHO Regional Office for Europe, Copenhagen, Denmark, 2004.

[36] G. Péczely, "Climatology," Nemzeti Tankönyvkiadó, Budapest, Hungary, 1979 (Hungarian).

[37] M. Bruse and H. Fleer, "Simulating surface-plant-air interactions inside urban environments with a three dimensional numerical model," *Environmental Modelling and Software*, vol. 13, no. 3-4, pp. 373–384, 1998.

[38] M. Bruse, ENVI-met website, http://www.envi-met.com/, 2004.

[39] Wyoming Weather Web, Weather information from the University of Wyoming, Department of Atmospheric Science, http://weather.uwyo.edu/upperair/europe.html, (WMO station number 12982).

[40] H. Mayer and P. Höppe, "Thermal comfort of man in different urban environments," *Theoretical and Applied Climatology*, vol. 38, no. 1, pp. 43–49, 1987.

[41] P. Höppe, "The physiological equivalent temperature—a universal index for the biometeorological assessment of the thermal environment," *International Journal of Biometeorology*, vol. 43, no. 2, pp. 71–75, 1999.

[42] A. Matzarakis and H. Mayer, "Another kind of environmental stress: thermal stress," *WMO Newsletter*, vol. 18, pp. 7–10, 1996.

[43] P. Cohen, O. Potchter, and A. Matzarakis, "Daily and seasonal climatic conditions of green urban open spaces in the Mediterranean climate and their impact on human comfort," *Building and Environment*, vol. 51, pp. 285–295, 2012.

[44] http://www.1800shadeu.com.au/shade_solutions/industry/schools/playground_shade/coloured_shade_sails_with_yell.

[45] http://www.shadecomforts.com/media/playground-shade-sails-7.html.

[46] http://www.1800shadeu.com.au/shade_solutions/structures/pyramid_shade/pyramid_shade_for_playground.

Hindawi Publishing Corporation
Advances in Meteorology
Volume 2013, Article ID 312572, 13 pages
http://dx.doi.org/10.1155/2013/312572

Research Article

Modification of Human-Biometeorologically Significant Radiant Flux Densities by Shading as Local Method to Mitigate Heat Stress in Summer within Urban Street Canyons

Hyunjung Lee,[1] Jutta Holst,[2] and Helmut Mayer[1]

[1] *Albert-Ludwigs University of Freiburg, Werthmannstraße 10, 79098 Freiburg, Germany*
[2] *Department of Physical Geography and Ecosystem Science, Lund University, Sölvegatan 12, 223 62 Lund, Sweden*

Correspondence should be addressed to Hyunjung Lee; hyunjung.lee@meteo.uni-freiburg.de

Received 8 April 2013; Revised 31 May 2013; Accepted 7 June 2013

Academic Editor: Tzu-Ping Lin

Increasing heat will be a significant problem for Central European cities in the future. Shading devices are discussed as a method to mitigate heat stress on citizens. To analyze the physical processes, which are characteristic of shading in terms of urban human-biometeorology, experimental investigations on the thermal effects of shading by a building and shading by tree canopies were conducted in Freiburg (Southwest Germany) during typical Central European summer weather. Urban human-biometeorology stands for the variables air temperature T_a, mean radiant temperature T_{mrt}, and physiologically equivalent temperature PET, that is the human-biometeorological concept to assess the thermal environment which was applied. The measuring setup consists of specific human-biometeorological stations, which enable the direct or indirect determination of T_a, T_{mrt}, and PET. With respect to both shading devices, the T_a reduction did not exceed 2°C, while PET as a measure for human heat stress was lowered by two thermal sensation steps according to the ASHRAE scale. As T_{mrt} has the role of a key variable for outdoor thermal comfort during Central European summer weather, all radiant flux densities relevant to the determination of T_{mrt} were directly measured and analyzed in detail. The results show the crucial significance of the horizontal radiant flux densities for T_{mrt} and consequently PET.

1. Introduction

Severe heat in summer is currently a problem for Central European cities, as both their design and citizens are not adapted to this meteorological hazard [1, 2]. For the future, results of regional climate simulations [3, 4] project not only a continuation of the long-term increase of near-surface air temperature T_a but also embedded heat waves, which will be more frequent and intense as well as lasting longer. The increasing severe heat will enhance the previous thermal strain for citizens into a considerable thermal stress, which causes extremely negative impacts on their efficiency, well-being, and health [5]. For example, the list of heat events during the period 2000–2007 [6] shows that the mortality rate in consequence of the heat wave of 2003 in Western Europe amounted to 19.490 in France and 5.250 in Germany. The demographic change in Central Europe is reflected by the age distribution of its population. Related to Germany, the percentage of people ≥65 years was 20% in 2008 and will be 29% in 2030 [7]. This development, which is similar to other countries in Central Europe, shows a gradual increase in elderly people; that is, the human vulnerability of risk groups with respect to severe heat is rising. Thereby, the accumulation impact of longer lasting heat on citizens has to be taken into account.

Given this background, urban planning faces the huge challenge to develop, apply, and validate methods to maintain human thermal comfort for citizens even under severe heat. It must be noted that severe heat is a regional phenomenon, which depends on the large-scale weather situation. The planning methods should include a redesign of buildings, streets, and open spaces in a preventive way that severe heat can be mitigated on the local urban scale [8, 9]. In this context, it has to be discussed whether these methods can be applied to Central European cities and to what extent [10]. Due to meteorological reasons, the assumption suggests that they will be

more effective for dry heat than humid heat periods. The scope of urban planning to reduce severe humid heat impacts on citizens is restricted as hardly any physical process exists that leads to a local reduction of moisture [11], which itself is governed by the large-scale weather conditions. Provided that it is not too low, the ventilation of cities has the potential to reduce the heat stress perceived by citizens. Therefore, all planning methods to mitigate heat stress on the urban scale should also include an improvement of the local ventilation conditions [12].

To cope with the need for action, urban planning needs quantitative fundamentals of urban human-biometeorology. For that purpose, results of investigations can be applied, which provide indications on the variation of human thermal comfort caused by changed urban design parameters [2, 13–15]. These investigations show a common feature: thermophysiological assessment indices are used, which were derived from the human heat budget. The physiologically equivalent temperature PET defined by Mayer and Höppe [16] represents one of those indices. Compared to similar indices, it has the advantage that many results for PET are available in the meantime, which has been obtained by numeric simulations or experiments worldwide [17–22]. They facilitate the comparative evaluation of thermal stress conditions for citizens. It will take some time, until the recently developed universal thermal climate index UTCI [23] reaches a similar basis of comparison. In addition, the current version of UTCI does not include a new approach to determine the mean radiant temperature T_{mrt} but recommends the use of existing simulation tools like the RayMan model [24].

In Central Europe, severe heat occurs only in summer, when day is longer than night. Therefore, urban planning prefers a double strategy for methods aiming at maintaining thermal comfort for citizens under severe heat. Methods, which are effective in the daytime, have a first priority, while methods, which are related only to nocturnal meteorological phenomena like thermally induced down-slope or mountain air flow, are often classified as secondary. The general objective of planning methods for the daytime conditions is to reduce the heat input into all urban spaces. This should be achieved in compliance with the targets of environmental protection, that is, avoidance of air conditioning systems. According to results of investigations on outdoor thermal comfort conducted in inland cities during clear-sky weather [2, 13–15, 18, 22, 25], the radiant exchange is the dominant meteorological factor affecting thermal comfort in the daytime. Therefore, the decrease of the direct solar radiation by shading can be the most effective method to reduce the heat entered into urban spaces [2, 13, 15, 25–31]. Transpiration from vegetation leads to a lowering of its surface temperature [32] including a slight decrease of T_a above the vegetation layer, but this effect does not reach a comparative magnitude of shading impacts on citizens.

Local shading of direct solar radiation within the urban canopy layer can be achieved by (i) optimized design of buildings, open spaces, and streets [2, 14, 15], (ii) man-made devices like awnings or sunshades, and (iii) street trees [2, 13, 25–31]. Under a human-biometeorological point of view, which includes aesthetic and psychological aspects, shading by street trees has the highest significance despite conflicting goals like impacts on the near-surface air flow or emission of BVOC as a precursor for the ozone formation [10].

The radiant exchange, which is relevant to the perception of heat by citizens [1, 25], can be quantified by T_{mrt}. It represents a measure for the heat of the short- and long-wave radiant flux densities from the three-dimensional environment absorbed by the human-biometeorological reference person and plays a fundamental role in the thermophysiological concept to assess the thermal environment [1, 2, 33].

In order to get a deeper understanding on the physical processes, which lead to a local reduction of heat for citizens, the main objective of this study is to quantify the human-biometeorological consequences of two effective shading methods, namely, shading by (i) a building and (ii) street trees. Against the background of existing studies on human-biometeorological shading effects, this study is focussed on the pattern of measured three-dimensional short- and long-wave radiant flux densities, which will be analyzed in a comparative way for both shading devices. This approach enables a physically based explanation of the spatiotemporal behaviour of T_{mrt} in contrast to T_a. Up to now, it is only available to some extent. As for inland cities in Central Europe, the daytime values of PET on typical summer days are strongly influenced by T_{mrt} [2, 13], the daytime pattern of PET can be interpreted by T_{mrt}. The analysis of the three-dimensional radiant fields should also give hints on the potential to manipulate physical surface properties aimed at an additional lowering of radiant flux densities from selected directions.

2. Materials and Methods

On typical Central European summer days during the period 2007–2010, several 1-day human-biometeorological measuring campaigns were conducted in different quarters of Freiburg (Southwest Germany) within the scope of the KLIMES project [1]. Their main objective has been the quantitative analysis of the influences of street design characteristics on those meteorological variables, which are necessary to calculate PET, that is, particularly T_a and T_{mrt}. In order to get a better insight into the pattern of radiant flux densities as well as T_{mrt} and PET during shading situations, two measuring campaigns were selected for this specific issue (Figure 1), one on July 15, 2007, and another on July 24, 2008. They were performed within the same WNW-ESE street canyon in the "Vauban" quarter but at different sites (Figure 1), which were about 300 m off each other. During each measuring campaign, parallel human-biometeorological measurements were conducted at a sunny and a shaded measuring site. As the weather conditions on both summer days were quite similar, the requirements for a comparison of the results, which can be regarded as representative for both shading situations, were met.

The specific objective of the measuring campaign on July 15, 2007, was the human-biometeorological analysis of shading of the direct solar radiation caused by a three-storey building (height: 15 m). The main measuring site was at

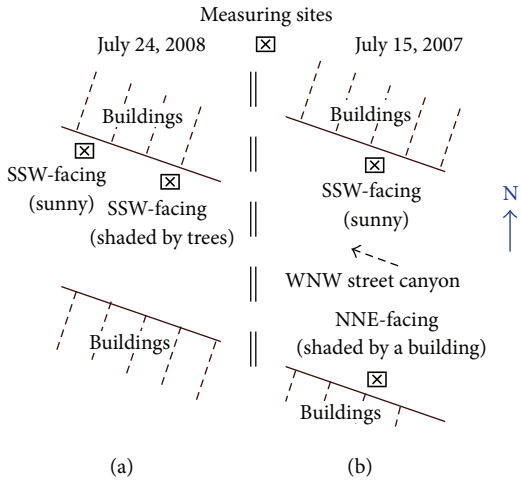

Figure 1: Location of the measuring sites during the human-biometeorological measuring campaigns within the same WNW street canyon in the "Vauban" quarter of Freiburg conducted on typical Central European summer days on July 15, 2007 (b) and July 24, 2008 (a).

Figure 2: Human-biometeorological measuring site at the NNE-facing sidewalk of a WNW street canyon in Freiburg, "Vauban" quarter, July 15, 2007.

the NNE-facing sidewalk about 1 m apart in front of this building (Figure 2). The site of comparison was at the opposite SSW-facing sidewalk in a distance of about 60 m.

The experimental investigation on July 24, 2008, addressed the human-biometeorological consequences of shading of the direct solar radiation by the canopy of five small leaved linden trees (Figure 3). They were planted about 10 m apart from a four-storey SSW-facing building, arranged parallel to the street axis, and spaced about 8 m apart from trunk to trunk of each tree. The main measuring site was at the sidewalk about 2.5 m apart in front of the building and about 7.5 m far from the stem of the centered small leaved linden tree. The individual tree height and crown diameter were about 25 m and 10 m, respectively. In the light of these, this site was almost shaded during the entire summer days. The site for a comparison was located in a distance of about 40 m at the same SSW-facing sidewalk about 2.5 m apart in front of another four-storey building but not influenced by trees.

Table 1: Aspect ratio H/W (H: building height, W: street width) and SVF_{90-270} (sky view factor related to the southern half of the upper hemisphere) at the measuring sites within the WNW street canyon in Freiburg, "Vauban" quarter.

	July 15, 2007		July 24, 2008	
	NNE-facing, shaded	SSW-facing, sunny	SSW-facing, sunny	SSW-facing, shaded
H/W	0.25	0.25	0.39	0.39
SVF_{90-270}	20%	65%	70%	6%

Figure 3: Human-biometeorological measuring sites at the sunny (in the front) and shaded (at the back) SSW-facing sidewalk of a WNW street canyon in Freiburg, "Vauban" quarter, July 24, 2008.

To characterize the measuring sites, Table 1 contains their sky view factors SVF_{90-270} related to the southern half of the upper hemisphere, that is, from east via south to west, and the aspect ratios H/W of the street canyon. According to [2, 13], SVF_{90-270} is more suitable for human-biometeorological investigations on thermal comfort in contrast to SVF for the complete upper hemisphere, because SVF_{90-270} is closely related to the direct solar radiation (Figure 4).

For the measurements, a specific human-biometeorological device was used, which consists of a stationary station (Figure 5) and a mobile station. Both are described in detail in [1, 2]. They measure all meteorological variables in the human-biometeorological reference height of 1.1 m that are necessary to calculate T_{mrt} and PET. For PET, the method was applied, which is described in detail in [1, 2, 13, 33].

To determine T_{mrt}, the approach by Höppe [34] was used. It required the measurement of the short- and long-wave radiant flux densities received by the human-meteorological reference person from the three-dimensional environment. For that purpose, the setup of the station in Figure 5 contains three cantilevers. A pair of two pyranometers and two pyrgeometers was attached to each of the three cantilevers

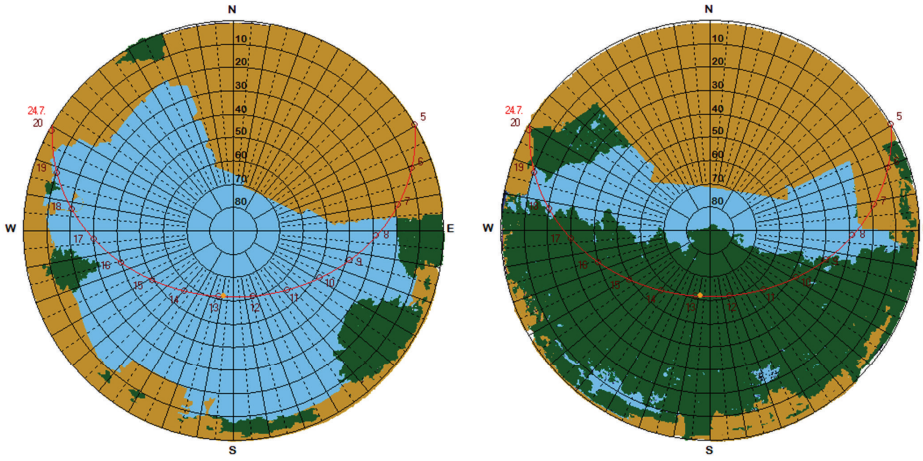

Figure 4: Fish-eye photos from the upper hemisphere at the sunny (a) and shaded (b) site during the human-biometeorological measuring campaign in Freiburg on July 24, 2008 [2, 13].

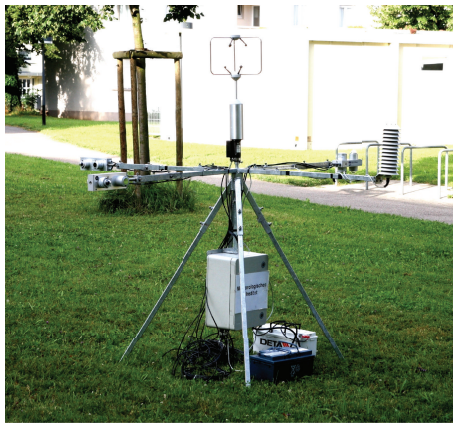

Figure 5: Stationary human-biometeorological station for experimental investigations to determine T_{mrt} and PET within urban structures in Freiburg.

in order to enable the parallel measurement of the two vertical and four horizontal short- and long-wave radiant flux densities. Similar measuring systems have proven to be successful in human-biometeorological investigations, which were conducted in Gothenburg, Sweden, [35], Szeged, Hungary, [36] and Lisbon, Portugal [37]. Based on this method, T_{mrt} (in °C) was calculated according to the Stefan-Boltzmann law by

$$T_{mrt} = \sqrt[4]{\frac{K^*_{abs} + L^*_{abs}}{\varepsilon_p \cdot \sigma}} - 273.15, \quad (1)$$

where K^*_{abs} is the sum of short-wave radiant flux densities from the three-dimensional environment absorbed by the human-biometeorological reference person, L^*_{abs} is the sum of long-wave radiant flux densities from the three-dimensional environment absorbed by the human-biometeorological reference person, ε_p is its long-wave emissivity, and σ is the Stefan-Boltzmann constant.

K^*_{abs} was determined by [34]

$$K^*_{abs} = \alpha_k \cdot \sum_{i=1}^{6} W_i \cdot K_i, \quad (2)$$

where α_k is the absorption coefficient of the reference person for the short-wave radiation, W_i are the weighting factors of the standing reference person for the three-dimensional radiant flux densities K_i (i = downward, upward, E, S, W, N); that is, W is 0.06 for the vertical and 0.22 for the horizontal radiant flux densities.

In the same way L^*_{abs} was calculated by

$$L^*_{abs} = \alpha_l \cdot \sum_{i=1}^{6} W_i \cdot L_i, \quad (3)$$

where α_l is the absorption coefficient of the reference person for the long-wave radiation.

Compared to a globe thermometer, which also enables the determination of T_{mrt} [35, 38], the set-up used in this study has two advantages, which are of importance for the discussion of urban planning methods against heat: (i) the differentiation between the effects of all short- and long-wave radiant flux densities is possible, and (ii) a differentiation of the radiant flux densities according to their spatial directions can be made.

For practical applications of PET like in urban planning, it is advisable to classify the PET values in terms of the ASHRAE thermal sensation scale, which represents a kind of standard. Based on results of suitable questionnaires for citizens and parallel experiments to determine PET, the PET classification scheme achieved for summer conditions in Freiburg [13] is shown in Table 2. This method, which was also applied in another investigations like in Gothenburg, Sweden, [39], Lisbon, Portugal, [37], Szeged, Hungary, [40], Taichung City, Taiwan [41], and Hong Kong [42], considers the acclimatization and adaptation of citizens to the local thermal environment.

Table 2: Ranges of the physiologically equivalent temperature PET for different warm levels of human thermal sensation according to the ASHRAE thermal sensation scale determined for summer conditions in Freiburg [13].

ASRAE thermal sensation scale		PET range (°C)
Name	Scale	
Slightly warm	+1	30–34
Warm	+2	35–40
Hot	+3	>40

Both are not included in the well-known classification scheme of PET by [43], as it has been developed from comparative numeric calculations of PMV and PET for different weather stations in Greece covering the period 1990–1999. Based on a linear regression analysis, the PMV thresholds according to [44] for different human thermal sensations were transferred into corresponding PET thresholds.

This method has two weaknesses. (i) Basically, the original PMV thresholds were only developed for indoor climate; that is, simplified approaches for the human heat budget as basis for PMV were used. They are only valid for slight deviations from the human thermal comfort. Due to the meteorological conditions in Greece, the deviations from the thermal comfort are much stronger at least in summer. Therefore, PMV should not be applied to outdoor conditions like in Greece. (ii) The PET classification scheme by [43] is not generally applicable because it is limited to an internal human heat production of 80 W and a heat transfer resistance of human clothing of 0.9 clo.

3. Results and Discussion

3.1. Shading by a Building. According to [2, 13], the results of the measuring campaign on July 15, 2007, show that the shading effect was only reflected by T_{mrt} and PET but hardly by T_a (Figure 6). It occurred from 10–16 CET and was caused by the building, which was located about 1 m apart in opposite direction to the NNE-facing measuring site. The shading led to a reduction of T_{mrt} by about 18°C and of PET by about 7°C. PET exceeded the thermophysiological threshold value under hot conditions in Freiburg (Table 2) only from 16–18 CET.

With respect to the strong T_{mrt} dependence of daytime PET in Central European cities in summer [2, 13], differentiated analyses of the short- and long-wave radiant flux densities give a deeper insight into their behaviour, which is relevant to T_{mrt}. In contrast to other studies [1], Figure 7 does not contain absolute values of the direction-dependent short-wave radiant flux densities K_i (i = down, up, E, S, W, and N) but normalized values related to the daily 1 h peak value of the short-wave radiant flux density from the upper hemisphere ($K_{down,max}$). Thus, results from different measuring campaigns can be easily compared. The results of $K_i/K_{down,max}$ show that the shading by the building led to relative K_i values below 10%. The geometry of the measuring site caused the strongest drop for K_{down}, K_E, and K_W.

Due to the standing position of the human-biometeorological reference person, which results in different weighting

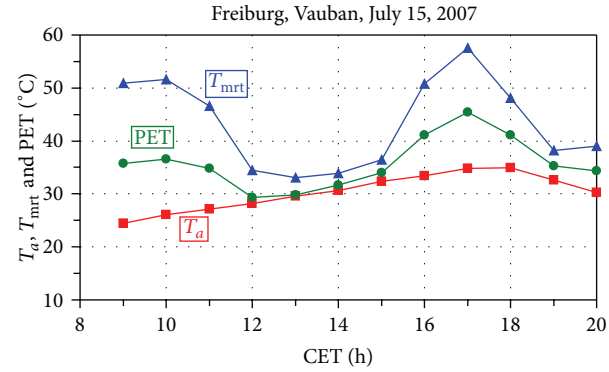

Figure 6: 1 h mean values of air temperature T_a, mean radiant temperature T_{mrt}, and physiologically equivalent temperature PET at the NNE-facing sidewalk of a WNW-ESE street canyon, "Vauban" quarter in Freiburg during typical Central European summer day.

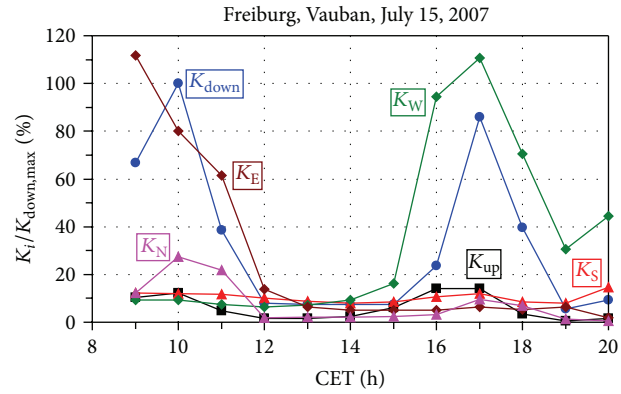

Figure 7: 1 h mean values of the short-wave radiant flux densities K_i (i = down, up, E, S, W, and N) reaching the human-biometeorological reference person from the three-dimensional environment, related to the daily 1 h peak value of K_{down} ($K_{down,max}$ = 659 W/m^2), NNE-facing sidewalk of a WNW-ESE street canyon, "Vauban" quarter in Freiburg during typical Central European summer day.

factors with respect to the radiant flux densities [2, 16, 33, 34], and its absorption coefficient (0.7) for K_i, the amounts of $K_{i,abs}$, that is, short-wave radiant flux densities from the three-dimensional environment absorbed by the human-biometeorological reference person, were lower (Figure 8) compared to K_i, in particular for $K_{down,abs}$ and $K_{up,abs}$ [1]. The shading by the building led to relative $K_{i,abs}$ values, which were about 7% for $K_{down,abs}$, 1% for $K_{up,abs}$, 25% for $K_{E,abs}$, 30% for $K_{S,abs}$, 18% for $K_{W,abs}$, and 7% for $K_{N,abs}$.

The response of the direction-dependent long-wave radiant flux densities L_i on the shading by the building (Figure 9) turned out to be distinctly weaker as compared to K_i. With the exception of L_{down}, that is, the long-wave radiant flux density from the upper hemisphere, the shading caused a drop of about 10% of the relative L_i values, which were related to the 1 h peak value of L_{up}, that is, long-wave radiant flux density from the lower hemisphere. It is noticeable that the L_{down} values were about 15% lower than the other L_i values, whose behaviour and range were quite similar.

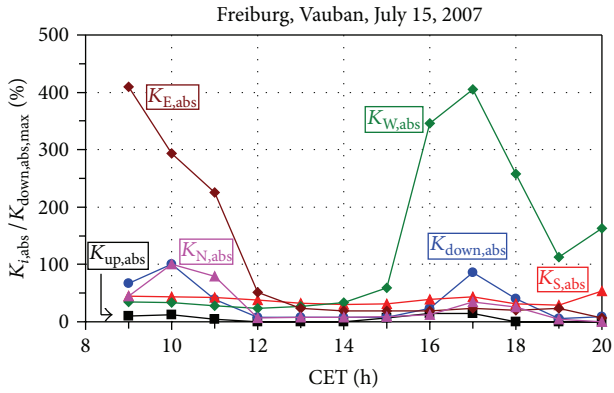

FIGURE 8: 1 h mean values of the short-wave radiant flux densities $K_{i,abs}$ (i = down, up, E, S, W, and N) from the three-dimensional environment absorbed by the human-biometeorological reference person, related to the 1 h peak value of $K_{down,abs}$ ($K_{down,abs,max}$ = 28 W/m^2), NNE-facing sidewalk of a WNW-ESE street canyon, "Vauban" quarter in Freiburg during typical Central European summer day.

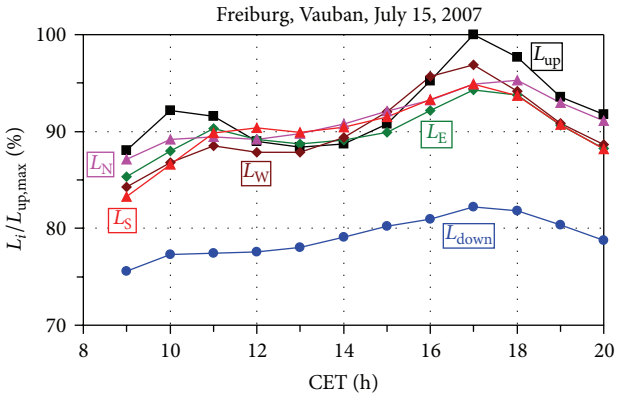

FIGURE 9: 1 h mean values of the long-wave radiant flux densities L_i (i = down, up, E, S, W, and N) reaching the human-biometeorological reference person from the three-dimensional environment, related to the 1 h peak value of L_{up} ($L_{up,max}$ = 533 W/m^2), NNE-facing sidewalk of a WNW-ESE street canyon, "Vauban" quarter in Freiburg during typical Central European summer day.

With respect to the long-wave radiant flux densities $L_{i,abs}$ from the three-dimensional environment absorbed by the human-biometeorological reference person, its absorption coefficient (0.97) for L_i led to a slight lowering of $L_{i,abs}$. In addition, a more pronounced reduction of $L_{i,abs}$ was caused by the weighting factors for radiant flux densities due to the standing position of the reference person (Figure 10). Due to the selected reference (1 h peak value of $L_{up,abs}$), the vertical radiant flux densities $L_{down,abs}$ and $L_{up,abs}$ were at least 200% lower than the horizontal $L_{i,abs}$ values, whereby $L_{up,abs}$ was by 13% higher than $L_{down,abs}$. The values of the four horizontal $L_{i,abs}$ (i = E, S, W, and N) were quite similar in their range and scattered around 330% on average. Interestingly, the reference values $K_{down,abs,max}$ (28 W/m^2) and $L_{up,abs,max}$ (31 W/m^2) were in a similar range.

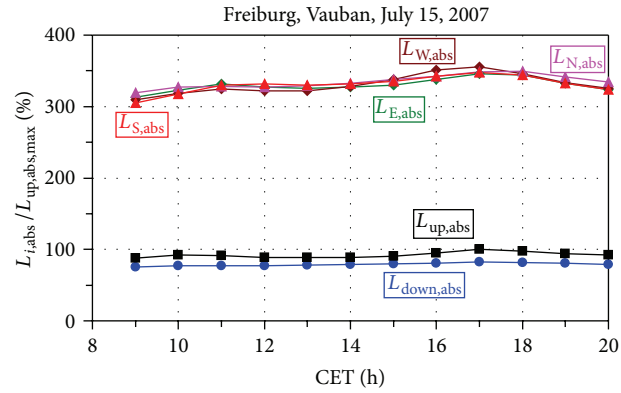

FIGURE 10: 1 h mean values of the long-wave radiant flux densities $L_{i,abs}$ (i = down, up, E, S, W, and N) from the three-dimensional environment absorbed by the human-biometeorological reference person, related to the 1 h peak value of $L_{up,abs}$ ($L_{up,abs,max}$ = 31 W/m^2), NNE-facing sidewalk of a WNW-ESE street canyon, "Vauban" quarter in Freiburg during typical Central European summer day.

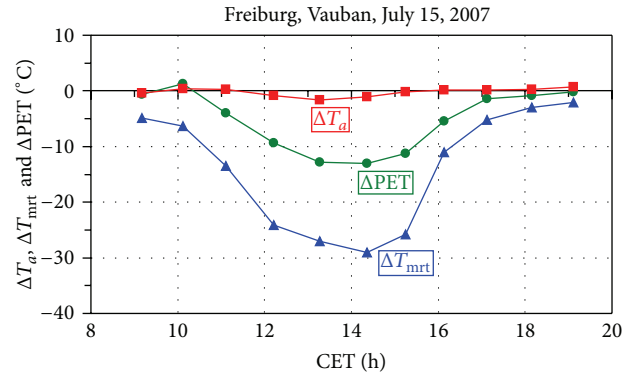

FIGURE 11: 1 h mean values of differences Δ of air temperature T_a, mean radiant temperature T_{mrt}, and physiologically equivalent temperature PET between the shaded NNE- and sunny SSW-facing sidewalk of a WNW-ESE street canyon, "Vauban" quarter in Freiburg during typical Central European summer day.

In order to assess the effectiveness of the shading by a building, the differences Δ of T_a, T_{mrt}, and PET between the shaded NNE- and sunny SSW-facing sidewalk were determined (Figure 11). The peak values of ΔT_a, ΔT_{mrt}, and ΔPET were –1.7°C, –29.0°C, and –13.1°C, respectively; that is, ΔT_{mrt} strongly reacted on the shading as it mainly affected the radiant exchange. The findings of similar investigations [1, 2, 13, 22, 24] that T_{mrt} turns out to be a key variable for PET during typical Central European summer weather can be confirmed by Figure 11. Therefore, the peak value of ΔPET was comparatively high. It corresponded to a mitigation of the human thermal sensation from "hot" to "slightly warm" according to the ASHRAE scale. Due to the physical processes that govern the heat exchange in the near-surface layer, the resulting variable T_a, which represents the sensible heat conditions, only showed a slight effect of the shading. As the human-biometeorological concept to assess the human perception of heat is not only related to the sensible heat,

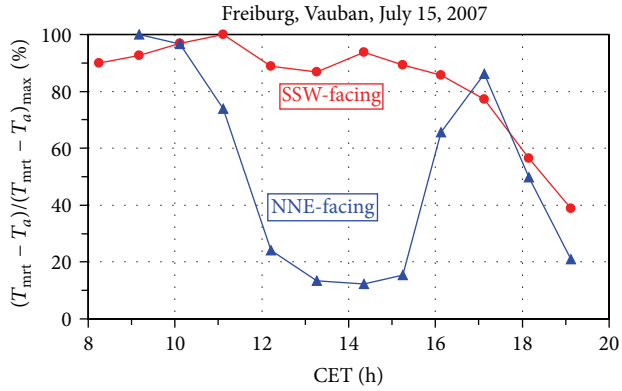

FIGURE 12: 1 h mean values of the difference between mean radiant temperature T_{mrt} and air temperature T_a, related to the 1 h peak value of $(T_{mrt} - T_a)$ at the shaded NNE-facing sidewalk ($(T_{mrt} - T_a)_{max}$ = 26.4°C) and sunny SSW-facing sidewalk ($(T_{mrt} - T_a)_{max}$ = 33.3°C) of a WNW-ESE street canyon, "Vauban" quarter in Freiburg during typical Central European summer day.

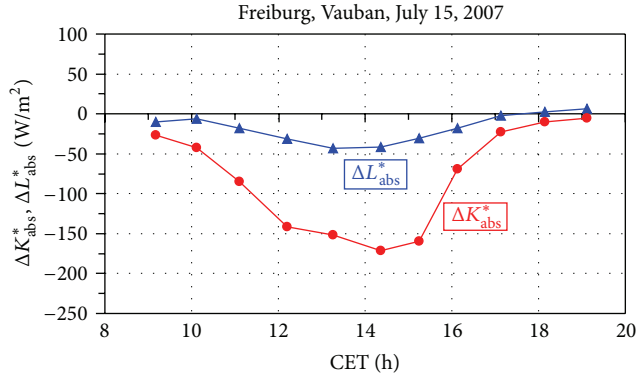

FIGURE 13: 1 h mean values of differences Δ of the sums of short-wave radiant flux densities (K^*_{abs}) and long-wave radiant flux densities (L^*_{abs}) from the three-dimensional environment absorbed by the human-biometeorological reference person between the shaded NNE- and sunny SSW-facing sidewalk of a WNW-ESE street canyon, "Vauban" quarter in Freiburg during typical Central European summer day.

T_a or the urban heat island intensity UHI is inappropriate to characterize the human thermal sensation [13–15].

At the sunny SSW-facing sidewalk, the peak difference between T_{mrt} and T_a was relatively high (33.3°C at 11 CET), while shading by the building reduced $(T_{mrt} - T_a)$ up to 3.2°C (14 CET) at the NNE-facing sidewalk. For the normalized $(T_{mrt} - T_a)$, it corresponds about 12% (Figure 12), whereas the normalized $(T_{mrt} - T_a)$ was higher than 80% at the sunny sidewalk during 10–16 CET, which can be regarded as the period with the strongest heat for citizens.

The difference Δ of the sums of the short-wave radiant flux densities (K^*_{abs}) from the three-dimensional environment absorbed by the human-biometeorological reference person between the shaded NNE- and sunny SSW-facing sidewalk was higher (Figure 13) than those of the sums of the long-wave radiant flux densities (L^*_{abs}). For ΔK^*_{abs}, the difference was the strongest (−171 W/m^2) around 14 CET, while the peak value of ΔL^*_{abs} amounted to −43 W/m^2 around 13 CET. From this it follows that shading by a building causes a stronger impact on K^*_{abs} than on L^*_{abs}. Therefore, the differences of T_{mrt} between the sunny and the shaded sidewalk of the street canyon were mainly caused by ΔK^*_{abs}.

The magnitude of T_{mrt} is governed by the values of K^*_{abs} and L^*_{abs}. Referred to $(K^*_{abs} + L^*_{abs})$, the relative K^*_{abs} for the sunny SSW-facing sidewalk did not exceed 30% (Figure 14), while it reached 6% at the shaded NNE-facing sidewalk. This implies that the relative L^*_{abs} comprised about 70% for the case of the sunny (see also [1]) and about 94% in the shaded situation. Consequently, shading not only reduces the three-dimensional radiant flux densities and, therefore, T_{mrt} but also leads to a higher portion of relative L^*_{abs} for T_{mrt} than in the sunny situation.

3.2. Shading by Tree Canopies. The shading effect by tree canopies, which was investigated in the measuring campaign conducted on July 24, 2008, in the same street canyon, started about 10 CET and lasted the entire day (Figures 4 and 15).

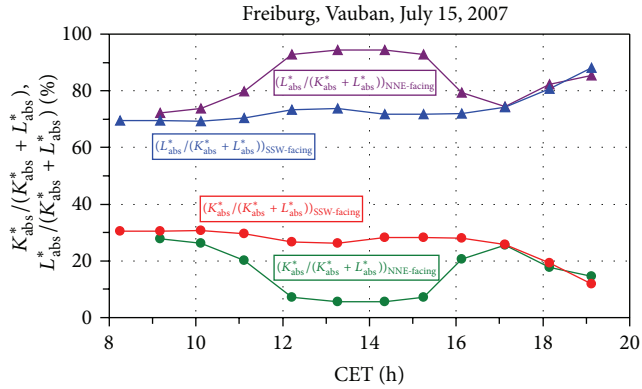

FIGURE 14: 1 h mean values of the sums of short-wave radiant flux densities (K^*_{abs}) and long-wave radiant flux densities (L^*_{abs}) from the three-dimensional environment absorbed by the human-biometeorological reference person, related to 1 h mean values of $(K^*_{abs} + L^*_{abs})$, at the shaded NNE- and sunny SSW-facing sidewalk of a WNW-ESE street canyon, "Vauban" quarter in Freiburg during typical Central European summer day.

As reflected by the results of both shading cases (Figures 6 and 15), T_a and PET were in a similar range, while T_{mrt} was about 5°C higher than T_a. According to the PET classification for Freiburg (Table 2), the PET values did not indicate any kind of thermal load.

The relative short-wave radiant flux densities hardly differentiated between both shading cases (Figures 7 and 16) with the exception that the shading by tree canopies extended over a longer time period; that is, K_W was also comparatively low in the afternoon. Due to the transmission of the short-wave radiation through the canopy [45], the relative K_{down} values for the case of the tree shading were about 4% higher than those for the shading through the building.

As for shading by a building, the relative $K_{i,abs}$ values at the measuring site shaded by tree canopies (Figure 17) also

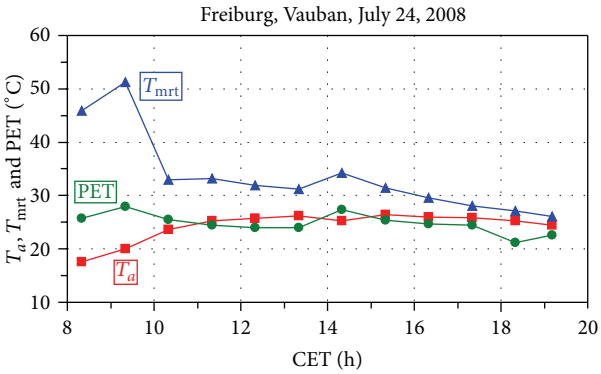

FIGURE 15: 1 h mean values of air temperature T_a, mean radiant temperature T_{mrt}, and physiologically equivalent temperature PET, SSW-facing sidewalk (shaded by tree canopies) of a WNW-ESE street canyon, "Vauban" quarter in Freiburg during typical Central European summer day.

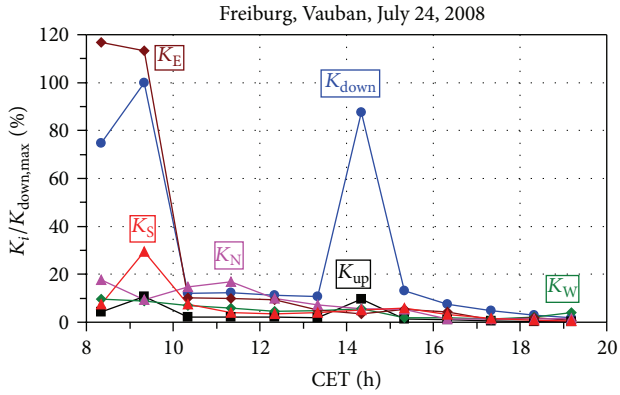

FIGURE 16: 1 h mean values of the short-wave radiant flux densities K_i (i = down, up, E, S, W, and N) reaching the human-biometeorological reference person from the three-dimensional environment, related to the 1 h peak value of K_{down} ($K_{down,max}$ = 600 W/m^2), SSW-facing sidewalk (shaded by tree canopies) of a WNW-ESE street canyon, "Vauban" quarter in Freiburg during typical Central European summer day.

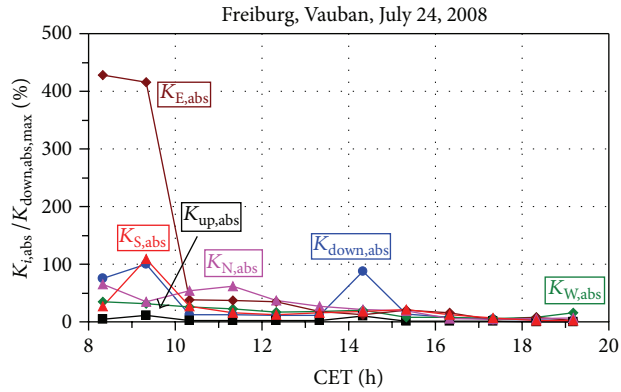

FIGURE 17: 1 h mean values of the short-wave radiant flux densities $K_{i,abs}$ (i = down, up, E, S, W, and N) from the three-dimensional environment absorbed by the human-biometeorological reference person, related to the 1 h peak value of $K_{down,abs}$ ($K_{down,abs,max}$ = 25 W/m^2), SSW-facing sidewalk (shaded by tree canopies) of a WNW-ESE street canyon, "Vauban" quarter in Freiburg during typical Central European summer day.

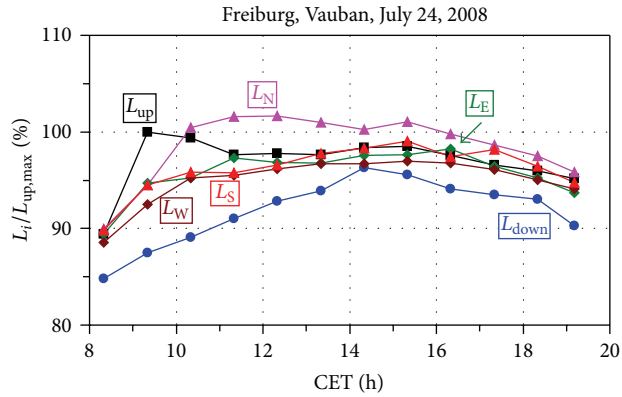

FIGURE 18: 1 h mean values of the long-wave radiant flux densities L_i (i = down, up, E, S, W, and N) reaching the human-biometeorological reference person from the three-dimensional environment, related to the 1 h peak value of L_{up} ($L_{up,max}$ = 474 W/m^2), SSW-facing sidewalk (shaded by tree canopies) of a WNW-ESE street canyon, "Vauban" quarter in Freiburg during typical Central European summer day.

reflected the short-wave radiation exchange, which is relevant to the calculation of T_{mrt} and was predetermined by the relative K_i values (Figure 16). The longer duration of the shading effect at the measuring site under the tree canopies was responsible for the comparatively low $K_{i,abs}$ values in the afternoon. With the exception of the relative $K_{down,abs}$ at about 14 CET, the relative $K_{i,abs}$ values in the afternoon were below 20% and showed a lower direction-dependent variability compared to the shading in the late morning. Around noon, the shading by tree canopies led to relative $K_{i,abs}$ values up to 11% for $K_{down,abs}$, 2% for $K_{up,abs}$, 18% for $K_{E,abs}$, 13% for $K_{S,abs}$, 17% for $K_{W,abs}$, and 27% for $K_{N,abs}$.

In contrast to Figure 9, where $L_{down}/L_{up,max}$ was continuously lower by at least 10% than the other relative L_i values, the temporal course of $L_{down}/L_{up,max}$ (Figure 18) was more pronounced and almost touched the other relative L_i values around 14 CET. As the shading by a building referred to about 4 hours around noon, the 1 h peak value of L_{up} occurred in the late afternoon (Figure 9), which caused some kind of a diurnal variation of the relative L_i values. As the shading by tree canopies extended over the entire afternoon, the 1 h peak value of L_{up} was already observed in the early morning (Figure 18). Due to the following shading at the measuring site, the temporal courses of the relative L_i values, with the exception of L_{down}, scattered around a near-constant level until the late afternoon. The specific location of the measuring site, that is, about 2.5 m apart in front of a SSW-facing building, was mainly responsible for the relative values of L_N, which were slightly above 100%.

Also for the shading by tree canopies, the relative $L_{up,abs}$ values were higher than the relative $L_{down,abs}$ values during

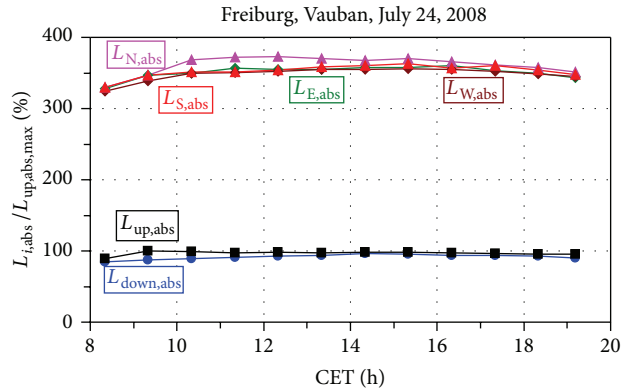

FIGURE 19: 1 h mean values of the long-wave radiant flux densities $L_{i,abs}$ (i = down, up, E, S, W, and N) from the three-dimensional environment absorbed by the human-biometeorological reference person, related to the 1 h peak value of $L_{up,abs}$ ($L_{up,abs,max}$ = 28 W/m^2), SSW-facing sidewalk (shaded by tree canopies) of a WNW-ESE street canyon, "Vauban" quarter in Freiburg during typical Central European summer day.

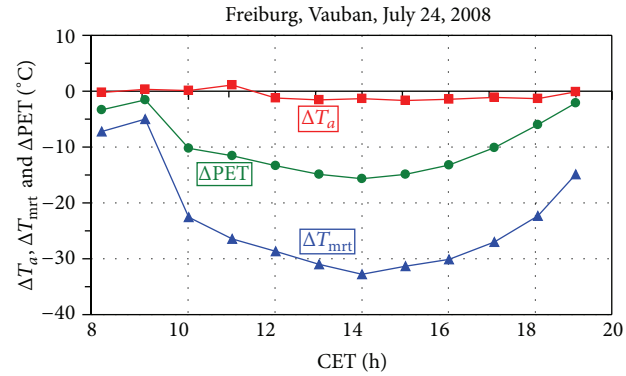

FIGURE 20: 1 h mean values of differences Δ of air temperature T_a, mean radiant temperature T_{mrt}, and physiologically equivalent temperature PET between a shaded (by tree canopies) and sunny SSW-facing sidewalk of a WNW-ESE street canyon, "Vauban" quarter in Freiburg during typical Central European summer day.

the complete measuring period (Figure 19) but by only 5% on average, while it was 13% for the shading by a building. The relative $L_{i,abs}$ values of the four horizontal directions i were at a higher mean level (350%) for the shading by tree canopies compared to the mean value of 330% for the shading by a building. As for this shading method, the reference values $K_{down,abs,max}$ (25 W/m^2) and $L_{up,abs,max}$ (28 W/m^2) for the shading by tree canopies were also in a similar range. For both shading options, $L_{up,abs,max}$ was by about 3 W/m^2 higher than $K_{down,abs,max}$, whereby both reference values were slightly higher for the shading by a building.

As both sites of this measuring campaign were located at the same SSW-facing sidewalk (Figure 1), the shading effect of the tree canopies can be determined by a comparison of the results for the shaded and the adjacent sunny site. The peak values of the differences Δ for the same variables like in Figure 11 between both sites are ΔT_a = −1.7°C, ΔT_{mrt} = −32.8°C, and ΔPET = −15.7°C (Figure 20). Compared to the Δ values for the shading by a building, the shading by tree canopies caused slightly higher peak values of ΔT_{mrt} and consequently also for ΔPET, while the peak value for ΔT_a was equal for both shading conditions. With respect to the physical processes, which are related to the shading by tree canopies, it is understandable that Δ was the strongest at the early afternoon for each of the three selected human-biometeorological variables.

Related to the mean values of T_a, T_{mrt}, and PET over 12–15 CET, that is, the period where the shading was effective during both measuring campaigns, the maximal relative reduction Δ (Table 3) was equal for T_a (6%). However, it was slightly higher for T_{mrt} (51%) and PET (41%) in the case of shading by tree canopies compared to ΔT_{mrt} (47%) and ΔPET (31%) for shading by a building.

In contrast to the measuring campaign on July 15, 2007, the peak difference between T_{mrt} and T_a (39.9°C) for the measuring campaign on July 24, 2008, which occurred in the afternoon, was distinctly higher at the sunny SSW-facing sidewalk. For the shaded SSW-facing sidewalk, the peak difference (31.2°C) was observed in the morning before the shading effect started. The longer lasting shading in the measuring campaign of July 24, 2008 was responsible for the continuous decrease of the normalized (T_{mrt}−T_a) values from 30% around 10 CET to 5% in the late afternoon (Figure 21). At the sunny SSW-facing sidewalk, the values of the normalized (T_{mrt} − T_a) started to decrease from the middle of the afternoon. This result is quite similar to those obtained for the comparable SSW-facing sidewalk in the measuring campaign a year earlier.

TABLE 3: Maximal relative reduction Δ of T_a, T_{mrt}, and PET by two shading methods related to the mean values of T_a, T_{mrt}, and PET over 12–15 CET, based on results of both human-biometeorological measuring campaigns in Freiburg during typical Central European summer weather.

Shading methods	ΔT_a	ΔT_{mrt}	ΔPET
Shading by a building (July 15, 2007)	6%	47%	31%
Shading by tree canopies (July 24, 2008)	6%	51%	41%

As for the measuring campaign in 2007, the differences Δ of the sums of the short-wave radiant flux densities (K^*_{abs}) between the shaded and sunny SSW-facing measuring sites were higher (Figure 22) than for the sums of the long-wave radiant flux densities (L^*_{abs}). For ΔK^*_{abs}, this difference was the strongest with −193 W/m^2 around 14 CET, while the peak value for ΔL^*_{abs} amounted to −43 W/m^2 and occurred one hour later. Despite differences of type and structure of the three-dimensional environment at the measuring sites, the peak ΔL^*_{abs} values do not differ between both measuring campaigns. Two essential reasons for this result, which is somewhat surprising at the first view, are the similar weather conditions and the unchanged orientation of the street canyon.

In contrast to the measuring campaign of 2007, the relative K^*_{abs} values obtained for the sunny sidewalk in the measuring campaign of 2008 slightly exceeded 30% (Figure 23). The peak value of 34% in the afternoon was

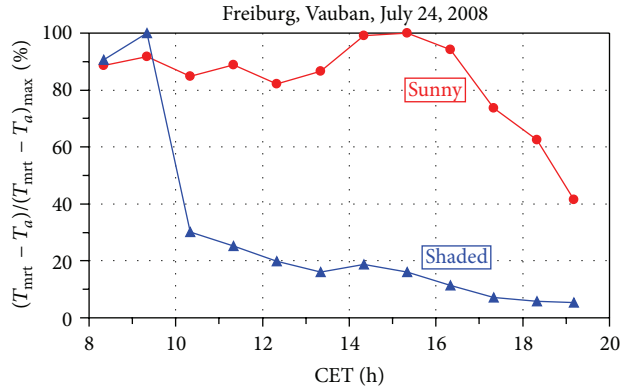

FIGURE 21: 1 h mean values of the difference between mean radiant temperature T_{mrt} and air temperature T_a, related to the 1 h peak value of $(T_{mrt} - T_a)$ at the shaded ($(T_{mrt} - T_a)_{max}$ = 31.2°C) and sunny ($(T_{mrt} - T_a)_{max}$ = 39.9°C) SSW-facing sidewalk of a WNW-ESE street canyon, "Vauban" quarter in Freiburg during typical Central European summer day.

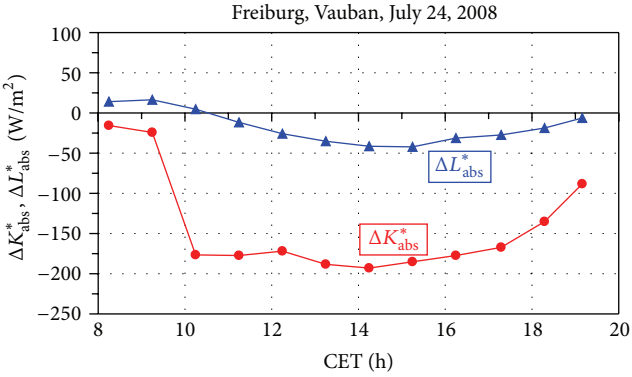

FIGURE 22: 1 h mean values of differences Δ of the sums of short-wave radiant flux densities (K^*_{abs}) and long-wave radiant flux densities (L^*_{abs}) from the three-dimensional environment absorbed by the human-biometeorological reference person between the shaded (by tree canopies) and sunny SSW-facing sidewalk of a WNW-ESE street canyon, "Vauban" quarter in Freiburg during typical Central European summer day.

equivalent to a minimum value for the relative L^*_{abs} of 66%. The shading by tree canopies caused a continuous decrease of the relative K^*_{abs} from 8% at the beginning of the shading up to 1% in the late afternoon. Accordingly, the relative L^*_{abs} increased from 92% to 99%. During the complete afternoon, the relative L^*_{abs} values for the shaded situation in 2008 were above 94%, which was the level under the shading condition by a building in 2007.

3.3. Discussion. Among several human-biometeorological experiments conducted during comparable weather conditions, that is, on typical Central European summer days, in different quarters of Freiburg from 2007–2010, two 1-day campaigns were selected to achieve generalizable results for the objectives of this study. Up to now, they were already known qualitatively, but these experiments enabled their

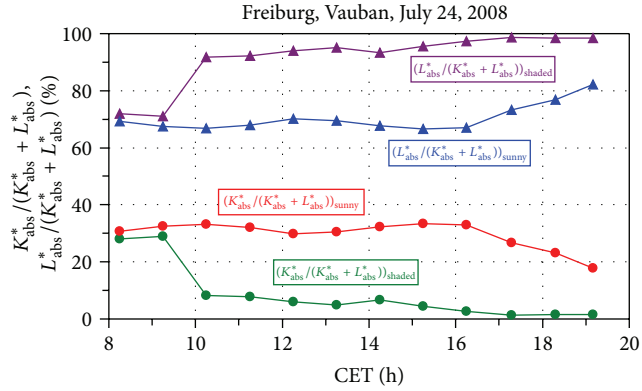

FIGURE 23: 1 h mean values of the sums of short-wave radiant flux densities (K^*_{abs}) and long-wave radiant flux densities (L^*_{abs}) from the three-dimensional environment absorbed by the human-biometeorological reference person, related to 1 h mean values of (K^*_{abs} + L^*_{abs}), at the shaded (by tree canopies) and sunny SSW-facing sidewalk of a WNW-ESE street canyon, "Vauban" quarter in Freiburg during typical Central European summer day.

TABLE 4: Coefficient of determination R^2 of linear regression functions f between 1 h mean values of different human-biometeorological variables, basis: experimental investigations on typical Central European summer days in various urban quarters of Freiburg from 2007–2010 (n: number of values).

function f	R^2	
	10–16 CET n = 200	22–5 CET n = 40
PET = f (T_{mrt})	0.892	0.616
PET = f (T_a)	0.589	0.892
PET = f (VP)	0.023	0.006
PET = f (v)	0.029	0.013
T_{mrt} = f (T_a)	0.308	0.825

quantification in a reliable way. By discussing the short- and long-wave radiant flux densities from the three-dimensional surroundings in detail, a deeper insight was provided into the radiation exchange. This is necessary for the physical understanding of the behaviour of T_{mrt} under different local environments.

Based on all human-biometeorological experiments in Freiburg concerning human heat stress during typical Central European summer weather, the results of a statistical analysis show that in the daytime PET was strongly governed by T_{mrt} (Table 4). This relationship was already indicated by the results of both case studies, which mainly addressed the variability of T_{mrt} for two shading methods.

During the daytime hours from 10–16 CET, that is, the period when citizens are badly affected by outdoor heat stress, the coefficient of determination R^2 of the linear regression between 1 h mean values of PET (°C) and T_{mrt} (°C)

$$\text{PET} = 0.581 \cdot T_{mrt} + 8.2 \quad (4)$$

was 0.892; that is, it was clearly higher than for the linear regression between PET and T_a (0.589).

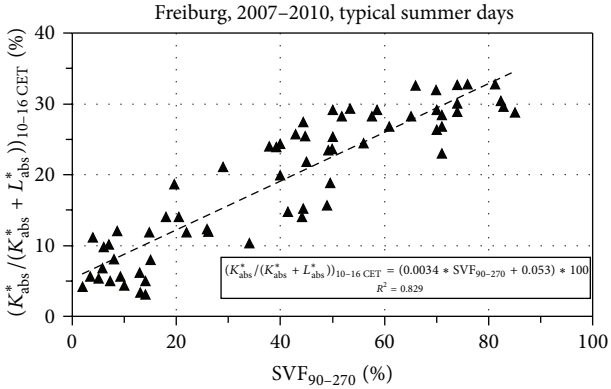

FIGURE 24: Relationship between mean values (10–16 CET) of $(K^*_{abs}/(K^*_{abs} + L^*_{abs}))$ and SVF_{90-270}, based on human-biometeorological measuring campaigns at different sites in Freiburg on typical summer days 2007–2010.

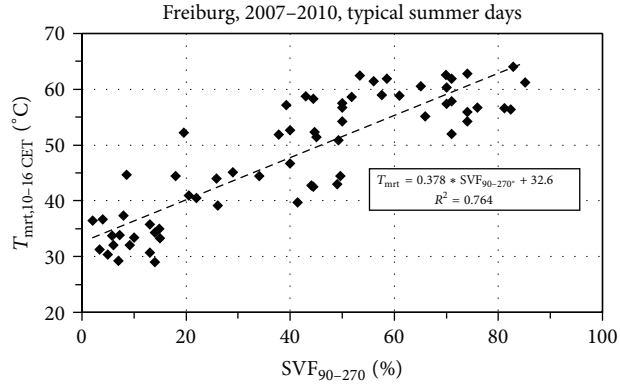

FIGURE 25: Relationship between mean values (10–16 CET) of T_{mrt} and SVF_{90-270}, based on human-biometeorological measuring campaigns at different sites in Freiburg on typical summer days 2007–2010 [2].

The distinctly lower significance of T_a and consequently of the urban heat island intensity for PET in the daytime was caused by the human-biometeorological assessment method for thermal comfort. It can be interpreted as a nesting of a smaller volume, that is, the volume of the standing human-biometeorological reference person, into the larger volume of an urban street canyon [13]. The thermal conditions within the latter volume can be described by T_a. As the human heat budget represents the thermophysiological basis for the perception of outdoor heat by citizens, additional processes besides those, which are responsible for T_a, have to be taken into account for the smaller volume. They are included in human-biometeorological variables like T_{mrt} or PET.

The relatively low R^2 values of the regressions between PET and vapour pressure VP as well as PET and wind speed v point out that the prevailing VP and v conditions during typical Central European summer weather just play a minor part for the human perception of heat in inland cities expressed by PET.

At night, the radiation exchange only consists of long-wave radiant flux densities. Therefore, R^2 of the linear regression between T_{mrt} and T_a was distinctly higher in the period 22–5 CET (0.825) than that for the daytime period 10–16 CET (0.308). As a result, R^2 was the highest in the night for the linear regression between PET and T_a (0.892).

This investigation in terms of two 1-day human-biometeorological experiments has shown that human thermal stress in the daytime indicated by PET can be reduced in the local urban scale, if the direct solar radiation is decreased by shading, which itself influences another short- and some long-wave radiant flux densities. As previously mentioned, SVF_{90-270} represents a suitable measure to characterize the spatial extent of shading in terms of urban human-biometeorology. A decreasing SVF_{90-270} indicates an increase of the spatial extent of shading in the southern half of the upper hemisphere.

Based on data of all measurement campaigns mentioned in Table 4, the mean relative K^*_{abs} determined for the period 10–16 CET linearly decreased with a lowering of SVF_{90-270} (Figure 24). This means that the mean relative L^*_{abs} over the same period increased with a lowering of SVF_{90-270}. As T_{mrt} depends on the sum of K^*_{abs} and L^*_{abs} (1), the contribution of relative L^*_{abs} for T_{mrt} was linearly increasing with decreasing SVF_{90-270}. However, it should be borne in mind that shading decreased the absolute values of both K^*_{abs} and L^*_{abs}, whereby this decrease was stronger for K^*_{abs} than for L^*_{abs}. Shading in terms of lower SVF_{90-270} also led to a lower absolute sum $(K^*_{abs} + L^*_{abs})$. Due to the dependence of T_{mrt} on this sum, a decreasing SVF_{90-270} also caused a lower T_{mrt} [2], whereby the relationship can be approximated by linear regression (Figure 25).

In the human-biometeorological concept to assess the thermal environment, the standing position of the reference person leads to a higher significance of the horizontal radiant flux densities. However, shading of the direction-dependent solar radiation also has consequences for the other radiant flux densities. Different shading methods mainly influence the short- and long-wave radiant flux densities directly in the spatial range of the shading device. Its extent varies dependent on the solar altitude, that is, time of day and year.

Due to the substantial significance of the horizontal radiant flux densities for the determination of T_{mrt} and consequently PET during summer weather, a simulation for an E-W street canyon (H/W = 1) with similar buildings at both sides was performed using the ENVI-met model. Related to the meteorological conditions of a day during the Central European heat wave of 2003, the results show that an extreme change of the albedo of the vertical walls of both buildings from 0.1 to 0.9 leads to modifications of short- and long-wave radiant flux densities, which result in an increase of T_{mrt} up to 30°C. This is mainly caused by the higher short-wave radiant flux densities reflected from the vertical walls. This result, which seems to be surprising at first view, does not agree with other investigations on the influence of changed albedo performed with the Green CTTC model [31], as they show a decrease of T_{mrt} with an increase of the albedo of vertical walls.

4. Conclusions

Among several human-biometeorological measuring campaigns conducted from 2007–2010 within different urban quarters in Freiburg during typical Central European summer weather, two measuring campaigns were selected in order to analyze the response of the human-biometeorological variables T_a, T_{mrt}, and PET on the shading of the direct solar radiation by (i) a building and (ii) tree canopies. As T_{mrt} and consequently PET reflect the shading effects much stronger than T_a, the behaviour of the short- and long-wave radiant flux densities from the three-dimensional environment, which are the basis to calculate T_{mrt}, was investigated in detail. Related to all human-biometeorological measuring campaigns in Freiburg, the achieved results for the two case studies have a general validity, because their weather conditions were always quite similar.

Results from regional climate simulations project for Central Europe that extreme summer heat like in 2003 will be the normality as from 2050 [3, 4]. By providing physical data, which can be used for the explanation of shading impacts and the preliminary fixing of specific shading devices, for example, with respect to its type or duration, this investigation contributes to the discussion on the effectiveness of shading impacts on maintaining human thermal comfort even under extreme summer heat.

Another advantage of this applied investigation design is the availability of reliable data on the short- and long-wave radiant flux densities from the three-dimensional environment, which can be used for the validation of results of simulation models for the three-dimensional radiation field within urban structures [24, 28]. This validation can lead to an update of the physical basis of the models, which is recommended to improve the accuracy of their results [35, 38].

The synopsis of all human-biometeorological experiments conducted during Central European summer weather in different urban structures of Freiburg from 2007–2010 points out that shading in terms of SVF_{90-270} causes not only lower relative K^*_{abs} and, therefore, higher relative L^*_{abs} values but also lower absolute values of the sum ($K^*_{abs} + L^*_{abs}$). They are responsible for the decrease of T_{mrt} with lower SVF_{90-270}. The analysis of all experimental results in terms of mean values for the period from 10 to 16 CET shows that a reduction of SVF_{90-270} by 10% through shading by tree canopies leads to a lowering of T_a by 0.2°C, T_{mrt} by 3.8°C, and PET by 1.4°C. These communal benefits are qualitatively visualized by Figure 26.

Figure 26: Human thermal comfort below the canopy of a vital linden tree on a typical Central European summer day (June 27, 2011) in Freiburg.

Acknowledgments

For the grants given to this research, the authors are indebted to the German Federal Ministry of Education and Research (BMBF), Project KLIMES ALUF (FZK: 01LS05020) within the scope of the research initiative "klimazwei," and the German-Israeli Foundation for Scientific Research and Development (GIF) under Grant no. 955-36.8/2007. The authors also give thanks to students and colleagues of the Meteorological Institute, Albert-Ludwigs-University of Freiburg, who supported the human-biometeorological measurements. The ENVI-met simulation reported in this study was conducted by Matthias Mühleis.

References

[1] H. Mayer, J. Holst, P. Dostal, F. Imbery, and D. Schindler, "Human thermal comfort in summer within an urban street canyon in central Europe," *Meteorologische Zeitschrift*, vol. 17, no. 3, pp. 241–250, 2008.

[2] J. Holst and H. Mayer, "Impacts of street design parameters on human-biometeorological variables," *Meteorologische Zeitschrift*, vol. 20, no. 5, pp. 541–552, 2011.

[3] J. Ballester, X. Rodó, and F. Giorgi, "Future changes in central Europe heat waves expected to mostly follow summer mean warming," *Climate Dynamics*, vol. 35, no. 7, pp. 1191–1205, 2010.

[4] J. Ballester, F. Giorgi, and X. Rodó, "Changes in European temperature extremes can be predicted from changes in PDF central statistics," *Climatic Change*, vol. 98, no. 1-2, pp. 277–284, 2010.

[5] R. S. Kovats and S. Hajat, "Heat stress and public health: a critical review," *Annual Review of Public Health*, vol. 29, pp. 41–55, 2008.

[6] S. N. Gosling, J. A. Lowe, G. R. McGregor, M. Pelling, and B. D. Malamud, "Associations between elevated atmospheric temperature and human mortality: a critical review of the literature," *Climatic Change*, vol. 92, no. 3-4, pp. 299–341, 2009.

[7] Federal Statistical Office of Germany, "Demographic change in Germany—issue 2011," Tech. Rep. 1, 2011.

[8] C. S. B. Grimmond, M. Roth, T. R. Oke et al., "Climate and more sustainable cities: climate information for improved planning and management of cities (producers/capabilities perspective)," *Procedia Environmental Sciences*, vol. 1, pp. 247–274, 2010.

[9] E. Ng, "Towards planning and practical understanding of the need for meteorological and climatic information in the design of high-density cities: a case-based study of Hong Kong," *International Journal of Climatology*, vol. 32, no. 4, pp. 582–598, 2012.

[10] W. Kuttler, "Climate change in urban areas—part 2: measures," *Environmental Sciences Europe*, vol. 23, pp. 1–15, 2011.

[11] W. Kuttler, S. Weber, J. Schonnefeld, and A. Hesselschwerdt, "Urban/rural atmospheric water vapour pressure differences

and urban moisture excess in Krefeld, Germany," *International Journal of Climatology*, vol. 27, no. 14, pp. 2005–2015, 2007.

[12] E. Ng, "Policies and technical guidelines for urban planning of high-density cities—air ventilation assessment (AVA) of Hong Kong," *Building and Environment*, vol. 44, no. 7, pp. 1478–1488, 2009.

[13] J. Holst and H. Mayer, "Urban human-biometeorology: investigations in freiburg (Germany) on human thermal comfort," *Urban Climate News*, no. 38, pp. 5–10, 2010.

[14] F. Ali-Toudert and H. Mayer, "Numerical study on the effects of aspect ratio and orientation of an urban street canyon on outdoor thermal comfort in hot and dry climate," *Building and Environment*, vol. 41, no. 2, pp. 94–108, 2006.

[15] F. Ali-Toudert and H. Mayer, "Effects of asymmetry, galleries, overhanging façades and vegetation on thermal comfort in urban street canyons," *Solar Energy*, vol. 81, no. 6, pp. 742–754, 2007.

[16] H. Mayer and P. Höppe, "Thermal comfort of man in different urban environments," *Theoretical and Applied Climatology*, vol. 38, no. 1, pp. 43–49, 1987.

[17] N. Kántor and J. Unger, "Benefits and opportunities of adopting GIS in thermal comfort studies in resting places: an urban park as an example," *Landscape and Urban Planning*, vol. 98, no. 1, pp. 36–46, 2010.

[18] L. Chen and E. Ng, "Outdoor thermal comfort and outdoor activities: a review of research in the past decade," *Cities*, vol. 29, no. 2, pp. 118–125, 2012.

[19] T.-P. Lin, K.-T. Tsai, R.-L. Hwang, and A. Matzarakis, "Quantification of the effects of thermal indices and sky view factor on park attendance," *Landscape and Urban Planning*, vol. 107, no. 2, pp. 137–146, 2012.

[20] A. M. Abdel-Ghany, I. M. Al-Helal, and M. R. Shady, "Human thermal comfort and heat stress in an outdoor urban arid environment: a case study," *Advances in Meteorology*, vol. 2013, Article ID 693541, 7 pages, 2013.

[21] P. Cohen, O. Potchter, and A. Matzarakis, "Human thermal perception of Coastal Mediterranean outdoor urban environments," *Applied Geography*, vol. 37, no. 1, pp. 1–10, 2013.

[22] D. Fröhlich and A. Matzarakis, "Modelling of changes in thermal bioclimate: examples based on urban spaces in Freiburg, Germany," *Theoretical and Applied Climatology*, vol. 111, no. 3-4, pp. 547–558, 2013.

[23] G. Jendritzky, R. de Dear, and G. Havenith, "UTCI-Why another thermal index?" *International Journal of Biometeorology*, vol. 56, no. 3, pp. 421–428, 2012.

[24] A. Matzarakis, F. Rutz, and H. Mayer, "Modelling radiation fluxes in simple and complex environments: basics of the RayMan model," *International Journal of Biometeorology*, vol. 54, no. 2, pp. 131–139, 2010.

[25] L. Shashua-Bar, D. Pearlmutter, and E. Erell, "The influence of trees and grass on outdoor thermal comfort in a hot-arid environment," *International Journal of Climatology*, vol. 31, no. 10, pp. 1498–1506, 2011.

[26] D. E. Bowler, L. Buyung-Ali, T. M. Knight, and A. S. Pullin, "Urban greening to cool towns and cities: a systematic review of the empirical evidence," *Landscape and Urban Planning*, vol. 97, no. 3, pp. 147–155, 2010.

[27] T.-P. Lin, A. Matzarakis, and R.-L. Hwang, "Shading effect on long-term outdoor thermal comfort," *Building and Environment*, vol. 45, no. 1, pp. 213–221, 2010.

[28] F. Lindberg and C. S. B. Grimmond, "The influence of vegetation and building morphology on shadow patterns and mean radiant temperatures in urban areas: model development and evaluation," *Theoretical and Applied Climatology*, vol. 105, no. 3-4, pp. 311–323, 2011.

[29] S. Oliveira, H. Andrade, and T. Vaz, "The cooling effect of green spaces as a contribution to the mitigation of urban heat: a case study in Lisbon," *Building and Environment*, vol. 46, no. 11, pp. 2186–2194, 2011.

[30] G. Gross, "Effects of different vegetation on temperature in an urban building environment. micro-scale numerical experiments," *Meteorologische Zeitschrift*, vol. 21, no. 4, pp. 399–412, 2012.

[31] L. Shashua-Bar, I. X. Tsiros, and M. Hoffman, "Passive cooling design options to ameliorate thermal comfort in urban streets of a mediterranean climate (athens) under hot summer conditions," *Building and Environment*, vol. 57, pp. 110–119, 2012.

[32] S. Leuzinger, R. Vogt, and C. Körner, "Tree surface temperature in an urban environment," *Agricultural and Forest Meteorology*, vol. 150, no. 1, pp. 56–62, 2010.

[33] P. Höppe, "The physiological equivalent temperature—a universal index for the biometeorological assessment of the thermal environment," *International Journal of Biometeorology*, vol. 43, no. 2, pp. 71–75, 1999.

[34] P. Höppe, "A new method to determine the mean radiant temperature outdoors," *Wetter und Leben*, vol. 44, no. 1–3, pp. 147–151, 1992.

[35] S. Thorsson, F. Lindberg, I. Eliasson, and B. Holmer, "Different methods for estimating the mean radiant temperature in an outdoor urban setting," *International Journal of Climatology*, vol. 27, no. 14, pp. 1983–1993, 2007.

[36] N. Kántor, L. Égerházi, and J. Unger, "Subjective estimation of thermal environment in recreational urban spaces—part 1: investigations in Szeged, Hungary," *International Journal of Biometeorology*, vol. 56, no. 6, pp. 1075–1088, 2012.

[37] S. Oliveira and H. Andrade, "An initial assessment of the bioclimatic comfort in an outdoor public space in Lisbon," *International Journal of Biometeorology*, vol. 52, no. 1, pp. 69–84, 2007.

[38] N. Kántor and J. Unger, "The most problematic variable in the course of human-biometeorological comfort assessment—the mean radiant temperature," *Central European Journal of Geosciences*, vol. 3, no. 1, pp. 90–100, 2011.

[39] S. Thorsson, M. Lindqvist, and S. Lindqvist, "Thermal bioclimatic conditions and patterns of behaviour in an urban park in Göteborg, Sweden," *International Journal of Biometeorology*, vol. 48, no. 3, pp. 149–156, 2004.

[40] N. Kántor, J. Unger, and Á. Gulyas, "Subjective estimations of thermal environment in recreational urban spaces—part 2: international comparison," *International Journal of Biometeorology*, vol. 56, no. 6, pp. 1089–1101, 2012.

[41] T.-P. Lin, "Thermal perception, adaptation and attendance in a public square in hot and humid regions," *Building and Environment*, vol. 44, no. 10, pp. 2017–2026, 2009.

[42] E. Ng and V. Cheng, "Urban human thermal comfort in hot and humid Hong Kong," *Energy and Buildings*, vol. 55, pp. 51–65, 2012.

[43] A. Matzarakis and H. Mayer, "Another kind of environmental stress: thermal stress," *WHO Newsletter*, vol. 18, pp. 7–10, 1996.

[44] G. Jendritzky, W. Sönning, and H. J. Swantes, "An objective evaluation method for the description of the thermal surroundings in urban and landscape planning ("Klima-Michel-Modell")," Academy Spatial Research Planning Report 28, 1979.

[45] J. Konarska, F. Lindberg, A. Larsson, S. Thorsson, and B. Holmer, "Transmissivity of solar radiation through the crowns of single urban trees," *Urban Climate News*, no. 46, pp. 20–24, 2012.